

# Aspects of Anomaly in Condensed Matter Physics

by

Weicheng Ye

A thesis  
presented to the University of Waterloo  
in fulfillment of the  
thesis requirement for the degree of  
Doctor of Philosophy  
in  
Physics

Waterloo, Ontario, Canada, 2023

© Weicheng Ye 2023

## Examining Committee Membership

The following served on the Examining Committee for this thesis. The decision of the Examining Committee is by majority vote.

External Examiner: William Witczak-Krempa  
Professor, Université de Montréal

Supervisor(s): Timothy H. Hsieh  
Adjunct Professor, University of Waterloo  
Roger G. Melko  
Professor, University of Waterloo

Internal Member: A. A. Burkov  
Professor, University of Waterloo

Internal-External Member: Ben Webster  
Professor, University of Waterloo

Other Member(s): Chong Wang  
Adjunct Professor, University of Waterloo

### **Author's Declaration**

This thesis consists of material all of which I authored or co-authored: see Statement of Contribution in the thesis. This is a true copy of the thesis, including any required final revisions, as accepted by my examiners.

I understand that my thesis may be made electronically available to the public.

## Statement of Contributions

This thesis is based on the following published articles:

- **Ye, Weicheng**, Meng Guo, Yin-Chen He, Chong Wang, and Liuju Zou. “Topological characterization of Lieb-Schultz-Mattis constraints and applications to symmetry-enriched quantum criticality.” *SciPost Physics* 13, no. 3 (2022): 066. [[arXiv: 2111.12097](#)] [1]
- **Ye, Weicheng**, and Liujun Zou. “Anomaly of  $(2 + 1)$ -Dimensional Symmetry-Enriched Topological Order from  $(3 + 1)$ -Dimensional Topological Quantum Field Theory.” *arXiv preprint arXiv:2210.02444* (2022). [2]

There are also several articles produced while Weicheng Ye is a Ph.D. student at the University of Waterloo but not included in the thesis:

- **Ye, Weicheng**, Sung-Sik Lee, and Liujun Zou. “Ultraviolet-Infrared Mixing in Marginal Fermi Liquids.” *Physical Review Letters*, 128, no. 10 (2022): 106402. [[arXiv: 2109.00004](#)] [3]
- Lin, Cheng-Ju, **Weicheng Ye**, Yijian Zou, Shengqi Sang, and Timothy H. Hsieh. “Probing sign structure using measurement-induced entanglement.” *Quantum* 7 (2023): 910. [[arXiv: 2205.05692](#)] [4]

Weicheng Ye acknowledges supports from the Natural Sciences and Engineering Research Council of Canada(NSERC) through Discovery Grants. Research at Perimeter Institute is supported in part by the Government of Canada through the Department of Innovation, Science and Industry Canada and by the Province of Ontario through the Ministry of Colleges and Universities.

## Abstract

Anomalies have proven to be an important tool for unraveling the enigmatic properties of strongly-coupled condensed matter systems. Especially, it provides powerful constraints on the emergibility problem, i.e., whether a quantum phase or phase transition can emerge in a many-body system. In this thesis, the focus is mainly on  $(2 + 1)$ -dimensional bosonic systems, and we explain how to identify the anomaly of various interesting systems in this category. We then apply these results to study the emergibility of a class of quantum critical states known as Stiefel Liquid, and discuss several interesting realizations uncovered using results from anomaly.

First of all, for a  $(2 + 1)$ -d lattice spin system, we derive the topological partition functions that characterize the Lieb-Schultz-Mattis constraints with  $G_s \times G_{int}$  symmetry, where  $G_s$  is an arbitrary space group in two spatial dimensions, and  $G_{int}$  is any internal symmetry whose projective representations are classified by  $(\mathbb{Z}_2)^k$  with  $k$  an integer. This LSM anomaly will be matched with the anomaly of IR states. We then calculate the anomaly of several IR states. One class of IR states we discuss is the recently-proposed Stiefel Liquid, with the well-known Deconfined Quantum Critical Point (DQCP) and U(1) Dirac Spin Liquid (DSL) unified as two special examples. We introduce the description of Stiefel Liquid using non-linear Sigma Model and explain how to get the anomaly from such description. Another class of IR states we consider is  $(2 + 1)$ -d symmetry-enriched topological order. And we explain the framework of getting the anomaly of topological order with a general symmetry action by identifying a  $(3 + 1)$ -d topological quantum field theory whose boundary hosts the original  $(2 + 1)$ -d symmetry-enriched topological order.

Finally, we apply these results and the framework of anomaly-matching to understand the emergibility of Stiefel Liquid, including DQCP, DSL, and the so-called non-Lagrangian Stiefel liquid. These states can emerge as a consequence of the competition between a magnetic state and a non-magnetic state. We identify all possible realizations of these states on systems with  $SO(3) \times \mathbb{Z}_2^T$  internal symmetry and either  $p6m$  or  $p4m$  lattice symmetry. Many interesting examples are discovered, including a DQCP adjacent to a ferromagnet, stable DSLs on square and honeycomb lattices, and a class of quantum critical spinquadrupolar liquids of which the most relevant spinful fluctuations carry spin-2. In particular, there is a realization of spin-quadrupolar DSL that is beyond the usual parton construction.

## Acknowledgements

First and foremost, I want to express my wholehearted appreciation to my Ph.D. advisors Prof. Timothy H. Hsieh and Prof. Chong Wang. I am really really blessed to have both of you as my invaluable guides through my Ph.D. years. I learn so so much from both of your numerous valuable comments and suggestions, great patience in my mistakes and blunders, and careful instructions during the whole process of my Ph.D. program, without which I will never successfully graduate and accomplish this thesis. I am also consistently amazed by both of your very unique approach to physics and your research enthusiasm, which I will benefit for the rest of my life. I remember vividly so many interesting topics Tim brought up on the lunch table of condensed matter physicists and I never cease to be amazed by the range and originality of many questions and comments. I also remember many hilarious jokes Chong made during many explanations and discussions. Particularly, I will always remember both of your unforgettable encouragement at the beginning of the covid and during my personal low points. Chong even said, and I quote, “just relax until you are ready for physics”, for which I will be grateful forever.

I would specially acknowledge Dr. Liujun Zou, whom I have so much academic contact with and whom I learn so much from. I really understand what “doing physics” means in everyday life from Liujun and I also learn so much from your most unique philosophy and approach towards physics. I am still learning what it means to do physics but I am so thankful that these lessons will follow me wherever I go.

I would like to thank my collaborators during my Ph.D program. I learn so much from your wisdom and my ways of doing physics are forged because of you. I am grateful to Prof. Sung-Sik Lee for many in-depths discussions during our collaboration. I am also grateful to Prof. Yin-Chen He for many sharp inspirations. Many thanks to my collaborators, Meng Guo, Cheng-Ju (Jacob) Lin, Shengqi Sang, and Yijian Zou. I also want to thank Arun Albert Debray, Zi-Wen Liu, Jinmin Yi, and Matthew Yu for current collaboration. I would also like to thank Leonardo A. Lessa, Han Ma, Ruochen Ma, Shan-Ming Ruan, Aaron Szasz, Lei Gioia Yang, and Keyou Zeng for stimulating discussions. Specially, I want to thank Aaron for guidance and encouragement during covid times, Zi-Wen for showing me the beauty of quantum information, Matt for listening to my chaotic nonsense about math that I do not understand, Yijian for helpful guidance and unique perspectives in condensed matter physics, and Shengqi for chatting with me during my solo time in my office. I would like to acknowledge my dissertation committee members, Prof. A. A. Burkov, Prof. Roger Melko, Prof. Ben Webster, and Prof. William Witczak-Krempa, for their time, extreme patience, and wisdom that enriches this thesis. I would also like to acknowledge

my undergraduate advisor Prof. Bin Chen, whose support in my undergraduate years and my pursuit in condensed matter physics deeply touches my heart.

I am deeply indebted to so many people that I am very fortunate to call friends. My everyday life with you is the very strength that takes me to the end of my Ph.D. years. I sincerely hope that I can recount every moment with you and I regret deeply if I forget any one of them. In particular, my sincere thanks goes to Yijian Zou, Yushao Chen, Shuwei Liu, and Ruochen Ma for sharing a flat with me and tolerating my wierd behaviors. And I also want to specially thank Ruozhen Gong, Qi Hu, Yuhan Liu, Zi-Wen Liu, Ruochen Ma, Shengqi Sang, Lei Gioia Yang, Matthew Yu, Jian-Hao Zhang, and Yijian Zou for their strong support during my postdoc applications and guidance in my future endeavors. I am confident about my future choice because of your wisdom.

At the very last, I want to dedicate this thesis to my grandparents, especially my grandfather. I remember vividly talking with you about fetching something inside a closed ball through “going to a higher dimension”. It is perhaps at this very moment that I want to start a career in science. My motivation for a very long time is to do something that makes you proud. I never achieve something that I am truly proud of. But still, here at the end of my Ph.D. years, I am sitting in your old house typing this thesis, and I dedicate this thesis to you.

## Dedication

*Dedicated to my grandparents.  
Because of whom I am less afraid of death.*



# Table of Contents

Examining Committee	ii
Author's Declaration	iii
Statement of Contributions	iv
Abstract	v
Acknowledgements	vi
Dedication	viii
List of Figures	xiv
List of Tables	xvii
<b>1 Introduction</b>	<b>1</b>
1.1 Exotic Quantum Phases of Matter . . . . .	1
1.1.1 Topological Order . . . . .	2
1.1.2 Stiefel Liquid . . . . .	3
1.2 Symmetry and Anomaly . . . . .	3
1.3 The Hypothesis of Emergibility . . . . .	6
1.4 Plan of the Thesis . . . . .	7

<b>2</b>	<b>Topological Characterization of LSM Constraints and LSM Anomaly</b>	<b>11</b>
2.1	Review of lattice homotopy and the connection to SPT . . . . .	12
2.1.1	$G_s = p6m$ . . . . .	14
2.1.2	$G_s = p4m$ . . . . .	16
2.2	Topological characterization of the LSM constraints . . . . .	17
2.2.1	$G_s = p6m$ . . . . .	22
2.2.2	$G_s = p4m$ . . . . .	24
2.2.3	Topological characterization of the LSM constraints in $(1 + 1)$ -d . . . . .	26
2.A	Topological partition function corresponding to LSM . . . . .	27
2.B	Fractionalization pattern involving both translation and glide symmetries . . . . .	29
2.C	Non-LSM fractionalization patterns . . . . .	30
2.D	Group Cohomology and $\mathbb{Z}_2$ Cohomology ring of wallpaper groups . . . . .	32
2.E	Topological invariants for all LSM constraints . . . . .	48
2.F	Topological characterization of LSM constraints in $(1 + 1)$ -d . . . . .	57
<b>3</b>	<b>Stiefel Liquid, non-linear Sigma Model and its Anomaly</b>	<b>60</b>
3.1	Stiefel Liquids as a NLSM . . . . .	61
3.2	Symmetry . . . . .	62
3.3	Anomaly . . . . .	63
3.4	Dynamics of Stiefel Liquids . . . . .	66
3.4.1	$SL^{(5)}$ : DQCP . . . . .	66
3.4.2	$SL^{(6)}$ : $U(1)$ Dirac spin liquid . . . . .	67
3.4.3	$SL^{(N \geq 7)}$ : non-Lagrangian Theory . . . . .	69
3.A	Effects of Relevant Operators on SL . . . . .	70
<b>4</b>	<b>Anomaly of <math>(2 + 1)</math>-Dimensional Symmetry-Enriched Topological Order</b>	<b>74</b>
4.1	Review of topological order with symmetry $G$ . . . . .	75
4.1.1	Review of UMTC notation . . . . .	75

4.1.2	Global symmetry . . . . .	77
4.2	(3 + 1)-d TQFT with finite group symmetry $G$ . . . . .	81
4.2.1	Characterizing the anomaly by bulk-boundary correspondence . . . . .	82
4.2.2	General construction of TQFT . . . . .	83
4.2.3	Handle decomposition . . . . .	89
4.2.4	Recipe for calculating the partition function . . . . .	91
4.3	Examples: finite group symmetry . . . . .	98
4.3.1	No symmetry . . . . .	98
4.3.2	$\mathbb{Z}_2^T$ . . . . .	99
4.3.3	$\mathbb{Z}_2 \times \mathbb{Z}_2$ . . . . .	101
4.3.4	$\mathbb{Z}_2^T \times \mathbb{Z}_2^T$ . . . . .	104
4.4	Generalization to connected Lie group symmetry . . . . .	112
4.4.1	Example: $SO(N)$ . . . . .	113
4.5	Other symmetry groups . . . . .	118
4.5.1	$O(N)^T$ . . . . .	118
4.5.2	$SO(N) \times \mathbb{Z}_2^T$ . . . . .	122
4.A	Derivation of Eq. (4.44) . . . . .	124
4.A.1	Vector Spaces . . . . .	124
4.A.2	Partition functions . . . . .	125
4.A.3	Inner Products . . . . .	127
4.A.4	Requirement from Invertibility . . . . .	129
4.B	An explicit expression of the $\eta$ -factor . . . . .	130
4.C	Consistency check of TQFT . . . . .	131
4.C.1	Independence on the handle decomposition . . . . .	131
4.C.2	Invariance under change of defects . . . . .	138
4.C.3	Gauge invariance . . . . .	141
4.C.4	Cobordism invariance . . . . .	142

4.C.5	Invertibility . . . . .	144
4.C.6	Generalization to connected Lie groups . . . . .	145
4.D	Identifying the manifold $\mathcal{M}$ from bordism . . . . .	146
4.E	More information about handle decomposition of manifolds . . . . .	148
4.E.1	$\mathbb{C}P^2$ . . . . .	149
4.E.2	$\mathbb{R}P^4$ . . . . .	149
4.E.3	$\mathbb{R}P^3 \times S^1$ . . . . .	150
4.E.4	$\mathbb{R}P^2 \times \mathbb{R}P^2$ . . . . .	151
<b>5</b>	<b>Emergibility of Symmetry-Enriched Quantum Criticality</b>	<b>152</b>
5.1	Methods of Calculation . . . . .	153
5.1.1	Example: anomaly matching for DQCP . . . . .	156
5.2	Deconfined quantum critical point and quantum critical spin liquids . . . . .	159
5.2.1	DQCP . . . . .	160
5.2.2	DSL . . . . .	164
5.2.3	$SL^{(7)}$ . . . . .	167
5.3	Quantum critical spin-quadrupolar liquids . . . . .	169
5.4	Stability under symmetry breaking . . . . .	172
5.A	More examples of the calculation of pullback . . . . .	173
5.A.1	$SU(2)_1$ and emergent anomaly . . . . .	174
5.A.2	DSL . . . . .	177
5.A.3	$SL^{(7)}$ . . . . .	180
5.A.4	Five dimensional representation of $SO(3)$ . . . . .	184
5.B	Strategy of exhaustive search of SEP and results . . . . .	185
5.C	Stable realizations on various lattice spin systems . . . . .	188
5.C.1	Stable realizations of DQCP . . . . .	189
5.C.2	Stable realizations of DSL . . . . .	189
5.C.3	Stable realizations of $SL^{(7)}$ . . . . .	192
5.D	Classical regular magnetic orders . . . . .	214
5.E	Stability of DSL realizations on $\text{NaYbO}_2$ and twisted bilayer $\text{WSe}_2$ . . . . .	220

<b>6 Summary and Discussion</b>	<b>222</b>
References	224
<b>APPENDIX</b>	<b>240</b>
<b>A Review of Mathematical Background</b>	<b>241</b>
A.1 Group cohomology . . . . .	241
A.2 Maps of group Cohomology . . . . .	243
A.3 Cup product and $\mathbb{Z}_2$ cohomology ring . . . . .	246
A.4 $SQ^1$ . . . . .	250

# List of Figures

1.1	If two states have the same emergent order and exact microscopic symmetry, and if they can be smoothly connected when symmetry-breaking perturbations are allowed, but are necessarily separated by a phase transition when the relevant symmetries are preserved, then these states are said to have symmetry-protected distinction. . . . .	4
2.1	Panel (a) shows the generators of the wallpaper group $p6m$ . In panel (b), the hexagon is a translation unit cell of the wallpaper group $p6m$ . It has three IWP, usually labelled by $a$ , $b$ and $c$ in crystallography, and they form the sites of the triangular, honeycomb and kagome lattices, respectively. The $C_6$ rotation center is at the type- $a$ IWP. . . . .	14
2.2	Panel (a) shows the generators of the wallpaper group $p4m$ . In panel (b), the square is a translation unit cell of the wallpaper group $p4m$ . It has three IWP, usually labelled by $a$ , $b$ and $c$ in crystallography. Type- $a$ and type- $b$ both form a square lattice. The $C_4$ rotation center in panel (a) is taken to be at the type- $a$ IWP. . . . .	16
2.3	Acting $G^{-1}T_1GT_1$ on an $SO(3)$ monopole. The first $T_1$ action is marked in blue, the following $G$ action is marked in red, the next $T_1$ action is marked in green, and the last $G^{-1}$ action is marked in purple. The dashed line is the reflection axis of $G$ . This figure shows that the operation $G^{-1}T_1GT_1$ moves an $SO(3)$ monopole along a trajectory that encloses a fundamental domain. . . . .	30
4.1	The illustration of some anyon diagram on $D^2 \times D^1$ , with some anyon lines ending on anyon $a$ and $\bar{a}$ put on the boundary. . . . .	87

4.2	Illustration of the usage of gluing formula, where orange, green and blue faces are attached to each other while the red line denotes the (common) boundary of the faces. . . . .	88
4.3	Illustration of a blue 0-handle, a green 1-handle and a purple 2-handle together with labels assigned to their attaching regions. The green shaded regions are the attaching regions $S^0 \times D^3$ of the 1-handle, and the purple shaded regions are the attaching regions $S^1 \times D^2$ of the 2-handle. The red line displays a defect, which crosses the 1-handle with the section being $D^3$ . We associate an anyon $a$ to the 2-handle. We also associate a vector $ a_1, \dots; b_1, \dots\rangle$ and a dual vector $\langle a_1, \dots; b_1, \dots $ to the attaching regions living on the 0-handle side and 1-handle side, respectively (these two sides are identified by the embedding map that attaches the 1-handle to the 0-handle). . . . .	91
4.4	Left: Illustration of a green orientable 1-handle and a purple non-orientable 1-handle, attached to the blue 0-handle. The manifold is supposed to be 4-dimensional but we draw a 2-dimensional plane for illustration. The dashed green circle and the the dashed purple circle are the induced cycles of the two 1-handles. Right: the Kirby diagrams for the green and purple 1-handles (the two figures in the middle), together with the anyon diagrams associated with these Kirby diagrams (the two figures in dashed ellipses). Pay attention how points on the two $D^3$ components of attaching regions $S^0 \times D^3$ are connected to each other via the 1-handle. . . . .	92
4.5	Illustration of the 1-handle. The 1-handle has the topology of a $D^4$ but we draw it as a $D^3$ for illustration. The shaded region represents a $\mathfrak{g}$ -defect for unitary $\mathfrak{g}$ , which cuts through the 1-handle along its $D^3$ plane (drawn as a $D^2$ plane here). The lower plane displays a dual vector $\langle a_1, a_2, a_3; b_1, b_2  _{(x,y,\mu,\nu,\rho)}$ that lives in the vector space associated to $D^3$ , i.e., $\mathcal{V}(D^3; (a_1, a_2, a_3; b_1, b_2)) \simeq V_{b_1, b_2}^{a_1, a_2, a_3}$ , while the upper plane displays a vector $  \mathfrak{g}a_1, \mathfrak{g}a_2, \mathfrak{g}a_3; \mathfrak{g}b_1, \mathfrak{g}b_2 \rangle_{(\mathfrak{g}x, \mathfrak{g}y, \tilde{\mu}, \tilde{\nu}, \tilde{\rho})}$ . The evaluation of the diagram is given by Eq. (4.114) if no defect is present. In the presence of the $\mathfrak{g}$ -defect we just need to add the $U$ -factor as in Eq. (4.43). See Remarks d,e for further treatment when $\mathfrak{g}$ is anti-unitary. . . . .	95
4.6	Suppose a $\mathfrak{g}$ -defect is on the green 1-handle. Following their arrows, anyons in the red and yellow (blue and purple) lines enter the upper (lower) $D^3$ ball and exit from the lower (upper) $D^3$ ball, and they are said to move “downward” (“upward”) and are acted by $\rho_{\mathfrak{g}}^{-1}$ ( $\rho_{\mathfrak{g}}$ ). . . . .	97

4.7	The Kirby diagram of $\mathbb{RP}^4$ . The two blue balls illustrate the attaching region of the 1-handle and the red lines illustrate the attaching region of the 2-handle. The 1-handle is nonorientable. . . . .	100
4.8	The Kirby diagram of $\mathbb{RP}^3 \times S^1$ . The blue balls and dark blue balls illustrate the two 1-handles, and the red lines and orange lines illustrate the two 2-handles. Both 1-handles are orientable. . . . .	102
4.9	Anyon diagram from the Kirby diagram of $\mathbb{RP}^3 \times S^1$ in Fig. 4.8. Pay attention to the extra topological twist of the orange line from the correct framing of the corresponding 2-handle. . . . .	103
4.10	The Kirby diagram of $\mathbb{RP}^2 \times \mathbb{RP}^2$ . The blue balls and dark blue balls illustrate two 1-handles and the red, orange and sand-dune lines illustrate three 2-handles. Both 1-handles are nonorientable. . . . .	104
4.11	Anyon diagram from the Kirby diagram of $\mathbb{RP}^2 \times \mathbb{RP}^2$ in Fig. 4.10. . . . .	105
4.12	Illustration of the 1-handle, with no defect present. The 1-handle has topology of a $D^4$ but we draw it as a $D^3$ for illustration. The lower plane displays a vector $(x, \nu, \mu)(y, \mu, \rho)$ that lives in the vector space associated to $D^3$ , i.e., $\mathcal{V}(D^3; (a_1, \dots; b_1, \dots)) \in V_{b_1, b_2}^{a_1, a_2, a_3}$ , while the upper plane hosts a dual vector. . . . .	126
4.13	Illustration of the calculation of $\langle l_a   l_b \rangle_{\mathcal{V}(S^1 \times D^2; \emptyset)}$ through $\mathcal{Z}(S^1 \times D^3)[l_{\bar{a}} \cup l_b]$ . . . . .	128
4.14	An illustration of the effect of 1-1 handle slide on the Kirby diagram, where the blue 1-handle slides past the darkblue 1-handle. On the anyon diagram the two red lines running upward become a bubble. . . . .	132
4.15	An illustration of the effect of isotopies where the red 2-handle crosses some defect on the darkblue 1-handle. On the anyon diagram the red line connecting the lower darkblue ball to itself becomes a red bubble. . . . .	135
4.16	Upper: An illustration of the effect of a 2-2 handle slide on the Kirby diagram, where the red 2-handle slides past the yellow 2-handle. Lower: An illustration of the change of framing after 2-2 handle slide. . . . .	136



# List of Tables

4.1	Basic Information about handle decomposition of various manifolds used in Section 4.3. See Appendix 4.E for more information about their handle decomposition. . . . .	98
4.2	Anomalies for all-fermion $\mathbb{Z}_2$ topological order with $\mathbb{Z}_2^T \times \mathbb{Z}_2^T$ symmetry, where symmetries do not permute anyons. <i>efmf</i> refers to the trivial symmetry fractionalization class. All classes have $\mathcal{I}_0 = -1$ and hence the beyond-cohomology anomaly. . . . .	109
4.3	Anomalies for all-fermion $\mathbb{Z}_2$ topological order with $\mathbb{Z}_2^T \times \mathbb{Z}_2^T$ symmetry, where $\mathcal{T}_1$ and $\mathcal{T}_2$ permute anyons, which is the reason for the subscripts for <i>e</i> and <i>m</i> . The meanings of the other symbols are the same as in Table 4.2. All classes have $\mathcal{I}_0 = -1$ and hence the beyond-cohomology anomaly. . . .	110
4.4	Anomalies for all-fermion $\mathbb{Z}_2$ topological order with $\mathbb{Z}_2^T \times \mathbb{Z}_2^T$ symmetry, where $\mathcal{T}_1$ and $\mathcal{T}_1\mathcal{T}_2$ permute anyons, which is the reason for the subscripts for <i>e</i> and <i>m</i> . The meanings of the other symbols are the same as in Table 4.2. All classes have $\mathcal{I}_0 = -1$ and hence the beyond-cohomology anomaly. .	110

- 5.1 Numbers of realizations for DQCP, DSL and  $SL^{(7)}$  in spin systems with a  $p6m$  (upper) or  $p4m$  (lower) lattice symmetry. Two realizations with symmetry actions related by a similarity transformation are considered as a single realization. The columns without (with) subscript “quad” represent realizations where the most relevant spinful excitations, i.e., the  $n$  modes that transform nontrivially under the  $SO(3)$  spin rotational symmetry, carry spin-1 (spin-2). No realization of DQCP has the  $n$  modes carrying spin-2. The numbers in parenthesis are the numbers of *stable* realizations. Here a stable DQCP means a realization that has a single relevant perturbation allowed by the microscopic symmetry, and a stable DSL,  $SL^{(7)}$ ,  $DSL_{\text{quad}}$  and  $SL_{\text{quad}}^{(7)}$  means a realization that has no relevant perturbation allowed by the microscopic symmetry. For all columns except  $SL_{\text{incom}}^{(7)}$ , the  $n$  modes are at high-symmetry momenta in the Brillouin zone. For  $SL^{(7)}$  realized on  $p4m$  symmetric lattices, there are realizations with some  $n$  modes at incommensurate momenta, and the column  $SL_{\text{incom}}^{(7)}$  documents the numbers of families of these realizations, where each family includes infinitely many realizations labeled by a momentum, which continuously interpolate between two realizations in the column  $SL^{(7)}$ . Two continuous families of realizations may share a common high-symmetry momentum, at which these two realizations turn out to be always distinct, in that symmetries other than translation are implemented distinctly. (23, 2) means that there are 23 families of realizations, such that as long as a given realization is in the “interiors” of the family (i.e., not all  $n$  modes are at high-symmetry momenta), the only symmetric relevant perturbation is the one that shifts the momenta of  $n$  modes, and there are 2 other families, such that this is still the case except at two exceptional points in the interior, where there is an additional symmetric relevant perturbation that changes the emergent order. The symmetry actions of the stable realizations are explicitly listed in *ReadMe.nb*. . . . . 161
- 5.2 Numbers of realizations for DQCP (top), DSL (middle) and  $SL^{(7)}$  (bottom) adjacent to some colinear, coplanar and non-coplanar magnetic orders, respectively, of triangular, kagome, honeycomb and square lattice spin-1/2 (or general half-integer-spin) systems (third column) and spin-1 (or general integer-spin) systems (fourth column). The numbers in parenthesis are the numbers of stable realizations (defined in the same way as in Table 5.1). F stands for Ferromagnetic while AF stands for Anti-ferromagnetic. “1 Incom” means that realizations of  $SL^{(7)}$  adjacent to tetrahedral umbrella order on the square lattice spin-1/2 systems belong to a continuous family of realizations, where the non-magnetic components of  $n$  can have continuously changing momenta. See Appendix 5.D for the spin configurations of these magnetic orders, and the attached code *ReadMe.nb* for the explicit symmetry actions. . . . . 162

# Chapter 1

## Introduction

### 1.1 Exotic Quantum Phases of Matter

Understanding quantum phases of matter and phase transitions is the central area of study in condensed matter physics. A groundbreaking result in this field is the Landau theory, which characterizes different phases and phase transitions according to whether symmetries are spontaneously broken or not [5]. However, modern condensed matter physics has revealed numerous intriguing phases and phase transitions that cannot be explained by Landau's paradigm [6, 7]. These phases and transitions often involve emergent low-energy degrees of freedom, and many theories, especially strongly interacting field theories, have been proposed to explain their kinematics and dynamics. As a result, the study of these systems has become a hotbed of exciting research in the field of condensed matter physics.

In particular, quantum spin liquids [8–10] are exotic states of matter that arise in certain materials at low temperatures. In these materials, the electrons responsible for magnetism (known as spins) do not settle into the usual ordered patterns that are observed in most magnets. Instead, the spins remain disordered even at very low temperatures, and exhibit long-range entanglement and other unusual quantum properties.

Quantum spin liquids are of great interest to physicists because they challenge our understanding of how materials behave at the quantum level. They also have potential applications in quantum computing and other advanced technologies. However, they are still not well understood, and much of their behavior remains a mystery. This suggests that to understand the behavior of these exotic states of matter, new concepts and theoretical frameworks are necessary and even unavoidable. In this thesis, we focus on  $(2 + 1)$ -d

bosonic quantum many-body systems, with an eye toward its application in understanding exotic phenomena surrounding quantum spin liquids and quantum magnetism.

From the theoretical point of view, quantum states with low-energy excitations described by well-defined quasiparticles, especially Landau symmetry-breaking orders, are relatively well-understood because of the weakly interacting nature of these theories in the IR. However, understanding quantum states that remain strongly coupled even at the lowest energy scale and therefore do not admit descriptions in terms of quasiparticles remains a great challenge theoretically.

When dealing with such states, one usually starts from a non-interacting mean-field theory and introduces fluctuations that are weak at some energy scale. Fluctuations may grow under renormalization group (RG) flow, in which case the low-energy theory will eventually become strongly coupled. Here, the mean-field theory can be formulated in terms of the original physical degrees of freedom (DOFs), such as spins, as is done for Landau symmetry-breaking orders. It can also be formulated in terms of more interesting objects called partons, which are “fractions” of local DOFs, examples of which include composite bosons/fermions in fractional quantum Hall effects and spinons in spin liquids. Fluctuations on top of a parton mean-field theory typically lead to a gauge theory, which forms the theoretical basis of a large number of exotic quantum phases in modern condensed matter physics. However, it is natural to envision that such perturbative arguments may fail to give quantitative or even qualitative predictions, and we may need fundamentally new tools to tackle systems beyond the perturbative regime.

### 1.1.1 Topological Order

One canonical example of such exotic states is topological order. Topological orders are interesting gapped quantum phases of matter beyond the conventional paradigm, and their discovery is one of the main forces that revolutionized modern quantum many-body physics [7]. Instead of being characterized by local order parameters associated with symmetries, in  $(2 + 1)$ -d they are characterized by *anyons*, quasiparticle excitations with nontrivial statistics that may be neither bosonic nor fermionic. The physical properties of a topological order are nicely summarized using the language of tensor category [11–14], and in particular in  $(2 + 1)$ -d bosonic systems the data of anyons forms an elegant mathematical structure called *unitary modular tensor category* (UMTC). In this thesis, we focus on bosonic topological orders in  $(2 + 1)$ -d, and will use the terms topological order and UMTC interchangeably.

### 1.1.2 Stiefel Liquid

Another interesting class of states we consider is called Stiefel Liquid (SL), proposed in Ref. [15]. The Stiefel Liquid is proposed to describe the quantum criticality resulting from the competition between magnetic and non-magnetic orders in quantum spin systems. Their effective theories are formulated in terms of a non-linear Sigma Model (NLSM) defined on a target space  $SO(N)/SO(4)$  ( $N \geq 5$ ), called Stiefel manifold, supplemented with a Wess-Zumino-Witten (WZW) term at level  $k$  ( $k \neq 0$ ) [16, 17]. We refer to an SL labeled by integers  $(N, k)$  as  $SL^{(N,k)}$ , and  $SL^{(N,k=1)}$  may also be simply written as  $SL^{(N)}$ . Stiefel Liquids are supposed to be an infinite family of quantum critical states. The well-known deconfined quantum critical point (DQCP) [18–21] and  $U(1)$  Dirac spin liquid (DSL) [22–24] are unified as the two simplest SLs, with  $N = 5$  and  $N = 6$ , respectively.  $SL^{(N \geq 7)}$  are conjectured to be *non-Lagrangian*, i.e., they are so strongly interacting, such that they cannot be described by any weakly-coupled continuum Lagrangian at any energy scale. Such non-Lagrangian states are beyond the paradigm of parton gauge mean-field theory familiar in the study of exotic quantum liquids in condensed matter physics.

## 1.2 Symmetry and Anomaly

The classification and understanding of exotic quantum phases does not necessarily depend on the presence of symmetry. However, it is well-known that symmetry can largely enrich the story of exotic quantum phases, leading to the concept of symmetry-enriched quantum phases, and there is rich interplay between exotic quantum phases and symmetry. For example, a non-trivial aspect of symmetry actions on a topological order is *symmetry fractionalization*, in the sense that symmetry actions on anyons may not form a representation of the symmetry group, but a projective representation. So we sometimes say that anyons carry “fractional” quantum numbers.

To be more specific, by now it is well appreciated that the universal long-distance and low-energy physics of most (if not all) quantum many-body systems are specified by two levels of data. The first level is characterized by what we refer to as the *emergent order*. In the language of renormalization group (RG), the emergent order is described by properties of the RG fixed point corresponding to this system, which are independent of the exact microscopic symmetry. For example, the RG fixed point corresponding to gapped states are described by certain topological quantum field theory (TQFT), or variants of it. Short-range entangled (SRE) states, i.e., states smoothly connected to a product state without quantum entanglement, are related to a trivial TQFT. In contrast, long-range entangled

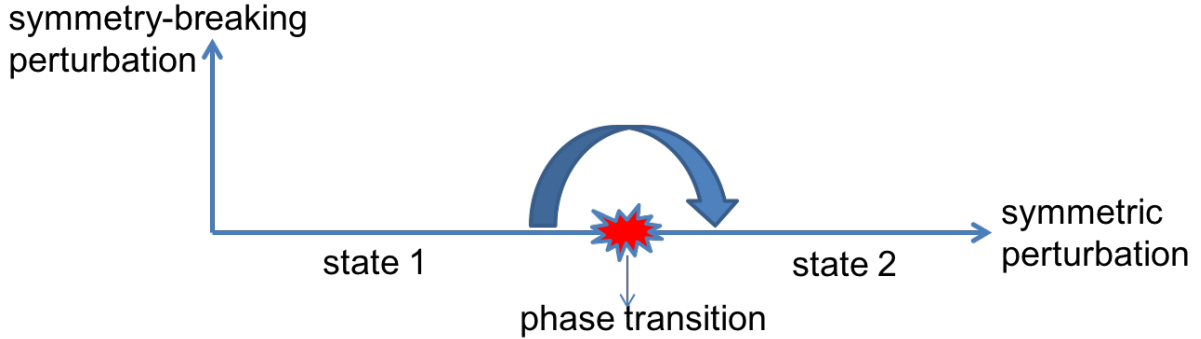


Figure 1.1: If two states have the same emergent order and exact microscopic symmetry, and if they can be smoothly connected when symmetry-breaking perturbations are allowed, but are necessarily separated by a phase transition when the relevant symmetries are preserved, then these states are said to have symmetry-protected distinction.

gapped states, which cannot be smoothly connected to product states, correspond to some nontrivial TQFT. On the other hand, gapless states have different emergent orders, and many of their RG fixed points are described by a conformal field theory (CFT). States described by different RG fixed points are distinct at the level of their emergent orders.

Even if two states have the same emergent order (RG fixed point), their exact microscopic symmetries provide a second level of data that may distinguish them. Two states with the same emergent order but different exact microscopic symmetries are considered distinct. If they have the same emergent order and the same exact microscopic symmetries, they may still have *symmetry-protected distinction*: they are not smoothly connected if certain symmetries are imposed, while they are if these symmetries are broken (see Fig. 1.1). Two SRE states with symmetry-protected distinction are referred to as different symmetry-protected topological phase (SPT), two topological orders with symmetry-protected distinction are referred to as different symmetry-enriched topological states (SETs), and two quantum critical states with symmetry-protected distinction are referred to as different symmetry-enriched criticality.

Given some emergent order and some exact microscopic symmetries, different realizations can be characterized by their symmetry embedding pattern (SEP), i.e., how the microscopic symmetries embed into the emergent symmetries of low-energy DOFs. This characterization has a number of advantages. First and most fundamentally, it captures the symmetry actions in an intrinsic and direct way. This is in contrast to the more common treatment of emergent gauge theories in condensed matter physics (e.g., for DQCP

and DSL), where one first considers the symmetry actions on gauge non-invariant operators (such as spinons) and then converts them into actions on local operators, which is indirect and sometimes complicated, especially when there is a  $(2 + 1)$ -d  $U(1)$  gauge field where the quantum numbers of the local monopole operators cannot be identified with those of any gauge-invariant composite of the matter fields, and when some symmetries act as duality between different gauge-theoretic formulations of the same critical state. Second, especially in the context of Stiefel Liquid, using this characterization we can easily read off the symmetry-breaking patterns of the ordered phases adjacent to the exotic quantum criticality. This information provides valuable guidance on where to look for these quantum critical states: if the corresponding ordered phases are found in a material or model, then exploring the vicinity of the phase diagram may result in the critical state. Third, using this characterization it is easy to check the stability of the critical state under various perturbations, e.g., spin-orbit couplings (SOC).

Interestingly, some realization of symmetry-enriched states are anomalous, in the sense that the corresponding symmetry action cannot be realized in a purely  $(2 + 1)$ -d style with on-site symmetry actions. On the contrary, it has to be realized on the boundary of a  $(3 + 1)$ -d SPT, so that the symmetry actions can be on-site. This is believed to be equivalent to the notion of a 't Hooft anomaly [25]. Given a symmetry group  $G$ , possible anomalies are classified by *group cohomology* or *cobordism*, and these different classes are in one-to-one correspondence with the SPT states in the  $(3 + 1)$ -d bulk that can potentially cancel the anomaly and host this anomalous state on its boundary [26–28].

Understanding the anomaly of quantum many-body systems is very important because the anomaly constrains the low-energy dynamics in a powerful way. If the system has some 't Hooft anomaly, then its ground state cannot be trivial, i.e., either the symmetries are spontaneously broken, or the ground state is gapless or topologically ordered. Going one step further, even more powerful constraint comes from anomaly matching. Since the anomaly can be viewed as a property of the higher dimensional bulk, it is an invariant under deformations of the original system. In particular, it is an invariant under renormalization group that should be the same in the UV and IR. For strongly interacting field theories, we do not have too many handles on their low-energy dynamics so far, and understanding their 't Hooft anomalies and considering anomaly matching serve as a powerful approach [15, 21, 29, 30]. In this thesis we systematically develop frameworks to calculate the anomaly of NLSMs (in Chapter 3) and SETs (in Chapter 4), which may serve as the starting point to study many exotic quantum phases using the concept of anomaly. We identify the anomaly as an element in the relevant cohomology or cobordism group, which can also be thought of as a topological partition function (TPF) characterizing the topological data of the system.

Such constraint imposed by 't Hooft anomaly on quantum many-body systems is reminiscent of Lieb-Schultz-Mattis (LSM) type constraint [31–33]. For instance, a simple example of LSM constraints states that in a  $(d + 1)$ -d lattice spin system with  $SO(3)$  spin rotation and lattice translation symmetries that are not explicitly or spontaneously broken, if each unit cell hosts an odd number of spin-1/2 moments, then the ground state must be exotic (i.e., topologically ordered or gapless).

In fact, there has been great progress in understanding LSM constraints in recent years [34–40], and in particular it was realized that LSM constraints can be captured by *LSM anomalies*, the quantum anomalies carried by the boundaries of some higher-dimensional topological crystalline phases. The LSM anomaly serves as the anomaly of the UV lattice system. Therefore, such relations between LSM constraints and anomalies can be very powerful in constraining the emergibility of a phase or phase transition, because the quantum anomaly of this phase or phase transition, which we refer to as its *IR anomaly*, must match with the LSM anomaly (in a sense to be sharpened later). In order to utilize these constraints, we need to compare the TPF of an LSM anomaly and an IR anomaly, and these constraints have been applied to various systems and shed important insights into the emergibility of some states [41–44]. In Chapter 2, we systematically identify the TPFs of the LSM anomaly relevant to our study. This topological characterization of the LSM constraints is the basis of a systematic framework that uses the LSM constraints to understand the emergibility of quantum phases and phase transitions in a many-body system.

### 1.3 The Hypothesis of Emergibility

A crucial question in condensed matter physics is what we call the question of *emergibility*: given an IR effective theory, can it emerge at low energies in a lattice system described by a local Hamiltonian? This question is generically rather challenging in strongly correlated systems, both theoretically and experimentally, due to the lack of i) theoretical tools to exactly solve the many-body ground state in the generic setting, and ii) experimentally accessible signatures that can unambiguously diagnose the nature of the phase or phase transition. In light of Lieb-Schultz-Mattis type constraint on emergibility, we will utilize the *hypothesis of emergibility*: given a  $(d + 1)$ -dimensional IR effective theory with symmetry  $G_{\text{IR}}$ , a necessary and sufficient condition for it to emerge from a lattice system with symmetry  $G_{\text{UV}}$  is that there is a symmetry embedding pattern (SEP), i.e., a homomorphism  $\varphi$

$$\varphi : G_{\text{UV}} \rightarrow G_{\text{IR}}, \tag{1.1}$$



such that the anomaly of this IR effective theory matches with the anomaly of the lattice system coming from the LSM-like constraint, in the sense that

$$\Omega_{UV} = \varphi^*(\Omega_{IR}) \tag{1.2}$$

where  $\Omega_{UV}$  describes the LSM-like anomaly of the lattice system,  $\Omega_{IR}$  is the anomaly of the IR effective theory, and  $\varphi^*$  is the pullback induced by  $\varphi$  (see Appendix A.2 for a review). In fact, the necessity of this condition has been established (i.e., 't Hooft anomaly-matching condition), and only the sufficiency of it is hypothetical. Although this hypothesis has not been proved so far, it is supported by many nontrivial examples. In the following we will *assume* the correctness of the hypothesis of emergibility.<sup>1</sup>

The hypothesis of emergibility provides an intrinsic characterization of the emergibility of an IR effective theory, without relying on any of its specific constructions. It is especially useful when there is no known lattice construction of this IR effective theory, but its anomaly is known. In Chapter 5 we will utilize this hypothesis to understand the emergibility of Stiefel Liquids (SLs). Due to the intrinsic absence of a weakly-coupled description, it is difficult to construct Stiefel Liquid states, especially non-Lagrangian Stiefel Liquids, on a lattice system by usual means. However, the anomalies of these SLs can be derived. With  $\Omega_{UV}$  derived in Chapter 2 (given by Eqs. (2.1) or (2.2)), we can check the emergibility of these states in various lattice spin systems, by checking the existence of SEPs that can match the anomalies. Based on this approach, some interesting realizations of the non-Lagrangian SLs on triangular and kagome lattices are proposed [15]. Here we will explore this problem more systematically.

## 1.4 Plan of the Thesis

The rest of the thesis is organized as follows:

- In Chapter 2, we derive the topological partition functions of the LSM constraints of the lattice spin systems of our interest. Motivated by the studies of quantum magnetism, we consider  $(2 + 1)$ -d spin systems with  $G_s \times G_{int}$  symmetry, where the lattice symmetry  $G_s$  is any of the 17 wallpaper groups, and  $G_{int}$  is any internal symmetry whose projective representations are classified by  $\mathbb{Z}_2^k$  with  $k$  some integer,

---

<sup>1</sup>When  $G_{UV}$  is trivial, the hypothesis says that every IR effective theory free from gravitational anomaly can be put on some discretized lattice system, which is generally believed to be true. Still, this statement can be thought of as the simplest yet nontrivial check or consequence of the hypothesis.

e.g.,  $G_{int} = SO(3) \times \mathbb{Z}_2^T$ , the combination of  $SO(3)$  spin rotational symmetry and time reversal symmetry. Given  $G_s \times G_{int}$ , there are still topologically distinct LSM constraints, specified by the projective representation (PR) under  $G_{int}$  carried by DOF of the system, and the spatial distribution of these DOF. For *all* cases, we derive the TPFs of the LSM anomalies. Similar analysis is also performed for  $(1+1)$ -d lattice spin systems. The structure of these topological partition functions is given in Eq. (2.1), where  $\eta$  is determined by the projective representation carried by the local degrees of freedom under the internal symmetry, and  $\lambda$  is determined by the locations of the local degrees of freedom. The characterization of  $\lambda$  for different space groups can be found in Sec. 2.2 and Appendix 2.E.

- In Chapter 3, we review the formulation of Stiefel liquid in terms of NLSM, indexed by two integers,  $N \geq 5$  and  $k \neq 0$ . The NLSM is defined on target manifold  $SO(N)/SO(4)$ , known as Stiefel manifold  $V_{N,N-4}$  (or simply  $V_N$  in this thesis), supplemented with a Wess-Zumino-Witten (WZW) term at level  $k$ . The Stiefel manifold can be parameterized using an  $N \times (N-4)$  matrix  $n_{ji}$  satisfying  $n^T n = I_{N-4}$ , where  $I_{N-4}$  is the  $(N-4)$ -dimensional identity matrix. The NLSM is defined using the action

$$S^{(N,k)}[n] = \frac{1}{2g} \int d^{2+1}x (\partial_\mu n^T \partial^\mu n) + k \cdot S_{\text{WZW}}^{(N)}.$$

We identify the symmetries of the Stiefel Liquids to be the standard Poincaré symmetry group plus

$$\frac{O(N)^T \times O(N-4)^T}{\mathbb{Z}_2}. \quad (1.3)$$

whose precise meaning is described in detail in Sec. 3.2. We then calculate the anomaly of the SLs using the NLSM formulation, discussed in detail in Sec. 3.3.

- In Chapter 4, for any SET with any symmetry group  $G$  (which may be discrete or continuous, Abelian or non-Abelian, contain anti-unitary elements and/or permute anyons), we develop a  $(3+1)$ -d topological quantum field theory (TQFT) defined on manifolds with a  $G$ -bundle structure, which describes the SPT state whose boundary can host this SET. Based on this TQFT, we establish a framework to calculate the anomaly of a  $(2+1)$ -d topological order with symmetry group  $G$ , by calculating the partition function of the corresponding TQFT on certain manifolds with some  $G$ -bundle structure. This procedure is spelled out in great detail for finite group symmetries and connected Lie groups, and is expressed compactly in Eq. (4.44) and (4.65), respectively.

We then apply this framework to specific examples. In particular, we calculate the *anomaly indicators* of various symmetry groups, including  $\mathbb{Z}_2^T$  (see Eqs. (4.46),(4.50)),  $\mathbb{Z}_2 \times \mathbb{Z}_2$  (see Eqs. (4.53),(4.54)),  $\mathbb{Z}_2^T \times \mathbb{Z}_2^T$  (see Eqs. (4.55),(4.56)),  $SO(N)$  (see Eq. (4.78)),  $O(N)^T$  (see Eqs. (4.95),(4.96)) and  $SO(N) \times \mathbb{Z}_2^T$  (see Eq. (4.106)), where  $\mathbb{Z}_2$  and  $\mathbb{Z}_2^T$  refer to a unitary and anti-unitary order-2 symmetry group, respectively, and  $O(N)^T$  denotes a symmetry group  $O(N)$  such that elements in  $O(N)$  with determinant  $-1$  are anti-unitary. Here anomaly indicators of symmetry group  $G$  refer to a family of quantities, expressed in terms of the data characterizing an SET, that can completely determine the anomaly of any topological order enriched by the symmetry group  $G$ . In addition, a byproduct of our analysis is an explicit formula for the  $SO(N)$  Hall conductance of an  $SO(N)$  symmetric topological order, expressed in terms of the data characterizing this SET (up to contributions from  $(2+1)$ -d invertible states) (see Eqs. (4.80),(4.81)). Moreover, for  $O(N)^T$ ,  $N \geq 5$  and  $SO(N) \times \mathbb{Z}_2^T$ ,  $N \geq 4$ , we show that certain anomalies cannot be realized by any SET, demonstrating the phenomenon of “symmetry-enforced gaplessness” [45].

- In Chapter 5, we apply these results to study the emergibility of Stiefel Liquids, including the well-known deconfined quantum critical point (DQCP),  $U(1)$  Dirac spin liquid (DSL), and the non-Lagrangian Stiefel liquid. We sketch how to use anomaly-matching to understand the emergibility of various Stiefel liquids. Detailed examples of calculations are presented in Sec. 5.1 and also in Appendix 5.A. We then present some interesting realizations of SLs in Secs. 5.2 and 5.3, while the complete results are summarized in the attached codes, which can be read with the instruction in Appendix 5.B. Table 5.1 records the total numbers of realizations in different cases, and Table 5.2 records the numbers of realizations that are adjacent to classical regular magnetic orders. The stability of each realization is also analyzed, which is recorded in the attached codes. In Appendix 5.C, we present all stable realizations on various familiar lattice systems. The highlighted examples in the main text include i) a deconfined quantum critical point between a ferromagnet and a valence bond solid, ii) stable  $U(1)$  Dirac spin liquids in spin-1/2 square and honeycomb lattices, iii) various realizations of the non-Lagrangian Stiefel liquid, and iv) realizations of SLs where the most relevant spinful excitations carry spin-2, which, in particular, include a  $U(1)$  Dirac spin liquid that cannot be described by the usual parton approach. We also demonstrate how to use our formalism to study the stability of these states under symmetry-breaking perturbations in Sec. 5.4, where we argue that the DSL can be stable in  $\text{NaYbO}_2$ . More analysis regarding  $\text{NaYbO}_2$  and twisted bilayer  $\text{WSe}_2$  is presented in Appendix 5.E.

- Multiple appendices are included at the end of each chapter or the whole thesis. They either provide further details or collect results that may be of general interest. For example, Appendix [A](#) is a review of the basic mathematical tools we use. Appendix [2.D](#) contains descriptions of all 17 wallpaper groups, as well as information about their  $\mathbb{Z}_2$  cohomology, including their  $\mathbb{Z}_2$  cohomology rings and all representative cochains at degree 1 and 2.

## Chapter 2

# Topological Characterization of LSM Constraints and LSM Anomaly

In this chapter, we develop a topological characterization of the LSM constraints applicable to a  $(2+1)$ -d lattice spin system, whose Hilbert space is a tensor product of local bosonic Hilbert spaces, and whose Hamiltonian is also local. We assume that the system has a symmetry group  $G = G_s \times G_{int}$ , where  $G_s$  is one of the 17 wallpaper groups and  $G_{int}$  is an internal symmetry group. Throughout this thesis, we consider  $G_{int}$  whose projective representations (PR) are classified by  $\mathbb{Z}_2^k$  with some  $k \in \mathbb{N}^+$ , i.e.,  $H^2(G_{int}, \text{U}(1)_\rho) = \mathbb{Z}_2^k$ <sup>1</sup>, with the subscript  $\rho$  indicating the complex conjugation action of any spacetime orientation reversal symmetry on the  $\text{U}(1)$  coefficient. Typical examples of such  $G_{int}$  include  $SO(3)$ ,  $SO(3) \times \mathbb{Z}_2^T$ ,  $\mathbb{Z}_2^T$ ,  $O(2)$ ,  $\mathbb{Z}_2 \times \mathbb{Z}_2$ , etc. These choices of  $G$  and  $G_{int}$  are motivated by the systems and models relevant to quantum magnetism. We will also perform a similar analysis for  $(1+1)$ -d lattice spin systems.

Some  $G_{int}$  may have multiple types of PR. For example, for  $G_{int} = SO(3) \times \mathbb{Z}_2^T$ ,  $H^2(SO(3) \times \mathbb{Z}_2^T, \text{U}(1)_\rho) = \mathbb{Z}_2^2$ , so there are 3 different types of nontrivial PR, corresponding to spinor under  $SO(3)$  while Kramers singlet under  $\mathbb{Z}_2^T$ , singlet under  $SO(3)$  while Kramers doublet under  $\mathbb{Z}_2^T$ , and spinor under  $SO(3)$  while Kramers doublet under  $\mathbb{Z}_2^T$ . In this thesis, we will mainly consider systems with at most one type of nontrivial PR, i.e., there may be some DOF carrying trivial PR under  $G_{int}$ , but all DOF with nontrivial PR carry the same type of nontrivial PR which we refer to as the *PR type of the system*. If all DOF

---

<sup>1</sup>In this thesis, a few different objects have the structure of  $\mathbb{Z}_2^k$  with some  $k \in \mathbb{N}$ . These  $k$ 's are independent unless explicitly claimed, and we will abuse the notation to use the same  $k$  when we make a statement about this  $\mathbb{Z}_2^k$  structure.

carry trivial PR, then the PR type of the system is said to be the trivial type. Many of our results can be straightforwardly generalized to the case where the system has DOF with different types of nontrivial PR, on which we sometimes explicitly comment.

This chapter is adapted from Section 2 of Ref. [1].

## 2.1 Review of lattice homotopy and the connection to SPT

To be self-contained, we begin by reviewing lattice homotopy [35], in a way that will lead to our topological characterization of the LSM constraints most easily.

All LSM constraints should be fully determined by the spatial distribution of the DOF in the system. The key idea of lattice homotopy is that, to characterize the LSM constraints for a given lattice system, one can always first smoothly deform the system so that all DOF are moved to the high-symmetry points of the corresponding wallpaper symmetry group, while preserving the  $G = G_s \times G_{int}$  symmetry during the process. These high-symmetry points are called the irreducible Wyckoff positions (IWP); their precise definition can be found in Ref. [35] and they are well documented for each space group in the standard crystallographic literature. All distributions of DOF that can be smoothly deformed into each other are referred to be in the same *lattice homotopy class*. Below we always assume that a smooth deformation has been performed, such that all DOF are located at some IWP. Then to determine the presence or absence of an LSM constraint, one can invoke one or multiple of the following 3 types of basic no-go theorems that preclude symmetric SRE (sym-SRE) ground states in various cases [35, 46]:

1. Define a fundamental domain to be a region that tiles the 2D space under the actions of translation and glide symmetries. When the total PR within a fundamental domain is nontrivial, a sym-SRE ground state is forbidden.
2. When there is a translation symmetry along a mirror axis, and the total PR within a translation unit along this mirror axis is nontrivial, a sym-SRE ground state is forbidden.
3. In our case, the PR of  $G_{int}$  are classified by  $\mathbb{Z}_2^k$ . Then if the total PR at a  $C_2$  rotation center is nontrivial, a sym-SRE ground state is forbidden. However, PR at a  $C_n$  rotation center for odd  $n$  does not forbid a sym-SRE ground state.

Note that these no-go theorems do not require the full wallpaper symmetry to be applicable. In particular, the first applies whenever there are translation or glide symmetries, the second applies whenever there are commuting translation and mirror symmetries, and the last applies whenever there is a rotation symmetry. When a full wallpaper symmetry is present, there are often multiple translations, glide reflections, mirror and rotation symmetries, so a given distribution of DOF may trigger multiple of these basic no-go theorems. It is straightforward to check that knowing which no-go theorems are triggered is actually also sufficient to know which lattice homotopy class this distribution of DOF is in.

One can see that, for a given wallpaper group  $G_s$  and a PR type of the system, the spatial distributions of DOF form an Abelian group, denoted by  $A_{\text{LH}}$ . Each group element in  $A_{\text{LH}}$  corresponds to a lattice homotopy class of distributions of DOF, the multiplication between two group elements corresponds to physically stacking two such distributions of DOF together, and the trivial group element corresponds to a distribution of DOF that is free of all 3 basic no-go theorems above (i.e., a distribution of DOF with no net nontrivial PR in any fundamental domain, any translation unit on any mirror axis, or any  $C_2$  rotation center). Due to the  $\mathbb{Z}_2$  nature of the PR, the inverse of each group element is itself, so  $A_{\text{LH}} = \mathbb{Z}_2^k$  with  $k \in \mathbb{N}$ .

It turns out that elements in  $A_{\text{LH}}$  are in one-to-one correspondence with different LSM constraints [35], i.e., the ground states emergible in systems with distributions of DOF corresponding to different group elements of  $A_{\text{LH}}$  must be different, in the sense that they have different emergent order or symmetry-protected distinction. As an example, the trivial element represents the absence of any LSM constraint, i.e., a sym-SRE ground state is allowed if the microscopic DOF of the system are arranged in a configuration corresponding to the trivial element. Therefore, the intuitive geometric picture based on lattice homotopy gives an elegant characterization and classification of LSM constraints. An important observation that will be very useful later is that the structure of  $A_{\text{LH}}$  only depends on  $G_s$  and the fact that all PR of  $G_{\text{int}}$  has a  $\mathbb{Z}_2$  nature, but not on other details of  $G_{\text{int}}$ .

When PR of  $G_{\text{int}}$  are  $\mathbb{Z}_2^k$ -classified with  $k > 1$ , the above discussion applies to the case where at most one type of nontrivial PR is present in the system. If all nontrivial PR are allowed to be present, all LSM constraints are classified by  $A_{\text{LH}}^k$ , i.e., each nontrivial PR can result in LSM constraints classified by  $A_{\text{LH}}$ , and nontrivial LSM constraints from different nontrivial PR are all different.

To make this discussion more concrete, below we consider two specific examples that will be relevant for the later part of the thesis.

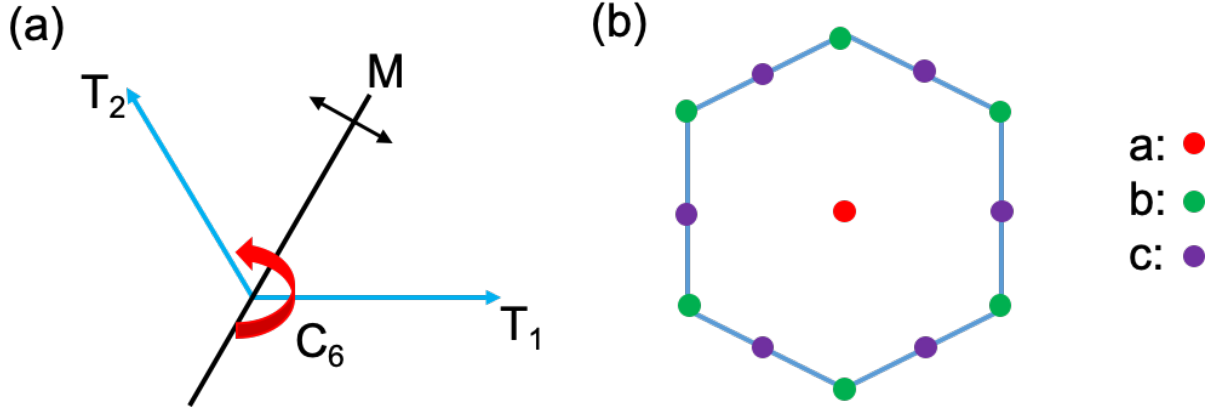


Figure 2.1: Panel (a) shows the generators of the wallpaper group  $p6m$ . In panel (b), the hexagon is a translation unit cell of the wallpaper group  $p6m$ . It has three IWP, usually labelled by  $a$ ,  $b$  and  $c$  in crystallography, and they form the sites of the triangular, honeycomb and kagome lattices, respectively. The  $C_6$  rotation center is at the type- $a$  IWP.

### 2.1.1 $G_s = p6m$

We start with the example where  $G_s = p6m$ , which is the symmetry group of triangular, kagome and honeycomb lattices. The generators, a translation unit cell and IWP of  $p6m$  are shown in Fig. 2.1. The translation vectors of  $T_1$  and  $T_2$  have the same length, and their angle is  $2\pi/3$ . There is also a 6-fold rotational symmetry, denoted by  $C_6$ . Finally, there is a mirror symmetry  $M$ , whose mirror axis passes through the  $C_6$ -center and bisects the translation vectors of  $T_1$  and  $T_2$ .

We wish to understand how to identify the distributions of DOF with the elements in  $A_{LH}$  in this example. First consider the case where all DOF in the system are in the trivial PR. This distribution of DOF is free of all the 3 basic no-go theorems, so it corresponds to the trivial element of  $A_{LH}$ , which physically implies that there is no LSM constraint associated with this distribution of DOF, and sym-SRE ground states are allowed. This is indeed the common belief.

Next, consider putting DOF with nontrivial PR on any of the three types of IWP. First, imagine putting DOF with nontrivial PR on the type- $b$  IWP. One can check that none of the 3 basic no-go theorems is triggered, so this distribution of DOF also corresponds to the trivial group element, and there should be no associated LSM constraint. Indeed, this configuration is where the DOF are on a honeycomb lattice, and it is known that sym-SRE ground states are allowed in this case [47–50], consistent with the absence of any LSM



constraint. Second, imagine putting DOF with nontrivial PR on the type-*a* IWP. One can check that all 3 basic no-go theorems are triggered, so this configuration should correspond to a nontrivial element in  $A_{\text{LH}}$ , and such a system has a nontrivial LSM constraint that precludes any sym-SRE ground state. The same is true if DOF with nontrivial PR are put on the type-*c* IWP. Moreover, one can also check that the distributions of DOF on type-*a* and type-*c* IWP are in different lattice homotopy classes, i.e., they cannot be smoothly deformed into each other. So they correspond to different group elements in  $A_{\text{LH}}$ , which indicates different LSM constraints. These two types of IWP form a triangular and kagome lattice, respectively, and there is indeed no known example of symmetric states that can emerge in both triangular and kagome lattices, without showing any difference in emergent order or symmetry-protected distinction.<sup>2</sup>

Finally, one can also consider putting DOF with nontrivial PR on multiple of the three types of IWP. For instance, putting these DOF on both type-*a* and type-*c* IWP is equivalent to stacking systems with DOF arranged on a triangular lattice and kagome lattice together, which corresponds to multiplying the two nontrivial group elements in the last paragraph.

Taken together, the above analysis indicates that the LSM constraints on a lattice with  $p6m$  symmetry are classified by  $A_{\text{LH}} = \mathbb{Z}_2^2$ , and the two generators can be taken to correspond to distributions of DOF on triangular and kagome lattices, respectively.

In the above, we have worked out  $A_{\text{LH}}$  by examining whether any of the basic no-go theorems is triggered by a distribution of DOF. To finish the discussion of this case with  $G_s = p6m$ , we demonstrate how the information about which basic no-go theorems are triggered can uniquely determine the lattice homotopy class. In this case, we just need to consider the third type of the basic no-go theorems. For this type of no-go theorems, there are two independent ones, triggered by putting DOF with nontrivial PR on the type-*a* and type-*c* IWP, respectively. So if we know which of the no-go theorems are triggered, we also know whether there are nontrivial PR carried by type-*a* and type-*c* IWP. From the previous discussion, this can uniquely determine the lattice homotopy class. This observation will be very useful when we construct a topological characterization of the LSM constraints later.

---

<sup>2</sup>In fact, even spontaneously-symmetry-breaking states (such as ferromagnetic states) realized on these two lattices should be distinct, because they have different anomalies. However, to the best of our knowledge, it is still an open problem to explicitly calculate the complete anomalies for these spontaneously-symmetry-breaking states, which is an interesting problem beyond the scope of the current paper.

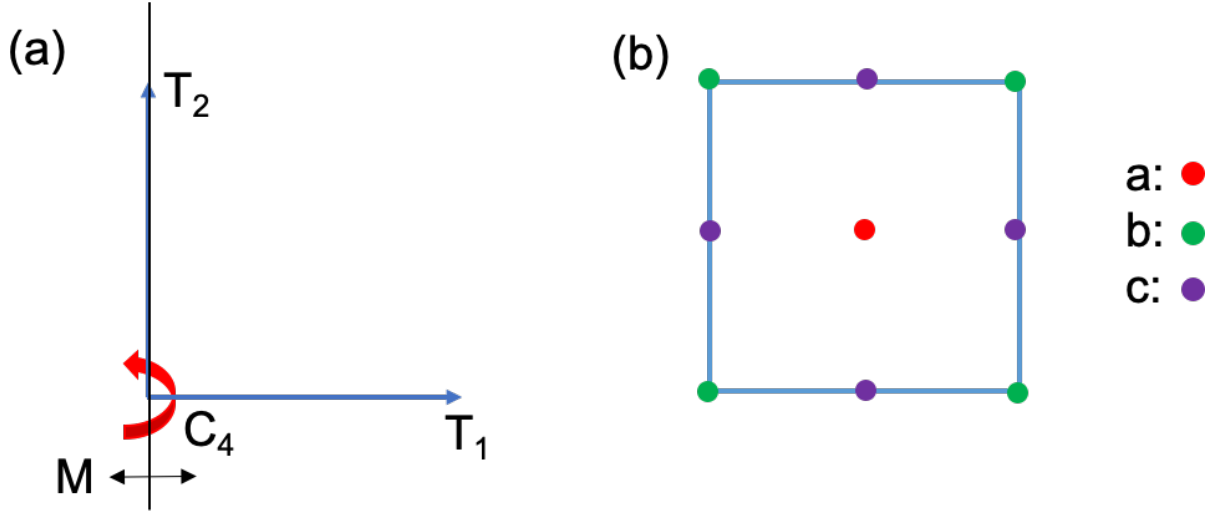


Figure 2.2: Panel (a) shows the generators of the wallpaper group  $p4m$ . In panel (b), the square is a translation unit cell of the wallpaper group  $p4m$ . It has three IWP, usually labelled by  $a$ ,  $b$  and  $c$  in crystallography. Type- $a$  and type- $b$  both form a square lattice. The  $C_4$  rotation center in panel (a) is taken to be at the type- $a$  IWP.

### 2.1.2 $G_s = p4m$

Warmed up with the example where  $G_s = p6m$ , now we can easily apply the similar analysis to the other 16 wallpaper groups. Here, we examine the case where  $G_s = p4m$ , which will be relevant to our later discussion.

The  $p4m$  group describes the symmetry of square and checkerboard lattices. The generators, a translation unit cell and IWP of  $p4m$  are shown in Fig. 2.2. The translation vectors of  $T_1$  and  $T_2$  have the same length and are perpendicular. There is also a 4-fold rotational symmetry, denoted by  $C_4$ . Finally, there is a mirror symmetry  $M$ , whose mirror axis passes through the  $C_4$ -center and is parallel to the translation vector of  $T_2$ . There are 3 types of IWP. The type- $a$  IWP is the 2-fold rotation centers of  $C_4^2$ , the type- $b$  IWP is the 2-fold rotation centers of  $T_1T_2C_4^2$ , and the type- $c$  IWP includes the 2-fold rotation centers of both  $T_1C_4^2$  and  $T_2C_4^2$ . Note that the type- $a$  and type- $b$  are actually also 4-fold rotation centers, and all three IWP lie on some mirror axes.

Below, we enumerate some distributions of DOF that correspond to different elements in  $A_{LH}$  in this case:

1. All DOF have trivial PR: trivial element in  $A_{\text{LH}}$ .
2. DOF with nontrivial PR at one of the three types of IWP: three different elements in  $A_{\text{LH}}$ .
3. DOF with nontrivial PR at multiple of the IWP: product of elements in the previous case.

This analysis implies that the LSM constraints on a lattice with  $p4m$  symmetry are classified by  $A_{\text{LH}} = \mathbb{Z}_2^3$ , and the three generators can be taken to correspond to distributions of DOF on the three types of IWP. Note that both the type- $a$  and type- $b$  IWP form a square lattice, and type- $c$  IWP form a checkerboard lattice. Again, it is easy to see that knowing which of the basic no-go theorems are triggered can uniquely determine the lattice homotopy class.

Before finishing the review, we note that it has also been realized that LSM constraints are intimately related to anomalies and higher dimensional SPTs [34, 36–39]. In the present context, our  $(2+1)$ -d system with DOF carrying PR can be viewed as a boundary of a  $(3+1)$ -d system made of stacked  $(1+1)$ -d SPTs protected by  $G_{\text{int}}$ , which are also classified by  $H^2(G_{\text{int}}, \text{U}(1)_\rho) = \mathbb{Z}_2^k$ . The spatial extension of these  $(1+1)$ -d SPTs is along the extra dimension. The boundaries of these SPTs carry the PR, whose types and locations precisely match with the DOF of the original  $(2+1)$ -d system, which have been moved to the IWP using lattice homotopy. Furthermore, the wallpaper symmetry  $G_s$  can be naturally extended into a symmetry of the  $(3+1)$ -d system. Then the  $(3+1)$ -d system is an SPT protected by  $G_s \times G_{\text{int}}$ , and a sym-SRE boundary of such a nontrivial SPT is forbidden due to the nontrivial quantum anomaly, which implies the LSM constraints. Moreover, different SPTs have different anomalies on the boundary, so their corresponding LSM constraints must be different, such that ground states emergible in systems with different LSM constraints must have distinction in their emergent order or symmetry-protected distinction. For these reasons, in the following we will view an LSM constraint and the  $(3+1)$ -d  $G_s \times G_{\text{int}}$  SPT corresponding to this LSM constraint on equal footing.

## 2.2 Topological characterization of the LSM constraints

The above picture of lattice homotopy and higher dimensional SPTs allows us to derive a topological characterization of the LSM constraints. In particular, we will identify the topological partition function (TPF) of the  $(3+1)$ -d SPT corresponding to each nontrivial LSM constraint for a given  $G_s$  and  $G_{\text{int}}$ .

To do it, we use the fact that the SPT of interest can be constructed by stacking the nontrivial  $(1+1)$ -d  $G_{int}$  SPT at various IWP. Suppose, in the language of Dijkgraaf-Witten theories [26, 51, 52], the TPF of this  $(1+1)$ -d SPT is encoded in a nontrivial cocycle in  $H^2(G_{int}, U(1)_\rho) \cong \mathbb{Z}_2^k$ , which can be represented by  $\exp(i\pi\eta(a_1, a_2))$ , where  $a_{1,2} \in G_{int}$  and  $\eta$  takes values in  $\{0, 1\}$  (taking  $\eta \in \{0, 1\}$  is valid since such SPTs are  $\mathbb{Z}_2^k$ -classified). To write down the TPF of the relevant  $(3+1)$ -d  $G_s \times G_{int}$  SPT, we view  $G_s$  on equal footing with  $G_{int}$ , keeping in mind that any orientation-reversal element in  $G_s$  should also complex conjugate the  $U(1)$  coefficient, in accordance with the crystalline equivalence principle [53]. Then the TPF can be encoded in a cocycle  $\Omega(g_1, g_2, g_3, g_4)$  in  $H^4(G_s \times G_{int}, U(1)_\rho)$ , where  $g_{1,2,3,4} \in G_s \times G_{int}$ . The picture based on lattice homotopy and stacks of  $(1+1)$ -d  $G_{int}$  SPT strongly suggests that  $\Omega(g_1, g_2, g_3, g_4)$  takes the form

$$\Omega(g_1, g_2, g_3, g_4) = e^{i\pi\lambda(l_1, l_2)\eta(a_3, a_4)} \quad (2.1)$$

where  $g_i \in G_s \times G_{int}$  is written as  $g_i = l_i \otimes a_i$ , with  $l_i \in G_s$  and  $a_i \in G_{int}$ , and  $\lambda$  also takes values in  $\{0, 1\}$ . Physically,  $\lambda$  encodes the information of which IWP host the  $(1+1)$ -d  $G_{int}$  SPT. The lattice homotopy picture further suggests that  $\lambda$  is completely determined by  $G_s$  and the lattice homotopy class corresponding to the particular LSM constraint, and should be the same for all  $G_{int}$  with  $\mathbb{Z}_2^k$ -classified PR and all PR types of the system. Such a cocycle implies that the TPF, in terms of lattice gauge theory on a triangulated manifold, takes the form

$$\mathcal{Z} = e^{i\pi \int_{\mathcal{M}_4} \lambda[A_s] \cup \eta[A_{int}]} \quad (2.2)$$

where  $\mathcal{M}_4$  is the 4 dimensional spacetime manifold of the SPT,  $A_s$  and  $A_{int}$  are the (1-form) gauge fields resulting from gauging  $G_s$  and  $G_{int}$ , respectively, and  $\exp(i\pi \int \eta[A_{int}])$  gives the TPF of the  $(1+1)$ -d  $G_{int}$  SPT. Note that although the TPF is constructed from a cup product of  $\lambda$  and  $\eta$ , generically  $\lambda$  (or  $\eta$ ) itself cannot be written as a cup product of  $A_s$  (or  $A_{int}$ ).

In Appendix 2.A, we show that the above expectation is indeed correct. Furthermore,  $\lambda(l_1, l_2)$  can be viewed as a representative cochain in  $H^2(G_s, \mathbb{Z}_2)$ . Assuming that the  $(1+1)$ -d  $G_{int}$  SPT is already understood (i.e., the  $\eta$  corresponding to the PR type of the system is known), the task to identify the TPF for the  $(3+1)$ -d  $G_s \times G_{int}$  SPT corresponding to the LSM constraints becomes identifying  $\lambda(l_1, l_2)$  for a given  $G_s$  and lattice homotopy class.

Before proceeding, let us pause to clarify what it means to identify  $\lambda(l_1, l_2)$ . After all, as reviewed in Appendix A.1,  $\lambda(l_1, l_2)$  changes under coboundary transformations, so it is not an invariant characterization of the LSM constraints. However, inequivalent  $\lambda$ 's can be

diagnosed by quantities related to it that are invariant under coboundary transformations. So identifying  $\lambda(l_1, l_2)$  really means identifying these *topological invariants*. To relate to some known results of such topological invariants, we define  $\omega(l_1, l_2) \equiv e^{i\pi\lambda(l_1, l_2)}$ , which encodes the same information as  $\lambda(l_1, l_2)$ . Then a topological invariant takes the form of  $\alpha[\omega]$ , a functional of  $\omega$ .

Now we proceed to derive these topological invariants. Because  $\lambda(l_1, l_2)$  or  $\omega(l_1, l_2)$  is the same for all  $G_{int}$ , it suffices to derive it in a particularly simple and illuminating case, i.e.,  $G_{int} = SO(3)$ . According to Sec. 2.1, in this case the  $(3+1)$ -d  $G_s \times G_{int}$  SPTs related to the LSM constraints are fully characterized by the spatial distribution of Haldane chains, i.e.,  $(1+1)$ -d SPT protected by the  $SO(3)$  symmetry. Therefore, to characterize the LSM constraints, all we have to do is to identify topological invariants for  $H^2(G_s, \mathbb{Z}_2)$  that can tell us which IWP host Haldane chains. To this end, we utilize the fact that, for a given spatial distribution of Haldane chains, which IWP host Haldane chains is fully encoded in which of the 3 basic no-go theorems are triggered. So if we can characterize the 3 basic no-go theorems using some topological invariants, we can further get the topological invariants corresponding to the LSM constraints.

To obtain the topological invariants corresponding to the 3 basic no-go theorems, it is useful to consider coupling the system to a probe gauge field of the  $SO(3)$  symmetry and examine the monopoles of this  $SO(3)$  gauge field, which is a method proven to be extremely powerful [44, 45, 54–58]. Because the wave function of the system acquires a  $-1$  topological phase factor when an  $SO(3)$  monopole circles around a Haldane chain<sup>3</sup>, we will see below that if any of the 3 basic no-go theorems is triggered, the  $G_s$  symmetry will fractionalize on the  $SO(3)$  monopole in a specific way, i.e., the  $SO(3)$  monopole will carry a specific projective representation of  $G_s$ . The symmetry fractionalization pattern of  $G_s$  on the  $SO(3)$  monopole will thus completely encode the LSM constraint. Since the fusion rule of the  $SO(3)$  monopole is determined by  $\pi_1(SO(3)) = \mathbb{Z}_2$  [59], the symmetry fractionalization patterns of  $G_s$  on the  $SO(3)$  monopole are classified by  $H^2(G_s, \mathbb{Z}_2)$  [42, 43, 60, 61]. So the LSM constraints can be characterized by elements in  $H^2(G_s, \mathbb{Z}_2)$ , consistent with the previous general discussion. This also implies that when  $G_{int} = SO(3)$ , for a given  $G_s$  and lattice homotopy class, the  $\lambda(l_1, l_2)$  in Eq. (2.1) should be precisely the element

---

<sup>3</sup>Consider moving a Haldane chain around an  $SO(3)$  monopole. The topological phase factor generated in this process is given by the topological partition function of the Haldane chain, calculated on the manifold defined by the spacetime trajectory it moves along, with a background  $SO(3)$  gauge bundle exerted by the  $SO(3)$  monopole. It is known that the topological partition function of a Haldane chain is  $e^{i\pi \int_{\mathcal{M}} w_2^{SO(3)}}$ , where  $w_2^{SO(3)}$  is the second Stiefel-Whitney class of the  $SO(3)$  gauge bundle. Furthermore,  $\int_{\mathcal{M}} w_2^{SO(3)} = 1$  around an  $SO(3)$  monopole. Therefore, there is a  $-1$  phase factor generated in this process, which also implies that moving an  $SO(3)$  monopole around a Haldane chain results in a  $-1$  topological phase factor.

in  $H^2(G_s, \mathbb{Z}_2)$  that describes the symmetry fractionalization pattern of  $G_s$  on the  $SO(3)$  monopole in the corresponding SPT. However, one should not expect that all symmetry fractionalization patterns captured by  $H^2(G_s, \mathbb{Z}_2)$  are related to LSM constraints. To see it, consider breaking the  $SO(3)$  symmetry to  $U(1)$ . Then the original LSM-related  $G_s \times SO(3)$  SPT will become a trivial  $G_s \times U(1)$  SPT, since the Haldane chain is trivialized upon this symmetry breaking. Therefore, the  $U(1)$  monopole, which is the descendent of the  $SO(3)$  monopole after symmetry breaking, should carry no nontrivial symmetry fractionalization pattern. It implies that certain nontrivial symmetry fractionalization pattern on the  $SO(3)$  monopoles, or certain elements in  $H^2(G_s, \mathbb{Z}_2)$ , may be unrelated to LSM constraints. We will see this explicitly below.

We start with the first no-go theorem, and focus on the case where only translation symmetry is important, and defer a similar discussion where the glide reflection is also important to Appendix 2.B. Denote the two translation generators by  $T_1$  and  $T_2$ , and apply the operation  $T_2^{-1}T_1^{-1}T_2T_1$  to an  $SO(3)$  monopole, which moves it around a translation unit cell. If each translation unit cell contains an odd (even) number of Haldane chains, this process results in a  $-1$  ( $1$ ) phase factor, which precisely characterizes how the translation symmetry fractionalizes on the  $SO(3)$  monopole. By slightly abusing the notation, we write the subgroup of  $G_s$  generated by  $T_1$  and  $T_2$  as  $T_1 \times T_2$ . The fractionalization patterns of the  $T_1 \times T_2$  symmetry should be classified by  $H^2(T_1 \times T_2, \mathbb{Z}_2) = \mathbb{Z}_2$ , so the aforementioned phase factor must be given by the unique nontrivial topological invariant in  $H^2(T_1 \times T_2, \mathbb{Z}_2)$ , i.e.,  $\alpha_1[\omega] = \frac{\omega(T_1, T_2)}{\omega(T_2, T_1)}$ . Denote two elements in this subgroup by  $l_1 = T_1^{x_1} T_2^{y_1}$  and  $l_2 = T_1^{x_2} T_2^{y_2}$ , with  $x_{1,2}, y_{1,2} \in \mathbb{Z}$ , a representative cochain that triggers this topological invariant is  $\omega(l_1, l_2) = (-1)^{y_1 x_2}$ .

Next, consider the second no-go theorem. Denote the generator of the relevant mirror symmetry by  $M$ , and suppose  $T$  generates a translation symmetry on the mirror plane. Note that this implies  $TM = MT$ . Apply the operation  $MT^{-1}MT$  to an  $SO(3)$  monopole, which moves it along a trajectory that encloses a translation unit along the mirror plane. Suppose there is an odd (even) number of Haldane chains in this translation unit, this process results in a  $-1$  ( $1$ ) phase factor, which precisely characterizes how the symmetry group generated by  $M$  and  $T$  fractionalizes on the  $SO(3)$  monopole. Write the subgroup of  $G_s$  generated by  $M$  and  $T$  as  $M \times T$ , the fractionalization patterns of the  $M \times T$  symmetry are classified by  $H^2(M \times T, \mathbb{Z}_2) = \mathbb{Z}_2^2$ . So there are two nontrivial topological invariants in  $H^2(M \times T, \mathbb{Z}_2)$ , and they can be written as  $\alpha_2[\omega] = \frac{\omega(T, M)}{\omega(M, T)}$  and  $\alpha_{\text{non-LSM}} = \frac{\omega(M, M)}{\omega(1, 1)}$ , where in the denominator 1 stands for the trivial group element in  $M \times T$ . Note that  $\alpha_{\text{non-LSM}} = -1$  would imply when the  $SO(3)$  symmetry is broken to  $U(1)$ , the resulting  $G_s \times U(1)$  state is a nontrivial SPT, since this represents a nontrivial symmetry fractionalization pattern of a  $U(1)$  monopole [56, 57]. According to the previous general discussion,  $\alpha_{\text{non-LSM}}$  should

be unrelated to LSM constraints of interest.

We can also directly see that  $\alpha_{\text{non-LSM}}$  is unrelated to the LSM constraints without considering breaking the  $SO(3)$  symmetry. Denote two elements in  $M \times T$  by  $l_1 = T^{x_1} M^{m_1}$  and  $l_2 = T^{x_2} M^{m_2}$ , with  $x_{1,2} \in \mathbb{Z}$  and  $m_{1,2} \in \{0, 1\}$ , representative cochains that trigger these two topological invariants are  $\omega(l_1, l_2) = (-1)^{m_1 x_2}$  and  $\omega(l_1, l_2) = (-1)^{m_1 m_2}$ , respectively. Suppose  $\lambda$  in Eq. (2.1) contains a piece  $\lambda(l_1, l_2) = m_1 m_2$ , such that  $\alpha_{\text{non-LSM}} = -1$ , from Eq. (2.2), we see the TPF of the  $(3+1)$ -d SPT contains a part given by  $\exp(i\pi \int (w_1^{TM})^2 w_2^{SO(3)})$ , where  $w_1^{TM}$  is the first Stiefel-Whitney class of the tangent bundle of the spacetime manifold, and  $w_2^{SO(3)}$  is the second Stiefel-Whitney class of the  $SO(3)$  gauge bundle. In writing this down, we have used that  $M$  is an orientation reversal symmetry and that the TPF of a Haldane chain is  $\exp(i\pi \int w_2^{SO(3)})$ . This means that when the symmetry is broken down to  $M \times SO(3)$ , the system is still a nontrivial SPT.<sup>4</sup> However, all SPTs corresponding to LSM constraints become trivial when the lattice symmetry contains only a mirror symmetry (as can be seen from lattice homotopy, or simply from the lack of basic no-go theorem that only requires a mirror symmetry as the lattice symmetry), and hence a contradiction. This again means  $\alpha_{\text{non-LSM}} = 1$  for SPTs corresponding to LSM constraints (see Appendix 2.C for the physics of the SPTs that trigger  $\alpha_{\text{non-LSM}}$ ). Therefore, the phase factor resulted from acting  $MT^{-1}MT$  to an  $SO(3)$  monopole must be given by  $\alpha_2$ .

Finally, consider the third no-go theorem. Denote the generator of the relevant 2-fold rotational symmetry by  $C_2$ , and apply  $C_2$  to an  $SO(3)$  monopole twice, which moves it around a  $C_2$  rotation axis. Suppose there is an odd (even) number of Haldane chains in this  $C_2$  rotation axis, this process results in a  $-1$  ( $1$ ) phase factor, which precisely characterizes how the  $C_2$  rotational symmetry fractionalizes on the  $SO(3)$  monopole. Write the subgroup of  $G_s$  generated by  $C_2$  also as  $C_2$ . The fractionalization patterns of the  $C_2$  symmetry are classified by  $H^2(C_2, \mathbb{Z}_2) = \mathbb{Z}_2$ , so the aforementioned phase factor must be given by the unique topological invariant in  $H^2(C_2, \mathbb{Z}_2)$ , i.e.,  $\alpha_3[\omega] = \frac{\omega(C_2, C_2)}{\omega(1, 1)}$ . Denote two elements in this subgroup by  $l_1 = C_2^{c_1}$  and  $l_2 = C_2^{c_2}$ , with  $c_{1,2} \in \{0, 1\}$ , a representative cochain that triggers this topological invariant is  $\omega(l_1, l_2) = (-1)^{c_1 c_2}$ .

In summary, we have found 4 basic types of symmetry fractionalization patterns of  $G_s$ , characterized by the above 4 types of topological invariants,  $\alpha_{1,2,3}$  and  $\alpha_{\text{non-LSM}}$ . The first

---

<sup>4</sup>In this SPT, the symmetry  $M$  fractionalizes on the  $SO(3)$  monopole, i.e., acting  $M$  twice on an  $SO(3)$  monopole yields a  $-1$  phase factor. This symmetry fractionalization pattern is captured by  $H^2(M, \mathbb{Z}_2) = \mathbb{Z}_2$ , whose unique topological invariant is  $\alpha_{\text{non-LSM}}$ . So  $\alpha_{\text{non-LSM}}$  should be identified as this phase factor. In Appendix 2.C, we further show that such an SPT can be constructed by putting on its  $M$  mirror plane a  $(2+1)$ -d  $\mathbb{Z}_2 \times SO(3)$  SPT, whose  $\mathbb{Z}_2$  domain walls are decorated with Haldane chains.

three are related to the 3 basic no-go theorems, thus to the LSM constraints, while the last is a non-LSM symmetry fractionalization pattern. As mentioned before, if  $G_{int} = SO(3)$  is broken to  $U(1)$ ,  $\alpha_{\text{non-LSM}}$  detects a nontrivial symmetry fractionalization pattern of a  $U(1)$  monopole, captured by a nontrivial element in  $H^2(G_s, U_\rho(1))$ <sup>5</sup>. One can also see that  $\alpha_{1,2,3} = -1$  does not imply that the descendent  $G_s \times U(1)$  SPT is nontrivial, since they correspond to trivial elements in  $H^2(G_s, U_\rho(1))$ . These 4 basic fractionalization patterns are clearly independent of each other, as they correspond to completely different  $(3+1)$ -d SPTs. Furthermore, for all 17 wallpaper groups  $G_s$ , these 4 types of fractionalization patterns give a complete set of topological invariants that can distinguish all elements of  $H^2(G_s, \mathbb{Z}_2)$ , as explicitly checked in Appendix 2.E. These actually mean that

$$A_{\text{LH}} = \ker[\tilde{i} : H^2(G_s, \mathbb{Z}_2) \rightarrow H^2(G_s, U(1)_\rho)] \quad (2.3)$$

where  $\tilde{i}$  is the map defined in Eq. (A.13).

With this in mind, to further derive the topological invariants corresponding to an LSM constraint, we just need to write down the complete set of independent topological invariants of  $H^2(G_s, \mathbb{Z}_2)$ , and bridge the combinations of these topological invariants with distributions of DOF. Then each combination is a topological invariant for an LSM constraint, which determines  $\lambda$  in Eq. (2.1). Combined with  $\eta$  corresponding to the PR type of the system, Eq. (2.1) or (2.2) gives the TPF of the  $(3+1)$ -d  $G_s \times G_{int}$  SPT corresponding to this LSM constraint. An advantage of this approach is its intuitive nature, i.e., everything can be done by simply inspecting the IWP. Below we perform this analysis in detail for the cases with  $G_s = p6m$  and  $G_s = p4m$ , which will be relevant to the discussion of symmetry-enriched criticality later in the thesis. In Appendix 2.E, we present all topological invariants that characterize  $H^2(G_s, \mathbb{Z}_2)$ , with  $G_s$  being any of the 17 wallpaper groups.

Before moving on, we stress again that the topological characterization of the LSM constraints obtained here applies to all  $G_{int}$  with  $\mathbb{Z}_2^k$ -classified PR and all PR types of the system, although it is derived in a special case with  $G_{int} = SO(3)$ .

### 2.2.1 $G_s = p6m$

All fractionalization patterns of  $p6m$  are classified by  $H^2(p6m, \mathbb{Z}_2) = \mathbb{Z}_2^4$ . As discussed in Sec. 2.1,  $p6m$  has two IWP related to LSM constraints, type-*a* and type-*c*. The former is the 2-fold rotation center of  $C_6^3$ , and the latter includes the 2-fold rotation centers of

---

<sup>5</sup>More precisely,  $H_{\text{Borel}}^2(G_s, U(1)_\rho)$ . Especially,  $H_{\text{Borel}}^2(p1, U(1)_\rho) \cong H^3(p1, \mathbb{Z}_\rho) = 0$ .



$T_1C_6^3$ ,  $T_2C_6^3$  and  $T_1T_2C_6^3$ . In addition,  $p6m$  also has two independent mirror symmetries,  $M$  and  $C_6^3M$ . Using the 4 types of basic topological invariants discussed above, we can immediately write down the complete set of independent topological invariants which can distinguish all elements in  $H^2(p6m, \mathbb{Z}_2)$ :

$$\begin{aligned}
\alpha_1^{p6m}[\omega] &= \frac{\omega(C_6^3, C_6^3)}{\omega(1, 1)} \\
\alpha_2^{p6m}[\omega] &= \frac{\omega(T_1C_6^3, T_1C_6^3)}{\omega(1, 1)} \\
\alpha_3^{p6m}[\omega] &= \frac{\omega(M, M)}{\omega(1, 1)} \\
\alpha_4^{p6m}[\omega] &= \frac{\omega(C_6^3M, C_6^3M)}{\omega(1, 1)}
\end{aligned} \tag{2.4}$$

Physically,  $\alpha_1^{p6m}$  and  $\alpha_2^{p6m}$  measure the PR at the type-*a* and type-*c* IWP, respectively, while  $\alpha_3^{p6m}$  and  $\alpha_4^{p6m}$  determine whether the  $(3+1)$ -d  $G_s \times G_{int}$  SPT contains a non-LSM component. Mathematically, the correctness, completeness and independence of these topological invariants can be checked using the representative cochains in Appendix 2.D.

Therefore, when  $\alpha_3^{p6m} = \alpha_4^{p6m} = 1$ , the combinations  $(\alpha_1^{p6m}, \alpha_2^{p6m})$  are the sought-for topological invariants that characterize the LSM constraints in a lattice with  $G_s = p6m$ . In particular,  $(\alpha_1^{p6m}, \alpha_2^{p6m}) = (-1, 1)$  and  $(\alpha_1^{p6m}, \alpha_2^{p6m}) = (1, -1)$  imply that there are DOF with nontrivial PR at the type-*a* and type-*c* IWP, respectively, which are the generators of  $A_{LH}$ , as discussed in Sec. 2.1. When at least one of  $\alpha_3^{p6m}$  and  $\alpha_4^{p6m}$  is  $-1$ , this combination does not correspond to any LSM constraint.

We remark that the choice of topological invariants is not unique. For example, the expression of  $\alpha_2^{p6m}[\omega]$  can be replaced by either  $\frac{\omega(T_2C_6^3, T_2C_6^3)}{\omega(1,1)}$  or  $\frac{\omega(T_1T_2C_6^3, T_1T_2C_6^3)}{\omega(1,1)}$ , because  $\frac{\omega(T_1C_6^3, T_1C_6^3)}{\omega(1,1)} = \frac{\omega(T_2C_6^3, T_2C_6^3)}{\omega(1,1)} = \frac{\omega(T_1T_2C_6^3, T_1T_2C_6^3)}{\omega(1,1)}$  for a cocycle  $\omega(g_1, g_2)$  in  $H^2(p6m, \mathbb{Z}_2)$ , as can be checked by using the representative cochains in Appendix 2.D. Physically, this just means that the 2-fold rotation centers of  $T_1C_6^3$ ,  $T_2C_6^3$  and  $T_1T_2C_6^3$  are related by symmetry, so the PR at these three rotation centers should be the same. We can also replace the expression of  $\alpha_2^{p6m}[\omega]$  by  $\frac{\omega(T_1, T_2)}{\omega(T_2, T_1)}$ , which tells us whether there is a net nontrivial PR in a translation unit cell and equals  $\alpha_1^{p6m}[\omega] \cdot \alpha_2^{p6m}[\omega]$ . This information combined with  $\alpha_1^{p6m}[\omega]$  also completely specifies which IWP host Haldane chains.

It is useful to notice some interesting relations between LSM constraints with  $G_s = p6m$  and those with  $G_s$  being a subgroup of  $p6m$ . In particular, consider the case where  $G_s = cmm$ , which is a subgroup of  $p6m$  generated by  $T_1$ ,  $T_2$ ,  $C_2 \equiv C_6^3$  and  $M$ . That is,

the 3-fold rotational symmetry generated by  $C_6^2$  is absent. This wallpaper group has 3 IWP, where the first is the 2-fold rotation center of  $C_2$ , the second is the 2-fold rotation center of  $T_1T_2C_2$ , and the last includes the 2-fold rotation centers of both  $T_1C_2$  and  $T_2C_2$ . Furthermore, there are two independent mirror symmetries, generated by  $M$  and  $C_2M$ . Similar analysis as before indicates that, for  $cm\bar{m}$ , the 3 LSM fractionalization patterns and 2 non-LSM fractionalization patterns are detected by topological invariants

$$\begin{aligned}
\alpha_1^{cm\bar{m}}[\omega] &= \frac{\omega(C_2, C_2)}{\omega(1, 1)} \\
\alpha_2^{cm\bar{m}}[\omega] &= \frac{\omega(T_1T_2C_2, T_1T_2C_2)}{\omega(1, 1)} \\
\alpha_3^{cm\bar{m}}[\omega] &= \frac{\omega(T_1C_2, T_1C_2)}{\omega(1, 1)} \\
\alpha_4^{cm\bar{m}}[\omega] &= \frac{\omega(M, M)}{\omega(1, 1)} \\
\alpha_5^{cm\bar{m}}[\omega] &= \frac{\omega(C_2M, C_2M)}{\omega(1, 1)}
\end{aligned} \tag{2.5}$$

So when  $\alpha_4^{cm\bar{m}} = \alpha_5^{cm\bar{m}} = 1$ , the combinations  $(\alpha_1^{cm\bar{m}}, \alpha_2^{cm\bar{m}}, \alpha_3^{cm\bar{m}})$  are the topological invariants that characterize the LSM constraints in a lattice with  $G_s = cm\bar{m}$ .

It is easy to see that the first IWP of  $cm\bar{m}$  is just the descendent of the type-*a* IWP of  $p6m$ , and the second and third IWP of  $cm\bar{m}$  are descendent of the type-*c* IWP of  $p6m$ . Moreover, the mirror symmetries of  $cm\bar{m}$  are also the descendent mirror symmetries of  $p6m$ . This means that the fractionalization pattern of  $p6m$  can be completely specified by that of its  $cm\bar{m}$  subgroup. More precisely, for a  $cm\bar{m}$  subgroup of  $p6m$ , we have

$$\begin{aligned}
\alpha_1^{p6m} &= \alpha_1^{cm\bar{m}}, & \alpha_2^{p6m} &= \alpha_2^{cm\bar{m}} = \alpha_3^{cm\bar{m}}, \\
\alpha_3^{p6m} &= \alpha_4^{cm\bar{m}}, & \alpha_4^{p6m} &= \alpha_5^{cm\bar{m}}
\end{aligned} \tag{2.6}$$

These relations allow us to focus on the  $cm\bar{m}$  subgroup of a  $p6m$  group when we consider its fractionalization classes, which sometimes simplifies the analysis.

### 2.2.2 $G_s = p4m$

Using similar analysis as before, it is easy to see that the LSM constraints for the case with  $G_s = p4m$  are classified by  $\mathbb{Z}_2^3$ , generated by distributions of DOF with nontrivial PR on

the 3 IWP. The 3 root LSM constraints can be detected by topological invariants

$$\begin{aligned}
\alpha_1^{p4m} &= \frac{\omega(C_4^2, C_4^2)}{\omega(1, 1)} \\
\alpha_2^{p4m} &= \frac{\omega(T_1 T_2 C_4^2, T_1 T_2 C_4^2)}{\omega(1, 1)} \\
\alpha_3^{p4m} &= \frac{\omega(T_1 C_4^2, T_1 C_4^2)}{\omega(1, 1)}
\end{aligned} \tag{2.7}$$

Again, the  $p4m$  symmetry requires that  $\frac{\omega(T_1 C_4^2, T_1 C_4^2)}{\omega(1, 1)} = \frac{\omega(T_2 C_4^2, T_2 C_4^2)}{\omega(1, 1)}$ . There are also non-LSM fractionalization patterns classified by  $\mathbb{Z}_2^3$ , with the following topological invariants for the corresponding generators:

$$\begin{aligned}
\alpha_4^{p4m}[\omega] &= \frac{\omega(M, M)}{\omega(1, 1)} \\
\alpha_5^{p4m}[\omega] &= \frac{\omega(T_1 M, T_1 M)}{\omega(1, 1)} \\
\alpha_6^{p4m}[\omega] &= \frac{\omega(C_4 M, C_4 M)}{\omega(1, 1)}
\end{aligned} \tag{2.8}$$

In the case with  $G_{int} = SO(3)$ , these three topological invariants imply that acting  $M$ ,  $T_1 M$  and  $C_4 M$  on an  $SO(3)$  monopole twice yields a  $-1$  phase factor, respectively.

Therefore, when  $\alpha_4^{p4m} = \alpha_5^{p4m} = \alpha_6^{p4m} = 1$ , the combinations  $(\alpha_1^{p4m}, \alpha_2^{p4m}, \alpha_3^{p4m})$  are the topological invariants that characterize the LSM constraints in a lattice with  $G_s = p4m$ .

Again, it is useful to note the relation between the LSM constraints for  $G_s = p4m$  and those for its subgroups. Let us consider the  $pmm$  subgroup of  $p4m$ , generated by  $T_1$ ,  $T_2$ ,  $M$  and  $C_2 \equiv C_4^2$ . That is, the 4-fold rotation is absent while the 2-fold rotation is retained in  $pmm$ . By inspecting the IWP of  $pmm$ , we can immediately write down the topological invariants corresponding to the LSM constraints

$$\begin{aligned}
\alpha_1^{pmm}[\omega] &= \frac{\omega(C_2, C_2)}{\omega(1, 1)} \\
\alpha_2^{pmm}[\omega] &= \frac{\omega(T_1 T_2 C_2, T_1 T_2 C_2)}{\omega(1, 1)} \\
\alpha_3^{pmm}[\omega] &= \frac{\omega(T_1 C_2, T_1 C_2)}{\omega(1, 1)} \\
\alpha_4^{pmm}[\omega] &= \frac{\omega(T_2 C_2, T_2 C_2)}{\omega(1, 1)}
\end{aligned} \tag{2.9}$$

and the topological invariants for the non-LSM fractionalization patterns

$$\begin{aligned}
\alpha_5^{pmm}[\omega] &= \frac{\omega(M, M)}{\omega(1, 1)} \\
\alpha_6^{pmm}[\omega] &= \frac{\omega(C_2M, C_2M)}{\omega(1, 1)} \\
\alpha_7^{pmm}[\omega] &= \frac{\omega(T_1M, T_1M)}{\omega(1, 1)} \\
\alpha_8^{pmm}[\omega] &= \frac{\omega(T_2C_2M, T_2C_2M)}{\omega(1, 1)}
\end{aligned} \tag{2.10}$$

So when all  $\alpha_5^{pmm} = \alpha_6^{pmm} = \alpha_7^{pmm} = \alpha_8^{pmm} = 1$ , the combinations  $(\alpha_1^{pmm}, \alpha_2^{pmm}, \alpha_3^{pmm}, \alpha_4^{pmm})$  are the topological invariants that characterize the LSM constraints in a lattice with  $G_s = pmm$ .

Furthermore, by examining the relation between IWP of  $p4m$  and the IWP of its  $pmm$  subgroup, we get

$$\begin{aligned}
\alpha_1^{p4m} &= \alpha_1^{pmm}, & \alpha_2^{p4m} &= \alpha_2^{pmm}, \\
\alpha_3^{p4m} &= \alpha_3^{pmm} = \alpha_4^{pmm}, \\
\alpha_4^{p4m} &= \alpha_5^{pmm} = \alpha_6^{pmm}, \\
\alpha_5^{p4m} &= \alpha_7^{pmm} = \alpha_8^{pmm}
\end{aligned} \tag{2.11}$$

So 5 of the 6 topological invariants for  $p4m$  can be determined by examining its  $pmm$  subgroup. To further determine the last topological invariant,  $\alpha_6^{p4m}$ , one can simply examine the subgroup generated by  $C_4M$ . This observation will also simplify some analysis.

### 2.2.3 Topological characterization of the LSM constraints in (1+1)-d

In the above we have derived the topological characterization of LSM constraints in (2+1)-d systems. Similar derivation can be carried out for (1+1)-d systems with  $G_s \times G_{int}$  symmetry, where  $G_s$  is one of the two line groups, and  $G_{int}$  is an internal symmetry group whose PR are  $\mathbb{Z}_2^k$ -classified. In this case, the lattice homotopy picture still applies in an analogous way, and there are (2+1)-d  $G_s \times G_{int}$  SPTs corresponding to each LSM constraint. Here we present the cocycle and TPF of these SPTs, and leave the details of derivation to Appendix 2.F.

When  $G_s = p1$ , the line group that contains only translation generated by  $T$ , the classification of LSM constraints is  $\mathbb{Z}_2$ , detected by the total PR inside each translation unit cell. The cocycle describing the  $(2+1)$ -d  $p1 \times G_{int}$  SPT related to the nontrivial LSM constraint is

$$\Omega(g_1, g_2, g_3) = e^{i\pi x_1 \eta(a_2, a_3)} \quad (2.12)$$

where  $g_i = T^{x_i} \otimes a_i$ , with  $x_i \in \mathbb{Z}$  and  $a_i \in G_{int}$ , for  $i = 1, 2, 3$ . The corresponding TPF can be written as

$$\mathcal{Z} = e^{i\pi \int_{\mathcal{M}_3} x \cup \eta[A_{int}]} \quad (2.13)$$

where  $\mathcal{M}_3$  is the  $(2+1)$ -d spacetime manifold the SPT lives in, and  $x$  is the gauge field corresponding to the translation symmetry.

When  $G_s = p1m$ , the line group that contains both translation  $T$  and mirror  $M$ , the classification of LSM constraints is  $\mathbb{Z}_2^2$ , detected by the total PR at the mirror centers of  $M$  and  $TM$ . For the case where only the mirror center of  $M$  has a net nontrivial PR, the corresponding cocycle is

$$\Omega(g_1, g_2, g_3) = e^{i\pi(x_1 + m_1)\eta(a_2, a_3)} \quad (2.14)$$

where  $g_i = T^{x_i} M^{m_i} \otimes a_i$ , with  $x_i \in \mathbb{Z}$ ,  $m_i \in \{0, 1\}$  and  $a_i \in G_{int}$ , for  $i = 1, 2, 3$ . The corresponding TPF can be written as

$$\mathcal{Z} = e^{i\pi \int_{\mathcal{M}_3} (x+m) \cup \eta[A_{int}]} \quad (2.15)$$

where  $x$  is still the gauge field of translation, and  $m$  is the gauge field of mirror symmetry. For the case where only the mirror center of  $TM$  has a net nontrivial PR, using similar notations, the corresponding cocycle and TPF are respectively

$$\Omega(g_1, g_2, g_3) = e^{i\pi x_1 \eta(a_2, a_3)} \quad (2.16)$$

and

$$\mathcal{Z} = e^{i\pi \int_{\mathcal{M}_3} x \cup \eta[A_{int}]} \quad (2.17)$$

## 2.A Topological partition function corresponding to LSM

In this appendix, we provide a more rigorous argument that the cocycle corresponding to the topological partition function (TPF) of the  $(3+1)$ -d  $G_s \times G_{int}$  SPT, whose boundary

has some LSM constraint, can indeed be written in the form of Eq. (2.1).<sup>6</sup>

To start, first recall that the lattice homotopy picture indicates that all LSM constraints for a given wallpaper group  $G_s$  are classified by a group  $A_{\text{LH}} = \mathbb{Z}_2^k$  with some integer  $k$ . This means that the sought-for cocycle in  $H^4(G_s \times G_{\text{int}}, \text{U}(1)_\rho)$  can be written as

$$\Omega(g_1, g_2, g_3, g_4) = e^{i\pi\kappa(g_1, g_2, g_3, g_4)} \quad (2.18)$$

with  $\kappa$  taking values in  $\{0, 1\}$ . This allows us to view  $\kappa(g_1, g_2, g_3, g_4)$  as a representative cochain in  $H^4(G_s \times G_{\text{int}}, \mathbb{Z}_2)$ , where the multiplication between two elements is implemented by the mod 2 addition of their corresponding representative cochains. Since  $H^4(G_s \times G_{\text{int}}, \mathbb{Z}_2) \simeq \bigoplus_{i=0}^4 H^i(G_s, \mathbb{Z}_2) \otimes H^{4-i}(G_{\text{int}}, \mathbb{Z}_2)$ , we can always write  $\Omega$  as

$$\Omega(g_1, g_2, g_3, g_4) = \prod_{i=0}^4 e^{i\pi\lambda_i(l_1, \dots, l_i)\eta_{4-i}(a_{i+1}, \dots, a_4)} \quad (2.19)$$

where each  $g_i \in G_s \times G_{\text{int}}$  is again written as  $g_i = l_i \otimes a_i$ , with  $l_i \in G_s$  and  $a_i \in G_{\text{int}}$ . Both  $\lambda_i$  and  $\eta_{4-i}$  take values in  $\{0, 1\}$ , and they can be viewed as representative cochains in  $H^i(G_s, \mathbb{Z}_2)$  and  $H^{4-i}(G_{\text{int}}, \mathbb{Z}_2)$ , respectively. Furthermore, we can view  $e^{i\pi\eta_{4-i}(a_{i+1}, \dots, a_4)}$  as a representative cochain in  $H^{4-i}(G_{\text{int}}, \text{U}(1)_\rho)$ , which can be physically interpreted as a  $G_{\text{int}}$  SPT living in  $3 - i$  spatial dimensions.

Previous studies of  $G_s \times G_{\text{int}}$  SPTs indicate that all these SPTs have a real-space construction, in which various lower dimensional SPTs (or invertible states) are decorated into various submanifolds of the entire crystal [39, 62, 63]. Indeed, the SPT relevant to LSM constraints can be constructed by putting copies of (1 + 1)-d  $G_{\text{int}}$  SPTs at various IWP of the wallpaper group  $G_s$ . Combining these two observations together, we conclude that in Eq. (2.19) only the factor with  $i = 2$  can possibly be related to LSM constraints, because only that factor can possibly be related to putting (1 + 1)-d  $G_{\text{int}}$  SPTs at various positions, while other factors involve SPTs living in the wrong dimension (e.g., the  $i = 1$  term means that some (2 + 1)-d  $G_{\text{int}}$  SPT is decorated into the system in some way). Moreover, for a

---

<sup>6</sup>Since the (3 + 1)-d  $G_s \times G_{\text{int}}$  SPT is captured by an element in  $H^4(G_s \times G_{\text{int}}, \text{U}(1)_\rho)$ , one may attempt to show the validity of Eq. (2.1) by combining the Kunneth decomposition  $H^4(G_s \times G_{\text{int}}, \text{U}(1)_\rho) \cong \bigoplus_{i=0}^4 H^i(G_s, H^{4-i}(G_{\text{int}}, \text{U}(1)_\rho))$  and the fact that the relevant (1 + 1)-d  $G_{\text{int}}$  SPT is captured by  $H^2(G_{\text{int}}, \text{U}(1)_\rho)$ , which suggests that in the Kunneth decomposition only the term  $H^2(G_s, H^2(G_{\text{int}}, \text{U}(1)_\rho))$  is relevant to the LSM constraints. Although intuitively appealing, this argument is flawed, because there is generically no unambiguous way to determine whether an element in  $H^4(G_s \times G_{\text{int}}, \text{U}(1)_\rho)$  is in  $H^2(G_s, H^2(G_{\text{int}}, \text{U}(1)_\rho))$ . Our argument below does not suffer from this ambiguity. Furthermore, even if we know that the relevant cocycle is in  $H^2(G_s, H^2(G_{\text{int}}, \text{U}(1)_\rho))$ , it requires an explanation why its representative cochain can necessarily be written as Eq. (2.1).

given PR type of the system,  $e^{i\pi\eta_2(a_3,a_4)}$  should be the cocycle corresponding to the  $(1+1)$ -d  $G_{int}$  SPT whose boundary hosts this particular PR.

Therefore, the cocycle related to LSM constraints can always be written in a form given by Eq. (2.1), and  $\lambda(l_1, l_2)$ , which is written as  $\lambda_2(l_1, l_2)$  in Eq. (2.19), can be viewed as a representative cochain in  $H^2(G_s, \mathbb{Z}_2)$ . Furthermore, according to the lattice homotopy picture,  $\lambda$  or  $\lambda_2$  should just encode the information of which IWP host  $(1+1)$ -d  $G_{int}$  SPTs, so it should be completely determined by  $G_s$  and the lattice homotopy class corresponding to each LSM constraint, and be the same for all  $G_{int}$  and all PR types of the system.

We remark that the above argument does not show that all cocycles in the form of Eq. (2.1) must be related to LSM constraints. In fact, in Sec. 2.2 we have found that some of them are not. Those SPTs can be constructed by inserting a  $(2+1)$ -d  $Z_2 \times G_{int}$  SPT on the mirror plane, such that the  $Z_2$  domain wall is decorated with a  $(1+1)$ -d  $G_{int}$  SPT. See Appendix 2.C for more detail.

We also remark that although we have assumed that the projective representations of  $G_{int}$  are  $\mathbb{Z}_2^k$ -classified with  $k$  some integer in the above argument, we expect that the topological partition functions corresponding to LSM constraints can always be written in a form similar to Eq. (2.1), for any  $G_{int}$ . Specially, if a PR type of  $G_{int}$  has order  $n$ , then the LSM-related cocycle takes the form

$$\Omega(g_1, g_2, g_3, g_4) = e^{i\frac{2\pi}{n}\lambda(l_1,l_2)\eta(a_3,a_4)} \quad (2.20)$$

where  $\lambda$  and  $\eta$  take integral values, and  $e^{\frac{2\pi i}{n}\eta(a_3,a_4)}$  is the cocycle corresponding to the relevant  $(1+1)$ -d  $G_{int}$  SPT. Moreover, this statement, including its special form Eq. (2.1), has been derived in the special cases where  $G_s$  contains only translation or only point group, using equivariant homology [40], and we expect that the method in Ref. [40] can be generalized to an arbitrary lattice symmetry group  $G_s$ . A systematic proof of this statement is beyond the scope of this thesis and we leave it for future work.

## 2.B Fractionalization pattern involving both translation and glide symmetries

Among all 17 wallpaper groups, there is only one group,  $pg$ , in which the fractionalization pattern has to be specified in a way that necessarily invokes the glide symmetry. In this appendix, we present its corresponding physical picture.

The group  $pg$  is generated by  $T_1$  and  $G$ , a translation and a glide reflection. The translation vector of  $T_1$  is flipped under  $G$ , and  $G^2$  is another translation along a direction perpendicular to the translation vector of  $T_1$ . These generators satisfy  $G^{-1}T_1GT_1 = 1$ .

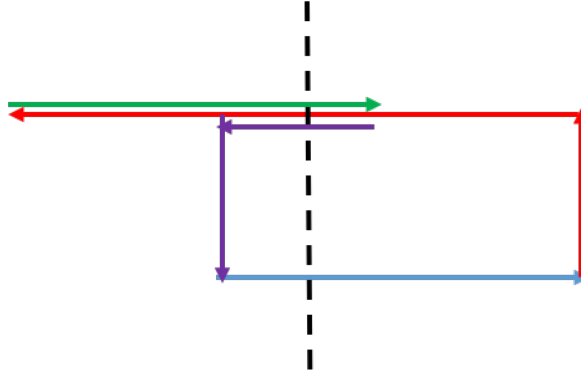


Figure 2.3: Acting  $G^{-1}T_1GT_1$  on an  $SO(3)$  monopole. The first  $T_1$  action is marked in blue, the following  $G$  action is marked in red, the next  $T_1$  action is marked in green, and the last  $G^{-1}$  action is marked in purple. The dashed line is the reflection axis of  $G$ . This figure shows that the operation  $G^{-1}T_1GT_1$  moves an  $SO(3)$  monopole along a trajectory that encloses a fundamental domain.

Consider the case where  $G_{int} = SO(3)$ . Just as in the main text, we gauge the  $SO(3)$  symmetry and examine the fractionalization pattern of  $pg$  on the  $SO(3)$  monopole by applying the operation  $G^{-1}T_1GT_1$  to an  $SO(3)$  monopole, which moves the monopole around the fundamental domain (see Fig. 2.3). If the fundamental domain contains an odd (even) number of Haldane chains, this process results in a  $-1$  ( $1$ ) phase factor, which is a signature of nontrivial (trivial) symmetry fractionalization pattern of the  $pg$  symmetry carried by the  $SO(3)$  monopole. Because  $H^2(pg, \mathbb{Z}_2) = \mathbb{Z}_2$ , there is only one nontrivial symmetry fractionalization pattern. A topological invariant detecting the nontrivial element in  $H^2(pg, \mathbb{Z}_2)$  is given in Eq. (2.118), so this must be the topological invariant that diagnoses the fractionalization pattern of the  $pg$  symmetry on an  $SO(3)$  monopole.

## 2.C Non-LSM fractionalization patterns

In this appendix, we discuss in more detail the  $M \times SO(3)$  SPT corresponding to  $\alpha_{\text{non-LSM}} = \frac{\omega(M,M)}{\omega(1,1)} = -1$ , which has TPF  $\exp(i\pi \int (w_1^{TM})^2 w_2^{SO(3)})$ . In particular, we will show that this SPT can be constructed by inserting into the mirror plane of  $M$  a  $(2+1)$ -d  $\mathbb{Z}_2 \times SO(3)$



SPT, whose  $\mathbb{Z}_2$  domain walls are decorated with Haldane chains. Moreover, we will show that for any  $G_{int}$  with  $\mathbb{Z}_2^k$ -classified PR, the  $(3+1)$ -d  $M \times G_{int}$  SPTs with  $\alpha_{\text{non-LSM}} = -1$  can always be constructed by inserting into the mirror plane of  $M$  a  $(2+1)$ -d  $\mathbb{Z}_2 \times G_{int}$  SPT, whose  $\mathbb{Z}_2$  domain walls are decorated with the relevant nontrivial  $(1+1)$ -d  $G_{int}$  SPT.

Focusing on the case with  $G_{int} = SO(3)$ , let us enumerate all  $(3+1)$ -d  $M \times SO(3)$  SPTs. According to the crystalline equivalence principle [53], the classification of these SPTs is the same as the classification of  $(3+1)$ -d  $\mathbb{Z}_2^T \times SO(3)$  SPTs, where  $\mathbb{Z}_2^T$  is a time reversal symmetry. It is known that the latter are classified by  $\mathbb{Z}_2^4$  (e.g., see Appendix F of Ref. [56] for the descriptions of the physical properties of these SPTs). So  $(3+1)$ -d  $M \times SO(3)$  SPTs are  $\mathbb{Z}_2^4$ -classified. According to Ref. [64], these SPTs can all be constructed by putting on the mirror plane of  $M$  some  $(2+1)$ -d invertible states that have at most a  $\mathbb{Z}_2 \times SO(3)$  symmetry (note that this  $\mathbb{Z}_2$  symmetry does not reverse the spacetime orientation). The  $(2+1)$ -d  $\mathbb{Z}_2 \times SO(3)$  SPTs are classified by  $H^3(\mathbb{Z}_2 \times SO(3), U(1)) = \mathbb{Z}_2 \times \mathbb{Z} \times \mathbb{Z}_2$ , where the Kunneth formula is used in calculating this classification. It is easy to read off the physical meaning of the root states of these  $(2+1)$ -d SPTs: one  $\mathbb{Z}_2$  factor represents SPTs protected purely by the  $\mathbb{Z}_2$  symmetry, the  $\mathbb{Z}$  factor represents spin quantum Hall states [65], which are SPTs protected purely by the  $SO(3)$  symmetry and has a TPF given by  $SO(3)$  Chern-Simons theories, and the other  $\mathbb{Z}_2$  factor must represent an SPT protected by both  $\mathbb{Z}_2$  and  $SO(3)$ . The decorated-domain-wall method [66] allows us to construct the SPT by decorating the  $\mathbb{Z}_2$  domain walls with a Haldane chain.

All the  $(2+1)$ -d  $\mathbb{Z}_2 \times SO(3)$  SPTs can be inserted into the mirror plane of  $M$  to construct a  $(3+1)$ -d  $M \times SO(3)$  SPT, and one can also insert an  $E_8$  state to the mirror plane. In total, these give the  $\mathbb{Z}_2^4$  classification of  $(3+1)$ -d  $M \times SO(3)$  SPTs. Note inserting a  $\mathbb{Z}_2$  SPT or an  $E_8$  state to the mirror plane results in a  $(3+1)$ -d SPT protected by  $M$  only, so these states will not have a TPF  $\exp(i\pi \int (w_1^{TM})^2 w_2^{SO(3)})$ , which shows that this SPT requires both  $M$  and  $SO(3)$  for protection. Now we are only left with the cases where the bosonic spin quantum Hall state and/or the state constructed from decorated domain wall is inserted into the mirror plane. To understand the physical properties of these states, we can refer to the corresponding  $(3+1)$ -d  $\mathbb{Z}_2^T \times SO(3)$  SPTs. If a spin quantum Hall state is decorated into the time reversal domain wall, the resulting state will have fermionic  $SO(3)$  monopoles. Using the correspondence between  $\mathbb{Z}_2^T \times SO(3)$  SPTs and  $M \times SO(3)$  SPTs, this indicates that if the spin quantum Hall state is inserted into the mirror plane, the  $SO(3)$  monopole will also be fermionic. However, the TPF  $\exp(i\pi \int (w_1^{TM})^2 w_2^{SO(3)})$  means that the  $SO(3)$  monopole is a boson (but carries nontrivial fractionalization pattern of the  $M$  symmetry). This means that the  $(3+1)$ -d SPT of interest must be obtained from inserting to the mirror plane the  $(2+1)$ -d SPT constructed from decorated domain wall.

In fact, one can explicitly demonstrate that a  $(3+1)$ -d  $M \times SO(3)$  SPT constructed

in this way indeed has an  $SO(3)$  monopole carrying the nontrivial fractionalization pattern of the  $M$  symmetry. To this end, it suffices to show a simpler version of this statement: suppose we break the  $SO(3)$  symmetry in this SPT to  $U(1)$ , the  $U(1)$  monopole in the resulting state will carry the nontrivial fractionalization pattern of  $M$ . This statement can be explicitly shown using the method in Ref. [57] (see Appendix B therein). This also means that upon this symmetry breaking, the resulting  $M \times U(1)$  symmetric state is a nontrivial SPT. According to the general discussion in Sec. 2.2, this implies that  $\alpha_{\text{non-LSM}}$  is unrelated to LSM constraints of interest.

The above discussion concerns about the case where  $G_{\text{int}} = SO(3)$ . Now we argue that for any  $G_{\text{int}}$  with  $\mathbb{Z}_2^k$ -classified PR,  $\alpha_{\text{non-LSM}}$  can be triggered in a  $(3+1)$ -d  $M \times G_{\text{int}}$  SPT constructed in a way similar to the above, and all we need to modify is to replace the Haldane chain decorated into the  $\mathbb{Z}_2$  domain wall by a  $(1+1)$ -d  $G_{\text{int}}$  SPT. To this end, it suffices to show that the TPF of this  $(3+1)$ -d  $M \times G_{\text{int}}$  SPT is  $e^{i\pi \int (w_1^{TM})^2 \eta}$ , where  $\eta \in H^2(G_{\text{int}}, \mathbb{Z}_2)$  and  $e^{i\pi \int \eta}$  is the TPF of the  $(1+1)$ -d  $G_{\text{int}}$  SPT. This can be shown by noting i) this SPT is its own inverse, and ii) this construction works for all such  $G_{\text{int}}$ . Then an argument very similar to that in Appendix 2.A suggests that the TPF of this SPT can indeed be written as  $e^{i\pi \int (w_1^{TM})^2 \eta}$ .

## 2.D Group Cohomology and $\mathbb{Z}_2$ Cohomology ring of wallpaper groups

In this appendix, we list the  $\mathbb{Z}_2$  cohomology rings of all 17 wallpaper groups. The calculation is done with the help of spectral sequence. See Appendix A.3 for some brief mathematical introduction of the relevant concepts, and Refs. [67–69] for more details. It turns out that for all wallpaper groups  $G_s$  except  $p4g$ , the cohomology ring can be written as

$$H^*(G_s, \mathbb{Z}_2) = \mathbb{Z}_2[A_\bullet, \dots, B_\bullet, \dots]/\text{relations} \quad (2.21)$$

with  $A_\bullet$  and  $B_\bullet$  the generators belonging to  $H^1(G_s, \mathbb{Z}_2)$  and  $H^2(G_s, \mathbb{Z}_2)$ , respectively. Subscripts “ $\bullet$ ” are the names of generators which differ for different  $G_s$ , and their meanings will often be clear in the context. As a result, all elements of the cohomology ring  $H^*(G_s, \mathbb{Z}_2)$  can be written as cup product of the generators  $A_\bullet$  and  $B_\bullet$ , but there are some relations that dictate that certain sums of cup products actually yield a trivial cohomology element. We will present all elements of  $H^1(G_s, \mathbb{Z}_2)$  and  $H^2(G_s, \mathbb{Z}_2)$  together with their representative cochains, as well as the complete set of the relations. This encodes the full information

of the cohomology ring  $H^*(G_s, \mathbb{Z}_2)$ . The situation for  $p4g$  is similar, but we need an extra degree-3 generator  $C \in H^3(p4g, \mathbb{Z}_2)$ , which, together with the generators in  $H^1(p4g, \mathbb{Z}_2)$  and  $H^2(p4g, \mathbb{Z}_2)$ , forms a complete set of generators of  $H^*(p4g, \mathbb{Z}_2)$ .

For later usage, we define a set of functions that take integers as their arguments:

$$P(x) = \begin{cases} 1, & x \text{ is odd} \\ 0, & x \text{ is even} \end{cases}, \quad P_c(x) = 1 - P(x), \quad Q(x) = (-1)^x, \quad (2.22)$$

$$[x]_a = \{y = x \pmod{a} | 0 \leq y < a\}, \quad P_{ab}(x) = \begin{cases} 1, & x = b \pmod{a} \\ 0, & \text{otherwise} \end{cases}$$

- Wallpaper group 1:  $p1$

This group is generated by  $T_1$  and  $T_2$ , two independent translations which are commutative,

$$T_1 T_2 = T_2 T_1. \quad (2.23)$$

An arbitrary group element in  $p1$  can be written as  $g = T_1^x T_2^y$ , with  $x, y \in \mathbb{Z}$ . For  $g_1 = T_1^{x_1} T_2^{y_1}$  and  $g_2 = T_1^{x_2} T_2^{y_2}$ , the group multiplication rule gives

$$g_1 g_2 = T_1^{x_1+x_2} T_2^{y_1+y_2}. \quad (2.24)$$

The  $\mathbb{Z}_2$  cohomology ring of  $p1$  is

$$\mathbb{Z}_2[A_x, A_y] / (A_x^2 = 0, A_y^2 = 0). \quad (2.25)$$

Here  $H^1(p1, \mathbb{Z}_2) = \mathbb{Z}_2^2$ , with generators  $\xi_1 = A_x$ ,  $\xi_2 = A_y$ , which have representative cochains,

$$\xi_1(g) = x, \quad \xi_2(g) = y. \quad (2.26)$$

$H^2(p1, \mathbb{Z}_2) = \mathbb{Z}_2$ , with generators  $\lambda_1 = A_x A_y$ , which have representative cochains,

$$\lambda_1(g_1, g_2) = y_1 x_2 \quad (2.27)$$

Indeed  $\lambda_1$  generates the LSM constraint.

- Wallpaper group 2:  $p2$

This group is generated by  $T_1$ ,  $T_2$  and  $C_2$ , two independent translations and a  $C_2$  rotational symmetry, with the following relations among generators

$$C_2^2 = 1, \quad C_2 T_1 C_2 = T_1^{-1}, \quad C_2 T_2 C_2 = T_2^{-1}, \quad T_1 T_2 = T_2 T_1. \quad (2.28)$$

An arbitrary group element in  $p2$  can be written as  $g = T_1^x T_2^y C_2^c$ , with  $x, y \in \mathbb{Z}$  and  $c \in \{0, 1\}$ . For  $g_1 = T_1^{x_1} T_2^{y_1} C_2^{c_1}$  and  $g_2 = T_1^{x_2} T_2^{y_2} C_2^{c_2}$ , the group multiplication rule gives

$$g_1 g_2 = T_1^{x_1+Q(c_1)x_2} T_2^{y_1+Q(c_1)y_2} C_2^{P(c_1+c_2)}. \quad (2.29)$$

The  $\mathbb{Z}_2$  cohomology ring of  $p2$  is

$$\mathbb{Z}_2[A_x, A_y, A_c]/(A_x^2 = A_x A_c, A_y^2 = A_y A_c) \quad (2.30)$$

Here  $H^1(p2, \mathbb{Z}_2) = \mathbb{Z}_2^3$ , with generators  $\xi_1 = A_x$ ,  $\xi_2 = A_y$ ,  $\xi_3 = A_c$ , which have representative cochains,

$$\xi_1(g) = x, \quad \xi_2(g) = y, \quad \xi_3(g) = c. \quad (2.31)$$

$H^2(p2, \mathbb{Z}_2) = \mathbb{Z}_2^4$ , with generators  $\lambda_1 = (A_x + A_c)(A_y + A_c)$ ,  $\lambda_2 = A_x(A_y + A_c)$ ,  $\lambda_3 = (A_x + A_c)A_y$ ,  $\lambda_4 = A_x A_y$ , which have representative cochains,

$$\begin{aligned} \lambda_1(g_1, g_2) &= y_1 x_2 + c_1(x_2 + y_2 + c_2) \\ \lambda_2(g_1, g_2) &= (y_1 + c_1)x_2 \\ \lambda_3(g_1, g_2) &= y_1 x_2 + c_1 y_2 \\ \lambda_4(g_1, g_2) &= y_1 x_2 \end{aligned} \quad (2.32)$$

The generators are chosen so that they have a 1-1 correspondence with topological invariants presented in Appendix 2.E. There we will also see that all of them,  $\lambda_1, \lambda_2, \lambda_3, \lambda_4$ , generate LSM constraints.

- Wallpaper group 3:  $pm$

This group is generated by  $T_1$ ,  $T_2$  and  $M$ , where  $T_1$  and  $T_2$  are translations with perpendicular translation vectors, and  $M$  is a mirror symmetry such that

$$M^2 = 1, \quad MT_1 M = T_1^{-1}, \quad MT_2 M = T_2, \quad T_1 T_2 = T_2 T_1. \quad (2.33)$$

An arbitrary element in  $pm$  can be written as  $g = T_1^x T_2^y M^m$ , with  $x, y \in \mathbb{Z}$  and  $m \in \{0, 1\}$ . For  $g_1 = T_1^{x_1} T_2^{y_1} M^{m_1}$  and  $g_2 = T_1^{x_2} T_2^{y_2} M^{m_2}$ , the group multiplication rule gives

$$g_1 g_2 = T_1^{x_1+Q(m_1)x_2} T_2^{y_1+y_2} M^{P(m_1+m_2)}. \quad (2.34)$$

The  $\mathbb{Z}_2$  cohomology ring of  $pm$  is

$$\mathbb{Z}_2[A_x, A_y, A_m]/(A_x^2 = A_x A_m, A_y^2 = 0) \quad (2.35)$$

Here  $H^1(pm, \mathbb{Z}_2) = \mathbb{Z}_2^3$ , with generators  $\xi_1 = A_x$ ,  $\xi_2 = A_y$ ,  $\xi_3 = A_m$ , which have representative cochains,

$$\xi_1(g) = x, \quad \xi_2(g) = y, \quad \xi_3(g) = m. \quad (2.36)$$

$H^2(pm, \mathbb{Z}_2) = \mathbb{Z}_2^4$ , with generators  $\lambda_1 = (A_x + A_m)A_y$ ,  $\lambda_2 = A_x A_y$ ,  $\lambda_3 = (A_x + A_m)A_m$ ,  $\lambda_4 = A_x A_m$ , which have representative cochains,

$$\begin{aligned} \lambda_1(g_1, g_2) &= y_1 x_2 + m_1 y_2 \\ \lambda_2(g_1, g_2) &= y_1 x_2 \\ \lambda_3(g_1, g_2) &= m_1(x_2 + m_2) \\ \lambda_4(g_1, g_2) &= m_1 x_2 \end{aligned} \quad (2.37)$$

In Appendix 2.E, we will see that  $\lambda_1, \lambda_2$  generate LSM constraints, while  $\lambda_3, \lambda_4$  correspond to non-LSM fractionalization patterns.

- Wallpaper group 4:  $pg$

This group is generated by  $T_1$  and  $G$ , where  $T_1$  is a translation and  $G$  is a glide reflection, such that

$$G^{-1}T_1G = T_1^{-1}. \quad (2.38)$$

Note that  $G^2$  is a translation along the direction perpendicular to the translation vector of  $T_1$ . An arbitrary element in  $pg$  can be written as  $g = T_1^x G^s$ , with  $x, s \in \mathbb{Z}$ . For  $g_1 = T_1^{x_1} G^{s_1}$  and  $g_2 = T_1^{x_2} G^{s_2}$ , the group multiplication rule gives

$$g_1 g_2 = T_1^{x_1 + Q(s_1)x_2} G^{s_1 + s_2}. \quad (2.39)$$

The  $\mathbb{Z}_2$  cohomology ring of  $pg$  is

$$\mathbb{Z}_2[A_x, A_s]/(A_x^2 = A_x A_s, A_s^2 = 0) \quad (2.40)$$

Here  $H^1(pg, \mathbb{Z}_2) = \mathbb{Z}_2^2$ , with generators  $\xi_1 = A_x$ ,  $\xi_2 = A_s$ , which have representative cochains,

$$\xi_1(g) = x, \quad \xi_2(g) = s. \quad (2.41)$$

$H^2(pg, \mathbb{Z}_2) = \mathbb{Z}_2$ , with generators  $\lambda_1 = A_x A_s$ , which have representative cochains,

$$\lambda_1(g_1, g_2) = s_1 x_2 \quad (2.42)$$

In Appendix 2.E, we will see that  $\lambda_1$  generates LSM constraints.

- Wallpaper group 5:  $cm$

This group is generated by  $T_1, T_2$  and  $M$ , two independent translations and a mirror symmetry whose mirror axis bisects the translation vectors of  $T_1$  and  $T_2$ . They satisfy

$$M^2 = 1, \quad MT_1M = T_2, \quad MT_2M = T_1, \quad T_1T_2 = T_2T_1. \quad (2.43)$$

An arbitrary element of  $cm$  can be written as  $g = T_1^x T_2^y M^m$ , with  $x, y \in \mathbb{Z}$  and  $m \in \{0, 1\}$ . For  $g_1 = T_1^{x_1} T_2^{y_1} M^{m_1}$  and  $g_2 = T_1^{x_2} T_2^{y_2} M^{m_2}$ , the group multiplication rule gives

$$g_1 g_2 = T_1^{x_1 + P_c(m_1)x_2 + P(m_1)y_2} T_2^{y_1 + P_c(m_1)y_2 + P(m_1)x_2} M^{P(m_1 + m_2)}. \quad (2.44)$$

The  $\mathbb{Z}_2$  cohomology ring of  $cm$  is

$$\mathbb{Z}_2[A_{x+y}, A_m, B_{xy}] / (A_{x+y}^2 = 0, A_{x+y}A_m = 0, B_{xy}A_{x+y} = 0, B_{xy}^2 = 0) \quad (2.45)$$

Here  $H^1(cm, \mathbb{Z}_2) = \mathbb{Z}_2^2$ , with two generators  $\xi_1 = A_{x+y}$ ,  $\xi_2 = A_m$ , which have representative cochains

$$\xi_1(g) = x + y, \quad \xi_2(g) = m. \quad (2.46)$$

$H^2(cm, \mathbb{Z}_2) = \mathbb{Z}_2^2$ , with generators  $\lambda_1 = B_{xy}$ ,  $\lambda_2 = A_m^2$ , which have representative cochains

$$\begin{aligned} \lambda_1(g_1, g_2) &= P_c(m_1)y_1x_2 + P(m_1)y_2(x_2 + y_1) \\ \lambda_2(g_1, g_2) &= m_1m_2 \end{aligned} \quad (2.47)$$

In Appendix 2.E, we will see that  $\lambda_1$  generates LSM constraints, while  $\lambda_2$  corresponds to non-LSM fractionalization patterns.

- Wallpaper group 6:  $pmm$

This group is generated by  $T_1, T_2, C_2$  and  $M$ , two translations with perpendicular translation vectors, a  $C_2$  rotation and a mirror symmetry such that

$$\begin{aligned} M^2 &= 1, & MC_2M &= C_2, & MT_1M &= T_1^{-1}, & MT_2M &= T_2 \\ C_2^2 &= 1, & C_2T_1C_2 &= T_1^{-1}, & C_2T_2C_2 &= T_2^{-1}, & T_1T_2 &= T_2T_1. \end{aligned} \quad (2.48)$$

Note that  $C_2M$  is another mirror symmetry that flips the translation vector of  $T_2$ . An arbitrary element in  $pmm$  can be written as  $g = T_1^x T_2^y C_2^c M^m$ , with  $x, y \in \mathbb{Z}$

and  $c, m \in \{0, 1\}$ . For  $g_1 = T_1^{x_1} T_2^{y_1} C_2^{c_2} M^{m_1}$  and  $g_2 = T_1^{x_2} T_2^{y_2} C_2^{c_2} M^{m_2}$ , the group multiplication rule gives

$$g_1 g_2 = T_1^{x_1+Q(c_1+m_1)x_2} T_2^{y_1+Q(c_1)y_2} C_2^{P(c_1+c_2)} M^{P(m_1+m_2)}. \quad (2.49)$$

The  $\mathbb{Z}_2$  cohomology ring of  $pmm$  is

$$\mathbb{Z}_2[A_x, A_y, A_c, A_m]/(A_x^2 = A_x(A_m + A_c), A_y^2 = A_y A_c) \quad (2.50)$$

Here  $H^1(pmm, \mathbb{Z}_2) = \mathbb{Z}_2^4$ , with generators  $\xi_1 = A_x$ ,  $\xi_2 = A_y$ ,  $\xi_3 = A_c$ ,  $\xi_4 = A_m$ , which have representative cochains,

$$\xi_1(g) = x, \quad \xi_2(g) = y, \quad \xi_3(g) = c, \quad \xi_4(g) = m. \quad (2.51)$$

$H^2(pmm, \mathbb{Z}_2) = \mathbb{Z}_2^8$ , with generators  $\lambda_1 = (A_x + A_c + A_m)(A_y + A_c)$ ,  $\lambda_2 = A_x A_y$ ,  $\lambda_3 = A_x(A_y + A_c)$ ,  $\lambda_4 = (A_x + A_c + A_m)A_y$ ,  $\lambda_5 = (A_x + A_c + A_m)A_m$ ,  $\lambda_6 = (A_y + A_c)A_m$ ,  $\lambda_7 = A_x A_m$ ,  $\lambda_8 = A_y A_m$ , which have representative cochains,

$$\begin{aligned} \lambda_1(g_1, g_2) &= (y_1 + c_1)x_2 + (c_1 + m_1)(y_2 + c_2) \\ \lambda_2(g_1, g_2) &= y_1 x_2 \\ \lambda_3(g_1, g_2) &= (y_1 + c_1)x_2 \\ \lambda_4(g_1, g_2) &= y_1 x_2 + (c_1 + m_1)y_2 \\ \lambda_5(g_1, g_2) &= m_1(x_2 + c_2 + m_2) \\ \lambda_6(g_1, g_2) &= m_1(y_2 + c_2) \\ \lambda_7(g_1, g_2) &= m_1 x_2 \\ \lambda_8(g_1, g_2) &= m_1 y_2 \end{aligned} \quad (2.52)$$

In Appendix 2.E, we will see that  $\lambda_1, \lambda_2, \lambda_3, \lambda_4$  generate LSM constraints, while  $\lambda_5, \lambda_6, \lambda_7, \lambda_8$  correspond to non-LSM fractionalization patterns.

- Wallpaper group 7:  $pmg$

This group is generated by  $T_1, T_2, C_2$  and  $M$ , two translations with perpendicular translation vectors, a 2-fold rotation and a mirror symmetry with mirror axis parallel to the translation vector of  $T_2$ , and displaced from the  $C_2$  rotation center by a quarter of the unit translation vector of  $T_1$ . They satisfy

$$\begin{aligned} M^2 &= 1, & MC_2M &= T_1C_2, & MT_1M &= T_1^{-1}, & MT_2M &= T_2, \\ C_2^2 &= 1, & C_2T_1C_2 &= T_1^{-1}, & C_2T_2C_2 &= T_2^{-1}, & T_1T_2 &= T_2T_1. \end{aligned} \quad (2.53)$$

An arbitrary element in  $pmg$  can be written as  $g = T_1^x T_2^y C_2^c M^m$ , with  $x, y \in \mathbb{Z}$  and  $c, m \in \{0, 1\}$ . For  $g_1 = T_1^{x_1} T_2^{y_1} C_2^{c_1} M^{m_1}$  and  $g_2 = T_1^{x_2} T_2^{y_2} C_2^{c_2} M^{m_2}$ , the group multiplication rule gives

$$g_1 g_2 = T_1^{x_1+Q(c_1+m_1)x_2+Q(c_1)c_2m_1} T_2^{y_1+Q(c_1)y_2} C_2^{P(c_1+c_2)} M^{P(m_1+m_2)}. \quad (2.54)$$

The  $\mathbb{Z}_2$  cohomology ring of  $pmg$  is

$$\mathbb{Z}_2[A_y, A_c, A_m]/(A_y^2 = A_c A_y, A_c A_m = 0) \quad (2.55)$$

Here  $H^1(pmg, \mathbb{Z}_2) = \mathbb{Z}_2^3$ , with generators  $\xi_1 = A_y$ ,  $\xi_2 = A_c$ ,  $\xi_3 = A_m$ , which have representative cochains,

$$\xi_1(g) = y, \quad \xi_2(g) = c, \quad \xi_3(g) = m. \quad (2.56)$$

$H^2(pmg, \mathbb{Z}_2) = \mathbb{Z}_2^4$ , with generators  $\lambda_1 = A_c(A_y + A_c)$ ,  $\lambda_2 = A_c A_y$ ,  $\lambda_3 = A_y A_m$ ,  $\lambda_4 = A_m^2$ , which have representative cochains,

$$\begin{aligned} \lambda_1(g_1, g_2) &= c_1(y_2 + c_2) \\ \lambda_2(g_1, g_2) &= c_1 y_2 \\ \lambda_3(g_1, g_2) &= m_1 y_2 \\ \lambda_4(g_1, g_2) &= m_1 m_2 \end{aligned} \quad (2.57)$$

In Appendix 2.E, we will see that  $\lambda_1, \lambda_2$  generate LSM constraints, while  $\lambda_3, \lambda_4$  correspond to non-LSM fractionalization patterns.

- Wallpaper group 8:  $pgg$

This group is generated by  $T_1, T_2, C_2$  and  $G_1$ , two translations with perpendicular translation vectors, a  $C_2$  rotation, and a glide reflection whose reflection axis is parallel to the translation vector of  $T_2$ , and displaced from the  $C_2$  center by a quarter of the unit translation vector of  $T_1$ . They satisfy

$$C_2^2 = 1, \quad G_1 C_2 G_1^{-1} = T_1 T_2 C_2, \quad C_2 T_1 C_2 = T_1^{-1}, \quad G_1 T_1 G_1^{-1} = T_1^{-1}, \quad G_1^2 = T_2. \quad (2.58)$$

An arbitrary element in  $pgg$  can be written as  $g = T_1^x T_2^y C_2^c G_1^s$ , with  $x, y \in \mathbb{Z}$  and  $c, s \in \{0, 1\}$ . For  $g_1 = T_1^{x_1} T_2^{y_1} C_2^{c_1} G_1^{s_1}$  and  $g_2 = T_1^{x_2} T_2^{y_2} C_2^{c_2} G_1^{s_2}$ , the group multiplication rule gives

$$g_1 g_2 = T_1^{x_1+Q(c_1+s_1)x_2+Q(c_1)c_2s_1} T_2^{y_1+Q(c_1)y_2+Q(c_1)c_2s_1+Q(c_1+c_2)s_1s_2} C_2^{P(c_1+c_2)} G_1^{P(s_1+s_2)} \quad (2.59)$$



The  $\mathbb{Z}_2$  cohomology ring of  $pgg$  is

$$\mathbb{Z}_2[A_c, A_s, B_{c(x+y)}]/(A_s^2 = 0, A_s A_c = 0, A_s B_{c(x+y)} = 0, B_{c(x+y)}^2 = A_c^2 B_{c(x+y)}) \quad (2.60)$$

Here  $H^1(pgg, \mathbb{Z}_2) = \mathbb{Z}_2^2$ , with generators  $\xi_1 = A_c$ ,  $\xi_2 = A_s$ , which have representative cochains,

$$\xi_1(g) = c, \quad \xi_2(g) = s. \quad (2.61)$$

$H^2(pgg, \mathbb{Z}_2) = \mathbb{Z}_2^2$ , with generators  $\lambda_1 = B_{c(x+y)} + A_c^2$ ,  $\omega_2 = B_{c(x+y)}$ , which have representative cochains,

$$\begin{aligned} \lambda_1(g_1, g_2) &= c_1(x_2 + y_2 + c_2) + (c_1 + c_2)s_1 s_2 + s_1 x_2 \\ \lambda_2(g_1, g_2) &= c_1(x_2 + y_2) + (c_1 + c_2)s_1 s_2 + s_1 x_2 \end{aligned} \quad (2.62)$$

In Appendix 2.E, we will see that  $\lambda_1, \lambda_2$  generate LSM constraints.

- Wallpaper group 9:  $cm$

This group is generated by  $T_1, T_2, C_2$  and  $M$ , two translations with translation vectors not perpendicular to each other, a  $C_2$  rotation, and a mirror symmetry whose mirror axis bisects the translation vectors of  $T_1$  and  $T_2$ . They satisfy

$$\begin{aligned} M^2 &= 1, & MC_2M &= C_2, & MT_1M &= T_2, & MT_2M &= T_1, \\ C_2^2 &= 1, & C_2T_1C_2 &= T_1^{-1}, & C_2T_2C_2 &= T_2^{-1}, & T_1T_2 &= T_2T_1. \end{aligned} \quad (2.63)$$

Note that  $C_2M$  is another mirror symmetry whose mirror axis bisects the translation vectors of  $T_1$  and  $T_2^{-1}$ . An arbitrary element in  $cm$  can be written as  $g = T_1^x T_2^y C_2^c M^m$ , with  $x, y \in \mathbb{Z}$  and  $c, m \in \{0, 1\}$ . For  $g_1 = T_1^{x_1} T_2^{y_1} C_2^{c_1} M^{m_1}$  and  $g_2 = T_1^{x_2} T_2^{y_2} C_2^{c_2} M^{m_2}$ , the group multiplication rule gives

$$g_1 g_2 = T_1^{x_1 + Q(c_1)X} T_2^{y_1 + Q(c_1)Y} C_2^{P(c_1 + c_2)} M^{P(m_1 + m_2)}, \quad (2.64)$$

where  $X$  and  $Y$  are defined as

$$\begin{aligned} X &= P_c(m_1)x_2 + P(m_1)y_2, \\ Y &= P_c(m_1)y_2 + P(m_1)x_2. \end{aligned} \quad (2.65)$$

The  $\mathbb{Z}_2$  cohomology ring of  $cm$  is

$$\mathbb{Z}_2[A_{x+y}, A_c, A_m, B_{xy}]/(A_{x+y}^2 = A_c A_{x+y}, A_{x+y} A_m = 0, B_{xy} A_{x+y} = 0, B_{xy}^2 = (A_c^2 + A_c A_m) B_{xy}) \quad (2.66)$$

Here  $H^1(cmm, \mathbb{Z}_2) = \mathbb{Z}_2^3$ , with generators  $\xi_1 = A_{x+y}$ ,  $\xi_2 = A_c$ ,  $\xi_3 = A_m$ , which have representative cochains,

$$\xi_1(g) = x + y, \quad \xi_2(g) = c, \quad \xi_3(g) = m. \quad (2.67)$$

$H^2(cmm, \mathbb{Z}_2) = \mathbb{Z}_2^5$ , with generators  $\lambda_1 = B_{xy} + A_c A_{x+y} + A_c^2 + A_m A_c$ ,  $\lambda_2 = B_{xy}$ ,  $\lambda_3 = A_c A_{x+y}$ ,  $\lambda_4 = (A_c + A_m)A_m$ ,  $\lambda_5 = A_c A_m$ , which have representative cochains,

$$\begin{aligned} \lambda_1(g_1, g_2) &= P_c(m_1)y_1x_2 + P(m_1)y_2(x_2 + y_1) + c_1(x_2 + y_2 + c_2 + m_2) \\ \lambda_2(g_1, g_2) &= P_c(m_1)y_1x_2 + P(m_1)y_2(x_2 + y_1) \\ \lambda_3(g_1, g_2) &= c_1(x_2 + y_2) \\ \lambda_4(g_1, g_2) &= m_1(c_2 + m_2) \\ \lambda_5(g_1, g_2) &= m_1c_2 \end{aligned} \quad (2.68)$$

In Appendix 2.E, we will that  $\lambda_1, \lambda_2, \lambda_3$  generate LSM constraints, while  $\lambda_4, \lambda_5$  correspond to non-LSM fractionalization pattern.

- Wallpaper group 10:  $p4$

This group is generated by  $T_1, T_2$  and  $C_4$ , two translations with perpendicular translation vectors that have equal length, and a 4-fold rotational symmetry, such that

$$C_4^4 = 1, \quad C_4 T_1 C_4^{-1} = T_2, \quad C_4 T_2 C_4^{-1} = T_1^{-1}, \quad T_1 T_2 = T_2 T_1. \quad (2.69)$$

An arbitrary element in  $p4$  can be written as  $g = T_1^x T_2^y C_4^c$ , with  $x, y \in \mathbb{Z}$  and  $c \in \{0, 1, 2, 3\}$ . For  $g_1 = T_1^{x_1} T_2^{y_1} C_4^{c_1}$  and  $g_2 = T_1^{x_2} T_2^{y_2} C_4^{c_2}$ , the group multiplication rule gives

$$g_1 g_2 = T_1^{x_1 + \Delta x(x_2, y_2, c_1)} T_2^{y_1 + \Delta y(x_2, y_2, c_1)} C_4^{[c_1 + c_2]_4} \quad (2.70)$$

where

$$\Delta x(x, y, c) = \begin{cases} x, & c = 0 \\ -y, & c = 1 \\ -x, & c = 2 \\ y, & c = 3 \end{cases}, \quad \Delta y(x, y, c) = \begin{cases} y, & c = 0 \\ x, & c = 1 \\ -y, & c = 2 \\ -x, & c = 3 \end{cases} \quad (2.71)$$

The  $\mathbb{Z}_2$  cohomology ring of  $p4$  is

$$\begin{aligned} \mathbb{Z}_2[A_c, A_{x+y}, B_{c^2}, B_{xy}] / (A_c^2 = 0, A_c A_{x+y} = 0, \\ B_{xy} A_{x+y} = B_{xy} A_c, B_{c^2} A_{x+y} = A_{x+y}^3 + B_{xy} A_{x+y}, \\ B_{xy}^2 = B_{c^2} B_{xy}) \end{aligned} \quad (2.72)$$

Here  $H^1(p4, \mathbb{Z}_2) = \mathbb{Z}_2^2$ , with generators  $\xi_1 = A_{x+y}$ ,  $\xi_2 = A_c$ , which have representative cochains,

$$\xi_1(g) = x + y, \quad \xi_2(g) = c. \quad (2.73)$$

$H^2(p4, \mathbb{Z}_2) = \mathbb{Z}_2^3$ , with generators  $\lambda_1 = B_{xy} + A_{x+y}^2 + B_{c^2}$ ,  $\lambda_2 = B_{xy}$ ,  $\lambda_3 = A_{x+y}^2$ , which have representative cochains,

$$\begin{aligned} \lambda_1(g_1, g_2) &= \lambda_2(g_1, g_2) + \lambda_3(g_1, g_2) + \frac{[c_1]_4 + [c_2]_4 - [c_1 + c_2]_4}{4} \\ \lambda_2(g_1, g_2) &= P_c(c_1)y_1x_2 + P(c_1)y_2(x_2 + y_1) \\ \lambda_3(g_1, g_2) &= P_{41}(c_1)x_2 + P_{42}(c_1)(x_2 + y_2) + P_{43}(c_1)y_2 \end{aligned} \quad (2.74)$$

In Appendix 2.E, we will see that  $\lambda_1, \lambda_2, \lambda_3$  generate LSM constraints.

- Wallpaper group 11:  $p4m$

This group is generated by  $T_1, T_2, C_4$  and  $M$ , where the first three generators have the same properties as those in  $p4$ , and the last generator  $M$  is a mirror symmetry that flips the translation vector of  $T_1$ , such that

$$\begin{aligned} M^2 &= 1, & MC_4M &= C_4^{-1}, & MT_1M &= T_1^{-1}, & MT_2M &= T_2, \\ C_4^4 &= 1, & C_4T_1C_4^{-1} &= T_2, & C_4T_2C_4^{-1} &= T_1^{-1}, & T_1T_2 &= T_2T_1. \end{aligned} \quad (2.75)$$

An arbitrary element in  $p4m$  can be written as  $g = T_1^x T_2^y C_4^c M^m$ , with  $x, y \in \mathbb{Z}$ ,  $c \in \{0, 1, 2, 3\}$  and  $m \in \{0, 1\}$ . For  $g_1 = T_1^{x_1} T_2^{y_1} C_4^{c_1} M^{m_1}$  and  $g_2 = T_1^{x_2} T_2^{y_2} C_4^{c_2} M^{m_2}$ , the group multiplication rule gives

$$g_1 g_2 = T_1^{x_1 + \Delta x(Q(m_1)x_2, y_2, c_1)} T_2^{y_1 + \Delta y(Q(m_1)x_2, y_2, c_1)} C_4^{[c_1 + Q(m_1)c_2]_4} M^{P(m_1 + m_2)} \quad (2.76)$$

where  $\Delta x(x, y, c)$  and  $\Delta y(x, y, c)$  are defined in Eq. (2.71).

The  $\mathbb{Z}_2$  cohomology ring of  $p4m$  is

$$\begin{aligned} \mathbb{Z}_2[A_c, A_{x+y}, A_m, B_{c^2}, B_{xy}] / ( &A_c(A_c + A_m) = 0, A_c A_{x+y} = 0, \\ &B_{xy} A_{x+y} = B_{xy}(A_c + A_m), \\ &B_{c^2} A_{x+y} = A_{x+y}^3 + A_m A_{x+y}^2 + B_{xy} A_{x+y}, \\ &B_{xy}^2 = B_{c^2} B_{xy}) \end{aligned} \quad (2.77)$$

Here  $H^1(p4m, \mathbb{Z}_2) = \mathbb{Z}_2^3$ , with generators  $\xi_1 = A_{x+y}$ ,  $\xi_2 = A_c$ ,  $\xi_3 = A_m$ , which have representative cochains,

$$\xi_1(g) = x + y, \quad \xi_2(g) = c, \quad \xi_3(g) = m. \quad (2.78)$$

$H^2(p4m, \mathbb{Z}_2) = \mathbb{Z}_2^6$ , with generators  $\lambda_1 = B_{xy} + A_{x+y}(A_{x+y} + A_m) + B_{c^2}$ ,  $\lambda_2 = B_{xy}$ ,  $\lambda_3 = A_{x+y}(A_{x+y} + A_m)$ ,  $\lambda_4 = A_m(A_m + A_{x+y} + A_c)$ ,  $\lambda_5 = A_m A_{x+y}$ ,  $\lambda_6 = A_m A_c$ , which have representative cochains,

$$\begin{aligned}
\lambda_1(g_1, g_2) &= \lambda_2(g_1, g_2) + \lambda_3(g_1, g_2) + \frac{[c_1]_4 + Q(m_1)[c_2]_4 - [c_1 + Q(m_1)c_2]_4}{4} \\
\lambda_2(g_1, g_2) &= P_c(c_1)y_1x_2 + P(c_1)y_2(x_2 + y_1) \\
\lambda_3(g_1, g_2) &= P_{41}(c_1)x_2 + P_{42}(c_1)(x_2 + y_2) + P_{43}(c_1)y_2 + m_1y_2 \\
\lambda_4(g_1, g_2) &= m_1(x_2 + y_2 + c_2 + m_2) \\
\lambda_5(g_1, g_2) &= m_1(x_2 + y_2) \\
\lambda_6(g_1, g_2) &= m_1c_2
\end{aligned} \tag{2.79}$$

In Appendix 2.E, we will see that  $\lambda_1, \lambda_2, \lambda_3$  generate LSM constraints, while  $\lambda_4, \lambda_5, \lambda_6$  correspond to non-LSM fractionalization patterns.

- Wallpaper group 12:  $p4g$

This group is generated by  $T_1, T_2, C_4$  and  $G$ . The first three generators have the same properties as those in  $p4$ , and the last generator  $G$  is a glide reflection whose reflection axis passes through the rotation center of  $C_4$  and bisects the translation vectors of  $T_1$  and  $T_2$ , such that

$$\begin{aligned}
C_4^4 &= 1, & C_4T_1C_4^{-1} &= T_2, & C_4T_2C_4^{-1} &= T_1^{-1}, & T_1T_2 &= T_2T_1, & (2.80) \\
G^2 &= T_1T_2, & GT_1G^{-1} &= T_2, & GT_2G^{-1} &= T_1, & GC_4G^{-1} &= T_2C_4^{-1}. & (2.81)
\end{aligned}$$

Note that there is also a mirror symmetry  $M = T_1^{-1}G$ . An arbitrary element in  $p4g$  can be written as  $g = T_1^x T_2^y C_4^c G^s$ , with  $x, y \in \mathbb{Z}$ ,  $c \in \{0, 1, 2, 3\}$  and  $s \in \{0, 1\}$ . For  $g_1 = T_1^{x_1} T_2^{y_1} C_4^{c_1} G^{s_1}$  and  $g_2 = T_1^{x_2} T_2^{y_2} C_4^{c_2} G^{s_2}$ , the group multiplication rule gives

$$g_1 g_2 = T_1^{x_1 + \Delta x(X, Y, c_1)} T_2^{y_1 + \Delta y(X, Y, c_1)} C_4^{[c_1 + Q(s_1)c_2]_4} G^{P(s_1 + s_2)} \tag{2.82}$$

where  $\Delta x(x, y, c)$  and  $\Delta y(x, y, c)$  are defined in Eq. (2.71), and

$$\begin{aligned}
X &= P_c(s_1)x_2 + P(s_1)y_2 + (P_{42}(c_2) + P_{43}(c_2))s_1 + \Delta x(s_1s_2, s_1s_2, [Q(s_1)c_2]_4) \\
Y &= P_c(s_1)y_2 + P(s_1)x_2 + (P_{41}(c_2) + P_{42}(c_2))s_1 + \Delta y(s_1s_2, s_1s_2, [Q(s_1)c_2]_4)
\end{aligned} \tag{2.83}$$

The  $\mathbb{Z}_2$  cohomology ring of  $p4g$  is

$$\begin{aligned} \mathbb{Z}_2[A_c, A_s, B_{c^2}, B_{c(x+y)}, C_{c^2(x+y)}] / (A_c^2 = 0, A_c A_s = 0, A_c B_{c(x+y)} = 0, \\ A_s B_{c(x+y)} = A_s B_{c^2}, \\ B_{c(x+y)}^2 = B_{c^2} B_{c(x+y)}, A_c C_{c^2(x+y)} = 0, \quad (2.84) \\ B_{c(x+y)} C_{c^2(x+y)} = B_{c^2} C_{c^2(x+y)}, \\ C_{c^2(x+y)}^2 = B_{c(x+y)}^3 + A_s B_{c^2} C_{c^2(x+y)}) \end{aligned}$$

Here  $H^1(p4g, \mathbb{Z}_2) = \mathbb{Z}_2^2$ , with generators  $\xi_1 = A_c$ ,  $\xi_2 = A_s$ , which have representative cochains,

$$\xi_1(g) = c, \quad \xi_2(g) = s. \quad (2.85)$$

$H^2(p4g, \mathbb{Z}_2) = \mathbb{Z}_2^3$ , with generators  $\lambda_1 = B_{c(x+y)} + B_{c^2}$ ,  $\lambda_2 = B_{c(x+y)}$ ,  $\lambda_3 = A_s^2$ , which have representative cochains,

$$\begin{aligned} \lambda_1(g_1, g_2) &= \lambda_2(g_1, g_2) + \frac{[c_1]_4 + Q(s_1)[c_2]_4 - [c_1 + Q(s_1)c_2]_4}{4} \\ \lambda_2(g_1, g_2) &= P_{40}(c_1)s_1(P_{43}(c_2) + (c_1 - c_2)s_2) + P_{41}(c_1)[P_c(s_1)y_2 + s_1(x_2 + 1 - P_{40}(c_2) + (c_1 - c_2)s_2)] \\ &\quad + P_{42}(c_1)[P_c(s_1)(x_2 + y_2) + s_1(x_2 + y_2 + P_{41}(c_2) + (c_1 - c_2)s_2)] \\ &\quad + P_{43}(c_1)[P_c(s_1)x_2 + s_1(y_2 + P_{42}(c_2) + (c_1 - c_2)s_2)] \\ \lambda_3(g_1, g_2) &= s_1 s_2 \end{aligned} \quad (2.86)$$

In Appendix 2.E, we will see that  $\lambda_1, \lambda_2$  generate LSM constraints, while  $\lambda_3$  corresponds to non-LSM fractionalization patterns.

Pay attention that there is a degree-3 generator  $C_{c^2(x+y)} \in H^3(p4g, \mathbb{Z}_2)$ . We do not have the explicit form of its representative cochain, but it can be determined by its pullback to the subgroup  $p4$  generated by  $T_1, T_2, C_4$ , which is  $A_{x+y}^3$ , as well as its pullback to the subgroup  $cm$  generated by  $T_1, T_2, T_2 C_2, T_1^{-1} G$ , which is  $A_{x+y}^3 + A_c^3 + B_{xy} A_m + A_c^2 A_m$ .

- Wallpaper group 13:  $p3$

This group is generated by  $T_1, T_2$  and  $C_3$ , two translations with translation vectors that have the same length and an angle of  $2\pi/3$ , and a 3-fold rotational symmetry, such that

$$C_3^3 = 1, \quad C_3 T_1 C_3^{-1} = T_2, \quad C_3 T_2 C_3^{-1} = T_1^{-1} T_2^{-1}, \quad T_1 T_2 = T_2 T_1. \quad (2.87)$$

An arbitrary element in  $p3$  can be written as  $g = T_1^x T_2^y C_3^c$ , with  $x, y \in \mathbb{Z}$  and  $c \in \{0, 1, 2\}$ . For  $g_1 = T_1^{x_1} T_2^{y_1} C_3^{c_1}$  and  $g_2 = T_1^{x_2} T_2^{y_2} C_3^{c_2}$ , the group multiplication rule gives

$$g_1 g_2 = T_1^{x_1 + \Delta x(x_2, y_2, c_1)} T_2^{y_1 + \Delta y(x_2, y_2, c_1)} C_3^{[c_1 + c_2]_3} \quad (2.88)$$

where

$$\Delta x(x, y, c) = \begin{cases} x, & c = 0 \\ -y, & c = 1 \\ -x + y, & c = 2 \end{cases}, \quad \Delta y(x, y, c) = \begin{cases} y, & c = 0 \\ x - y, & c = 1 \\ -x, & c = 2 \end{cases} \quad (2.89)$$

The  $\mathbb{Z}_2$  cohomology ring of  $p3$  is

$$\mathbb{Z}_2[B_{xy}]/(B_{xy}^2 = 0) \quad (2.90)$$

Here  $H^1(p3, \mathbb{Z}_2) = 0$ , while  $H^2(p3, \mathbb{Z}_2) = \mathbb{Z}_2$ , with generator  $\lambda_1 = B_{xy}$ , which have representative cochain,

$$\begin{aligned} \lambda_1(g_1, g_2) = & P_{30}(c_1)y_1x_2 + P_{31}(c_1) \left( \frac{y_2(y_2 - 1)}{2} + y_2(x_2 + y_1) \right) \\ & + P_{32}(c_1) \left( \frac{x_2(x_2 - 1)}{2} + y_1x_2 + y_2(x_2 + y_1) \right) \end{aligned} \quad (2.91)$$

In Appendix 2.E, we will see that  $\lambda_1$  generates LSM constraints.

- Wallpaper group 14:  $p3m1$

This group is generated by  $T_1, T_2, C_3$  and  $M$ , where the first three generators have the same properties as those in  $p3$ , and the last one is a mirror symmetry whose mirror axis passes through the  $C_3$  center, and is perpendicular to the angle that bisects the two translation vectors of  $T_1$  and  $T_2$ , such that

$$\begin{aligned} M^2 = 1, \quad MC_3M = C_3^{-1}, \quad MT_1M = T_2^{-1}, \quad MT_2M = T_1^{-1}, \\ C_3^3 = 1, \quad C_3T_1C_3^{-1} = T_2, \quad C_3T_2C_3^{-1} = T_1^{-1}T_2^{-1}, \quad T_1T_2 = T_2T_1. \end{aligned} \quad (2.92)$$

An arbitrary element in  $p3m1$  can be written as  $g = T_1^x T_2^y C_3^c M^m$ , with  $x, y \in \mathbb{Z}$ ,  $c \in \{0, 1, 2\}$  and  $M \in \{0, 1\}$ . For  $g_1 = T_1^{x_1} T_2^{y_1} C_3^{c_1} M^{m_1}$  and  $g_2 = T_1^{x_2} T_2^{y_2} C_3^{c_2} M^{m_2}$ , the group multiplication rule gives

$$g_1 g_2 = T_1^{x_1 + \Delta x(X, Y, c_1)} T_2^{y_1 + \Delta y(X, Y, c_1)} C_3^{[c_1 + Q(m_1)c_2]_3} M^{P(m_1 + m_2)} \quad (2.93)$$

where  $\Delta x(x, y, c)$  and  $\Delta y(x, y, c)$  are defined in Eq. (2.89), and

$$\begin{aligned} X &= P_c(m_1)x_2 - P(m_1)y_2 \\ Y &= P_c(m_1)y_2 - P(m_1)x_2 \end{aligned} \quad (2.94)$$

The  $\mathbb{Z}_2$  cohomology ring of  $p3m1$  is

$$\mathbb{Z}_2[A_m, B_{xy}]/(B_{xy}^2 = 0) \quad (2.95)$$

Here  $H^1(p3m1, \mathbb{Z}_2) = 0$ , with generator  $\xi_1 = A_m$ , which have representative cochain,

$$\xi_1(g) = m. \quad (2.96)$$

$H^2(p3m1, \mathbb{Z}_2) = \mathbb{Z}_2^2$ , with generators  $\lambda_1 = B_{xy}$ ,  $\lambda_2 = A_m^2$ , which have representative cochains,

$$\begin{aligned} \lambda_1(g_1, g_2) &= P_{30}(c_1)[P_c(m_1)y_1x_2 + m_1y_2(x_2 + y_1)] \\ &+ P_{31}(c_1) \left[ P_c(m_1) \left( \frac{y_2(y_2 - 1)}{2} + y_2(x_2 + y_1) \right) + m_1 \left( \frac{x_2(x_2 + 1)}{2} + y_1x_2 \right) \right] \\ &+ P_{32}(c_1) \left[ P_c(m_1) \left( \frac{x_2(x_2 - 1)}{2} + y_1x_2 + y_2(x_2 + y_1) \right) + m_1 \left( \frac{y_2(y_2 + 1)}{2} + y_1(x_2 + y_2) \right) \right] \quad (2.97) \\ \lambda_2(g_1, g_2) &= m_1m_2 \end{aligned}$$

In Appendix 2.E, we will see that  $\lambda_1$  generates LSM constraints, while  $\lambda_2$  corresponds to non-LSM fractionalization pattern.

- Wallpaper group 15:  $p31m$

This group is generated by  $T_1$ ,  $T_2$ ,  $C_3$  and  $M$ , where the first three generators have the same properties as those in  $p3$  and  $p3m1$ , and the last one is a mirror symmetry whose mirror axis passes through the  $C_3$  center and bisects the translation vectors of  $T_1$  and  $T_2$ , such that

$$\begin{aligned} M^2 &= 1, & MC_3M &= C_3^{-1}, & MT_1M &= T_2, & MT_2M &= T_1, \\ C_3^3 &= 1, & C_3T_1C_3^{-1} &= T_2, & C_3T_2C_3^{-1} &= T_1^{-1}T_2^{-1}, & T_1T_2 &= T_2T_1. \end{aligned} \quad (2.98)$$

An arbitrary element in  $p31m$  can be written as  $g = T_1^x T_2^y C_3^c M^m$ , with  $x, y \in \mathbb{Z}$ ,  $c \in \{0, 1, 2\}$  and  $M \in \{0, 1\}$ . For  $g_1 = T_1^{x_1} T_2^{y_1} C_3^{c_1} M^{m_1}$  and  $g_2 = T_1^{x_2} T_2^{y_2} C_3^{c_2} M^{m_2}$ , the group multiplication rule gives

$$g_1 g_2 = T_1^{x_1 + \Delta x(X, Y, c_1)} T_2^{y_1 + \Delta y(X, Y, c_1)} C_3^{[c_1 + Q(m_1)c_2]_3} M^{P(m_1 + m_2)} \quad (2.99)$$

where  $\Delta x(x, y, c)$  and  $\Delta y(x, y, c)$  are defined in Eq. (2.89), and

$$\begin{aligned} X &= P_c(m_1)x_2 + P(m_1)y_2 \\ Y &= P_c(m_1)y_2 + P(m_1)x_2 \end{aligned} \quad (2.100)$$

The  $\mathbb{Z}_2$  cohomology ring of  $p31m$  is

$$\mathbb{Z}_2[A_m, B_{xy}]/(B_{xy}^2 = 0) \quad (2.101)$$

Here  $H^1(p31m, \mathbb{Z}_2) = 0$ , with generator  $\xi_1 = A_m$ , which have representative cochain,

$$\xi_1(g) = m. \quad (2.102)$$

$H^2(p31m, \mathbb{Z}_2) = \mathbb{Z}_2^2$ , with generator  $\lambda_1 = B_{xy}$ ,  $\lambda_2 = A_m^2$ , which have representative cochains,

$$\begin{aligned} \lambda_1(g_1, g_2) &= P_{30}(c_1) [P_c(m_1) y_1 x_2 + m_1 y_2 (x_2 + y_1)] \\ &\quad + P_{31}(c_1) \left[ P_c(m_1) \left( \frac{y_2(y_2 + 1)}{2} + x_2 + y_2(x_2 + y_1) \right) + m_1 \left( \frac{x_2(x_2 + 1)}{2} + y_2 + y_1 x_2 \right) \right] \\ &\quad + P_{32}(c_1) \left[ P_c(m_1) \left( \frac{x_2(x_2 - 1)}{2} + y_2 + y_1 x_2 + y_2(x_2 + y_1) \right) + m_1 \left( \frac{y_2(y_2 - 1)}{2} + x_2 + y_1(x_2 + y_2) \right) \right] \\ \lambda_2(g_1, g_2) &= m_1 m_2 \end{aligned} \quad (2.103)$$

In Appendix 2.E, we will see that  $\lambda_1$  generates LSM constraints while  $\lambda_2$  corresponds to non-LSM fractionalization pattern.

- Wallpaper group 16:  $p6$

This group is generated by  $T_1$ ,  $T_2$  and  $C_6$ , two translations with translation vectors that have the same length and an angle of  $2\pi/3$ , and a 6-fold rotational symmetry, such that

$$C_6^6 = 1, \quad C_6 T_1 C_6^{-1} = T_1 T_2, \quad C_6 T_2 C_6^{-1} = T_1^{-1}, \quad T_1 T_2 = T_2 T_1. \quad (2.104)$$

An arbitrary element in  $p6$  can be written as  $g = T_1^x T_2^y C_6^c$ , with  $x, y \in \mathbb{Z}$  and  $c \in \{0, 1, 2, 3, 4, 5\}$ . For  $g_1 = T_1^{x_1} T_2^{y_1} C_6^{c_1}$  and  $g_2 = T_1^{x_2} T_2^{y_2} C_6^{c_2}$ , the group multiplication rule gives

$$g_1 g_2 = T_1^{x_1 + \Delta x(x_2, y_2, c_1)} T_2^{y_1 + \Delta y(x_2, y_2, c_1)} C_6^{[c_1 + c_2]_6} \quad (2.105)$$

where

$$\Delta x(x, y, c) = \begin{cases} x, & c = 0 \\ x - y, & c = 1 \\ -y, & c = 2 \\ -x, & c = 3 \\ -x + y, & c = 4 \\ y, & c = 5 \end{cases}, \quad \Delta y(x, y, c) = \begin{cases} y, & c = 0 \\ x, & c = 1 \\ x - y, & c = 2 \\ -y, & c = 3 \\ -x, & c = 4 \\ -x + y, & c = 5 \end{cases} \quad (2.106)$$



The  $\mathbb{Z}_2$  cohomology ring of  $p6$  is

$$\mathbb{Z}_2[A_c, B_{xy}]/(B_{xy}^2 = A_c^2 B_{xy}) \quad (2.107)$$

Here  $H^1(p6, \mathbb{Z}_2) = \mathbb{Z}_2$ , with generator  $\xi_1 = A_c$ , which have representative cochain,

$$\xi_1(g) = c. \quad (2.108)$$

$H^2(p6, \mathbb{Z}_2) = \mathbb{Z}_2^2$ , with generators  $\lambda_1 = B_{xy} + A_c^2$ ,  $\lambda_2 = B_{xy}$ , which have representative cochains,

$$\begin{aligned} \lambda_1(g_1, g_2) &= \lambda_2(g_1, g_2) + \frac{[c_1]_6 + [c_2]_6 - [c_1 + c_2]_6}{6} \\ \lambda_2(g_1, g_2) &= P_{60}(c_1)y_1x_2 + P_{61}(c_1)\left(\frac{x_2(x_2-1)}{2} + y_1x_2 + y_2(x_2 + y_1)\right) \\ &\quad + P_{62}(c_1)\left(\frac{y_2(y_2+1)}{2} + x_2 + y_2(x_2 + y_1)\right) + P_{63}(c_1)(x_2 + y_2 + y_1x_2) \\ &\quad + P_{64}(c_1)\left(\frac{x_2(x_2-1)}{2} + y_2 + y_1x_2 + y_2(x_2 + y_1)\right) + P_{65}(c_1)\left(\frac{y_2(y_2+1)}{2} + y_2(x_2 + y_1)\right) \end{aligned} \quad (2.109)$$

In Appendix 2.E, we will see that  $\lambda_1, \lambda_2$  generate LSM constraints.

- Wallpaper group 17:  $p6m$

This group is generated by  $T_1, T_2, C_6$  and  $M$ , where the first three generators have the same properties as those in  $p6$ , and the last one is a mirror symmetry whose mirror axis passes through the  $C_6$  center and bisects  $T_1$  and  $T_2$ , such that

$$\begin{aligned} M^2 &= 1, & MC_6M &= C_6^{-1}, & MT_1M &= T_2, & MT_2M &= T_1, \\ C_6^6 &= 1, & C_6T_1C_6^{-1} &= T_1T_2, & C_6T_2C_6^{-1} &= T_1^{-1}, & T_1T_2 &= T_2T_1. \end{aligned} \quad (2.110)$$

An arbitrary element in  $p6m$  can be written as  $g = T_1^x T_2^y C_6^c M^m$ , with  $x, y \in \mathbb{Z}$ ,  $c \in \{0, 1, 2, 3, 4, 5\}$  and  $m \in \{0, 1\}$ . For  $g_1 = T_1^{x_1} T_2^{y_1} C_6^{c_1} M^{m_1}$  and  $g_2 = T_1^{x_2} T_2^{y_2} C_6^{c_2} M^{m_2}$ , the group multiplication rule gives

$$g_1 g_2 = T_1^{x_1 + \Delta x(X, Y, c_1)} T_2^{y_1 + \Delta y(X, Y, c_1)} C_6^{[c_1 + Q(m_1)c_2]_6} M^{P(m_1 + m_2)} \quad (2.111)$$

where  $\Delta x(x, y, c)$  and  $\Delta y(x, y, c)$  are defined in Eq. (2.106), and  $X$  and  $Y$  are defined in Eq. (2.100).

The  $\mathbb{Z}_2$  cohomology ring of  $p6m$  is

$$\mathbb{Z}_2[A_c, A_m, B_{xy}]/(B_{xy}^2 = (A_c^2 + A_c A_m) B_{xy}) \quad (2.112)$$

Here  $H^1(p6m, \mathbb{Z}_2) = \mathbb{Z}_2^2$ , with generator  $\xi_1 = A_c$ ,  $\xi_2 = A_m$ , which have representative cochains,

$$\xi_1(g) = c, \quad \xi_2(g) = m. \quad (2.113)$$

$H^2(p6m, \mathbb{Z}_2) = \mathbb{Z}_2^4$ , with generators  $\lambda_1 = B_{xy} + A_c^2 + A_c A_m$ ,  $\lambda_2 = B_{xy}$ ,  $\lambda_3 = (A_c + A_m)A_m$ ,  $\lambda_4 = A_c A_m$ , which have representative cochains,

$$\begin{aligned} \lambda_1(g_1, g_2) &= \lambda_2(g_1, g_2) + \frac{[c_1]_6 + Q(m_1)[c_2]_6 - [c_1 + Q(m_1)c_2]_6}{6} \\ \lambda_2(g_1, g_2) &= P_{60}(c_1) [P_c(m_1)y_1x_2 + m_1y_2(x_2 + y_1)] \\ &\quad + P_{61}(c_1) \left[ P_c(m_1) \left( \frac{x_2(x_2 - 1)}{2} + y_1x_2 + y_2(x_2 + y_1) \right) + m_1 \left( \frac{y_2(y_2 - 1)}{2} + y_1(x_2 + y_2) \right) \right] \\ &\quad + P_{62}(c_1) \left[ P_c(m_1) \left( \frac{y_2(y_2 + 1)}{2} + x_2 + y_2(x_2 + y_1) \right) + m_1 \left( \frac{x_2(x_2 + 1)}{2} + y_2 + y_1x_2 \right) \right] \\ &\quad + P_{63}(c_1) [P_c(m_1)(x_2 + y_2 + y_1x_2) + m_1(x_2 + y_2 + y_2(x_2 + y_1))] \\ &\quad + P_{64}(c_1) \left[ P_c(m_1) \left( \frac{x_2(x_2 - 1)}{2} + y_2 + y_1x_2 + y_2(x_2 + y_1) \right) + m_1 \left( \frac{y_2(y_2 - 1)}{2} + x_2 + y_1(x_2 + y_2) \right) \right] \\ &\quad + P_{65}(c_1) \left[ P_c(m_1) \left( \frac{y_2(y_2 + 1)}{2} + y_2(x_2 + y_1) \right) + m_1 \left( \frac{x_2(x_2 + 1)}{2} + y_1x_2 \right) \right] \\ \lambda_3(g_1, g_2) &= m_1(c_2 + m_2) \\ \lambda_4(g_1, g_2) &= m_1c_2 \end{aligned} \quad (2.114)$$

In Appendix 2.E, we will see that  $\lambda_1, \lambda_2$  generate LSM constraints, while  $\lambda_3, \lambda_4$  correspond to non-LSM fractionalization patterns.

## 2.E Topological invariants for all LSM constraints

In this appendix, for each of the 17 wallpaper groups, we present the topological invariants for all LSM constraints and topological invariants for all non-LSM fractionalization patterns. These topological invariants can all be written down by simply inspecting the IWP and/or the mirror axes of the relevant wallpaper groups, and they correspond to various  $(3 + 1)$ -d  $G_s \times G_{int}$  SPTs that can be constructed in a manner described in Sec. 2.2. This physics-based reasoning implies that the topological invariants we present here are complete and independent. In Appendix 2.D, we also provide explicit expressions of the representative cochains that correspond to each of the topological invariants, which show mathematically that the topological invariants here are indeed complete and independent.

- Wallpaper group 1:  $p1$

All points in space correspond to the same IWP for  $p1$ . The fractionalization patterns of  $p1$  are classified by  $H^2(p1, \mathbb{Z}_2) = \mathbb{Z}_2$ . There is only one nontrivial fractionalization

pattern  $T_1T_2 = -T_2T_1$ , detected by the topological invariant

$$\alpha_1[\omega] = \frac{\omega(T_1, T_2)}{\omega(T_2, T_1)}. \quad (2.115)$$

This fractionalization pattern is related to the first of the 3 basic no-go theorems in Sec. 2.1, so it corresponds to an LSM constraint, and the classification of LSM constraints is  $\mathbb{Z}_2$ . It is straightforward to check that  $\alpha_1[(-1)^{\lambda_1}] = -1$ , where  $\lambda_1$  is defined in Appendix 2.D.

- Wallpaper group 2:  $p2$

There are 4 different IWP for  $p2$ , which are rotation centers for  $C_2$ ,  $T_1C_2$ ,  $T_2C_2$  and  $T_1T_2C_2$ , respectively. The fractionalization patterns of  $p2$  are classified by  $H^2(p2, \mathbb{Z}_2) = \mathbb{Z}_2^4$ . All fractionalization patterns are generated by 4 root patterns, detected by the topological invariants,

$$\begin{aligned} \alpha_1[\omega] &= \frac{\omega(C_2, C_2)}{\omega(1, 1)} \\ \alpha_2[\omega] &= \frac{\omega(T_1C_2, T_1C_2)}{\omega(1, 1)} \\ \alpha_3[\omega] &= \frac{\omega(T_2C_2, T_2C_2)}{\omega(1, 1)} \\ \alpha_4[\omega] &= \frac{\omega(T_1T_2C_2, T_1T_2C_2)}{\omega(1, 1)} \end{aligned} \quad (2.116)$$

corresponding to  $C_2^2 = -1$ ,  $(T_1C_2)^2 = -1$ ,  $(T_2C_2)^2 = -1$  and  $(T_1T_2C_2)^2 = -1$  respectively. All these topological invariants are related to the third of the 3 basic no-go theorems in Sec. 2.1, so they all correspond to LSM constraints, and the classification of LSM constraints is  $\mathbb{Z}_2^4$ . It is straightforward to check that  $\alpha_i[(-1)^{\lambda_j}] = (-1)^{\delta_{ij}}$  for  $i, j = 1, \dots, 4$ , where  $\lambda_i$  is defined in Appendix 2.D.

- Wallpaper group 3:  $pm$

There are 2 different IWP for  $pm$ , which are the mirror axes for  $M$  and  $T_1M$ , respectively. The fractionalization patterns of  $pm$  are classified by  $H^2(pm, \mathbb{Z}_2) = \mathbb{Z}_2^4$ . All fractionalization patterns are generated by 4 root patterns, detected by the topolog-

ical invariants

$$\begin{aligned}
\alpha_1[\omega] &= \frac{\omega(T_2, M)}{\omega(M, T_2)} \\
\alpha_2[\omega] &= \frac{\omega(T_2, T_1 M)}{\omega(T_1 M, T_2)} \\
\alpha_3[\omega] &= \frac{\omega(M, M)}{\omega(1, 1)} \\
\alpha_4[\omega] &= \frac{\omega(T_1 M, T_1 M)}{\omega(1, 1)}
\end{aligned} \tag{2.117}$$

The first two topological invariants are related to the second of the 3 basic no-go theorems, so they correspond to LSM constraints, and the classification of LSM constraints is  $\mathbb{Z}_2^2$ . The last two are non-LSM fractionalization patterns. It is straightforward to check that  $\alpha_i[(-1)^{\lambda_j}] = (-1)^{\delta_{ij}}$  for  $i, j = 1, \dots, 4$ , where  $\lambda_i$  is defined in Appendix 2.D.

- Wallpaper group 4:  $pg$

All points in space belong to one IWP of  $pg$ . The fractionalization patterns of  $pg$  are classified by  $H^2(pg, \mathbb{Z}_2) = \mathbb{Z}_2$ . There is only one nontrivial fractionalization pattern, detected by the topological invariant

$$\alpha_1[\omega] = \frac{\omega(T_1 G^{-1}, T_1 G) \omega(T_1, G)}{\omega(G^{-1}, G) \omega(T_1, G^{-1})} \tag{2.118}$$

corresponding to the symmetry fractionalization pattern  $G^{-1} T_1 G T_1 = -1$ . This topological invariant is related to the first of the 3 basic no-go theorems, so it corresponds to an LSM constraint, and the classification of LSM constraints is  $\mathbb{Z}_2$ . It is straightforward to check that  $\alpha_1[(-1)^{\lambda_1}] = -1$ , where  $\lambda_1$  is defined in Appendix 2.D.

- Wallpaper group 5:  $cm$

The group  $cm$  has one IWP, which includes points along the mirror axis of  $M$ . The fractionalization patterns of  $cm$  are classified by  $H^2(cm, \mathbb{Z}_2) = \mathbb{Z}_2^2$ . All fractionalization patterns are generated by 2 root patterns, detected by the topological invariants

$$\begin{aligned}
\alpha_1[\omega] &= \frac{\omega(T_1 T_2, M)}{\omega(M, T_1 T_2)} \\
\alpha_2[\omega] &= \frac{\omega(M, M)}{\omega(1, 1)}
\end{aligned} \tag{2.119}$$

The first topological invariant is related to the second of the 3 basic no-go theorems, so it corresponds to an LSM constraint, and the classification of LSM constraints is  $\mathbb{Z}_2$ . The second one is a non-LSM fractionalization pattern. It is straightforward to check that  $\alpha_i[(-1)^{\lambda_j}] = (-1)^{\delta_{ij}}$  for  $i, j = 1, 2$ , where  $\lambda_i$  is defined in Appendix 2.D.

- Wallpaper group 6:  $pmm$

There are 4 different IWP for  $pmm$ , which are the intersecting point of  $M$  and  $C_2M$ , the intersecting point of  $T_1M$  and  $C_2M$ , the intersecting point of  $M$  and  $T_2C_2M$ , and the intersecting point of  $T_1M$  and  $T_2C_2M$ . Note that these 4 IWP can also be respectively viewed as the rotation centers for the following four  $C_2$  rotations:  $C_2$ ,  $T_1C_2$ ,  $T_2C_2$  and  $T_1T_2C_2$ . The fractionalization patterns of  $pmm$  are classified by  $H^2(pmm, \mathbb{Z}_2) = \mathbb{Z}_2^8$ . All fractionalization patterns are generated by 8 root patterns, detected by the topological invariants

$$\begin{aligned}
\alpha_1[\omega] &= \frac{\omega(C_2, C_2)}{\omega(1, 1)} \\
\alpha_2[\omega] &= \frac{\omega(T_1T_2C_2, T_1T_2C_2)}{\omega(1, 1)} \\
\alpha_3[\omega] &= \frac{\omega(T_1C_2, T_1C_2)}{\omega(1, 1)} \\
\alpha_4[\omega] &= \frac{\omega(T_2C_2, T_2C_2)}{\omega(1, 1)} \\
\alpha_5[\omega] &= \frac{\omega(M, M)}{\omega(1, 1)} \\
\alpha_6[\omega] &= \frac{\omega(C_2M, C_2M)}{\omega(1, 1)} \\
\alpha_7[\omega] &= \frac{\omega(T_1M, T_1M)}{\omega(1, 1)} \\
\alpha_8[\omega] &= \frac{\omega(T_2C_2M, T_2C_2M)}{\omega(1, 1)}
\end{aligned} \tag{2.120}$$

The first four topological invariants are related to the third of the 3 basic no-go theorems, so they correspond to LSM constraints, and the classification of LSM constraints is  $\mathbb{Z}_2^4$ . The last four are non-LSM fractionalization patterns. It is straightforward to check that  $\alpha_i[(-1)^{\lambda_j}] = (-1)^{\delta_{ij}}$  for  $i, j = 1, \dots, 8$ , where  $\lambda_i$  is defined in Appendix 2.D.

- Wallpaper group 7:  $pmg$

There are 3 different IWP for  $pmg$ . The first includes the rotation centers of  $C_2$  and  $T_1C_2$ , the second includes the rotation centers of  $T_2C_2$  and  $T_1T_2C_2$ , and the third includes the mirror axes of  $M$  and  $T_1M$ . The fractionalization patterns of  $pmg$  are classified by  $H^2(pmg, \mathbb{Z}_2) = \mathbb{Z}_2^4$ . All fractionalization patterns are generated by 4 root patterns, detected by the topological invariants

$$\begin{aligned}
\alpha_1[\omega] &= \frac{\omega(C_2, C_2)}{\omega(1, 1)} \\
\alpha_2[\omega] &= \frac{\omega(T_1T_2C_2, T_1T_2C_2)}{\omega(1, 1)} \\
\alpha_3[\omega] &= \frac{\omega(T_2, M)}{\omega(M, T_2)} \\
\alpha_4[\omega] &= \frac{\omega(M, M)}{\omega(1, 1)}
\end{aligned} \tag{2.121}$$

The first two topological invariants are related to the third of the 3 basic no-go theorems, and the third is related to the second of the 3 basic no-go theorems, so they correspond to LSM constraints, and the classification of LSM constraints is  $\mathbb{Z}_2^3$ . The fourth topological invariant is a non-LSM fractionalization pattern. It is straightforward to check that  $\alpha_i[(-1)^{\lambda_j}] = (-1)^{\delta_{ij}}$  for  $i, j = 1, \dots, 4$ , where  $\lambda_i$  is defined in Appendix 2.D.

- Wallpaper group 8:  $pgg$

There are 2 different IWP for  $pgg$ . The first includes the rotation centers of  $C_2$  and  $T_1T_2C_2$ , and the second includes the rotation centers of  $T_1C_2$  and  $T_2C_2$ . The fractionalization patterns of  $pgg$  are classified by  $H^2(pgg, \mathbb{Z}_2) = \mathbb{Z}_2^2$ . All fractionalization patterns are generated by 2 root patterns, detected by the topological invariants

$$\begin{aligned}
\alpha_1[\omega] &= \frac{\omega(C_2, C_2)}{\omega(1, 1)} \\
\alpha_2[\omega] &= \frac{\omega(T_1C_2, T_1C_2)}{\omega(1, 1)}
\end{aligned} \tag{2.122}$$

Both topological invariants are related to the third of the 3 basic no-go theorems, so they both correspond to LSM constraints, and the classification of LSM constraints is  $\mathbb{Z}_2^2$ . It is straightforward to check that  $\alpha_i[(-1)^{\lambda_j}] = (-1)^{\delta_{ij}}$  for  $i, j = 1, 2$ , where  $\lambda_i$  is defined in Appendix 2.D.

- Wallpaper group 9:  $cm\bar{m}$

There are 3 different IWP for  $cm\bar{m}$ . The first is the 2-fold rotation center of  $C_2$ , the second is the 2-fold rotation center of  $T_1T_2C_2$ , and the third includes the 2-fold rotation centers of  $T_1C_2$  and  $T_2C_2$ .

The fractionalization patterns of  $cm\bar{m}$  are classified by  $H^2(cm\bar{m}, \mathbb{Z}_2) = \mathbb{Z}_2^5$ . All fractionalization patterns are generated by 5 root patterns, detected by the topological invariants

$$\begin{aligned}
\alpha_1[\omega] &= \frac{\omega(C_2, C_2)}{\omega(1, 1)} \\
\alpha_2[\omega] &= \frac{\omega(T_1T_2C_2, T_1T_2C_2)}{\omega(1, 1)} \\
\alpha_3[\omega] &= \frac{\omega(T_1C_2, T_1C_2)}{\omega(1, 1)} \\
\alpha_4[\omega] &= \frac{\omega(M, M)}{\omega(1, 1)} \\
\alpha_5[\omega] &= \frac{\omega(C_2M, C_2M)}{\omega(1, 1)}
\end{aligned} \tag{2.123}$$

The first three topological invariants are related to the third of the 3 basic no-go theorems, so they correspond to LSM constraints, and the classification of LSM constraints is  $\mathbb{Z}_2^3$ . The last two are non-LSM fractionalization patterns. It is straightforward to check that  $\alpha_i[(-1)^{\lambda_j}] = (-1)^{\delta_{ij}}$  for  $i, j = 1, \dots, 5$ , where  $\lambda_i$  is defined in Appendix 2.D.

- Wallpaper group 10:  $p4$

There are 3 different IWP for  $p4$ . The first is the 2-fold rotation center of  $C_4^2$ , the second is the 2-fold rotation center of  $T_1T_2C_4^2$ , and the third includes the 2-fold rotation centers of  $T_1C_4^2$  and  $T_2C_4^2$ . Note that the first two IWP are also 4-fold rotation centers. The fractionalization patterns of  $p4$  are classified by  $H^2(p4, \mathbb{Z}_2) = \mathbb{Z}_2^3$ . All fractionalization patterns are generated by 3 root patterns, detected by the

topological invariants

$$\begin{aligned}
\alpha_1[\omega] &= \frac{\omega(C_4^2, C_4^2)}{\omega(1, 1)} \\
\alpha_2[\omega] &= \frac{\omega(T_1 T_2 C_4^2, T_1 T_2 C_4^2)}{\omega(1, 1)} \\
\alpha_3[\omega] &= \frac{\omega(T_1 C_4^2, T_1 C_4^2)}{\omega(1, 1)}
\end{aligned} \tag{2.124}$$

All these topological invariants are related to the third of the 3 basic no-go theorems, so they all correspond to LSM constraints, and the classification of LSM constraints is  $\mathbb{Z}_2^3$ . It is straightforward to check that  $\alpha_i[(-1)^{\lambda_j}] = (-1)^{\delta_{ij}}$  for  $i, j = 1, \dots, 3$ , where  $\lambda_i$  is defined in Appendix 2.D.

- Wallpaper group 11:  $p4m$

There are 3 different IWP for  $p4m$ , just like  $p4$ . The first is the 2-fold rotation center of  $C_4^2$ , the second is the 2-fold rotation center of  $T_1 T_2 C_4^2$ , and the third includes the 2-fold rotation centers for  $T_1 C_4^2$  and  $T_2 C_4^2$ . All these IWP are also on some mirror axes, and the first two are also 4-fold rotation centers. The fractionalization patterns of  $p4m$  are classified by  $H^2(p4m, \mathbb{Z}_2) = \mathbb{Z}_2^6$ . All fractionalization patterns are generated by 6 root patterns, detected by the topological invariants

$$\begin{aligned}
\alpha_1[\omega] &= \frac{\omega(C_4^2, C_4^2)}{\omega(1, 1)} \\
\alpha_2[\omega] &= \frac{\omega(T_1 T_2 C_4^2, T_1 T_2 C_4^2)}{\omega(1, 1)} \\
\alpha_3[\omega] &= \frac{\omega(T_1 C_4^2, T_1 C_4^2)}{\omega(1, 1)} \\
\alpha_4[\omega] &= \frac{\omega(M, M)}{\omega(1, 1)} \\
\alpha_5[\omega] &= \frac{\omega(T_1 M, T_1 M)}{\omega(1, 1)} \\
\alpha_6[\omega] &= \frac{\omega(C_4 M, C_4 M)}{\omega(1, 1)}
\end{aligned} \tag{2.125}$$

The first three topological invariants are related to the third of the 3 basic no-go theorems, so they correspond to LSM constraints, and the classification of LSM



constraints is  $\mathbb{Z}_2^3$ . The last three are non-LSM constraints. It is straightforward to check that  $\alpha_i[(-1)^{\lambda_j}] = (-1)^{\delta_{ij}}$  for  $i, j = 1, \dots, 6$ , where  $\lambda_i$  is defined in Appendix 2.D.

- Wallpaper group 12:  $p4g$

There are 2 different IWP for  $p4g$ . The first includes the 2-fold rotation centers of  $C_4^2$  and  $T_1T_2C_4^2$ , and the second includes the 2-fold rotation centers of  $T_1C_4^2$  and  $T_2C_4^2$ . Note that the first IWP are also 4-fold rotation centers, and they do not lie on any mirror axis. The second IWP lies on some mirror axes. The fractionalization patterns of  $p4g$  are classified by  $H^2(p4g, \mathbb{Z}_2) = \mathbb{Z}_2^3$ . All fractionalization patterns are generated by 3 root patterns, detected by the topological invariants

$$\begin{aligned}\alpha_1[\omega] &= \frac{\omega(C_4^2, C_4^2)}{\omega(1, 1)} \\ \alpha_2[\omega] &= \frac{\omega(T_1C_4^2, T_1C_4^2)}{\omega(1, 1)} \\ \alpha_3[\omega] &= \frac{\omega(T_1^{-1}G, T_1^{-1}G)}{\omega(1, 1)}\end{aligned}\tag{2.126}$$

The first two topological invariants are related to the third of the 3 basic no-go theorems, so they correspond to LSM constraints, and the classification of LSM constraints is  $\mathbb{Z}_2^2$ . The last one is a non-LSM fractionalization pattern. It is straightforward to check that  $\alpha_i[(-1)^{\lambda_j}] = (-1)^{\delta_{ij}}$  for  $i, j = 1, \dots, 3$ , where  $\lambda_i$  is defined in Appendix 2.D.

- Wallpaper group 13:  $p3$

There are 3 IWP for  $p3$ , and they are all 3-fold rotation centers. The fractionalization patterns of  $p3$  are classified by  $H^2(p3, \mathbb{Z}_2) = \mathbb{Z}_2$ . All fractionalization patterns are generated by a root pattern, detected by the topological invariant

$$\alpha[\omega] = \frac{\omega(T_1, T_2)}{\omega(T_2, T_1)}\tag{2.127}$$

This topological invariant is related to the first of 3 basic no-go theorems, so it corresponds to an LSM constraint, and the classification of LSM constraints is  $\mathbb{Z}_2$ . It is straightforward to check that  $\alpha_1[(-1)^{\lambda_1}] = -1$  for  $i, j = 1, \dots, 8$ , where  $\lambda_1$  is defined in Appendix 2.D.

- Wallpaper group 14:  $p3m1$

There are 3 different IWP for  $p3m1$ , and they are all 3-fold rotation centers, just as in  $p3$ , but they also lie on the mirror axes. The fractionalization patterns of  $p3m1$  are classified by  $H^2(p3m1, \mathbb{Z}_2) = \mathbb{Z}_2^2$ . All fractionalization patterns are generated by 2 root patterns, detected by the topological invariants

$$\begin{aligned}\alpha_1[\omega] &= \frac{\omega(T_1, T_2)}{\omega(T_2, T_1)} \\ \alpha_2[\omega] &= \frac{\omega(M, M)}{\omega(1, 1)}\end{aligned}\tag{2.128}$$

The first topological invariant is related to the first of the 3 basic no-go theorems, so it corresponds to an LSM constraint, and the classification of LSM constraints is  $\mathbb{Z}_2$ . The second one is a non-LSM fractionalization pattern. It is straightforward to check that  $\alpha_i[(-1)^{\lambda_j}] = (-1)^{\delta_{ij}}$  for  $i, j = 1, 2$ , where  $\lambda_i$  is defined in Appendix 2.D.

- Wallpaper group 15:  $p31m$

There are 3 different IWP for  $p31m$ , and they are all 3-fold rotation centers, just as in  $p3$ , but only one of them also lies on the mirror axes. The fractionalization patterns of  $p31m$  are classified by  $H^2(p31m, \mathbb{Z}_2) = \mathbb{Z}_2^2$ . All fractionalization patterns are generated by 2 root patterns, detected by the topological invariants

$$\begin{aligned}\alpha_1[\omega] &= \frac{\omega(T_1 T_2, M)}{\omega(M, T_1 T_2)} \\ \alpha_2[\omega] &= \frac{\omega(M, M)}{\omega(1, 1)}\end{aligned}\tag{2.129}$$

The first topological invariant is related to the second of the 3 basic no-go theorems, so it corresponds to an LSM constraint, and the classification of LSM constraints is  $\mathbb{Z}_2$ . The second is a non-LSM fractionalization pattern. It is straightforward to check that  $\alpha_i[(-1)^{\lambda_j}] = (-1)^{\delta_{ij}}$  for  $i, j = 1, 2$ , where  $\lambda_i$  is defined in Appendix 2.D.

- Wallpaper group 16:  $p6$

There are 3 different IWP for  $p6$ , and they are centers of 6-fold, 3-fold and 2-fold rotations, respectively. The fractionalization patterns of  $p6$  are classified by  $H^2(p6, \mathbb{Z}_2) = \mathbb{Z}_2^2$ . All fractionalization patterns are generated by 2 root patterns,

detected by the topological invariants

$$\begin{aligned}\alpha_1[\omega] &= \frac{\omega(C_6^3, C_6^3)}{\omega(1, 1)} \\ \alpha_2[\omega] &= \frac{\omega(T_1 C_6^3, T_1 C_6^3)}{\omega(1, 1)}\end{aligned}\tag{2.130}$$

Both topological invariants are related to the third of the 3 basic no-go theorems, so they both correspond to LSM constraints, and the classification of LSM constraints is  $\mathbb{Z}_2^2$ . It is straightforward to check that  $\alpha_i[(-1)^{\lambda_j}] = (-1)^{\delta_{ij}}$  for  $i, j = 1, 2$ , where  $\lambda_i$  is defined in Appendix 2.D.

- Wallpaper group 17:  $p6m$

There are 3 different IWP for  $p6m$ . Just as  $p6$ , they are 6-fold, 3-fold and 2-fold rotation centers, respectively. Here all IWP also lie on some mirror axes. The fractionalization patterns of  $p6m$  are classified by  $H^2(p6m, \mathbb{Z}_2) = \mathbb{Z}_2^4$ . All fractionalization patterns are generated by 4 root patterns, detected by topological invariants

$$\begin{aligned}\alpha_1[\omega] &= \frac{\omega(C_6^3, C_6^3)}{\omega(1, 1)} \\ \alpha_2[\omega] &= \frac{\omega(T_1 C_6^3, T_1 C_6^3)}{\omega(1, 1)} \\ \alpha_3[\omega] &= \frac{\omega(M, M)}{\omega(1, 1)} \\ \alpha_4[\omega] &= \frac{\omega(C_6^3 M, C_6^3 M)}{\omega(1, 1)}\end{aligned}\tag{2.131}$$

The first two topological invariants are related to the third of the 3 basic no-go theorems, and they correspond to LSM constraints, and the classification of LSM constraints is  $\mathbb{Z}_2^2$ . The last two are non-LSM fractionalization patterns. It is straightforward to check that  $\alpha_i[(-1)^{\lambda_j}] = (-1)^{\delta_{ij}}$  for  $i, j = 1, \dots, 4$ , where  $\lambda_i$  is defined in Appendix 2.D.

## 2.F Topological characterization of LSM constraints in $(1+1)$ -d

In this appendix, we present the derivation of the topological characterization of the LSM constraints for  $(1+1)$ -d  $G_s \times G_{int}$  symmetric spin systems, where the results are already

given in Sec. 2.2.3.

First, we note that an argument similar to the one in Appendix 2.A for the  $(2 + 1)$ -d case shows that in this case the relevant cocycle can be written as

$$\Omega(g_1, g_2, g_3) = e^{i\pi\lambda(l_1)\eta(a_2, a_3)} \quad (2.132)$$

where  $g_i \in G_s \times G_{int}$  is written as  $g_i = l_i \otimes a_i$ , with  $l_i \in G_s$  and  $a_i \in G_{int}$ . The cocycle for the nontrivial  $(1 + 1)$ -d  $G_{int}$  SPT is precisely  $e^{i\pi\eta(a_1, a_2)}$ , and  $\lambda$  can be viewed as a cocycle in  $H^1(G_s, \mathbb{Z}_2)$ . Furthermore,  $\lambda$  is determined completely by  $G_s$  and the lattice homotopy class, and it is the same for all  $G_{int}$  with  $\mathbb{Z}_2^k$ -classified PR and for all PR type of the system.

When  $G_s = p1$ , the line group that only contains translation generated by  $T$ , the lattice homotopy picture implies that the LSM constraints in this case are classified by  $\mathbb{Z}_2$ , and the only nontrivial LSM constraint corresponds to the case where the total PR inside each translation unit cell is nontrivial. On the other hand,  $H^1(p1, \mathbb{Z}_2) = \mathbb{Z}_2$ , so there is also only one nontrivial cocycle. Writing an element in  $p1$  as  $T^x$  with  $x \in \mathbb{Z}$ ,  $\lambda(T^x) = [x]_2$  is a representative cochain of the nontrivial element in  $H^1(p1, \mathbb{Z}_2)$ . So we can identify the cocycle corresponding to the nontrivial LSM constraint as

$$\Omega(g_1, g_2, g_3) = e^{i\pi x_1 \eta(a_2, a_3)} \quad (2.133)$$

When  $G_s = p1m$ , the line group that contains a translation generated by  $T$  and a mirror symmetry generated by  $M$ , with commutation relation  $MTM = T^{-1}$ , there are two IWP in each translation unit cell, which are the mirror centers of  $M$  and  $TM$ , respectively. The lattice homotopy picture implies that the LSM constraints in this case are classified by  $\mathbb{Z}_2^2$ , and the two root LSM constraints can be taken to correspond to the cases where the total PR at one of the two IWP is nontrivial. On the other hand,  $H^1(p1m, \mathbb{Z}_2) = \mathbb{Z}_2^2$ , so all nontrivial cocycles in  $H^1(p1m, \mathbb{Z}_2)$  must correspond to some nontrivial LSM constraint. These cocycles can be generated by two roots represented by  $\lambda_1(T^x M^m) = x + m$  and  $\lambda_2(T^x M^m) = x$ , with  $x \in \mathbb{Z}$  and  $m \in \{0, 1\}$ . So the cocycles corresponding to the LSM constraints can also be generated by

$$\begin{aligned} \Omega_1(g_1, g_2, g_3) &= e^{i\pi(x_1 + m_1)\eta(a_2, a_3)} \\ \Omega_2(g_1, g_2, g_3) &= e^{i\pi x_1 \eta(a_2, a_3)} \end{aligned} \quad (2.134)$$

where  $g_i \in G_s \times G_{int}$  is written as  $g_i = T^{x_i} M^{m_i} \otimes a_i$ , with  $a_i \in G_{int}$ .

Now our task is just to identify  $\Omega_1$  and  $\Omega_2$  with the distributions of DOF that trigger the LSM constraint. To this end, first note that if  $M$  is broken while  $T$  is preserved, both  $\Omega_1$

and  $\Omega_2$  reduces to Eq. (2.133), which implies that both of them correspond to a distribution of DOF with a net nontrivial PR inside each translation unit cell. So one of them must correspond to the case where the mirror center of  $M$  hosts a nontrivial PR, while the other corresponds to the case where the mirror center of  $TM$  hosts a nontrivial PR. Suppose the mirror center of  $TM$  hosts a nontrivial PR, then after breaking the translation symmetry while keeping  $M$  unbroken, the system should have no LSM constraint. Only  $\Omega_2$  satisfies this condition, so this distribution of DOF is identified with  $\Omega_2$ , and  $\Omega_1$  corresponds to the case where the mirror center of  $M$  hosts a nontrivial PR.

# Chapter 3

## Stiefel Liquid, non-linear Sigma Model and its Anomaly

In this chapter, we discuss a particular class of quantum spin liquid, called Stiefel Liquid (SL), which is described in the IR by a non-linear Sigma Model (NLSM) with the target manifold Stiefel manifold, supplemented with a nontrivial Wess-Zumino-Witten (WZW) term. The motivation for SLs is to describe exotic quantum criticality arising from the competition between magnetic orders and non-magnetic orders, which we will discuss in detail in Section 5. Recall that each SL will be labeled by two integers  $(N, k)$ , with  $N \geq 5$  and  $k \neq 0$ . We will denote a SL corresponding to  $(N, k)$  by  $\text{SL}^{(N,k)}$ . Since we will mostly focus on the case with  $k = 1$ , we will also use the shorthand  $\text{SL}^{(N)}$  to denote  $\text{SL}^{(N,k=1)}$ . We propose that  $(N = 5, k = 1)$  corresponds to DQCP and  $(N = 6, k = 1)$  corresponds to U(1) DSL. We argue that SLs have a large emergent symmetry which is anomalous. The anomaly of a NLSM with a nontrivial WZW term can be calculated by a standard trick in mathematics called transgression, and we illustrate the calculation in SL and derive its anomaly. We end with a few comments on the dynamics of SLs.

Part of this chapter is adapted from Refs. [1, 15] while the calculation of the anomaly directly using the formulation of NLSM is newly written.

### 3.1 Stiefel Liquids as a NLSM

Recall that a NLSM with the target manifold  $V$  has fields corresponding to maps from the spacetime manifold  $\mathcal{M}$  to the target manifold  $V$ , i.e.,

$$f : \mathcal{M} \rightarrow V \quad (3.1)$$

where  $\mathcal{M}$  is the  $(d + 1)$ -dimensional spacetime manifold.

Now suppose that  $V$  is the Stiefel manifold  $V_{N,N-4}$  ( $N \geq 5$ ) [70]. For simplicity, in this thesis we will mostly use the abbreviated notation  $V_N$  if we want to emphasize the explicit  $N$ -dependence. One way to define the manifold  $V_N$  is as the coset space  $SO(N)/SO(4)$ . It can also be defined as the manifold constructed from  $(N - 4)$ -frames in the  $N$ -dimensional Euclidean space. Accordingly, a point on the Stiefel manifold can be labeled by an  $N$ -by- $(N - 4)$  real matrix, denoted by  $n$ , such that the columns of  $n$  are orthonormal, i.e.,  $n^T n = I_{N-4}$ , with  $I_{N-4}$  the  $(N - 4)$ -dimensional identity matrix. Therefore, the DOF of a SL can be characterized by a spacetime-dependent matrix  $n$ , supplemented with the orthonormal condition  $n^T n = I_{N-4}$ . A canonical action for the fields  $n$  can be simply

$$S_0[n] = \frac{1}{2g} \int d^{d+1}x \operatorname{Tr}(\partial_\mu n^T \partial^\mu n) \quad (3.2)$$

where the  $n$  in the square bracket indicates the dependence of the action on the configuration of  $n$ .

Interestingly, because  $H^4(V_N, \mathbb{Z}) \cong \mathbb{Z}$  is nontrivial, a nontrivial WZW term based on the closed 4-form on  $V$  can be defined for any  $N \geq 5$  in three dimensional spacetime [16, 17, 71]. To define this WZW term, we will first add one more dimension to the physical spacetime and extend the matrix  $n$  into this extra dimension. Denote the coordinate of the extra dimension by  $u$ , and the extended matrix by  $n^e$ , such that  $n^e(x, y, t, u = 0) = n(x, y, t)$  and  $n^e(x, y, t, u = 1) = n^r$ , with  $n^r$  a fixed reference matrix with entries  $(n^r)_{ji} = \delta_{ji}$ , where  $(\cdot)_{ji}$  represents the entry in the  $j$ th row and  $i$ th column of the relevant matrix. For notational brevity, in the following we will drop the superscript “e” in the extended matrix and simply write it as  $n$ , and the meaning of the matrix  $n$  should be clear from the context. This amounts to putting the three-dimensional spacetime on the boundary of a four-dimensional manifold  $D^3$ .

Then it is proposed in Ref. [15] that the WZW term on  $V_N$  can be given by the following (real-time) action:

$$S_{\text{WZW}}^{(N)}[n] = \frac{2\pi}{\Omega_4} \int_0^1 du \int d^3x \sum_{i,i'=1}^{N-4} \det(\tilde{n}_{(ii')}) \quad (3.3)$$

where the  $N$ -by- $N$  matrix  $\tilde{n}_{(ii')}$  is given by

$$\tilde{n}_{(ii')} = (n, \partial_x n_i, \partial_y n_i, \partial_t n_{i'}, \partial_u n_{i'}) \quad (3.4)$$

where  $n_i$  represents the  $i$ th column of  $n$  (the repeated indices  $i$  and  $i'$  are not summed over on the right hand side of Eq. (3.4)). That is, the first  $N - 4$  columns of  $\tilde{n}_{ii'}$  are just  $n$ , and its last 4 columns are derivatives of the columns of  $n$  arranged in the above way. More explicitly,

$$\det(\tilde{n}_{(ii')}) = \frac{1}{(N-4)!} \epsilon^{i_1 i_2 \dots i_{N-4}} \epsilon^{j_1 j_2 \dots j_N} n_{j_1 i_1} n_{j_2 i_2} \dots n_{j_{N-4} i_{N-4}} \partial_x n_{j_{N-3} i} \partial_y n_{j_{N-2} i} \partial_t n_{j_{N-1} i'} \partial_u n_{j_N i'} \quad (3.5)$$

where the  $\epsilon$ 's are the fully antisymmetric symbols with rank  $N - 4$  and  $N$ , respectively. And  $\Omega_4$  is the volume of a four-dimensional sphere  $S^4$ .

Taken together, the effective action of  $\text{SL}^{(N)}$  is given by

$$S^{(N)}[n] = S_0[n] + S_{\text{WZW}}^{(N)}[n] \quad (3.6)$$

The effective action of  $\text{SL}^{(N,k)}$  is the level- $k$  generalization of Eq. (3.6):

$$S^{(N,k)} = S_0 + k \cdot S_{\text{WZW}}^{(N)}. \quad (3.7)$$

## 3.2 Symmetry

In addition to the Poincaré symmetry, the actions in Eqs. (3.6) and (3.7) are invariant under an  $SO(N)$  transformation, which acts as:

$$n \rightarrow Ln, L \in SO(N), \quad (3.8)$$

and another  $SO(N - 4)$  transformation, which acts as

$$n \rightarrow nR, R \in SO(N - 4). \quad (3.9)$$

Notice that for even  $N$ , the two  $\mathbb{Z}_2$  centers  $L = -I_N$  and  $R = -I_{N-4}$  act identically. So  $S^{(N)}$  and  $S^{(N,k)}$  have a continuous symmetry group  $\tilde{I}^{(N)}$ , where  $\tilde{I}^{(N)} = (SO(N) \times SO(N-4))/\mathbb{Z}_2$  for even  $N$  and  $\tilde{I}^{(N)} = SO(N) \times SO(N-4)$  for odd  $N$ .



Besides this continuous symmetry,  $S^{(N)}$  and  $S^{(N,k)}$  also have discrete charge conjugation, reflection, and time reversal symmetries, i.e.,  $\mathcal{C}$ ,  $\mathcal{R}$  and  $\mathcal{T}$ . A particular implementation of these discrete symmetries for  $N \geq 6$  is

$$\begin{aligned} \mathcal{C} : n_{ji} &\rightarrow (-1)^{f_{ji}} n_{ji} \\ \mathcal{R} : n_{ji} &\rightarrow \begin{cases} n_{ji}, & j \leq N-1 \\ -n_{ji}, & j = N \end{cases} \\ \mathcal{T} : n_{ji} &\rightarrow \begin{cases} n_{ji}, & i \leq N-5 \\ -n_{ji}, & i = N-4 \end{cases} \end{aligned} \quad (3.10)$$

with  $f_{ji} = 1$  if  $(j = N \ \& \ i < N-4)$  or  $(j < N \ \& \ i = N-4)$ , and  $f_{ji} = 0$  otherwise. Notice that  $\mathcal{R}$  and  $\mathcal{T}$  also need to flip a spatial or temporal coordinate, respectively.

To combine the continuous symmetry with the discrete symmetry, an illuminating procedure is to enlarge the symmetry group  $SO(N)$  and  $SO(N-4)$  in  $\tilde{I}^{(N)}$  to  $O(N)$  and  $O(N-4)$ , respectively. However, the improper rotation of neither the  $O(N)$  nor the  $O(N-4)$  is a symmetry due to the WZW term, but the combination of an improper rotation with a reversal of a spatial or temporal coordinate is still a symmetry of the theory. Moreover, notice that the operation with  $L = -I_N \in O(N)$  and  $R = -I_{N-4} \in O(N-4)$  has no action on  $n$ , no matter whether  $N$  is even or odd. Hence, the full symmetry group of SL is the Poincaré symmetry plus

$$I^{(N)} = \frac{O(N)^T \times O(N-4)^T}{\mathbb{Z}_2} \quad (3.11)$$

The  $O(N)$  acts as  $n \rightarrow Ln$  with  $L \in O(N)$ , and the  $O(N-4)$  acts as  $n \rightarrow nR$  with  $R \in O(N-4)$ . The superscript ‘‘T’’ represents a locking condition: an improper rotation of either the  $O(N)$  or  $O(N-4)$  is a symmetry if and only if it is combined with a spacetime orientation reversal symmetry. This locking condition is one of the reasons why  $SL^{(N \geq 7)}$  may be non-Lagrangian (see Section 3.4.3). The  $\mathbb{Z}_2$  subgroup that is modded out is generated by  $(-I_N, -I_{N-4}) \in O(N) \times O(N-4)$ . For  $N = 5$ ,  $n$  reduces to a 5-component vector, and  $I^{(5)}$  is simply  $O(5)^T$  symmetry that acts by left multiplication on  $n$ , such that the improper rotation is combined with a spacetime orientation reversal symmetry.

### 3.3 Anomaly

In this section, we calculate the anomaly of SLs using the formulation of NLSM. The calculation essentially follows the general recipe in Ref. [71]. See also Refs. [51, 72, 73].

First, let us recall the concept of transgression in algebraic topology. We start with a fibration

$$F \xrightarrow{i} E \xrightarrow{p} B \quad (3.12)$$

with total space  $E$ , fibre  $F$  and base manifold  $B$ . Given an element  $\omega \in H^{d+1}(B, \mathbb{Z})$  such that  $p^*(\omega) = 0 \in H^{d+1}(E, \mathbb{Z})$ . Then for a specific cochain representative  $\bar{\omega} \in C^{d+1}(B, \mathbb{Z})$  representing  $\omega$ , we can find a cochain  $\tilde{\Gamma} \in C^d(E, \mathbb{Z})$  such that  $d\tilde{\Gamma} = p^*(\bar{\omega})$ . Restrict  $\tilde{\Gamma}$  to the fibre  $F$  we get an element  $\bar{\Gamma} \in C^n(F, \mathbb{Z})$  such that  $d\bar{\Gamma} = 0$ , i.e.,  $\bar{\Gamma} \in Z^n(F, \mathbb{Z})$  and defines an element  $\Gamma \in H^n(F, \mathbb{Z})$ . It is straightforward to check that  $\Gamma$  defined this way is independent of the choice of specific cochain representatives  $\bar{\omega}$  and  $\tilde{\Gamma}$ . We say that  $\omega$  is the *transgression* of  $\Gamma$ .

Now we go to a  $d$ -dimensional NLSM with the target manifold  $V$  and we specialize to the case where  $V = G/H$ , with natural  $G$  action on  $V$ . The WZW term in  $(d+1)$ -dimension is captured by an element  $\Gamma \in H^{d+1}(V, \mathbb{Z})$ . Suppose that we want to gauge the symmetry  $G$ . This means that we want to extend the WZW term  $\Gamma[f]$  to  $\tilde{\Gamma}[f, A]$  to account for the nontrivial background  $G$  gauge field. However,  $\tilde{\Gamma}[f, A]$  may not define a proper WZW term in the following sense. Consider the following fibration

$$G/H \rightarrow BH \rightarrow BG \quad (3.13)$$

where  $BG$  and  $BH$  are classifying spaces of  $G$  and  $H$ , respectively. Before gauging the fields of the NLSM correspond to maps  $f : \mathcal{M} \rightarrow G/H$  where  $\mathcal{M}$  is the spacetime manifold. Now after gauging the allowed fields do not have to be the original fields, i.e., do not have to correspond to maps  $f : \mathcal{M} \rightarrow G/H$ , since points on  $G/H$  can be identified by  $G$ -action. Still, they should correspond to maps  $\tilde{f} : \mathcal{M} \rightarrow BH$ . Then  $\tilde{\Gamma}$  should correspond to an element in  $C^d(BH, \mathbb{Z})$ . But  $\tilde{\Gamma}$  is not necessarily closed and we must have  $d\tilde{\Gamma} = p^*(\omega)$  for some  $\omega \in H^{d+2}(BG, \mathbb{Z})$ . This  $\omega$  can be thought of as the TPF of a bulk SPT that cancels the anomaly on the boundary, described by the NLSM. Hence the  $\omega$ , which is the transgression of  $\Gamma$ , is the anomaly we seek for.

For our purpose,  $V = SO(N)/SO(4)$  and we wish to gauge the full symmetry with symmetry group  $I^{(N)}$ . Therefore, we can take  $G$  to be  $I^{(N)}$  and  $H$  to be  $\frac{O(4)^T \times O(N-4)}{\mathbb{Z}_2}$ , which embeds into  $G$  as follows:

$$(g_1, g_2) \rightarrow \left( \left( \begin{array}{c} g_1 \\ g_2 \end{array} \right), g_2 \right) \quad (3.14)$$

where we treat  $g_1 \in O(4)$  and  $g_2 \in O(N-4)$  as a  $4 \times 4$  and  $(N-4) \times (N-4)$  matrix, which combine into one  $N \times N$  matrix in  $O(N)$ . Here the superscript ‘‘T’’ also represents the locking condition.

In the context of SLs, we have  $H^4(V, \mathbb{Z}) \cong \mathbb{Z}$  while  $H^i(V, \mathbb{Z}) = 0, i = 1, 2, 3$ . Consider the Serre spectral sequence associated to the fibration  $G/H \rightarrow BH \rightarrow BG$ , we immediately see that in this case the transgression of an element  $\Gamma \in H^4(V, \mathbb{Z})$  is the image of  $\Gamma$  under the differential at the fifth page, i.e.,

$$d_5 : H^4(V, \mathbb{Z}) \rightarrow H^5(BG, \mathbb{Z}_\rho) \quad (3.15)$$

where now we use  $\rho$  to emphasize that  $\mathbb{Z}$  is a module twisted by  $\rho : G \rightarrow \mathbb{Z}_2$  denoting the anti-unitary elements. Moreover, every element in  $H^5(BG, \mathbb{Z}_\rho)$  whose pullback to  $H^5(BH, \mathbb{Z}_\rho)$  is trivial must be in the image of  $d_5$ . Combining this fact with the fact that  $H^4(V, \mathbb{Z}) \cong \mathbb{Z}$ , we see that such elements must form a group  $\mathbb{Z}_n$  with some integer  $n$ . Therefore, to identify the transgression, we simply need to identify all elements in  $H^5(BG, \mathbb{Z}_\rho)$  such that its pullback to  $H^5(BH, \mathbb{Z}_\rho)$  is trivial. Then the transgression of  $k \in H^4(V, \mathbb{Z})$  is nothing but  $k$  times the generator of such elements.<sup>1</sup> In this way, we obtain the anomaly of  $\text{SL}^{(N,k)}$  described by a NLSM supplemented with a level  $k$  WZW term.

From the explicit calculation of group cohomology, we see that for  $k = 1$ , when  $N$  is odd the anomaly is  $\mathbb{Z}_2$  classified, while when  $N$  is even the anomaly is  $\mathbb{Z}_4$  classified. To obtain a more explicit formula for the anomaly, we can consider the projection

$$p_{\text{SL}} : \tilde{I}^{(N)} \equiv O(N)^T \times O(N-4)^T \rightarrow \frac{O(N)^T \times O(N-4)^T}{\mathbb{Z}_2} \quad (3.16)$$

and the pullback of  $\Omega$  induced by the projection is given by  $\tilde{\Omega} = e^{i\pi\tilde{L}} \in H^4(\tilde{I}^{(N)}, \text{U}(1)_\rho) \cong H^5(\tilde{I}^{(N)}, \mathbb{Z}_\rho)$ , where

$$\tilde{L} = w_4^{O(N)} + w_4^{O(N-4)} + \left[ w_2^{O(N-4)} + \left( w_1^{O(N-4)} \right)^2 \right] \left( w_2^{O(N)} + w_2^{O(N-4)} \right) + \left( w_1^{O(N-4)} \right)^4 \quad (3.17)$$

supplemented with a constraint  $w_1^{TM} + w_1^{O(N)} + w_1^{O(N-4)} = 0 \pmod{2}$ , which originates from the locking between the spacetime orientation reversals and the improper rotations of  $O(N)$  and  $O(N-4)$ . Here  $w_i^{O(N)}$ ,  $w_i^{O(N-4)}$  and  $w_i^{TM}$  are the  $i$ -th Stiefel-Whitney classes of the  $O(N)$ ,  $O(N-4)$  gauge bundles and the tangent bundle of the spacetime manifold, respectively.

---

<sup>1</sup>In principle there can be multiple generators, which have to be differentiated by e.g., explicit topological invariants. For our purpose, when  $N$  is odd, the anomaly is  $\mathbb{Z}_2$  classified and we do not need to address this issue. When  $N$  is even, the anomaly is  $\mathbb{Z}_4$  classified, but in most of our applications we will pullback the element to a  $\mathbb{Z}_2$  quotient group, where the images of the two  $\mathbb{Z}_4$  generators are the same. Therefore, fortunately in this thesis we do not have to address this ambiguity.

Still, for even  $N$ ,  $\tilde{\Omega}$  does not capture the full anomaly since the anomaly is  $\mathbb{Z}_4$  classified. Especially, when  $N$  is even and  $k$  is an odd multiple of 2, there is still nontrivial anomaly but its pullback to  $\tilde{I}^{(N)}$  is trivial. The anomaly can only be trivialized for even  $N$  with  $k$  a multiple of 4.

For odd  $N$ ,  $\tilde{\Omega}$  completely characterizes  $\Omega$ . Moreover, because  $O(N)^T = SO(N) \times \mathbb{Z}_2^T$ ,  $H^4(G_{\text{IR}}, U(1)_\rho)$  has the structure of  $\mathbb{Z}_2^k$  with some  $k \in \mathbb{N}$ , and there exists  $L_{\text{IR}} \in H^4(G_{\text{IR}}, \mathbb{Z}_2)$  such that  $\Omega_{\text{IR}} = e^{i\pi L_{\text{IR}}}$ . Now notice that the pullback from  $H^4(G_{\text{IR}}, \mathbb{Z}_2)$  to  $H^4(\tilde{G}_{\text{IR}}, \mathbb{Z}_2)$  induced by  $p_{\text{SL}}$  is injective, and hence we can uniquely identify  $L_{\text{IR}}$  from  $\tilde{L}_{\text{IR}}$ . The result is

$$L_{\text{IR}} = w_4^{SO(N)} + w_4^{SO(N-4)} + \left( w_2^{SO(N)} + w_2^{SO(N-4)} \right) w_2^{SO(N-4)} + \begin{cases} w_1^2 w_2^{SO(N)}, & N = 1 \pmod{8} \\ w_1^2 w_2^{SO(N-4)}, & N = 3 \pmod{8} \\ w_1^2 (w_2^{SO(N)} + w_1^2), & N = 5 \pmod{8} \\ w_1^2 (w_2^{SO(N-4)} + w_1^2), & N = 7 \pmod{8} \end{cases} \quad (3.18)$$

where  $w_i^{SO(N)}$  and  $w_i^{SO(N-4)}$  are the  $i$ -th Stiefel-Whitney class of the  $SO(N)$  and  $SO(N-4)$  gauge bundles. Considering enlarging  $SO(N)$  and  $SO(N-4)$  to  $O(N)$  and  $O(N-4)$ ,  $w_1$  is sum of the first Stiefel-Whitney classes of the  $O(N)$  and  $O(N-4)$  gauge bundles. Due to the locking between spacetime orientation reversals and improper rotations of  $O(N)$  and  $O(N-4)$ ,  $w_1$  can also be viewed as the first Stiefel-Whitney class of the tangent bundle of the spacetime manifold.

## 3.4 Dynamics of Stiefel Liquids

In this section, we first argue that the special case  $\text{SL}^{(5)}$  and  $\text{SL}^{(6)}$  correspond to the canonical examples of DQCP and  $U(1)$  DSL, which partly motivate the proposal of SL. We then discuss some dynamical properties of Stiefel Liquids, based on both numerics and theoretical arguments.

### 3.4.1 $\text{SL}^{(5)}$ : DQCP

The classic DQCP was proposed as a critical theory for a quantum phase transition between a Neel antiferromagnetic order (AF) and a valence-bond solid (VBS) on a square lattice [18, 19]. This transition is considered to be beyond the Landau-Ginzburg-Wilson-Fisher

paradigm if it is continuous, since the symmetry respected by either of these two phases is not a subgroup of the symmetry of the other.

The original formulation of the DQCP is in terms of two flavors of bosons coupled to a dynamical U(1) gauge field, and over the years many dual formulations have been proposed [20, 21]. Especially, there is a formulation written in terms of a NLSM with target manifold  $S^4$  supplemented with a nontrivial WZW term. Recall that  $S^4$  is precisely the Stiefel manifold  $V_5$ , then we immediately see that  $SL^{(5)}$  exactly corresponds to DQCP.

In the context of DQCP, the field  $\mathbf{n}$  is a 5-component unit vector, whose first 3 and last 2 components can be thought of as the order parameters of the AF and the VBS, respectively. So this is a formulation directly based on local DOFs.

The Neel-VBS transition is driven by a rank-2 anisotropy term  $\lambda(n_1^2 + n_2^2 + n_3^2 - n_4^2 - n_5^2)$ , with  $\lambda < 0$  favoring the Neel order and  $\lambda > 0$  favoring the VBS order. At weak coupling the sigma model orders spontaneously and the Neel-VBS transition driven by the anisotropy will be first order. The DQCP, as a continuous Neel-VBS transition, then requires a nontrivial fixed point at strong coupling. This fixed point must have a full emergent  $O(5)^T$  symmetry with anomaly  $\exp(\pi i w_4^{O(5)^T})$ .

It is now widely accepted [21, 74–77] that the hypothesized strong-coupling fixed point does not exist, and the theory flows all the way to the weakly coupled, first-order transition regime. However, there exists a region, around a nontrivial coupling strength  $g^*$ , where the RG flow is slow, also known as “walking” [78]. Consequently, the system behaves almost like a critical point up to a large length scale. A theory for the walking behavior in the sigma model has been proposed in Refs. [75, 76]. In the critical regime, which can be approximated by a CFT, the relevant operators are the  $SO(5)$  vector and symmetric traceless rank-2 tensor, and possibly time-reversal breaking  $SO(5)$  singlet.

### 3.4.2 $SL^{(6)}$ : U(1) Dirac spin liquid

The U(1) DSL was introduced as a critical quantum liquid that can emerge in certain spin systems [22, 23]. We wish to argue that it corresponds precisely to  $SL^{(6)}$ . Its standard formulation is in terms of 4 flavors of gapless Dirac fermions minimally coupled to a dynamical U(1) gauge field, with the Lagrangian

$$\mathcal{L} = \sum_{i=1}^4 \bar{\psi}_i i \not{D}_a \psi_i + \frac{1}{4e^2} f_{\mu\nu} f^{\mu\nu} \quad (3.19)$$

where  $\not{D}_a$  is the covariant derivative of the Dirac fermions,  $\psi$ , which are coupled to the dynamical U(1) gauge field,  $a$ , whose field strength is  $f_{\mu\nu} = \partial_\mu a_\nu - \partial_\nu a_\mu$ . The Dirac fermion  $\psi$  is *not* a local (gauge invariant) excitation here. Naively the simplest local operators are fermion biliners like  $\bar{\psi}_i \psi_j$ . It turns out that the most important local operators are the monopole operators [79, 80] – these are operators that insert U(1) gauge flux, in units of  $2\pi$ , into the system.

The symmetries of the DSL are discussed in detail in Refs. [79–81]. In particular, it indeed has an  $\tilde{I}^{(6)} = (O(6)^T \times O(2)^T)/Z_2$  symmetry. In particular, the Dirac fermions transform under a flavor  $SU(4)$  which is the spinor group of the  $SO(6)$ . The fermion bilinears  $\bar{\psi}_i \psi_j$  form a “singlet  $\oplus$  adjoint” representation under  $SO(6)$ . The  $U(1)_{\text{top}} \in O(2)$  corresponds to the conservation of gauge flux, with conserved current  $j_\mu = \epsilon_{\mu\nu\lambda} \partial^\nu a^\lambda / (2\pi)$  (the subscript “top” is due to the fact that this current conservation does not rely on the detailed equations of motion and is therefore “topological”). By definition only monopole operators are charged under the  $U(1)_{\text{top}}$ . It turns out [79] that the most fundamental monopoles also transform as a vector under the  $SO(6)$ . More concretely, the monopole can be represented by a 6-component complex bosonic field  $\Phi$ , such that the  $SO(6)$  rotates the components of  $\Phi$ , and the  $U(1)_{\text{top}}$  acts by multiplying  $\Phi$  by a phase factor. Hence we can identify the monopole operators  $\Phi$  as the fields  $n$  appearing explicitly in the formulation of NLSM. Therefore, the DOF and symmetries match between the gauge-theoretic formulation and the NLSM formulation

Naturally, the  $\Phi$  operators are supposed to be the most fundamental local operators in the theory, in the sense that any other local operator can be built up using the  $\Phi$ 's. In particular, according to the formulation of NLSM, we can classify (the most relevant) operators according to the representations of these operators under  $SO(6)$  and  $SO(2)$  symmetry, and denote them as  $(R_L, R_R)$ , where  $R_L$  and  $R_R$  denote representations under  $SO(6)$  and  $SO(2)$ , respectively. In this notation the  $\Phi$  operators can be denoted as  $(V_L, V_R)$ , where  $V_L$  and  $V_R$  stand for vector representations under  $SO(6)$  and  $SO(2)$ , respectively. The singlet mass operator  $\bar{\psi}\psi$  is identified as

$$\bar{\psi}_i \psi_i \sim i \epsilon^{abcdef} (\Phi_a^\dagger \Phi_b - \Phi_a \Phi_b^\dagger) (\Phi_c^\dagger \Phi_d - \Phi_c \Phi_d^\dagger) (\Phi_e^\dagger \Phi_f - \Phi_e \Phi_f^\dagger)$$

where  $a, b, c, d, e, f = 1, 2, 3, 4, 5, 6$ . This is a singlet under  $SO(6)$  and  $SO(2)$  but breaks time-reversal symmetry. The adjoint mass operator (i.e.,  $\bar{\psi}_i \psi_j - \bar{\psi}_k \psi_k \delta_{ij}/4$ ) is identified as the rank-2 antisymmetric tensor of  $\Phi$  that is neutral under the  $U(1)_{\text{top}}$ , i.e.,  $i(\Phi_a^\dagger \Phi_b - \Phi_b^\dagger \Phi_a)$ . Hence, we can identify the adjoint mass operator as the operator  $(A_L, A_R)$  in the formulation of NLSM, where  $A_L$  and  $A_R$  represent antisymmetric rank-2 tensor of  $SO(6)$  and  $SO(2)$ , respectively.

Various numerical studies of DSL (e.g. see a recent conformal bootstrap study [82] and references therein) give (indirect) support that the only relevant operators in these states are either conserved currents as well as the three operators listed above, i.e., time-reversal-breaking operators (singlet mass operator), or Lorentz scalar operators in the representations  $(V_L, V_R)$  ( $\Phi$ ) and  $(A_L, A_R)$  (adjoint mass). The effects of these relevant operators are complicated: some of them change the emergent order of the state, but others do not (see Appendix 3.A for more details).

### 3.4.3 $\text{SL}^{(N \geq 7)}$ : non-Lagrangian Theory

The dynamics of  $\text{SL}^{(N \geq 7)}$  have not been fully established yet. In particular, we cannot find any gauge-theoretic formulation for  $\text{SL}^{(N)}$  with  $N \geq 7$ . In fact, due to their delicate symmetry structure, we conjecture that the conformally invariant fixed points corresponding to  $\text{SL}^{(N \geq 7)}$  are non-Lagrangian, i.e., they have no description in terms of a weakly-coupled renormalizable continuum Lagrangian at any scale.

A suggestive argument, but not rigorous proof, supporting that  $\text{SL}^{(N > 6)}$  are non-Lagrangian is as follows. The key observation is that it appears unlikely for such Lagrangians to realize the  $SO(N)$ ,  $SO(N - 4)$  and reflection symmetries of  $\text{SL}^{(N)}$ . To see it, let us start with even  $N$ . Usually in such a Lagrangian, symmetries like  $SO(N)$  and  $SO(N - 4)$  are flavor symmetries, and there is a reflection symmetry that commutes with flavor symmetries. However, due to the locking between spacetime orientation reversals and improper rotations of  $O(N)$  and  $O(N - 4)$ ,  $\text{SL}^{(N)}$  has no such a reflection symmetry. This suggests that  $SO(N)$  and  $SO(N - 4)$  cannot be simultaneously flavor symmetries. In the special case of  $N = 6$ , which does have a renormalizable Lagrangian description, indeed only  $SO(6)$  but not  $SO(2)$  can be identified as a flavor symmetry. In this example, the  $SO(2)$  is realized as the flux conservation symmetry in the gauge theoretic formulation. For  $N > 6$ , there is no known generalization of the flux conservation symmetry that can give rise to symmetries like  $SO(N - 4)$ . This indicates  $\text{SL}^{(N > 6)}$  with an even  $N$  may be non-Lagrangian. Due to the cascade structure of SLs [15], it also suggests all  $\text{SL}^{(N > 6)}$  are non-Lagrangian.

We emphasize that the above is just a suggestive argument, but not a rigorous proof. There can be ways to get around the above obstruction, by, e.g., implementing some symmetries via dualities, considering Lagrangians in very complicated forms, showing that Lagrangians with smaller symmetries can have emergent symmetries of the SLs, etc. After finding a Lagrangian that can realize the symmetries of a SL, one still needs to make sure that its anomaly and low-energy dynamics match with the SL, which appears also challeng-

ing. If all these nontrivial challenges can be overcome and a renormalizable Lagrangian can be found to describe the SL at the end, we believe this process can generate new insights and teach us some valuable general lessons of quantum field theories.

Numerical studies [82] suggests that the only relevant operators in these states are the same as the case for  $N = 6$ , i.e., they are either conserved currents, or time-reversal-breaking operators, or Lorentz scalar operators in the representations  $(V_L, V_R)$  and  $(A_L, A_R)$ , where  $V_L$  ( $V_R$ ) and  $A_L$  ( $A_R$ ) represent the vector and antisymmetric rank-2 tensor of  $SO(N)$  ( $SO(N-4)$ ), respectively. We discuss the effects of these relevant operators in more detail in Appendix 3.A.

### 3.A Effects of Relevant Operators on SL

In this appendix, we discuss the effects of relevant operators on the DQCP ( $SL^{(5)}$ ), DSL ( $SL^{(6)}$ ) and  $SL^{(7)}$ . Because the low-energy dynamics of these states are not fully settled down, this discussion is also conjectural, and it is important to study these issues in a more rigorous manner in the future. However, given our understanding of these states, we believe the expectations below are reasonable.

For all SLs, the  $(V_L, V_R)$  operator (or the  $SO(5)$  vector for DQCP) should change the emergent order of the state. Due to the cascade structure among SLs [15], it is natural that this operator will just drive  $SL^{(N)}$  to  $SL^{(N-1)}$  (for DQCP, it simply gaps out the state). The time-reversal breaking operator that is a flavor singlet is likely to drive the state into a semion topological order, and this expectation is supported by the gauge-theoretic formulations of DQCP and DSL, as well as the fact that the semion topological order can match the anomaly of  $SL^{(N)}$  if time reversal is broken (for all  $N \geq 5$ ) [15]. The  $(A_L, A_R)$  operator (for all  $N \geq 6$ ) is expected to convert  $SL^{(N)}$  into certain spontaneous-symmetry-breaking state, as supported from the gauge-theoretic formulation of DSL [20, 81, 83]. For DQCP, the traceless symmetric rank-2 tensor of  $SO(5)$  drives the state into a spontaneous-symmetry-breaking state, and this operator is the tuning operator of the Neel-VBS transition in the standard realization of DQCP [18, 19]. All these operators change the emergent order of the states.

The remaining relevant operators to be discussed are the conserved current operators, whose effects on various states are complicated. It turns out that some of them can change the emergent order of the states, while others only shift the “zero momenta”.

The simplest way to discuss it is perhaps to start from DSL, which has a relatively



simple gauge-theoretic formulation in terms of  $N_f = 4$  QED<sub>3</sub>:

$$\mathcal{L} = \sum_{i=1}^4 \bar{\psi}_i i \not{D}_a \psi_i - \frac{1}{4e^2} f_{\mu\nu} f^{\mu\nu} \quad (3.20)$$

There are conserved currents due to the  $SO(6)$  and  $SO(2)$  symmetries, where a natural basis of the  $SO(6)$  currents is  $\bar{\psi} \gamma_\mu T^{su(4)} \psi$ , with  $\gamma_\mu$  the Dirac matrices and  $T^{(su(4))}$  the generators of  $su(4)$  in its fundamental representation, and the  $SO(2)$  currents are  $\epsilon_{\mu\nu\lambda} \partial^\nu a^\lambda / (2\pi)$ , with  $a$  the emergent U(1) gauge field. If the time component of the  $SO(6)$  currents is added as a perturbation to the DSL, the Dirac fermions will be doped and acquire a finite Fermi surface, so the emergent order of the state changes. If the time component of the  $SO(2)$  currents is added, the Dirac fermions will experience magnetic fields, Landau levels will form, and the emergent order of the state also changes. Below we discuss the effect of the spatial components of the currents.

For the  $SO(6)$  spatial currents, depending on the choice of  $T^{(su(4))}$  and  $\gamma_\mu$ , various effects can be triggered. For example, the current  $\bar{\psi} \gamma_x \sigma_{30} \psi$  merely shifts the positions of the Dirac cones in the momentum space in a flavor-dependent way, which does not really change the emergent order of DSL (here  $\sigma_{ij} \equiv \sigma_i \otimes \sigma_j$ , where  $\sigma_{i=0,1,2,3}$  are the identity and standard Pauli matrices). The same is true for  $\bar{\psi} (\gamma_x \sigma_{30} + \gamma_y \sigma_{03}) \psi$ . However, as another example,  $\bar{\psi} (\gamma_x \sigma_{23} + \gamma_y \sigma_{33}) \psi$  actually converts the 4 Dirac cones into 2 pairs of quadratic band touching (and another 2 pairs of gapped bands), which does change the emergent order of the state. By examining the effect of different spatial currents, one can see more complicated patterns. Although a systematic description of the effects of these spatial currents is lacking, it can be analyzed in a case-by-case manner. These spatial currents can all be converted into the language of  $SL^{(6)}$ , in terms of the  $6 \times 2$  matrix  $n$ . For example, using Appendix E of Ref. [15], we see that  $\bar{\psi} \gamma_x \sigma_{30} \psi \sim n_{3i} \partial_x n_{4i}$ ,  $\bar{\psi} (\gamma_x \sigma_{30} + \gamma_y \sigma_{03}) \psi \sim n_{3i} \partial_x n_{4i} + n_{1i} \partial_y n_{2i}$ , and  $\bar{\psi} (\gamma_x \sigma_{23} + \gamma_y \sigma_{33}) \psi \sim n_{4i} \partial_x n_{6i} + n_{5i} \partial_y n_{6i}$ .

Next we turn to the  $SO(2)$  spatial current, which in the language of  $SL^{(6)}$  is  $n_{i1} \partial_{x,y} n_{i2}$ , and in the gauge theory is the electric field of the emergent U(1) gauge field. It is not obvious what this perturbation does to the DSL. However, we argue that its effect is also to shift the zero momenta. To see it, we consider  $N_f = 2$  QED<sub>3</sub>, with Lagrangian

$$\mathcal{L} = \sum_{i=1}^2 \bar{\psi}_i i \not{D}_a \psi_i - \frac{1}{4e^2} f_{\mu\nu} f^{\mu\nu} \quad (3.21)$$

This theory is argued to describe the easy-plane DQCP, which has an emergent  $O(4)$  unitary symmetry (not to be confused with the DQCP we have been discussing, which has

an emergent  $SO(5)$  unitary symmetry) [21]. In this theory,  $\bar{\psi}\gamma_{x,y}\sigma_3\psi$  clearly only shifts the zero momenta without changing the emergent order of the state. On the other hand, the improper  $\mathbb{Z}_2$  rotation of the  $O(4)$  symmetry maps this operator into the electric fields of the emergent  $U(1)$  gauge fields [21], which means that the electric fields also play the role of shifting the zero momenta without changing the emergent order. So we propose that in DSL (i.e.,  $SL^{(6)}$ ), the  $SO(2)$  spatial currents also only shift the zero momenta, but maintain the emergent order.

Now we turn to DQCP ( $SL^{(5)}$ ), which has a couple of gauge-theoretic formulations [21]. From any of these formulations, one can see that the time component of the  $SO(5)$  currents changes the emergent order of the state. The formulation that has a manifest  $O(5)^T$  symmetry is an  $SU(2)$  gauge theory with 2 flavors of Dirac fermions, where the  $SO(5)$  symmetry is the flavor symmetry of these Dirac fermions. Under similar consideration of the  $SO(6)$  spatial currents in DSL, we see that the effects of the  $SO(5)$  spatial currents in DQCP are also complicated and need to be analysed in a case-by-case manner: some of them changes the emergent order of the states, while others only shift the zero momenta without changing the emergent order.

We remark that the effects of the spatial currents actually impose very strong constraints on the possible results of our anomaly-based framework of emergibility. Within this framework, it is easy to see that all realizations of DQCP and DSL on  $p6m \times O(3)^T$  and  $p4m \times O(3)^T$  symmetric lattice spin systems must have all entries of  $n$  locating at some high-symmetry momenta in the Brillouin zone, because all possible symmetry embedding patterns satisfy this condition. This means that in all realizations, it is impossible to have a spatial current operator that is allowed by the microscopic symmetries and can shift the zero momenta. As we have explicitly checked, this is indeed true for all realizations obtained in our anomaly-based framework, which can be viewed as a highly nontrivial sanity check of this framework – It nicely corroborates the validity of the hypothesis of emergibility, the proposal that DSL can indeed be described by  $SL^{(6)}$ , and the dynamics of DSL.

Finally, we turn to  $SL^{(7)}$ , whose low-energy dynamics is poorly understood so far. It is still likely that the time component of the  $SO(7)$  and  $SO(3)$  currents will change the emergent order. For the spatial currents, we propose the following rule. Writing an  $SO(7)$  spatial current operator as a sum of terms of the form  $n_{i_1j}\partial_{x,y}n_{i_2j}$ , then we consider the effect of the same operator in DSL (it turns out that all such operators allowed by our microscopic symmetries only involve at most 4 rows of  $n$ , so its corresponding operator in DSL can always be found). If this operator changes the emergent order of DSL, then it also changes the emergent order of  $SL^{(7)}$ , and if it only shifts the zero momenta of DSL, it also only shifts the zero momenta of  $SL^{(7)}$ . For the  $SO(3)$  spatial currents, it can be expanded

as a sum as  $\sim a_1 n_{i1} \partial_x n_{i2} + a_2 n_{i1} \partial_x n_{i3} + a_3 n_{i2} \partial_x n_{i3} + b_1 n_{i1} \partial_y n_{i2} + b_2 n_{i1} \partial_y n_{i3} + b_3 n_{i2} \partial_y n_{i3}$ . We propose to first convert it into an  $SO(7)$  spatial current  $\sim a_1 n_{1i} \partial_x n_{2i} + a_2 n_{1i} \partial_x n_{3i} + a_3 n_{2i} \partial_x n_{3i} + b_1 n_{1i} \partial_y n_{2i} + b_2 n_{1i} \partial_y n_{3i} + b_3 n_{2i} \partial_y n_{3i}$ . If this  $SO(7)$  spatial current changes the emergent order (only shifts zero momenta) using the the above criterion, then the original  $SO(3)$  spatial current also changes the emergent order (only shifts zero momenta).

The above proposal is of course conjectural, and more rigorous work is needed to fully settle it down. However, this proposal is supported by our results of anomaly-matching. We have checked all realizations of  $SL^{(7)}$  obtained from the anomaly-based framework of emergibility, and found that the current operators that can shift zero momenta (according to the above proposal) are allowed by microscopic symmetries in a realization if and only if this realization belongs to a family where the momenta of some entries of  $n$  can change continuously.

# Chapter 4

## Anomaly of $(2 + 1)$ -Dimensional Symmetry-Enriched Topological Order

In this chapter, we construct a  $(3 + 1)$ -d TQFT given the data of a UMTC and  $G$ -action on the UMTC. This TQFT is supposed to correspond to the SPT which hosts the symmetry-enriched topological order described by the UMTC with given  $G$ -action on its boundary. The partition functions of this TQFT on certain representative manifolds equipped with appropriate  $G$  bundles give the anomaly indicators of  $(2 + 1)$ -d bosonic topological orders enriched with a finite group symmetry  $G$ , which may be Abelian or non-Abelian, contain anti-unitary elements and permute anyons. Via this framework, besides reproducing the known anomaly indicators of  $G = \mathbb{Z}_2^T$ , we have calculated the anomaly indicators of  $G = \mathbb{Z}_2 \times \mathbb{Z}_2$  and  $G = \mathbb{Z}_2^T \times \mathbb{Z}_2^T$ , which have not been previously derived as far as we know. The usage of these anomaly indicators have been demonstrated in the example of all-fermion  $\mathbb{Z}_2$  topological orders. This framework is generalized to the case where the relevant symmetry is a connected Lie group, and we use it to derive the anomaly indicator for  $SO(N)$ . As a byproduct, we also obtain the expressions of the Hall conductance of an  $SO(N)$  symmetric topological order, written in terms of data characterizing this symmetry-enriched topological order. We explain how to use these results to calculate the anomaly indicators for some other symmetry groups without the need of further calculation, and explicitly derive the anomaly indicators for symmetry groups  $O(N)^T$  and  $SO(N) \times \mathbb{Z}_2^T$ . In particular, we show that certain anomalies associated with these symmetries cannot be realized by any topological order.

This chapter is adapted from Ref. [2]

## 4.1 Review of topological order with symmetry $G$

### 4.1.1 Review of UMTC notation

In this subsection we briefly review relevant concepts and notations that we use to describe UMTCs. For a more comprehensive review of these concepts and notations, see e.g., Refs. [60, 84, 85] for a more physics oriented introduction, or Refs. [11, 12, 86, 87] for a more mathematical treatment.

A category consists of objects and morphisms between those objects. In a UMTC  $\mathcal{C}$ , there is a finite set of simple objects  $a$ . They are referred to as (simple) anyons in the context of topological orders. The set of morphisms  $\text{Hom}(a, b)$  between two objects  $a$  and  $b$  in a UMTC  $\mathcal{C}$  forms a  $\mathbb{C}$ -linear vector space. The vector space is referred to as the topological state space in the context of topological order. For example,  $\text{Hom}(a, b)$  can be viewed as the Hilbert space of states on a 2-sphere that hosts anyons  $a$  and  $\bar{b}$  (see Eq. (4.35)).

Moreover, a UMTC  $\mathcal{C}$  has the structure of fusion and braiding. Fusion means that there is a bifunctor  $\times$  such that acting it on anyons  $a$  and  $b$  we have

$$a \times b \cong \sum_c N_{ab}^c c \quad (4.1)$$

where  $N_{ab}^c$  is interpreted as the dimension of the topological state space of two anyons  $a$  and  $b$  fusing into a third anyon  $c$ . There are two related vector spaces,  $V_{ab}^c$  and  $V_c^{ab}$ , referred to as the fusion and splitting vector spaces, respectively. The two vector spaces are dual to each other, and depicted graphically as:

$$(d_c/d_a d_b)^{1/4} \begin{array}{c} c \\ \uparrow \\ \mu \\ \swarrow \quad \searrow \\ a \quad b \end{array} = \langle a, b; c |_\mu \in V_{ab}^c, \quad (4.2)$$

$$(d_c/d_a d_b)^{1/4} \begin{array}{c} a \quad b \\ \swarrow \quad \searrow \\ \mu \\ \uparrow \\ c \end{array} = |a, b; c\rangle_\mu \in V_c^{ab}, \quad (4.3)$$

where  $\mu = 1, \dots, N_{ab}^c$ ,  $d_a$  is the *quantum dimension* of  $a$ , and the factors  $\left(\frac{d_c}{d_a d_b}\right)^{1/4}$  are a normalization convention for the diagrams.

In this thesis, we will use the convention that the splitting space is referred to as the vector space, corresponding to “ket” in Dirac’s notation, while the fusion space is the dual

vector space, corresponding to “bra” in Dirac’s notation. Diagrammatically, inner products of the vector space are formed by stacking vertices so the fusing/splitting lines connect

$$\begin{array}{c} c \\ \uparrow \\ \mu \\ \circlearrowleft \\ a \quad b \\ \circlearrowright \\ c' \quad \mu' \\ \uparrow \end{array} = \delta_{cc'} \delta_{\mu\mu'} \sqrt{\frac{d_a d_b}{d_c}} \quad \begin{array}{c} \zeta \\ \uparrow \end{array} \quad (4.4)$$

which can be applied inside more complicated diagrams.

More generally, for any integer  $n$  and  $m$  there are vector spaces  $V_{b_1, b_2, \dots, b_m}^{a_1, a_2, \dots, a_n}$ , which are referred to as the fusion space of  $m$  anyons into  $n$  anyons. These vector spaces have a natural basis in terms of tensor products of the elementary splitting spaces  $V_c^{ab}$  and fusion spaces  $V_{ab}^c$ . For instance, we have

$$V_d^{abc} \cong \sum_e V_e^{ab} \otimes V_d^{ec} \cong \sum_f V_d^{af} \otimes V_f^{bc} \quad (4.5)$$

The two vector spaces are related to each other by a basis transformation referred to as  $F$ -symbols, which is diagrammatically shown as follows

$$\begin{array}{c} a \quad b \quad c \\ \swarrow \quad \searrow \\ \alpha \quad \beta \\ \downarrow \\ e \\ \downarrow \\ d \end{array} = \sum_{f, \mu, \nu} [F_d^{abc}]_{(e, \alpha, \beta), (f, \mu, \nu)} \begin{array}{c} a \quad b \quad c \\ \swarrow \quad \searrow \\ \nu \quad \mu \\ \downarrow \\ d \end{array} \quad (4.6)$$

The basis transformations are required to be unitary transformations, i.e.

$$\left[ (F_d^{abc})^{-1} \right]_{(f, \mu, \nu)(e, \alpha, \beta)} = \left[ (F_d^{abc})^\dagger \right]_{(f, \mu, \nu)(e, \alpha, \beta)} = [F_d^{abc}]_{(e, \alpha, \beta)(f, \mu, \nu)}^* \quad (4.7)$$

There is also a trivial anyon denoted by  $1$  such that  $1 \times a = a \times 1 = a$ . We denote  $\bar{a}$  as the anyon conjugate to  $a$ , for which  $N_{a\bar{a}}^1 = 1$ , i.e.

$$a \times \bar{a} = 1 + \dots \quad (4.8)$$

Note that  $\bar{a}$  is unique for a given  $a$ .

The  $R$ -symbols define the braiding properties of the anyons, and are defined via the the following diagram:

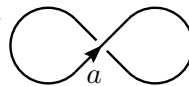
$$\begin{array}{c} a \quad b \\ \swarrow \quad \searrow \\ \mu \\ \downarrow \\ c \uparrow \end{array} = \sum_\nu [R_c^{ab}]_{\mu\nu} \begin{array}{c} a \quad b \\ \swarrow \quad \searrow \\ \nu \\ \downarrow \\ c \uparrow \end{array} \quad (4.9)$$

Under a basis transformation,  $\Gamma_c^{ab} : V_c^{ab} \rightarrow V_c^{ab}$ , the  $F$  and  $R$  symbols change according to:


$$\begin{aligned} F_{def}^{abc} &\rightarrow \tilde{F}_d^{abc} = \Gamma_e^{ab} \Gamma_d^{ec} F_{def}^{abc} [\Gamma_f^{bc}]^\dagger [\Gamma_d^{af}]^\dagger \\ R_c^{ab} &\rightarrow \tilde{R}_c^{ab} = \Gamma_c^{ba} R_c^{ab} [\Gamma_c^{ab}]^\dagger. \end{aligned} \quad (4.10)$$

where we have suppressed splitting space indices and dropped brackets on the  $F$ -symbol for shorthand. In this thesis, we refer to this basis transformation as a *vertex basis transformation*.

On the other hand, physical quantities, like the topological twist  $\theta_a$  and the modular  $S$ -matrix  $S_{ab}$ , should always be basis-independent combinations of the data. The *topological twist*  $\theta_a$  is defined via the diagram:

$$\theta_a = \theta_{\bar{a}} = \sum_{c,\mu} \frac{d_c}{d_a} [R_c^{aa}]_{\mu\mu} = \frac{1}{d_a} \text{diagram} \quad (4.11)$$


Finally, the *modular S-matrix*  $S_{ab}$ , is defined as

$$S_{ab} = D^{-1} \sum_c N_{\bar{a}b}^c \frac{\theta_c}{\theta_a \theta_b} d_c = \frac{1}{D} \text{diagram} \quad , \quad (4.12)$$


where  $D = \sqrt{\sum_a d_a^2}$  is the *total dimension* of the UMTC.

## 4.1.2 Global symmetry

We now consider a UMTC  $\mathcal{C}$  which is equipped with a global symmetry group  $G$ . Mathematically speaking, by definition,  $G$  associates a monoidal functor  $\rho_{\mathbf{g}}$  modulo natural isomorphism to each  $\mathbf{g} \in G$ , which should satisfy various consistency conditions. In this subsection we break down the definition and review the concepts and notations related to global symmetry  $G$ . For a more comprehensive review, see e.g., Refs. [60, 86, 88].

First of all, as a functor,  $\rho_{\mathbf{g}}$  acts on the anyon labels and the topological state spaces. For an individual element  $\mathbf{g} \in G$ ,  $\mathbf{g}$  can permute the anyons and we use  $\mathfrak{g}a$  to denote the (simple) anyon we get after the  $\mathbf{g}$  action on the (simple) anyon labeled by  $a$ . Moreover,  $\mathbf{g}$  also has an action on the topological state space, which is a  $\mathbb{C}$ -linear or  $\mathbb{C}$ -anti-linear operator on the fusion space, depending on whether  $\mathbf{g}$  is unitary or anti-unitary. We denote this action on individual topological state space as  $\rho_{\mathbf{g}}$  as well:

$$\rho_{\mathbf{g}} : V_c^{ab} \rightarrow V_{\mathfrak{g}c}^{\mathfrak{g}a \mathfrak{g}b}. \quad (4.13)$$

And in particular we have

$$N_{\mathfrak{g}_a \mathfrak{g}_b}^{\mathfrak{g}_c} = N_{ab}^c \quad (4.14)$$

To account for anti-unitary symmetry, we associate a  $\mathbb{Z}_2$  grading  $q(\mathfrak{g})$  (and related  $\sigma(\mathfrak{g})$ ) as follows

$$q(\mathfrak{g}) = \begin{cases} 0 & \text{if } \mathfrak{g} \text{ is unitary} \\ 1 & \text{if } \mathfrak{g} \text{ is anti-unitary} \end{cases} \quad (4.15)$$

$$\sigma(\mathfrak{g}) = \begin{cases} 1 & \text{if } \mathfrak{g} \text{ is unitary} \\ * & \text{if } \mathfrak{g} \text{ is anti-unitary} \end{cases} \quad (4.16)$$

where  $*$  denotes complex conjugation.

Assembling the above information in the component form, we can write the action of  $\rho_{\mathfrak{g}}$  on the topological state space as a matrix  $U_{\mathfrak{g}}(\mathfrak{g}_a, \mathfrak{g}_b; \mathfrak{g}_c)_{\mu\nu}$

$$\rho_{\mathfrak{g}}|a, b; c\rangle_{\mu} = \sum_{\nu} U_{\mathfrak{g}}(\mathfrak{g}_a, \mathfrak{g}_b; \mathfrak{g}_c)_{\mu\nu} K^{q(\mathfrak{g})}|\mathfrak{g}_a, \mathfrak{g}_b; \mathfrak{g}_c\rangle_{\nu}, \quad (4.17)$$

where  $U_{\mathfrak{g}}(\mathfrak{g}_a, \mathfrak{g}_b; \mathfrak{g}_c)$  is an  $N_{ab}^c \times N_{ab}^c$  matrix, and  $K$  denotes complex conjugation which appears when  $q(\mathfrak{g}) = 1$  and the action  $\rho_{\mathfrak{g}}$  is  $\mathbb{C}$ -anti-linear. As a convention, we will also use  $U_{\mathfrak{g}}^{-1}(\mathfrak{g}_a, \mathfrak{g}_b; \mathfrak{g}_c)$  to denote the matrix inverse of  $U_{\mathfrak{g}}(\mathfrak{g}_a, \mathfrak{g}_b; \mathfrak{g}_c)$ , even when  $\mathfrak{g}$  is anti-unitary.

Under a vertex basis transformation,  $\Gamma_c^{ab} : V_c^{ab} \rightarrow V_c^{ab}$ ,  $U_{\mathfrak{g}}(a, b; c)_{\mu\nu}$  transforms to

$$\tilde{U}_{\mathfrak{g}}(a, b, c) = \left[ \Gamma_{\mathfrak{g}_c}^{\mathfrak{g}_a \mathfrak{g}_b} \right]^{\sigma(\mathfrak{g})} U_{\mathfrak{g}}(a, b, c) \left[ (\Gamma_c^{ab})^{-1} \right], \quad (4.18)$$

with the shorthand  $\bar{\mathfrak{g}} = \mathfrak{g}^{-1}$ . Moreover, to preserve the structure of braiding and fusion, under the action of  $\rho_{\mathfrak{g}}$ , the  $F$  and  $R$  symbols should transform according to the following rules:

$$\begin{aligned} \rho_{\mathfrak{g}}[F_{def}^{abc}] &= U_{\mathfrak{g}}(\mathfrak{g}_a, \mathfrak{g}_b; \mathfrak{g}_e) U_{\mathfrak{g}}(\mathfrak{g}_e, \mathfrak{g}_c; \mathfrak{g}_d) F_{\mathfrak{g}_d \mathfrak{g}_e \mathfrak{g}_f}^{\mathfrak{g}_a \mathfrak{g}_b \mathfrak{g}_c} U_{\mathfrak{g}}^{-1}(\mathfrak{g}_b, \mathfrak{g}_c; \mathfrak{g}_f) U_{\mathfrak{g}}^{-1}(\mathfrak{g}_a, \mathfrak{g}_f; \mathfrak{g}_d) = K^{q(\mathfrak{g})} F_{def}^{abc} K^{q(\mathfrak{g})} \\ \rho_{\mathfrak{g}}[R_c^{ab}] &= U_{\mathfrak{g}}(\mathfrak{g}_b, \mathfrak{g}_a; \mathfrak{g}_c) R_{\mathfrak{g}_c}^{\mathfrak{g}_a \mathfrak{g}_b} U_{\mathfrak{g}}(\mathfrak{g}_a, \mathfrak{g}_b; \mathfrak{g}_c)^{-1} = K^{q(\mathfrak{g})} R_c^{ab} K^{q(\mathfrak{g})}, \end{aligned} \quad (4.19)$$

where we have suppressed the additional indices that appear when  $N_{ab}^c > 1$ . Accordingly, the basis-independent quantity, including the topological twist  $\theta_a$  and the modular  $S$ -matrix  $S_{ab}$ , should be invariant or complex-conjugated under the action of  $\rho_{\mathfrak{g}}$ , i.e.,

$$\begin{aligned} S_{\mathfrak{g}_a \mathfrak{g}_b} &= S_{ab}^{\sigma(\mathfrak{g})}, \\ \theta_{\mathfrak{g}_a} &= \theta_a^{\sigma(\mathfrak{g})}, \end{aligned} \quad (4.20)$$



Finally, we demand that  $\rho_{\mathfrak{g}}$  satisfy the group multiplication rule up to a natural isomorphism denoted by  $\eta(\mathfrak{g}, \mathfrak{h})$ , i.e.,

$$\eta(\mathfrak{g}, \mathfrak{h}) : \quad \rho_{\mathfrak{g}} \circ \rho_{\mathfrak{h}} \Longrightarrow \rho_{\mathfrak{gh}} \quad (4.21)$$

By the definition of natural isomorphism, first of all, for every anyon  $a$ ,  $\eta(\mathfrak{g}, \mathfrak{h})$  assigns a morphism  $\eta_{\mathfrak{gh}a}(\mathfrak{g}, \mathfrak{h}) \in \text{Hom}(\mathfrak{g}(\mathfrak{h}a), \mathfrak{gh}a)$  to  $\mathfrak{gh}a$ . In order for this morphism to be an isomorphism, we need to have

$$\mathfrak{g}(\mathfrak{h}a) = \mathfrak{gh}a, \quad (4.22)$$

and accordingly,  $\eta_{\mathfrak{gh}a}(\mathfrak{g}, \mathfrak{h})$  can be identified with just a  $U(1)$  phase for simple anyon  $a$ . Secondly, the definition of natural isomorphism demands that, on the topological state space  $|\mathfrak{gh}a, \mathfrak{gh}b; \mathfrak{gh}c\rangle_{\mu}$ , the action of  $\rho_{\mathfrak{g}} \circ \rho_{\mathfrak{h}}$  should be equal to the action of  $\rho_{\mathfrak{gh}}$  up to a phase  $\frac{\eta_a(\mathfrak{g}, \mathfrak{h})\eta_b(\mathfrak{g}, \mathfrak{h})}{\eta_c(\mathfrak{g}, \mathfrak{h})}$ , i.e., we should have

$$\frac{\eta_a(\mathfrak{g}, \mathfrak{h})\eta_b(\mathfrak{g}, \mathfrak{h})}{\eta_c(\mathfrak{g}, \mathfrak{h})} = U_{\mathfrak{g}}(a, b; c)^{-1} K^{q(\mathfrak{g})} U_{\mathfrak{h}}(\bar{\mathfrak{g}}a, \bar{\mathfrak{g}}b; \bar{\mathfrak{g}}c)^{-1} K^{q(\mathfrak{g})} U_{\mathfrak{gh}}(a, b; c), \quad (4.23)$$

This phase is often denoted by  $\kappa_{\mathfrak{g}, \mathfrak{h}}(a, b; c)$  in the literature [60].

We also wish to impose a third constraint on  $\eta(\mathfrak{g}, \mathfrak{h})$  coming from the constraint of associativity of symmetry actions. Namely, we wish that the two different ways of connecting  $\rho_{\mathfrak{g}} \circ \rho_{\mathfrak{h}} \circ \rho_{\mathfrak{k}}$  with  $\rho_{\mathfrak{ghk}}$  through natural isomorphism  $\eta$  are identically the same, i.e., we wish to have

$$\eta_a(\mathfrak{g}, \mathfrak{h})\eta_a(\mathfrak{gh}, \mathfrak{k}) = \eta_a(\mathfrak{g}, \mathfrak{hk})\eta_{\bar{\mathfrak{g}}a}(\mathfrak{h}, \mathfrak{k})^{\sigma(\mathfrak{g})}, \quad (4.24)$$

The action  $\rho_{\mathfrak{g}}$  above defines an element  $\mathfrak{O} \in \mathcal{H}_{[\rho]}^3(G, \mathcal{A})$  [60, 88, 89]. Eq. (4.24) can be satisfied only when  $\mathfrak{O}$  is trivial. If  $\mathfrak{O}$  is non-trivial, then  $\mathfrak{O}$  is referred to as the *obstruction to symmetry fractionalization*<sup>1</sup>. Different solutions  $\eta_a(\mathfrak{g}, \mathfrak{h})$  of Eq. (4.23) together with (4.24) corresponding to the same  $\rho_{\mathfrak{g}}$  are referred to as different *symmetry fractionalization classes*.

Finally, we identify different choices of  $\rho_{\mathfrak{g}}$  up to natural isomorphism  $\gamma(\mathfrak{g})$ , i.e., we identify two sets of functors  $\rho_{\mathfrak{g}}$  and  $\tilde{\rho}_{\mathfrak{g}}$  if they are connected to each other by some natural isomorphism  $\gamma(\mathfrak{g})$

$$\gamma(\mathfrak{g}) : \quad \rho_{\mathfrak{g}} \Longrightarrow \tilde{\rho}_{\mathfrak{g}}, \quad (4.25)$$

---

<sup>1</sup>In this thesis, we will always assume that this obstruction is absent, and it can be straightforwardly checked for specific examples that we consider in the paper.

and this changes  $U_{\mathbf{g}}(a, b; c)$  and  $\eta_a(\mathbf{g}, \mathbf{h})$  in the following way [60]:

$$\begin{aligned} U_{\mathbf{g}}(a, b; c) &\rightarrow \frac{\gamma_a(\mathbf{g})\gamma_b(\mathbf{g})}{\gamma_c(\mathbf{g})}U_{\mathbf{g}}(a, b; c) \\ \eta_a(\mathbf{g}, \mathbf{h}) &\rightarrow \frac{\gamma_a(\mathbf{g}\mathbf{h})}{\gamma_a(\mathbf{g})(\gamma_{\bar{g}_a}(\mathbf{h}))^{\sigma(\mathbf{g})}}\eta_a(\mathbf{g}, \mathbf{h}) \end{aligned} \quad (4.26)$$

In this thesis we refer to this transformation as the *symmetry action gauge transformation*. Different gauge inequivalent choices of  $\{\eta\}$  and  $\{U\}$  characterize distinct symmetry fractionalization classes [60]. In this thesis we will always fix the gauge

$$\begin{aligned} \eta_1(\mathbf{g}, \mathbf{h}) = \eta_a(\mathbf{1}, \mathbf{g}) = \eta_a(\mathbf{g}, \mathbf{1}) = 1 \\ U_{\mathbf{g}}(1, b; c) = U_{\mathbf{g}}(a, 1; c) = 1. \end{aligned} \quad (4.27)$$

Moreover, we choose  $\rho_1$  to always be the identity functor. When  $G$  is continuous, we further choose  $\rho_{\mathbf{g}}$  such that  $\rho_{\mathbf{g}}$ 's for different  $\mathbf{g}$ 's in the same connected component are the same functor.

One can show that distinct symmetry fractionalization classes form a torsor over  $\mathcal{H}_\rho^2(G, \mathcal{A})$ . That is, different possible symmetry fractionalization classes can be related to each other by elements of  $\mathcal{H}_\rho^2(G, \mathcal{A})$ , where  $\mathcal{A}$  is an Abelian group whose group elements correspond to the Abelian anyons in this UMTC, and the group multiplication corresponds to the fusion of these Abelian anyons. In particular, given an element  $[\mathbf{t}] \in \mathcal{H}_\rho^2(G, \mathcal{A})$ , we can go from one symmetry fractionalization class with data  $\eta_a(\mathbf{g}, \mathbf{h})$  to another with data  $\tilde{\eta}_a(\mathbf{g}, \mathbf{h})$  given by

$$\tilde{\eta}_a(\mathbf{g}, \mathbf{h}) = \eta_a(\mathbf{g}, \mathbf{h})M_{a, \mathbf{t}(\mathbf{g}, \mathbf{h})} \quad (4.28)$$

where  $\mathbf{t}(\mathbf{g}, \mathbf{h}) \in \mathcal{A}$  is a representative 2-cocycle for the cohomology class  $[\mathbf{t}]$  and  $M_{a, \mathbf{t}(\mathbf{g}, \mathbf{h})} = \frac{\theta_{a \times \mathbf{t}(\mathbf{g}, \mathbf{h})}}{\theta_a \theta_{\mathbf{t}(\mathbf{g}, \mathbf{h})}}$  is the double braid between  $a$  and  $\mathbf{t}(\mathbf{g}, \mathbf{h})$  [90].

In the case where the permutation  $\rho$  is trivial, there is always a canonical notion of a trivial symmetry fractionalization class, where  $\eta_a(\mathbf{g}, \mathbf{h}) = 1$  for all anyon  $a$  and all  $\mathbf{g}, \mathbf{h} \in G$ . In this case, an element of  $\mathcal{H}^2(G, \mathcal{A})$  is sufficient to completely characterize the symmetry fractionalization class.

As the take-home message, the data  $\{\rho_{\mathbf{g}}; U_{\mathbf{g}}(a, b; c), \eta_a(\mathbf{g}, \mathbf{h})\}$  defines a categorical  $G$  action on  $\mathcal{C}$ , satisfying various consistency conditions, especially Eqs. (4.19), (4.23) and (4.24).

Sometimes we need to consider the symmetry actions of two different groups  $G_1$  and  $G_2$  on a UMTC  $\mathcal{C}$ , with data  $\{\rho_{\mathbf{g}}^{(1)}; U_{\mathbf{g}}^{(1)}(a, b; c), \eta_a^{(1)}(\mathbf{g}, \mathbf{h})\}$  and  $\{\rho_{\mathbf{g}}^{(2)}; U_{\mathbf{g}}^{(2)}(a, b; c), \eta_a^{(2)}(\mathbf{g}, \mathbf{h})\}$ ,

respectively. We say that a map  $f : G_1 \rightarrow G_2$  is compatible with these symmetry actions on  $\mathcal{C}$  if for any  $\mathbf{g}_1 \in G_1$ ,  $\rho_{\mathbf{g}_1}^{(1)}$  and  $\rho_{f(\mathbf{g}_1)}^{(2)}$  are two functors connected to each other by a natural isomorphism  $\gamma(\mathbf{g}_1)$  as in Eq. (4.25), i.e.,

$$\gamma(\mathbf{g}_1) : \rho_{\mathbf{g}_1}^{(1)} \Longrightarrow \rho_{f(\mathbf{g}_1)}^{(2)}, \quad (4.29)$$

In particular,  $\mathbf{g}_1$  and  $f(\mathbf{g}_1)$  are either both unitary or both anti-unitary, and they permute anyons in exactly the same way. Moreover, up to a symmetry action gauge transformation their actions on the topological state space satisfy

$$U_{f(\mathbf{g}_1)}^{(2)}(a, b; c) = U_{\mathbf{g}_1}^{(1)}(a, b; c) \quad (4.30)$$

for any anyons  $a, b, c \in \mathcal{C}$ . All maps between symmetries considered in this thesis are in fact maps compatible with symmetry actions on some UMTC  $\mathcal{C}$  if not stated explicitly.

Given such a map, we say that the symmetry fractionalization class  $\eta^{(1)}$  of  $G_1$  is the *pullback* of the symmetry fractionalization class  $\eta^{(2)}$  of  $G_2$ , if, under the gauge choice leading to Eq. (4.30), we have

$$\eta_a^{(1)}(\mathbf{g}, \mathbf{h}) = \eta_a^{(2)}(f(\mathbf{g}), f(\mathbf{h})) \quad (4.31)$$

for any  $\mathbf{g}, \mathbf{h} \in G_1$  and any  $a \in \mathcal{C}$ . It is straightforward to see that  $\eta_a^{(1)}(\mathbf{g}, \mathbf{h})$  defined this way satisfies Eqs. (4.23) and (4.24), as long as  $\eta_a^{(2)}(\mathbf{g}, \mathbf{h})$  does.

## 4.2 (3 + 1)-d TQFT with finite group symmetry $G$

A UMTC  $\mathcal{C}$  defines a (3 + 1)-d TQFT via a path integral state sum construction due originally to Crane and Yetter [91], and the state sum construction is extended to orientable or nonorientable manifolds with  $G$ -bundle structure in Ref. [92], where  $G$  is a finite group. In this section, after explaining the relation of the partition function to anomaly, we review the approach of Refs. [93–95] to give a more formal definition of the TQFT along the lines of Refs. [96, 97], and demonstrate how to compute the partition function of this TQFT. In particular, we also extend the approach to allow for an extra  $G$ -bundle structure, where  $G$  is a finite group symmetry that may contain anti-unitary elements, in which case the manifold under consideration can be non-orientable. While Ref. [92] explicitly uses a cellulation of a manifold, our approach here utilizes a handle decomposition of a manifold, which is reviewed in Sec. 4.2.3. As a result, our calculation is simpler and will produce closed-form expressions for partition functions and anomaly indicators.

In this section, usually when we refer to a manifold  $\mathcal{M}$ , we assume that there is a  $G$ -bundle structure  $\mathcal{G}$  defined on it as well, and an orientation has been chosen if  $\mathcal{M}$  is orientable.<sup>2</sup>

### 4.2.1 Characterizing the anomaly by bulk-boundary correspondence

In the field theoretic language, a  $(d+1)D$   $G$ -symmetric theory is anomalous if it cannot be gauged, i.e., its partition function evaluated on a  $(d+1)D$  manifold with a  $G$ -bundle cannot be made gauge invariant by local deformations. However, there exists an appropriate  $(d+1+1)D$   $G$ -symmetric invertible bulk theory [99, 100] whose boundary can host the original  $(d+1)D$  theory, such that the combined theory is anomaly-free. So we can characterize the anomaly of the boundary utilizing properties of the bulk. Specifically, the topological part of the partition function of the  $(d+1)D$  theory (i.e., the part of the partition function that is insensitive to dynamical details and only concerns the anomaly) on some  $(d+1)D$  manifold  $\mathcal{N}$  can be defined as the partition function of a  $(d+1+1)D$  invertible bulk theory on some  $(d+1+1)D$  manifold  $\mathcal{M}$  with  $\partial\mathcal{M} = \mathcal{N}$ , i.e.,

$$\mathcal{Z}_{d+1}(\mathcal{N}) \equiv \mathcal{Z}_{d+1+1}(\mathcal{M}; \partial\mathcal{M} = \mathcal{N}) \quad (4.32)$$

Yet as an intrinsic  $(d+1)D$  theory the partition function for fixed  $\mathcal{N}$  should be independent of the choice of  $\mathcal{M}$ . Hence on closed  $(d+1+1)D$  manifold  $\mathcal{M}$  we are supposed to have  $\mathcal{Z}_{d+1+1}(\mathcal{M}; \partial\mathcal{M} = \emptyset) = 1$ . Therefore, any  $\mathcal{Z}_{d+1+1}(\mathcal{M}; \partial\mathcal{M} = \emptyset) \neq 1$  suggests that the boundary theory on  $\mathcal{N}$  is anomalous, and the class of anomaly is encoded in the bulk partition function, which should be a gauge invariant U(1) phase factor. Below we will use this bulk partition function to characterize the boundary anomaly.<sup>3</sup>

The case that concerns us is a  $(2+1)$ -d symmetry-enriched topological order described by a UMTC  $\mathcal{C}$  and a global symmetry  $G$ . In the case where  $G$  is trivial, the UMTC indeed defines a  $(3+1)$ -d invertible TQFT called the *Crane-Yetter model* [91]. However, the physical system that the Crane-Yetter model defines is trivial in the sense that the partition function on any close 4-manifold can be tuned to 1 without closing the gap or breaking

---

<sup>2</sup>Even for non-orientable  $\mathcal{M}$ , we still need to choose an orientation of  $T\mathcal{M} \oplus \xi$ , where  $T\mathcal{M}$  is the tangent bundle of  $\mathcal{M}$  and  $\xi$  denotes the associated vector bundle of the gauge bundle  $\mathcal{G}$  [98, 99]. See Appendix 4.D.

<sup>3</sup>In the literature, we usually say that there exists a bulk  $G$ -SPT that can “cancel” the anomaly on the boundary, such that the total partition function of the combined bulk and boundary system is gauge invariant. According to our convention, the partition function of such bulk  $G$ -SPT should be the inverse of  $\mathcal{Z}_{d+1+1}(\mathcal{M}; \partial\mathcal{M} = \emptyset)$  that we present here.

any symmetry (in fact no symmetry is imposed at all in this model). Mathematically, the partition function corresponds to some element that belongs to  $\text{Hom}(\Omega_4^{SO}(\star), \text{U}(1)) \cong \text{U}(1)$ , and all these elements are smoothly connected to the trivial element. This means that there is no intrinsic topological order in the bulk defined by the UMTC  $\mathcal{C}$  in this way [13, 101–103]. Nevertheless, the  $(3 + 1)$ -d theory on a manifold with boundary hosts a  $(2 + 1)$ -d topological state at its boundary, whose anyon excitations are described by the UMTC  $\mathcal{C}$  [104]. Moreover, the partition function of the Crane-Yetter model is related to the *framing anomaly* of the  $(2 + 1)D$  topological state, as discussed in Refs. [94, 105].

In the presence of symmetries, the  $(3 + 1)$ -d bulk is generically an SPT state. The partition function of this SPT state corresponds to some element of the cobordism group  $\Omega_{SO}^4((BG)^{q-1})$ , with  $q : G \rightarrow \mathbb{Z}_2$  as in Eq. (4.15) labeling anti-unitary symmetries (see Appendix 4.D for the precise definition)<sup>4</sup>. Therefore, in order to understand the SPT, we just need to calculate the partition function on a few *representative manifolds*, given by the generators of the dual bordism group  $\Omega_4^{SO}((BG)^{q-1})$ . A complete set of such partition functions, expressed in terms of the data characterizing  $(2 + 1)$ -d symmetry-enriched topological orders, are the *anomaly indicators*. The values of these anomaly indicators for a given symmetry-enriched topological order characterize its anomaly, corresponding to an element in the relevant cohomology or cobordism group.<sup>5</sup> Namely, there is an injection that maps the possible values of the anomaly indicators to elements of the relevant cohomology or cobordism group.<sup>6</sup>

## 4.2.2 General construction of TQFT

In this subsection we review the basic facts about TQFT that concern us in the context of topological order, which ultimately lead to our recipe for calculating the partition function in Sec. 4.2.4. The presentation here loosely follows Refs. [94, 97, 108]. See also Ref. [95]. This subsection is rather formal, and readers uninterested in the origin of various rules of the calculations can skip this subsection and take the recipe in Sec. 4.2.4 as the definition of our TQFT.

---

<sup>4</sup>To ease the notation, we will omit the superscript  $q - 1$  when  $G$  contains unitary symmetries only.

<sup>5</sup>More precisely, after choosing a basis of the cohomology or cobordism group, the anomaly indicators are the expansion coefficients of the element under this basis.

<sup>6</sup>For a finite group  $G$ , because any  $(3 + 1)$ -d SPT can have symmetric topologically ordered boundary, this injection should be a bijection [106, 107]. However, for a continuous group  $G$ , because sometimes the  $(3 + 1)$ -d SPT cannot have any symmetric topologically ordered boundary [45, 56, 57], this injection is generically not surjective.

According to Ref. [96], an  $n$ -dimensional TQFT for oriented manifolds (with no  $G$ -bundle structure), taking values in  $\mathbb{C}$ , requires the specification of the following information:

- a. For every closed oriented  $n$ -dimensional manifold  $\mathcal{M}$ , a  $\mathbb{C}$ -number  $\mathcal{Z}(\mathcal{M}) \in \mathbb{C}$ .
- b. For every closed oriented  $(n - 1)$ -dimensional manifold  $\mathcal{N}$ , a  $\mathbb{C}$ -linear vector space  $\mathcal{V}(\mathcal{N})$ . When  $\mathcal{N}$  is empty, the vector space  $\mathcal{V}(\mathcal{N})$  is canonically isomorphic to  $\mathbb{C}$ .
- c. For every oriented  $n$ -dimensional manifold  $\mathcal{M}$ , a vector  $|\mathcal{Z}(\mathcal{M})\rangle$  of the vector space  $\mathcal{V}(\partial\mathcal{M})$ . When  $\partial\mathcal{M} = \emptyset$ , this vector space is canonically identified with  $\mathbb{C}$ , and gives the same  $\mathbb{C}$ -number as we get in [a].

They should satisfy a series of consistency conditions that we do not specify here. We usually choose a set of orthonormal basis vectors  $\{|\beta_{\partial\mathcal{M}}\rangle\}$  for  $\mathcal{V}(\partial\mathcal{M})$ , and then  $|\mathcal{Z}(\mathcal{M})\rangle$  can be written as sum of basis vectors, i.e.,  $|\mathcal{Z}(\mathcal{M})\rangle = \sum_{\beta} \langle\beta_{\partial\mathcal{M}}|\mathcal{Z}(\mathcal{M})\rangle |\beta_{\partial\mathcal{M}}\rangle$ . We call the inner product  $\langle\beta_{\partial\mathcal{M}}|\mathcal{Z}(\mathcal{M})\rangle$  the partition function of  $\mathcal{M}$  with *label*  $|\beta_{\partial\mathcal{M}}\rangle$  put on  $\partial\mathcal{M}$ , and denote it by  $\mathcal{Z}(\mathcal{M}; \beta_{\partial\mathcal{M}})$ .

One of the most important facts of TQFT is that the partition function  $\mathcal{Z}(\mathcal{M})$  of some  $n$ -manifold  $\mathcal{M}$  can be evaluated via the gluing formula. Let us cut a closed  $n$ -manifold  $\mathcal{M}$  along some  $(n - 1)$ -manifold  $\mathcal{N}$ , then we get a new  $n$ -manifold  $\mathcal{M}_{\text{cut}}$  with boundary  $\partial\mathcal{M}_{\text{cut}} = \mathcal{N} \cup \overline{\mathcal{N}}$ , where  $\overline{\mathcal{N}}$  is the same manifold  $\mathcal{N}$  with opposite orientation. From the axioms of TQFT we have the following gluing formula:

$$\mathcal{Z}(\mathcal{M}) = \sum_{\beta} \frac{\mathcal{Z}(\mathcal{M}_{\text{cut}}; \beta_{\mathcal{N}})}{\langle\beta_{\mathcal{N}}|\beta_{\mathcal{N}}\rangle_{\mathcal{V}(\mathcal{N})}}. \quad (4.33)$$

Here  $\{\beta_{\mathcal{N}}\}$  is a set of orthonormal basis for  $\mathcal{V}(\mathcal{N})$ .

From the gluing formula, it is clear that in order to calculate the partition function on some complicated manifold  $\mathcal{M}$ , we can chop  $\mathcal{M}$  up into simpler pieces and calculate the partition functions of the individual pieces, so that we can obtain the partition function of the original manifold  $\mathcal{M}$  with the help of the gluing formula Eq. (4.33). Therefore, in order to understand the TQFT, which in principle is defined on any manifold that can be arbitrarily complex, the hope is that it suffices to specify a relatively small amount of information about  $\mathcal{M}_{\text{cut}}$  and  $\mathcal{N}$ .

Yet the manifold  $\mathcal{N}$  as an  $(n - 1)$ -manifold can be very complicated as well, and thus  $\mathcal{V}(\mathcal{N})$  can be very complicated. The idea of *2-extended TQFT* is to extend the construction once down, i.e., we wish to extend the construction of TQFT properly to incorporate the

case where  $\mathcal{N}$  has boundaries as well, and  $\mathcal{V}(\mathcal{N})$  can also be obtained by gluing relatively simple pieces together. This extension will further simplify the analysis and the calculation of the partition function. We will also immediately see that the data of a UMTC can be manifestly incorporated into the construction, since we will soon put anyons on an  $(n-2)$ -manifold  $\mathcal{O}$ .

Specifically, to specify the data of a *2-extended* TQFT, beyond the data of an ordinary TQFT, we need to put an object of some  $\mathbb{C}$ -linear category, reminiscent of anyons, on “the boundary of the boundary”. More precisely, on top of the information defining an ordinary TQFT, this further information includes

- d. For every closed oriented  $(n-2)$ -manifold  $\mathcal{O}$ , a  $\mathbb{C}$ -linear category  $\mathcal{C}(\mathcal{O})$ . When  $\mathcal{O}$  is empty, the category  $\mathcal{C}(\mathcal{O})$  is canonically isomorphic to the category of  $\mathbb{C}$ -linear vector spaces.
- e. For every oriented  $(n-1)$ -manifold  $\mathcal{N}$ , an object  $\mathcal{V}(\mathcal{N})$  of the category  $\mathcal{C}(\partial\mathcal{N})$ . When  $\partial\mathcal{N} = \emptyset$ , this object is canonically identified with a  $\mathbb{C}$ -linear vector space, and gives the same  $\mathbb{C}$ -linear vector space as we get in [b].

Similar to the fact that a vector can be written as sum of basis vectors, an object can be written as a (direct) sum of simple objects  $\{\beta_{\mathcal{O}}\}$  for  $\mathcal{C}(\mathcal{O})$  a semisimple category. Therefore, similar to the previous analysis of ordinary TQFT, we will also associate an object  $\beta_{\partial\mathcal{N}}$  to  $\partial\mathcal{N}$  and call  $\text{Hom}(\beta_{\partial\mathcal{N}}, \mathcal{V}(\mathcal{N}))$  the vector space of  $\mathcal{N}$  with *label*  $\beta_{\partial\mathcal{N}}$  put on  $\partial\mathcal{N}$ , and denote it by  $\mathcal{V}(\mathcal{N}; \beta_{\partial\mathcal{N}})$ .

From this construction, we define the vector space  $\mathcal{V}(\mathcal{N}; \beta_{\partial\mathcal{N}})$  associated to  $\mathcal{N}$  with boundary  $\partial\mathcal{N} \neq \emptyset$ , after putting labels  $\beta_{\partial\mathcal{N}}$  on the boundary. Moreover,  $\mathcal{V}(\mathcal{N}; \beta_{\partial\mathcal{N}})$  can be obtained by chopping  $\mathcal{N}$  along some  $(n-2)$ -manifold  $\mathcal{O}$  and using “gluing formula” similar to Eq. (4.33).

Now we specialize to the TQFT that concerns us the most, i.e., a TQFT defined on 4-dimensional manifolds from the data of a UMTC  $\mathcal{C}$ . We can start using the language of anyons and topological state spaces. We define  $\mathcal{C}(\mathcal{O})$  as  $\mathcal{C}^{\otimes n}$  where  $n$  is the number of connected components of  $\mathcal{O}$ . In particular, when  $\mathcal{O} = \emptyset$ , we say  $n = 0$  and  $\mathcal{C}^{\otimes 0}$  is defined as the UMTC with only object 1, i.e., a trivial anyon. Therefore, for closed  $(n-1)$ -manifold  $\mathcal{N}$  with  $\partial\mathcal{N} = \emptyset$ , e.g.,  $S^3$ ,  $\mathcal{V}(\mathcal{N})$  is a 1-dimensional  $\mathbb{C}$ -vector space, i.e., we have

$$\mathcal{V}(S^3) \simeq \mathbb{C} \tag{4.34}$$

To finish the definition of the TQFT, we associate the object 1 to  $\mathcal{N} = D^3$ . When writing down the vector space of  $D^3$  given some label on  $\partial D^3 = S^2$ , sometimes we need to

associate a direction of the flow of anyons, i.e., whether an anyon comes into or out of the  $S^2$  ball. This choice is similar to the choice of an orientation of  $\mathcal{N}$ , and when  $\mathcal{N} = \partial\mathcal{M}$  it can be the same as or opposite to the orientation induced from  $\mathcal{M}$ . Now we assign  $a_1, \dots$  anyons coming out of  $S^2$  and  $b_1, \dots$  anyons coming into  $S^2$ , and we have the canonical identification of the vector space given such labels as the topological state space of fusing  $b_1, \dots$  anyons into  $a_1, \dots$  anyons, i.e.,

$$\mathcal{V}(D^3; (a_1, \dots; b_1, \dots)) \simeq V_{b_1, \dots}^{a_1, \dots} \quad (4.35)$$

After this assignment, we can in principle identify all vector spaces associated to  $\mathcal{N}$  with some label on  $\partial\mathcal{N}$ . For example, for  $S^2 \times D^1$  with trivial anyon on the boundary, we have

$$\mathcal{V}(S^2 \times D^1; \emptyset) \simeq \mathbb{C} \quad (4.36)$$

For  $S^1 \times D^2$  with trivial anyon on the boundary, we have

$$\mathcal{V}(S^1 \times D^2; \emptyset) \simeq \mathbb{C}^{|\mathcal{C}|} \quad (4.37)$$

where  $|\mathcal{C}|$  denotes the number of simple anyons in  $\mathcal{C}$ , and  $\emptyset$  denotes the trivial anyon on the boundary. A basis vector in  $\mathcal{V}(S^1 \times D^2; \emptyset)$  corresponds to putting an anyon loop labeled by  $a \in \mathcal{C}$  along  $S^1 \times \{\text{pt}\} \subset S^1 \times D^2$ , where  $\{\text{pt}\}$  denotes a point in  $D^2$ .

We mention that in Ref. [94],  $\mathcal{V}(\mathcal{N}; \beta_{\partial\mathcal{N}})$  is defined as the space of formal linear superpositions (with complex coefficients) of all anyon diagrams, which can end on the anyons labeled by  $\beta_{\partial\mathcal{N}}$  on the boundary  $\partial\mathcal{N}$ , modulo the equivalence from local relations given by fusion of anyon lines,  $F$ -moves, and  $R$ -moves, i.e.,

$$\mathcal{V}(\mathcal{N}; \beta_{\partial\mathcal{N}}) = \mathbb{C}[\mathcal{C}(\mathcal{N}; \beta_{\partial\mathcal{N}})] / \sim, \quad (4.38)$$

where  $\mathcal{C}(\mathcal{N}; \beta_{\partial\mathcal{N}})$  denotes the set of all such anyon diagrams and  $\sim$  is the equivalence given by these local relations. This serves as a nice diagrammatic illustration of the vector spaces defined above, as simply illustrated in Fig. 4.1. (See also Ref. [104] for the connection to Hamiltonian formalism.) In Appendix 4.A.1 we rederive various vector spaces mentioned using the above definition, which serves as a nice consistency check.

Another piece of information that we should attribute to the vector space is the inner product in  $\mathcal{V}(\mathcal{N}; \beta_{\partial\mathcal{N}})$ . Following the expectation from gluing formula as in Eq. (4.40), the inner product in  $\mathcal{V}(\mathcal{N}; \beta_{\partial\mathcal{N}})$  is supposed to be the partition function of  $\mathcal{N} \times D^1$  with the labels on the boundary of  $\mathcal{N}$  and  $\overline{\mathcal{N}}$  attached to each other:

$$\langle x|y \rangle_{\mathcal{V}(\mathcal{N}; \beta_{\partial\mathcal{N}})} = \mathcal{Z}(\mathcal{N} \times D^1; \bar{x} \cup y), \quad (4.39)$$



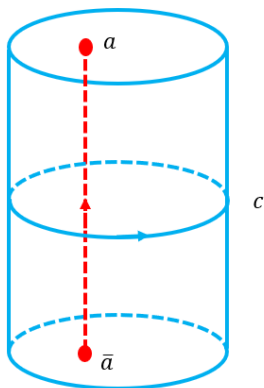


Figure 4.1: The illustration of some anyon diagram on  $D^2 \times D^1$ , with some anyon lines ending on anyon  $a$  and  $\bar{a}$  put on the boundary.

where  $x, y$  are two vectors in  $\mathcal{V}(\mathcal{N}; \beta_{\partial\mathcal{N}})$  and  $\bar{x}$  is the dual vector of  $x$  in the dual vector space  $\mathcal{V}(\bar{\mathcal{N}}; \bar{\beta}_{\partial\bar{\mathcal{N}}})$ .

For our purpose, we have to deal with manifold  $\mathcal{M}$  with an additional  $G$ -bundle structure  $\mathcal{G}$ . Now we specialize to a finite symmetry group  $G$ , and thus a  $G$ -bundle  $\mathcal{G}$  is fully characterized by the holonomy around all noncontractible cycles of  $\mathcal{M}$ . Such noncontractible cycles are generators of  $\pi_1(\mathcal{M})$  that we call 1-cycles, and the holonomy assigns a group element  $\mathbf{g} \in G$  to every generator of  $\pi_1(\mathcal{M})$ . To facilitate the usage of gluing formula, we can use a defect network to represent the holonomy, and the  $G$ -bundle structure is completely determined by which group elements (i.e., defects) we put on noncontractible cycles of  $\mathcal{M}$ , up to conjugation by elements in  $G$ .

According to the general recipe in Ref. [97], the category  $\mathcal{C}(\mathcal{O})$  and the vector space  $\mathcal{V}(\mathcal{N})$  should be equipped with a categorical  $G$ -action. This is precisely the data  $\{\rho_{\mathbf{g}}; U_{\mathbf{g}}(a, b; c), \eta_a(\mathbf{g}, \mathbf{h})\}$  in Sec. 4.1.2 that defines a categorical  $G$  action on  $\mathcal{C}$ . Labels should be acted by  $\rho_{\mathbf{g}}$  or  $\rho_{\mathbf{g}}^{-1}$  when crossing a defect corresponding to the group element  $\mathbf{g}$  (whether it is  $\rho_{\mathbf{g}}$  or  $\rho_{\mathbf{g}}^{-1}$  will be explained later). Moreover, a 1-cycle of  $\mathcal{M}$ , thought of as a 1-morphism in the language of higher category, should be assigned a functor acting on vector spaces, while a 2-cycle of  $\mathcal{M}$ , thought of as a 2-morphism in the language of higher category, should be assigned a natural isomorphism acting on objects. The former precisely gives an extra piece  $U_{\mathbf{g}}(a, b; c)$  in the partition function, which will be referred to as a  $U$ -factor; the latter gives an extra piece  $\eta_a(\mathbf{g}, \mathbf{h})$  in the partition function, which will be referred to as an  $\eta$ -factor. Because of Eq. (4.24), we do not need 3- or higher morphisms to connect different compositions of 2-morphisms, hence introducing appropriate  $U$ -factors and  $\eta$ -factors is

enough to determine such TQFT and calculate the partition function of it.

Finally, we collect the above results to write down the gluing formula for the TQFT, which is the main tool for the calculation of the partition function of the TQFT

$$\mathcal{Z}(\mathcal{M}, \mathcal{G}) = \sum_{\beta} \frac{\mathcal{Z}(\mathcal{M}_{\text{cut}}, \mathcal{G}_{\text{cut}}; \beta_{\mathcal{N}}, \beta_{\partial\mathcal{N}})}{\langle \beta_{\mathcal{N}} | \beta_{\mathcal{N}} \rangle_{\mathcal{V}(\mathcal{N}; \beta_{\partial\mathcal{N}})}}. \quad (4.40)$$

Here,  $\mathcal{M}$  is an  $n$ -dimensional closed manifold with a  $G$ -bundle structure  $\mathcal{G}$ , and we cut  $\mathcal{M}$  along  $\mathcal{N}$  to get a new manifold  $\mathcal{M}_{\text{cut}}$  with boundary and corner.  $\{\beta_{\partial\mathcal{N}}\}$  is a set of simple anyons we put on  $\partial\mathcal{N}$  after the cut, while  $\{\beta_{\mathcal{N}}\}$  is a set of orthonormal basis states for  $\mathcal{V}(\mathcal{N}; \beta_{\partial\mathcal{N}})$ . Notice that we should sum up both kinds of labels, collectively denoted by  $\beta$ .

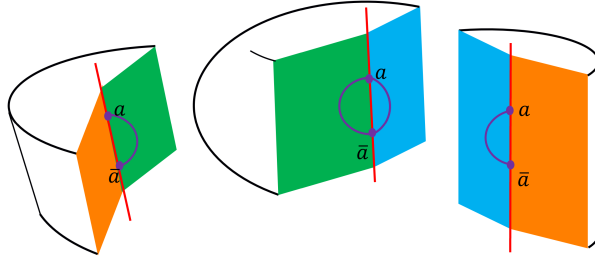


Figure 4.2: Illustration of the usage of gluing formula, where orange, green and blue faces are attached to each other while the red line denotes the (common) boundary of the faces.

With the help of the language of higher category [97], this definition of TQFT can be extended all the way to 0-dimensional points, giving rise to a *fully-extended TQFT*. For example, Crane-Yetter model has already been established as a fully-extended TQFT [95, 109, 110]. Although it is cumbersome to directly check that our construction satisfies all the consistency conditions of a fully-extended TQFT, we believe the TQFT that we are working with is indeed a fully-extended TQFT, given the infinity category presented in Ref. [95], equipped with  $G$  action. For most of our exposition, it is enough to consider 2-extended TQFT. But being a fully-extended TQFT does allow us to chop the target 4-manifold  $\mathcal{M}$  up in any way we like, without worrying about some small-dimensional submanifold on the boundary of which no data is defined. In particular, we can chop  $\mathcal{M}$  up into  $D^4$  pieces, which is essentially the handle decomposition that we will review in the next subsection.

### 4.2.3 Handle decomposition

In this section, we review basic facts about handle decomposition that will be used in this thesis. Some standard textbooks of handle decomposition and 4-manifold topology are Refs. [111–113]. Handle decompositions of specific manifolds used in this thesis are summarized in Appendix 4.E.

Handle decomposition is nothing but a canonical way of chopping an  $n$ -dimensional manifold up into simple pieces of  $D^n$ , where every  $D^n$  piece is called a *handle*. Every smooth manifold admits a handle decomposition [111]. A handle decomposition of an  $n$ -manifold  $\mathcal{M}$  is a decomposition of  $\mathcal{M}$  into 0-handles, 1-handles,  $\dots$ ,  $n$ -handles. The union of all 0-handles, 1-handles,  $\dots$ ,  $m$ -handles is called the  $m$ -handlebody of this handle decomposition for  $m \leq n$ , temporarily denoted by  $\mathcal{M}^{(m)}$  here. A handle decomposition can always be done such that lower-handles are first specified, and higher handles are attached along their *attaching regions* to the boundary of the already-specified lower handlebodies by embedding maps. Specifically, for an  $n$ -dimensional  $k$ -handle, it is topologically equivalent to  $D^k \times D^{n-k}$  and its attaching region is the part of its boundary that is topologically equivalent to  $\partial(D^k) \times D^{n-k} \cong S^{k-1} \times D^{n-k}$ . The attaching region is attached to  $\mathcal{M}^{(k-1)}$  via an *embedding map*<sup>7</sup>:

$$\varphi : S^{k-1} \times D^{n-k} \rightarrow \partial\mathcal{M}^{(k-1)} \quad (4.41)$$

A handle decomposition is specified by specifying all handles and the embedding maps that attach all handles together. See Fig. 4.3 for an illustration of 1-handles and 2-handles together with their attaching regions.

There is some formal analogy between handle decompositions and cell decompositions. In fact, it is often useful to think of a handle decomposition as a “thickened” version of a cell decomposition. For example, one can take a triangulation or cellulation of an  $n$ -dimensional manifold  $\mathcal{M}$ , and thicken the 0-cells into  $n$ -balls  $D^n$ . Next, one can thicken the 1-cells to  $n$ -balls as well, and glue them to the boundary of 0-cells along two  $D^{n-1}$  pieces of  $S^0 \times D^{n-1} \subset \partial(D^n)$ . The 2-cells can be thickened to  $n$ -balls, and glued to the boundary of 0- and 1- cells along  $S^1 \times D^{n-2}$ , and so on.

For a connected  $n$ -manifold  $\mathcal{M}$ , we can choose to have only one 0-cell. A handle decomposition of  $\mathcal{M}$  with a unique 0-handle then determines a presentation of  $\pi_1(\mathcal{M})$ .

---

<sup>7</sup>When there are multiple  $k$ -handles, the first of them is attached to  $\mathcal{M}^{(k-1)}$  in this way, which results a manifold  $\mathcal{M}^{(k-1),1}$ . Then one needs to attach the second  $k$ -handle to  $\mathcal{M}^{(k-1),1}$  in a similar way. This procedure continues until all  $k$ -handles are attached to result in  $\mathcal{M}^{(k)}$ . The manifold obtained this way is independent of the sequence of attachment.

Namely, each 1-handle together with the 0-handle forms an  $S^1 \times D^{n-1}$  and determines a generator of  $\pi_1(\mathcal{M})$ , and the attaching region  $S^1 \times D^{n-2}$  of each 2-handle gives a relation among the generators (as this  $S^1$  is always contractible). This is also what we expect from cell decompositions. We will sometimes call the cycle formed this way from joining a 1-handle with the 0-handle the *induced (1-)cycle* of the 1-handle, as shown in Fig. 4.4.

Given a  $k$ -handle, in order to specify how it is attached to lower handles  $\mathcal{M}^{(k-1)}$ , we just need to specify the attaching region, which requires the following two pieces of information:

1. How  $S^{k-1} \times \{\text{pt}\}$  is embedded in  $\partial\mathcal{M}^{(k-1)}$ , where  $\{\text{pt}\} \in D^{n-k}$  is any point in the interior of  $D^{n-k}$ .
2. How to choose a trivialization in the tubular neighborhood of  $S^{k-1} \times \{\text{pt}\}$  in  $\partial\mathcal{M}'$  that is supposed to be identified with  $\partial(D^k) \times D^{n-k}$ .

The second piece of information is called the *framing* of the  $k$ -handle. This information is not directly present in cell decomposition. In particular, the framing of a 1-handle is classified by  $\pi_0(O(1)) \cong \mathbb{Z}_2$ , and is given by whether the induced cycle of the 1-handle is orientable or not. With slight abuse, if this induced cycle is orientable (non-orientable), we will say that the 1-handle is orientable (non-orientable). The framing of 2-handle is classified by  $\pi_1(O(2)) \cong \mathbb{Z}$ , which is the self-intersection number of  $S^1 \times \{\text{pt}\}$  on the boundary of the 0-handle (see Ref. [112] for more information regarding this).

Now let us specialize to 4-dimensional manifolds. In order to illustrate the handle decomposition, we introduce *Kirby diagrams*. Suppose we have some 4-dimensional closed connected manifold  $\mathcal{M}$ . We assume that there is a unique 0-handle  $D^4$ , whose boundary  $S^3$  can be thought of as  $\mathbb{R}^3 \cup \{\infty\}$ . We then try to draw the attaching regions of the remaining handles in  $\mathbb{R}^3$ . The attaching region of each 1-handle is two copies of  $D^3$ , which we draw as a pair of round balls. For 2-handles whose attaching regions are  $S^1 \times D^2$ , we draw the image of  $S^1 \times \{\text{pt}\} \subset S^1 \times D^2$  on  $\mathbb{R}^3$ , and pay attention that in  $\mathbb{R}^3$  circles can be knotted and linked. It is known that 3-handles and 4-handles are uniquely defined once we have determined how 1-handles and 2-handles are attached.

We must then deal with framings. Specifically, given whether the induced cycle of some 1-handle is orientable or non-orientable, we need to connect points on the two balls in different ways. Specifically, the two balls are glued together by the 1-handle with the opposite (same) orientation if the cycle is orientable (non-orientable). In this thesis, for an orientable 1-handle points related to each other by mirror reflection through the plane perpendicularly bisecting the lines joining their centers are connected to each other, as in Ref. [111, 112]. For a non-orientable 1-handle, we use the convention that parallel points,

e.g., the bottom points or the top points of two balls, are connected to each other by the 1-handle, in contrast to the convention in Ref. [112]. These are illustrated in Fig. 4.4. For 2-handles, we need to add the correct amount of topological twists to account for the correct framing. One important way to determine the linking and framing of 2-handles is through the intersection form and mod-2 intersection form of  $\mathcal{M}$  [111], which can be calculated relatively easily in algebraic topology.

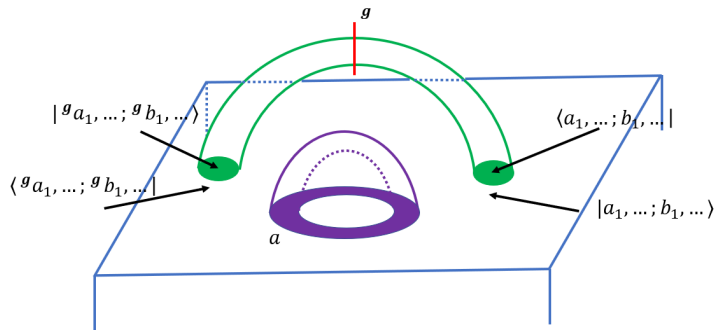


Figure 4.3: Illustration of a blue 0-handle, a green 1-handle and a purple 2-handle together with labels assigned to their attaching regions. The green shaded regions are the attaching regions  $S^0 \times D^3$  of the 1-handle, and the purple shaded regions are the attaching regions  $S^1 \times D^2$  of the 2-handle. The red line displays a defect, which crosses the 1-handle with the section being  $D^3$ . We associate an anyon  $a$  to the 2-handle. We also associate a vector  $|a_1, \dots; b_1, \dots\rangle$  and a dual vector  $\langle a_1, \dots; b_1, \dots|$  to the attaching regions living on the 0-handle side and 1-handle side, respectively (these two sides are identified by the embedding map that attaches the 1-handle to the 0-handle).

#### 4.2.4 Recipe for calculating the partition function

Having laid down the foundation, in this subsection we spell out the recipe for calculating the partition function on any  $(3 + 1)$ -d manifold  $\mathcal{M}$  equipped with a  $G$ -bundle  $\mathcal{G}$ , given the data of a UMTC  $\mathcal{C}$  and the data of symmetry action of some finite group  $G$  on  $\mathcal{C}$ . This recipe is summarized by Eq. (4.44). Note that  $\mathcal{G}$  is fully characterized by the holonomy around all noncontractible cycles of  $\mathcal{M}$ , and we will use a defect network to represent the holonomy. In Appendix 4.C, without resorting to its origin or its relation to gluing formula, we directly check that the partition function constructed here indeed satisfies various desired properties, including the independence on the handle decomposition, gauge invariance, cobordism invariance, etc., by directly manipulating the formula in Eq. (4.44).

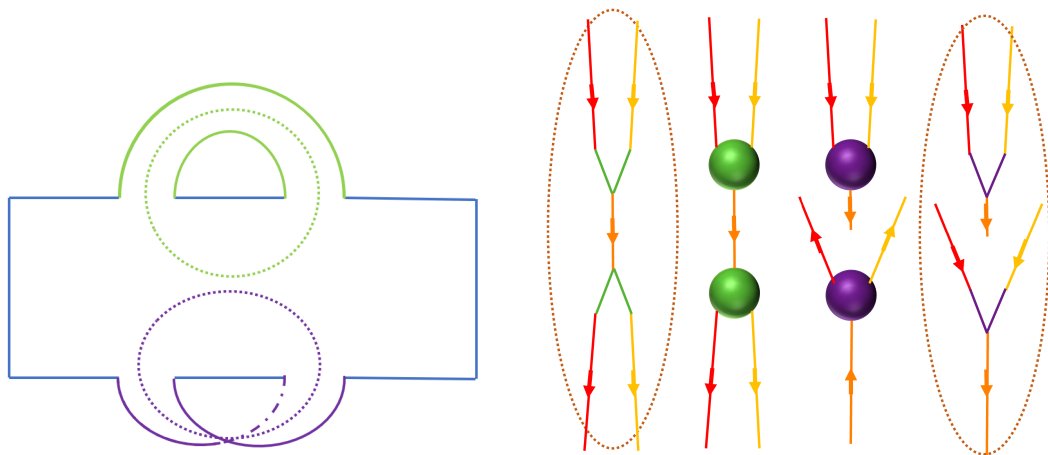


Figure 4.4: Left: Illustration of a green orientable 1-handle and a purple non-orientable 1-handle, attached to the blue 0-handle. The manifold is supposed to be 4-dimensional but we draw a 2-dimensional plane for illustration. The dashed green circle and the dashed purple circle are the induced cycles of the two 1-handles. Right: the Kirby diagrams for the green and purple 1-handles (the two figures in the middle), together with the anyon diagrams associated with these Kirby diagrams (the two figures in dashed ellipses). Pay attention how points on the two  $D^3$  components of attaching regions  $S^0 \times D^3$  are connected to each other via the 1-handle.

The basic formula for the calculation is the gluing formula Eq. (4.40). For a specific handle decomposition of the manifold  $\mathcal{M}$ , we have [95]

$$\mathcal{Z}(\mathcal{M}, \mathcal{G}) = \sum_{\beta \in \mathcal{L}} \prod_{j=0}^4 \prod_{h \in j\text{-handle}} \frac{\mathcal{Z}(h; \beta_{\partial h})}{\langle \beta_{\tilde{\partial} h} | \beta_{\tilde{\partial} h} \rangle_{\mathcal{V}(\tilde{\partial} h; \beta_{\partial(\tilde{\partial} h)})}} \quad (4.42)$$

Here  $\beta \in \mathcal{L}$  denotes all labels on the attaching regions of all  $j$ -handles,  $\mathcal{Z}(h; \beta_{\partial h})$  is the partition function of some  $j$ -handle  $h$  with label  $\beta_{\partial h}$  on the boundary  $\partial h$ , and  $\langle \beta_{\tilde{\partial} h} | \beta_{\tilde{\partial} h} \rangle_{\mathcal{V}(\tilde{\partial} h; \beta_{\partial(\tilde{\partial} h)})}$  is the squared norm of the state  $|\beta_{\tilde{\partial} h}\rangle$  in the vector space  $\mathcal{V}(\tilde{\partial} h; \beta_{\partial(\tilde{\partial} h)})$  associated with the 3D manifold of the attaching region  $\tilde{\partial} h$  of  $h$ . From the formula we need to calculate various norms and the partition function on various handles given a prescribed label. We repeat the calculation of Refs. [93–95] in Appendix 4.A, which concerns manifolds without a general  $G$ -bundle structure. A major innovation we introduce in this thesis is how to deal with a  $G$ -bundle structure, and we discuss it in detail for finite group  $G$  below.

The recipe for calculating the partition function  $\mathcal{Z}(\mathcal{M}, \mathcal{G})$  of the manifold  $\mathcal{M}$  with a  $G$ -bundle structure  $\mathcal{G}$  on  $\mathcal{M}$ , with  $G$  a finite group, is summarized here.

1. Identify a handle decomposition of the manifold  $\mathcal{M}$ . On each 1-handle put appropriate defects according to the  $G$ -bundle structure  $\mathcal{G}$ , as in Fig. 4.3.
2. The  $S^1$  boundary of each 2-handle is separated by the defects into segments. Associate an anyon  $a$  to an arbitrary segment on the  $S^1$  boundary of each 2-handle, and the anyons on the other segments are related to  $a$  by the  $G$ -actions given by the defects. Write down the  $\eta$ -factor coming from the natural isomorphism for  $a$  that connects the functor of successive  $G$ -actions and the identity functor. (See Remark g below for more details.)
3. Associate a dual vector  $\langle a_1, \dots; b_1, \dots |_{\mu\dots} K^{q(\mathfrak{g})}$ <sup>8</sup> and a vector  $|\mathfrak{g}a_1, \dots; \mathfrak{g}b_1, \dots\rangle_{\tilde{\mu}\dots}$  to the two  $D^3$  planes of the attaching region  $S^0 \times D^3$  of every 1-handle as in Fig. 4.5, where  $a_1, \dots$  and  $b_1, \dots$  are labels of anyons running out of and into the lower  $D^3$  plane of the attaching region of the 1-handle, respectively. Write down the  $U$ -factor from<sup>9</sup>

$$\langle a_1, \dots; b_1, \dots |_{\mu\dots} K^{q(\mathfrak{g})} \rho_{\mathfrak{g}}^{-1} | \mathfrak{g}a_1, \dots; \mathfrak{g}b_1, \dots \rangle_{\tilde{\mu}\dots} = U_{\mathfrak{g}}^{-1} (\mathfrak{g}a_1, \dots; \mathfrak{g}b_1, \dots)_{\tilde{\mu}\dots, \mu\dots} \quad (4.43)$$

<sup>8</sup>See Remark e in the following paragraphs for some further explanation of the factor  $K^{q(\mathfrak{g})}$ .

<sup>9</sup>The assignment of  $\rho_{\mathfrak{g}}^{-1}$  instead of e.g.,  $\rho_{\bar{\mathfrak{g}}}$  is just to match the convention of Ref. [92].

4. Evaluate the anyon diagram from the Kirby diagram  $\langle K \rangle$  of  $\mathcal{M}$ , given the prescribed anyon labels associated to the  $S^1$  lines corresponding to 2-handles and vectors associated to the  $D^3$  balls corresponding to 1-handles as in Fig. 4.3.
5. Assemble the result as follows:

$$\mathcal{Z}(\mathcal{M}, \mathcal{G}) = D^{-\chi+2(N_4-N_3)} \times \sum_{\text{labels}} \left( \frac{\prod_{2 \text{ handle } i} d_{a_i}}{\prod_{1 \text{ handle } x} \left( \prod_{2 \text{ handle } j \text{ across } x} d_{a_j} \right)^{1/2}} \right) \quad (4.44)$$

$$\times \left( \prod_i (\eta\text{-factors})_i \right) \times \left( \prod_x (U\text{-factors})_x \times \langle K \rangle \right)$$

Here  $N_k$  is the number of  $k$ -handles in this handle decomposition, and  $\chi \equiv N_0 - N_1 + N_2 - N_3 + N_4$  is the Euler number of  $\mathcal{M}$ .

There are a few extra points that may clarify the meanings or ease the computation. We summarize them below:

- a. Without loss of generality, we assume that  $\mathcal{M}$  is connected. Then the numbers of 0- and 4-handles in the handle decomposition of  $\mathcal{M}$  can be chosen to be 1. If  $\mathcal{M}$  is disconnected, then the partition function is the product of the partition functions on each of its disconnected components.
- b. Since  $G$  is finite, the  $G$ -bundle is fully characterized by the holonomy around non-contractible cycles. Recall that noncontractible cycles are the induced cycles of some 1-handles. Therefore, we interpret a holonomy labeled by group element  $\mathbf{g}$  around such a cycle as a defect we put across the associated 1-handle along its  $D^3$  plane, such that each anyon gets acted upon by  $\mathbf{g}$  when crossing this defect. Without loss of generality, we assume that no defect intersects the 0-handle, which can always be achieved.
- c. If  $G$  contains unitary symmetries only,  $\mathcal{M}$  is always oriented. On the other hand, in the presence of anti-unitary symmetries,  $\mathcal{M}$  can be an unorientable manifold with a nontrivial first Stiefel-Whitney class  $w_1^{TM}$ . Moreover, there must be a  $\mathbf{g}$ -defect on each non-orientable cycle, where  $\mathbf{g}$  is an anti-unitary symmetry. On the anyon diagram, anyons should flip the direction of the flow after crossing such  $\mathbf{g}$ -defect, as illustrated in Figs. 4.4 (pay special attention to the right two graphs of the lower figure).



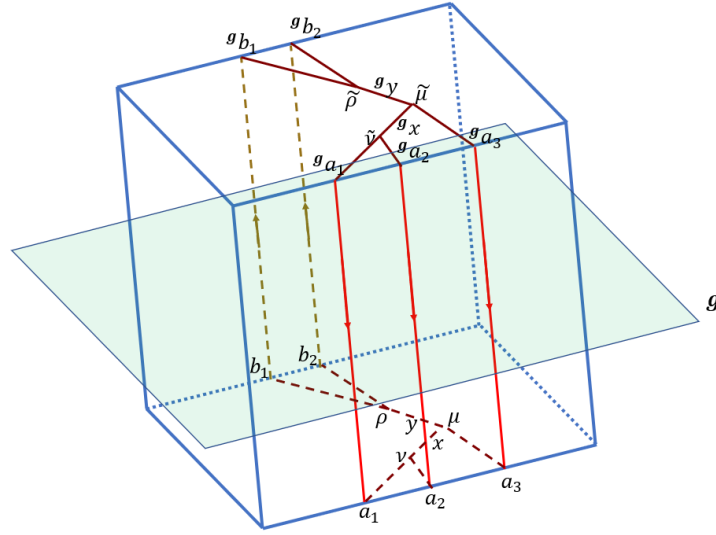


Figure 4.5: Illustration of the 1-handle. The 1-handle has the topology of a  $D^4$  but we draw it as a  $D^3$  for illustration. The shaded region represents a  $\mathbf{g}$ -defect for unitary  $\mathbf{g}$ , which cuts through the 1-handle along its  $D^3$  plane (drawn as a  $D^2$  plane here). The lower plane displays a dual vector  $\langle a_1, a_2, a_3; b_1, b_2 |_{(x, y, \mu, \nu, \rho)}$  that lives in the vector space associated to  $D^3$ , i.e.,  $\mathcal{V}(D^3; (a_1, a_2, a_3; b_1, b_2)) \simeq V_{b_1, b_2}^{a_1, a_2, a_3}$ , while the upper plane displays a vector  $| \mathfrak{g}a_1, \mathfrak{g}a_2, \mathfrak{g}a_3; \mathfrak{g}b_1, \mathfrak{g}b_2 \rangle_{(\mathfrak{g}x, \mathfrak{g}y, \tilde{\mu}, \tilde{\nu}, \tilde{\rho})}$ . The evaluation of the diagram is given by Eq. (4.114) if no defect is present. In the presence of the  $\mathbf{g}$ -defect we just need to add the  $U$ -factor as in Eq. (4.43). See Remarks d,e for further treatment when  $\mathbf{g}$  is anti-unitary.

- d. It is of paramount importance to keep track of the framing of 1-handles and 2-handles when drawing and evaluating the Kirby diagram. Let us emphasize that we use the convention according to which, for an orientable 1-handle, points on each pair of  $D^3$  balls related to each other by a reflection with respect to the plane perpendicularly bisecting the centers of these  $D^3$  balls are connected to each other by the 1-handle, while, for a non-orientable 1-handle, points on the pair of  $D^3$  balls are connected to each other by the 1-handle, if these points are related to each other by a translation that relates the two  $D^3$  balls. This convention is illustrated in Fig. 4.4. For 2-handles, we should pay special attention to whether we should add extra topological twists/kinks to the Kirby diagram as in Eq. (4.11), accounting for the correct self-intersection number of the  $S^1$  loop associated to the 2-handle.
- e. We further comment on assigning vectors and dual vectors to 1-handles and 0-handles. Note that when we attach a 1-handle and a 0-handle, we should assign a vector and a dual vector to the 1-handle and the 0-handle respectively as in Fig. 4.3. In a Kirby diagram, we can put the two  $D^3$  balls corresponding to a single 1-handle on the upper and lower parts of the diagram, and associate the dual vector  $\langle \mathbf{g}a_1, \dots; \mathbf{g}b_1, \dots |$  and the vector  $K^{q(\mathbf{g})}|a_1, \dots; b_1, \dots \rangle$  to the upper and lower ball, respectively. As illustrated in the lower figure of Fig. 4.4, according to the convention in Remark d, if  $\mathbf{g}$  is anti-unitary we draw  $K^{q(\mathbf{g})}|a_1, \dots; b_1, \dots \rangle$  in the same way as a dual vector on the anyon diagram. According to this convention, on the 1-handle we assign a dual vector  $\langle a_1, \dots; b_1, \dots | K^{q(\mathbf{g})}$  and a vector  $|\mathbf{g}a_1, \dots; \mathbf{g}b_1, \dots \rangle$ , and therefore the  $U$ -factor is given by Eq. (4.43), as illustrated in Fig. 4.5.
- f. In this convention, anyons running “upward” in the 1-handles are acted upon by  $\rho_{\mathbf{g}}$  while anyons running “downward” in the 1-handles are acted upon by  $\rho_{\mathbf{g}}^{-1}$ , when we put a  $\mathbf{g}$ -defect across the 1-handle, as in Fig. 4.6.
- g. Here we explain how to get  $\eta$ -factors in detail. In general, the  $S^1$  line of a 2-handle is separated into multiple segments by the defects. Starting from an arbitrary segment on this  $S^1$  line with anyon label  $a$ , we move along the  $S^1$  line on the Kirby diagram and use the above prescription to get a functor describing the successive symmetry actions, which takes the form  $\rho_{\mathbf{g}_1}^{s_1} \circ \rho_{\mathbf{g}_2}^{s_2} \circ \dots$ , where  $\mathbf{g}_{1,2,\dots}$  denotes the defect and  $s_{1,2,\dots} = 1$  ( $s_{1,2,\dots} = -1$ ) if the anyon crosses this defect in the “upward” (“downward”) direction. Note that this  $S^1$  is contractible, so consistency requires that the combination of all these defects is a trivial defect, i.e.,  $\mathbf{g}_1^{s_1} \mathbf{g}_2^{s_2} \dots = \mathbf{1}$ . The  $\eta$ -factor associated with this 2-handle comes from the natural isomorphism that connects  $\rho_{\mathbf{g}_1}^{s_1} \circ \rho_{\mathbf{g}_2}^{s_2} \circ \dots$  and the identity functor. The explicit expression of the  $\eta$ -factor is not unique, and different expressions can be converted into each other using Eq. (4.24).

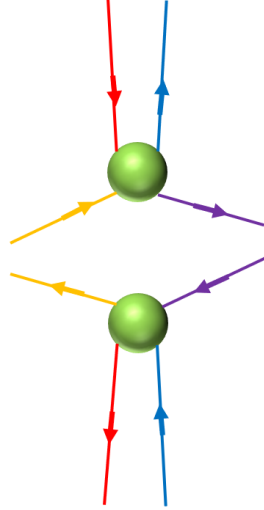


Figure 4.6: Suppose a  $\mathfrak{g}$ -defect is on the green 1-handle. Following their arrows, anyons in the red and yellow (blue and purple) lines enter the upper (lower)  $D^3$  ball and exit from the lower (upper)  $D^3$  ball, and they are said to move “downward” (“upward”) and are acted by  $\rho_{\mathfrak{g}}^{-1}$  ( $\rho_{\mathfrak{g}}$ ).

In Appendix 4.B, we present such an expression explicitly. In the following, we demonstrate this analysis via concrete examples.

First consider the situation where  $C$  is a  $\mathbb{Z}_2$  generator and some anyon  $a$  associated to a 2-handle crosses a  $C$ -defect twice. Then there is a natural isomorphism  $\eta(C, C)$  connecting  $\rho_C \circ \rho_C$  to the identity functor, which gives the desired  $\eta$ -factor to be  $\eta_a(C, C)$ . With slight abuse of notation, we will say that  $\rho_C \circ \rho_C$  acting on  $a$  gives a phase  $\eta_a(C, C)$ . As another example, consider the situation where  $C_1, C_2$  are any two generators of a unitary symmetry such that  $C_1 C_2 = C_2 C_1$ , and  $a$  is acted upon by  $\rho_{C_2} \circ \rho_{C_1} \circ \rho_{C_2}^{-1} \circ \rho_{C_1}^{-1}$ . Then connecting  $\rho_{C_2} \circ \rho_{C_1}$  to  $\rho_{C_2 C_1}$  gives a phase  $\eta_a(C_2, C_1)$ , while connecting  $\rho_{C_2 C_1}$  to  $\rho_{C_1} \circ \rho_{C_2}$  gives another phase  $1/\eta_a(C_1, C_2)$ . By definition, the composition of  $\rho_{C_1} \circ \rho_{C_2}$  with  $\rho_{C_2}^{-1} \circ \rho_{C_1}^{-1}$  is the identity functor. Therefore, the desired  $\eta$ -factor is  $\frac{\eta_a(C_2, C_1)}{\eta_a(C_1, C_2)}$ .

### 4.3 Examples: finite group symmetry

After spelling out the recipe for calculation, in this section we go to specific examples of finite group symmetries that concern us the most, including the case of no symmetry (i.e., Crane-Yetter model),  $\mathbb{Z}_2^T$ ,  $\mathbb{Z}_2 \times \mathbb{Z}_2$  and  $\mathbb{Z}_2^T \times \mathbb{Z}_2^T$ . We will calculate the anomaly indicators of these symmetries, which are the partition functions defined in Sec. 4.2 evaluated on appropriate manifolds with certain bundle structures (see Appendix 4.D for how to identify the manifolds and bundle structures that are relevant to the anomaly indicators). Especially, the calculation of the anomaly indicators of the mutual anomaly of  $\mathbb{Z}_2 \times \mathbb{Z}_2$  and  $\mathbb{Z}_2^T \times \mathbb{Z}_2^T$  is new, and their results are given by Eq. (4.53) and Eq. (4.55), respectively.

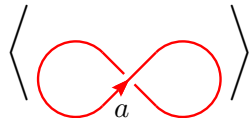
Manifold $\mathcal{M}$	Orientability	0-handles	1-handles	2-handles	3-handles	4-handles
$\mathbb{C}\mathbb{P}^2$	Yes	1	0	1	0	1
$\mathbb{R}\mathbb{P}^4$	No	1	1	1	1	1
$\mathbb{R}\mathbb{P}^3 \times S^1$	Yes	1	2	2	2	1
$\mathbb{R}\mathbb{P}^2 \times \mathbb{R}\mathbb{P}^2$	No	1	2	3	2	1

Table 4.1: Basic Information about handle decomposition of various manifolds used in Section 4.3. See Appendix 4.E for more information about their handle decomposition.

#### 4.3.1 No symmetry

Even in the absence of any symmetry, the partition function is not completely trivial and it reduces to the original Crane-Yetter model [91, 102]. Since the partition function is a cobordism invariant, to evaluate the partition function on any oriented  $4D$  manifold, we just need to evaluate it on the generating manifold of  $\Omega_4^{SO}(\star) \cong \mathbb{Z}$ , which is  $\mathbb{C}\mathbb{P}^2$ .

The minimum handle decomposition of  $\mathbb{C}\mathbb{P}^2$  contains 1 0-handle, 1 2-handle and 1 4-handle, as listed in Table 4.1. No symmetry defect is present, so there is no appearance of  $\eta$ -factor or  $U$ -factor. Given label  $a$  to the anyon associated with the 2-handle, the Kirby diagram is evaluated as

$$\left\langle \text{Kirby diagram} \right\rangle = d_a \theta_a \quad (4.45)$$


The topological twist reflects the +1 intersection number of  $\mathbb{CP}^2$ . Assembling all factors as in Eq. (4.44), we have

$$\mathcal{Z}(\mathbb{CP}^2) = \frac{1}{D} \sum_a d_a^2 \theta_a \quad (4.46)$$

It is well-known that the right hand side of this expression is related to the *chiral central charge*  $c \bmod 8$ , i.e.,

$$e^{2\pi ic/8} = \frac{1}{D} \sum_a d_a^2 \theta_a \quad (4.47)$$

Physically, the partition function  $\mathcal{Z}(\mathbb{CP}^2)$  and the chiral central charge gives the thermal Hall conductance of the  $(2+1)$ -d topological order, which is very well-known in the literature [84, 114].

An important fact in 4-dimensional topology is that any oriented manifold  $\mathcal{M}$  is cobordant with  $\#(\mathbb{CP}^2)^{\sigma(\mathcal{M})}$ , i.e., the connected sum of  $\sigma(\mathcal{M})$  copies of  $\mathbb{CP}^2$ , where  $\sigma(\mathcal{M})$  is the *intersection number* of  $\mathcal{M}$  [113]. Then the partition function on any oriented manifold  $\mathcal{M}$  is given by

$$\mathcal{Z}_{\text{CY}}(\mathcal{M}) = e^{(2\pi ic/8) \cdot \sigma(\mathcal{M})}, \quad (4.48)$$

which is indeed the correct form of the Crane-Yetter model [101, 102, 115].

### 4.3.2 $\mathbb{Z}_2^T$

For the group  $\mathbb{Z}_2^T$ , the bordism group that we should consider is  $\Omega_4^O(\star) \cong \mathbb{Z}_2 \oplus \mathbb{Z}_2$ , and the two  $\mathbb{Z}_2$  factors are generated by  $\mathbb{CP}^2$  and  $\mathbb{RP}^4$ , respectively.  $\mathcal{I}_0 \equiv \mathcal{Z}(\mathbb{CP}^2)$  has been calculated in Section 4.3.1 and given by Eq. (4.46), which is referred to as the “beyond-cohomology” anomaly indicator for  $\mathbb{Z}_2^T$ . In fact, in the presence of anti-unitary symmetry, there is always this “beyond-cohomology” anomaly indicator  $\mathcal{I}_0 = \mathcal{Z}(\mathbb{CP}^2)$ . Below we present the calculation for the partition function on  $\mathbb{RP}^4$ , which is referred to as the “incohomology” anomaly indicator for  $\mathbb{Z}_2^T$ . These anomaly indicators are first conjectured in Ref. [116] and derived in Ref. [94]. We will see that this is the simplest example involving 1-handle in the handle decomposition of the manifold.

The minimal handle decomposition of  $\mathbb{RP}^4$  contains 1 0-handle, 1 1-handle, 1 2-handle, 1 3-handle and 1 4-handle, as listed in Table 4.1. Since  $\mathbb{RP}^4$  is non-orientable, we should

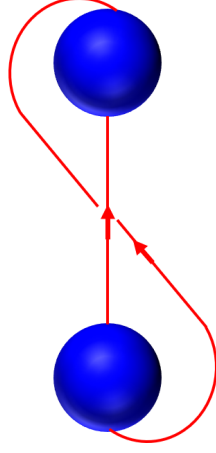


Figure 4.7: The Kirby diagram of  $\mathbb{R}P^4$ . The two blue balls illustrate the attaching region of the 1-handle and the red lines illustrate the attaching region of the 2-handle. The 1-handle is nonorientable.

consider the effect of the “ $\mathbb{Z}_2^T$ -defect”, or more commonly referred to as a *crosscap*, across the 1-handle. Namely, in the Kirby diagram shown in Fig. 4.7, the 1-handle (represented by the pair of blue balls) is crossed by such a  $\mathcal{T}$ -defect, with  $\mathcal{T}$  the generator of  $\mathbb{Z}_2^T$ .

Now we put anyon  $a$  and  $\mathcal{T}a$  on the  $S^1$  line of the 2-handle. Following remark g in Sec. 4.2.4, the  $\eta$ -factor from the 2-handle is given by action  $\rho_{\mathcal{T}} \circ \rho_{\mathcal{T}}$  on  $a$ , which is  $\eta_a(\mathcal{T}, \mathcal{T})$ . On the 1-handle we associate a dual vector  $\langle \mathcal{T}a; a |$  and a vector  $|a; \mathcal{T}a \rangle$ , and they are nonzero only when  $\mathcal{T}a = a$ . Pay attention that after touching the crosscap, the direction of the flow of one of the anyons should change. Specifically, comparing Fig. 4.7 and the diagram in Eq. (4.49), the curvy red line changes the direction of the flow. Also note that when  $\mathcal{T}a = a$ ,  $\eta_a(\mathcal{T}, \mathcal{T})$  is invariant under the gauge transformation Eq. (4.26). According to Eq. (4.27), the  $U$ -factor from the 1-handle is simply 1. Finally, the Kirby diagram in Fig. 4.7 can be translated to the following anyon diagram and evaluated as

$$\left\langle \begin{array}{c} \tau_a \\ \bullet \\ \bullet \\ a \\ \bullet \\ \bullet \\ a \\ \bullet \\ \tau_a \end{array} \right\rangle = d_a \theta_a \tag{4.49}$$

Again, there is a factor of  $\theta_a$  coming from the +1 framing of the 2-handle.

Assembling all factors, we have

$$\mathcal{Z}(\mathbb{RP}^4; \mathcal{T}) = \frac{1}{D} \sum_{\tau_{a=a}^a} d_a \theta_a \times \eta_a(\mathcal{T}, \mathcal{T}) \quad (4.50)$$

This is precisely the in-cohomology anomaly indicator for  $\mathbb{Z}_2^T$  symmetry [94, 116].

In summary, the beyond-cohomology anomaly indicator for  $\mathbb{Z}_2^T$  symmetry is  $\mathcal{I}_0 = \mathcal{Z}(\mathbb{CP}^2)$ , given by Eq. (4.46), while the in-cohomology anomaly indicator for  $\mathbb{Z}_2^T$  symmetry is  $\mathcal{I}_1 = \mathcal{Z}(\mathbb{RP}^4; \mathcal{T})$ , given by Eq. (4.50).<sup>10</sup> As such, the anomaly/partition function  $\mathcal{O}$  can be written as

$$\mathcal{O} = (\mathcal{I}_0)^{(w_2^{TM})^2} \cdot (\mathcal{I}_1)^{t^4} \quad (4.51)$$

where  $t$  is the generator of  $\mathcal{H}^1(\mathbb{Z}_2, \mathbb{Z}_2)$ , and  $(w_2^{TM})^2$  is the generator of the beyond-cohomology piece of anomaly.

### 4.3.3 $\mathbb{Z}_2 \times \mathbb{Z}_2$

Let us go to the simplest non-trivial group involving unitary symmetry only:  $\mathbb{Z}_2 \times \mathbb{Z}_2$ . The anomalies of  $\mathbb{Z}_2 \times \mathbb{Z}_2$  in  $(2+1)$ -dimension are classified by  $\mathbb{Z}_2 \oplus \mathbb{Z}_2$ , and the representative manifold is  $\mathbb{RP}^3 \times S^1$  with two different  $\mathbb{Z}_2 \times \mathbb{Z}_2$ -bundles, one with a  $C_1$  defect across the noncontractible cycle of  $\mathbb{RP}^3$  and a  $C_2$  defect across  $S^1$ , and the other with a  $C_2$  defect across the noncontractible cycle of  $\mathbb{RP}^3$  and a  $C_1$  defect across  $S^1$ , where  $C_1$  and  $C_2$  are two  $\mathbb{Z}_2$  generators of  $\mathbb{Z}_2 \times \mathbb{Z}_2$ .

Without loss of generality, let us first put a  $C_1$  defect across the noncontractible cycle of  $\mathbb{RP}^3$  and a  $C_2$  defect across  $S^1$ . The minimum handle decomposition of  $\mathbb{RP}^3 \times S^1$  contains 1 0-handle, 2 1-handle, 2 2-handle, 2 3-handle and 1 4-handle, as listed in Table 4.1. The Kirby diagram and the associated anyon diagram are drawn in Figs. 4.8 and 4.9, respectively.

Now we put anyon  $a$  and  $b$  on a red and orange segment of the 2-handles, respectively, and anyons on other segments can be obtained by symmetry actions on  $a$  and  $b$ , as shown in Fig. 4.9. From the two 1-handles we have two constraints  ${}^{C_1}a = a$  and  $a \times b \times {}^{C_1}b \rightarrow {}^{C_2}a$ . The second constraint means that  ${}^{C_2}a$  should be in the fusion channel of  $a$ ,  $b$  and  ${}^{C_1}b$ .

<sup>10</sup>Notice that  $\mathcal{I}_0$  and  $\mathcal{I}_1$  are numbers that will serve as coefficients in front of a certain basis in the expression of the anomaly.

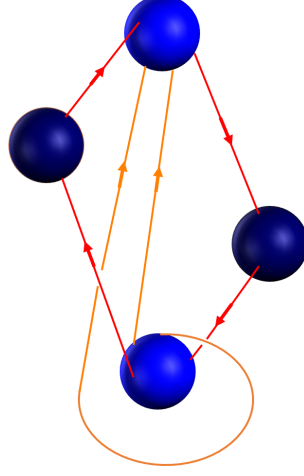


Figure 4.8: The Kirby diagram of  $\mathbb{RP}^3 \times S^1$ . The blue balls and dark blue balls illustrate the two 1-handles, and the red lines and orange lines illustrate the two 2-handles. Both 1-handles are orientable.

The  $\eta$ -factor from anyon  $a$  is given by action  $\rho_{C_1}^{-1} \circ \rho_{C_2} \circ \rho_{C_1} \circ \rho_{C_2}^{-1}$  on  $a$ , which is  $\frac{\eta_a(C_2, C_1)}{\eta_a(C_1, C_2)}$ . The  $\eta$ -factor from anyon  $b$  is given by action  $\rho_{C_1}^{-1} \circ \rho_{C_1}^{-1}$  on  $b$ , which is  $\frac{1}{\eta_b(C_1, C_1)}$ . The  $U$ -factor from the blue 1-handle is  $U_{C_1}^{-1}(a, b; x)_{\mu\tilde{\mu}} U_{C_1}^{-1}(x, {}^{C_1}b; {}^{C_2}a)_{\nu\tilde{\nu}}$ , while the  $U$ -factor from the darkblue 1-handle is simply 1 according to Eq. (4.27). Finally, we need to evaluate the anyon diagram Fig. 4.8, which is

$$d_a d_b \frac{\theta_x}{\theta_a} \left( R_u^{b, C_1 b} \right)_{\rho\sigma} \left( F_{C_2 a}^{a, b, C_1 b} \right)_{(x, \tilde{\mu}, \tilde{\nu})(u, \sigma, \alpha)}^* \left( F_{C_2 a}^{a, C_1 b, b} \right)_{(C_1 x, \mu, \nu)(u, \rho, \alpha)} \quad (4.52)$$

Assembling all factors as in Eq. (4.44), we have

$$\begin{aligned} \mathcal{Z}(\mathbb{RP}^3 \times S^1; C_1, C_2) &= \frac{1}{D^2} \sum_{\substack{a, b, x, u \\ \mu\nu\tilde{\mu}\tilde{\nu}\rho\sigma\alpha \\ C_1 a = a \\ a \times b \times C_1 b \rightarrow C_2 a}} d_b \frac{\theta_x}{\theta_a} \left( R_u^{b, C_1 b} \right)_{\rho\sigma} \left( F_{C_2 a}^{a, b, C_1 b} \right)_{(x, \tilde{\mu}, \tilde{\nu})(u, \sigma, \alpha)}^* \left( F_{C_2 a}^{a, C_1 b, b} \right)_{(C_1 x, \mu, \nu)(u, \rho, \alpha)} \\ &\quad \times U_{C_1}^{-1}(a, b; x)_{\tilde{\mu}\mu} U_{C_1}^{-1}(x, {}^{C_1}b; {}^{C_2}a)_{\tilde{\nu}\nu} \times \frac{1}{\eta_b(C_1, C_1)} \frac{\eta_a(C_2, C_1)}{\eta_a(C_1, C_2)} \end{aligned} \quad (4.53)$$

It is straightforward to check that this expression is invariant under the vertex basis transformation Eqs. (4.10),(4.18) and the symmetry action gauge transformation Eq. (4.26).



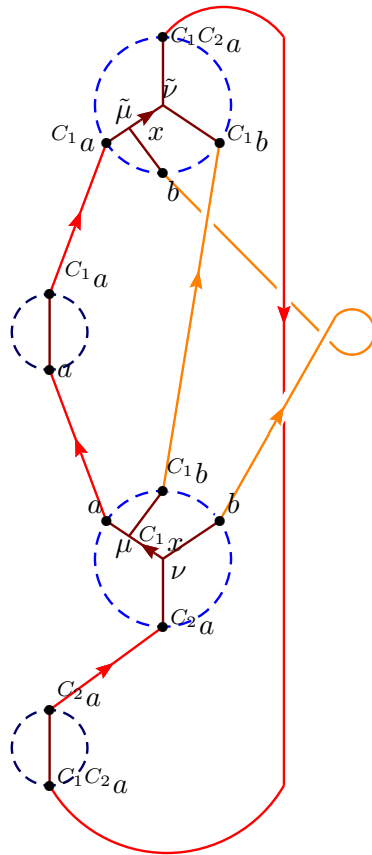


Figure 4.9: Anyon diagram from the Kirby diagram of  $\mathbb{RP}^3 \times S^1$  in Fig. 4.8. Pay attention to the extra topological twist of the orange line from the correct framing of the corresponding 2-handle.

The general proof of the cobordism invariance and invertibility of this partition function (see Appendix 4.C) indicates that this expression is  $\pm 1$ .

Therefore, the two anomaly indicators of  $\mathbb{Z}_2 \times \mathbb{Z}_2$  symmetry are  $\mathcal{I}_1 = \mathcal{Z}(\mathbb{RP}^3 \times S^1; C_1, C_2)$  and  $\mathcal{I}_2 = \mathcal{Z}(\mathbb{RP}^3 \times S^1; C_2, C_1)$ , given by Eq. (4.53), and the anomaly  $\mathcal{O} \in \mathcal{H}^4(\mathbb{Z}_2 \times \mathbb{Z}_2, \text{U}(1))$  can be written as

$$\mathcal{O} = (\mathcal{I}_1)^{c_1^3 c_2} \cdot (\mathcal{I}_2)^{c_2^3 c_1}, \quad (4.54)$$

where  $c_1$  and  $c_2$  are two generators of  $\mathcal{H}^1(\mathbb{Z}_2 \times \mathbb{Z}_2, \mathbb{Z}_2)$  corresponding to  $C_1$  and  $C_2$ , respectively.

#### 4.3.4 $\mathbb{Z}_2^T \times \mathbb{Z}_2^T$

Finally, let us consider the group  $\mathbb{Z}_2^T \times \mathbb{Z}_2^T$ . The anomalies of  $\mathbb{Z}_2^T \times \mathbb{Z}_2^T$  in  $(2+1)$ -dimension are classified by  $(\mathbb{Z}_2)^4$ . Suppose the two anti-unitary generators of  $\mathbb{Z}_2^T \times \mathbb{Z}_2^T$  are  $\mathcal{T}_1$  and  $\mathcal{T}_2$ . The representative manifold for the four  $\mathbb{Z}_2$  pieces are  $\mathbb{CP}^2$ ,  $\mathbb{RP}^4$  with a  $\mathcal{T}_1$  defect across the crosscap,  $\mathbb{RP}^4$  with a  $\mathcal{T}_2$  defect across the crosscap, and  $\mathbb{RP}^2 \times \mathbb{RP}^2$  with a  $\mathcal{T}_1$  defect across the crosscap of the first  $\mathbb{RP}^2$  piece and a  $\mathcal{T}_2$  defect across the crosscap of the second  $\mathbb{RP}^2$  piece. Given the result Eq. (4.50), we just need to focus on the last manifold.

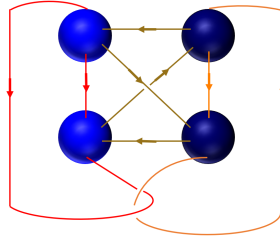


Figure 4.10: The Kirby diagram of  $\mathbb{RP}^2 \times \mathbb{RP}^2$ . The blue balls and dark blue balls illustrate two 1-handles and the red, orange and sand-dune lines illustrate three 2-handles. Both 1-handles are nonorientable.

The minimum handle decomposition of  $\mathbb{RP}^2 \times \mathbb{RP}^2$  contains 1 0-handle, 2 1-handle, 3 2-handle, 2 3-handle and 1 4-handle, as listed in Table 4.1. The Kirby diagram and the associated anyon diagram are drawn in Figs. 4.10 and 4.11, respectively.

Now we put anyon  $a$ ,  $b$  and  $c$  on a red, orange and sand-dune segment of the 2-handles, respectively, and anyons on other segments can be obtained by symmetry actions on  $a$ ,  $b$  and

$c$ , as shown in Fig. 4.11. From the two 1-handles we have two constraints  $\mathcal{T}_1 a \times \mathcal{T}_2 c \times c \rightarrow a$  and  $\mathcal{T}_1 c \times c \times b \rightarrow \mathcal{T}_2 b$ .

The  $\eta$ -factor from anyon  $a$  is given by action  $\rho_{\mathcal{T}_1} \circ \rho_{\mathcal{T}_1}$  on  $a$ , which is  $\eta_a(\mathcal{T}_1, \mathcal{T}_1)$ . The  $\eta$ -factor from anyon  $b$  is given by action  $\rho_{\mathcal{T}_2} \circ \rho_{\mathcal{T}_2}$  on  $b$ , which is  $\eta_b(\mathcal{T}_1, \mathcal{T}_1)$ . The  $\eta$ -factor from anyon  $c$  is given by action  $\rho_{\mathcal{T}_2} \circ \rho_{\mathcal{T}_1} \circ \rho_{\mathcal{T}_2}^{-1} \circ \rho_{\mathcal{T}_1}^{-1}$  on  $c$ , which is  $\frac{\eta_c(\mathcal{T}_2, \mathcal{T}_1)}{\eta_c(\mathcal{T}_1, \mathcal{T}_2)}$ . The  $U$ -factor from the blue 1-handle is  $U_{\mathcal{T}_1}^{-1}(\mathcal{T}_1 a, \mathcal{T}_2 c; x)_{\mu_x \tilde{\mu}_x} U_{\mathcal{T}_1}^{-1}(x, c; a)_{\nu_x \tilde{\nu}_x}$ , and the  $U$ -factor from the darkblue 1-handle is  $U_{\mathcal{T}_2}^{-1}(\mathcal{T}_1 c, y; \mathcal{T}_2 b)_{\mu_y \tilde{\mu}_y} U_{\mathcal{T}_2}^{-1}(c, b; y)_{\nu_y \tilde{\nu}_y}$ . Finally, we need to evaluate the anyon diagram Fig. 4.10.

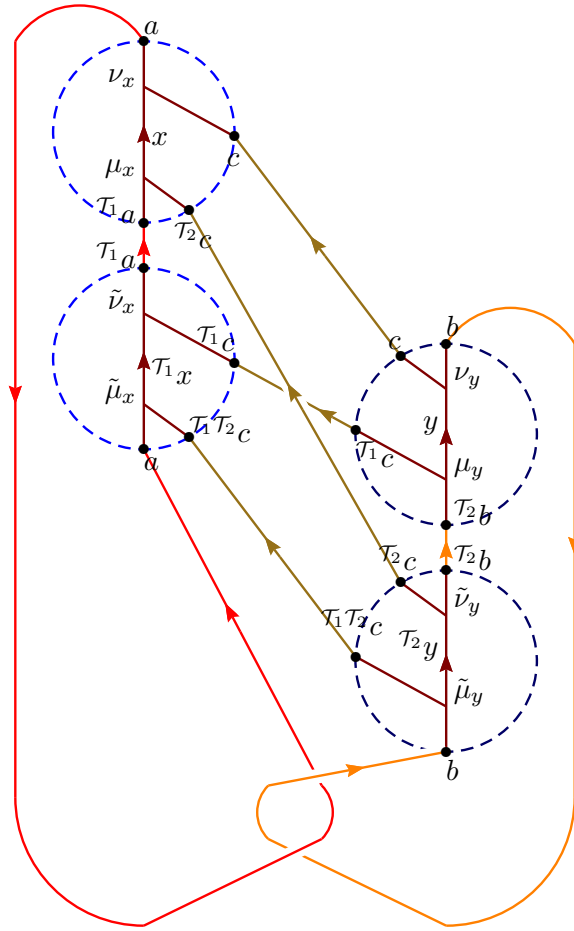


Figure 4.11: Anyon diagram from the Kirby diagram of  $\mathbb{RP}^2 \times \mathbb{RP}^2$  in Fig. 4.10.

Assembling all factors, we have

$$\begin{aligned}
\mathcal{Z}(\mathbb{RP}^2 \times \mathbb{RP}^2; \mathcal{T}_1, \mathcal{T}_2) &= \frac{1}{D^3} \sum_{\substack{a,b,c,x,y,u,v \\ \mu_x \nu_x \mu_y \nu_y \tilde{\mu}_x \tilde{\nu}_x \tilde{\mu}_y \tilde{\nu}_y \rho \sigma \tau \alpha \beta \gamma \delta \\ \mathcal{T}_1 a \times \mathcal{T}_2 c \times c \rightarrow a \\ \mathcal{T}_1 c \times c \times b \rightarrow \mathcal{T}_2 b}} d_c d_v \frac{\theta_v}{\theta_a \theta_b} \left( R_u^{\mathcal{T}_1 c, \mathcal{T}_2 c} \right)_{\rho \sigma} \\
&\times \left( F_v^{a, \mathcal{T}_1 \mathcal{T}_2 c, \mathcal{T}_2 y} \right)_{(\mathcal{T}_1 x, \tilde{\mu}_x, \alpha)(b, \tilde{\mu}_y, \tau)}^* \left( F_{\mathcal{T}_2 y}^{\mathcal{T}_2 c, \mathcal{T}_1 c, y} \right)_{(u, \rho, \beta)(\mathcal{T}_2 b, \mu_y, \tilde{\nu}_y)}^* \\
&\times \left( F_x^{\mathcal{T}_1 x, \mathcal{T}_1 c, \mathcal{T}_2 c} \right)_{(\mathcal{T}_1 a, \tilde{\nu}_x, \mu_x)(u, \sigma, \gamma)}^* \left( F_v^{\mathcal{T}_1 x, u, y} \right)_{(x, \gamma, \delta)(\mathcal{T}_2 y, \beta, \alpha)}^* \left( F_v^{x, c, b} \right)_{(a, \nu_x, \tau)(y, \nu_y, \delta)}^* \\
&\times U_{\mathcal{T}_1}^{-1}(\mathcal{T}_1 a, \mathcal{T}_2 c; x)_{\mu_x \tilde{\mu}_x} U_{\mathcal{T}_1}^{-1}(x, c; a)_{\nu_x \tilde{\nu}_x} U_{\mathcal{T}_2}^{-1}(\mathcal{T}_1 c, y; \mathcal{T}_2 b)_{\mu_y \tilde{\mu}_y}^* U_{\mathcal{T}_2}^{-1}(c, b; y)_{\nu_y \tilde{\nu}_y}^* \times \eta_a(\mathcal{T}_1, \mathcal{T}_1) \eta_b(\mathcal{T}_2, \mathcal{T}_2) \frac{\eta_c(\mathcal{T}_2, \mathcal{T}_1)}{\eta_c(\mathcal{T}_1, \mathcal{T}_2)}
\end{aligned} \tag{4.55}$$

It is straightforward to check that this expression is invariant under the vertex basis transformation Eqs. (4.10), (4.18) and the symmetry action gauge transformation Eq. (4.26). Again, the general proof of the cobordism invariance and invertibility of this partition function (see Appendix 4.C) indicates this expression is  $\pm 1$ .

Therefore, the four anomaly indicators of  $\mathbb{Z}_2^T \times \mathbb{Z}_2^T$  symmetry are  $\mathcal{I}_0 = \mathcal{Z}(\mathbb{CP}^2)$ , given by Eq. (4.46),  $\mathcal{I}_1 = \mathcal{Z}(\mathbb{RP}^4; \mathcal{T}_1)$ ,  $\mathcal{I}_2 = \mathcal{Z}(\mathbb{RP}^4; \mathcal{T}_2)$ , given by Eq. (4.50), and  $\mathcal{I}_3 = \mathcal{Z}(\mathbb{RP}^2 \times \mathbb{RP}^2; \mathcal{T}_1, \mathcal{T}_2)$ , given by Eq. (4.50). When extracting the cohomology element from the anomaly indicators, we should be careful that the manifold  $\mathbb{RP}^2 \times \mathbb{RP}^2$  has nontrivial  $(w_2^{TM})^2$  as well. As a result, the anomaly/partition function  $\mathcal{O}$  can be written as

$$\mathcal{O} = (\mathcal{I}_0)^{(w_2^{TM})^2} \cdot (\mathcal{I}_1)^{t_1^4} \cdot (\mathcal{I}_2)^{t_2^4} \cdot (\mathcal{I}_0 \mathcal{I}_3)^{t_1^2 t_2^2}, \tag{4.56}$$

where  $t_1$  and  $t_2$  are two generators of  $\mathcal{H}^1(\mathbb{Z}_2^T \times \mathbb{Z}_2^T, \mathbb{Z}_2)$  corresponding to  $\mathcal{T}_1$  and  $\mathcal{T}_2$ , respectively, and  $(w_2^{TM})^2$  is the generator of the beyond-cohomology piece of anomaly.

## All-fermion $\mathbb{Z}_2$ topological order

In order to demonstrate the power of the new anomaly indicators, in this subsection we systematically study a concrete example, the all-fermion  $\mathbb{Z}_2$  topological order, which is a cousin of the standard  $\mathbb{Z}_2$  topological order but all its nontrivial anyons are fermions [54, 84, 117, 118]. We will classify all  $\mathbb{Z}_2^T \times \mathbb{Z}_2^T$  symmetry fractionalization classes for this topological order, and calculate the anomaly for each class. We will see that the anomalies of some symmetry fractionalization classes can be obtained using (generalizations of) methods developed in the previous literature, but we also point out examples of symmetry fractionalization classes whose anomalies can only be calculated using the anomaly indicators derived here, as far as we can tell.

The data of the underlying UMTC of the all-fermion  $\mathbb{Z}_2$  topological order is collected in Ref. [84]. In particular, it has four simple anyons,  $1, e, m, \psi = e \times m$ . We can label an anyon  $a$  by two  $\mathbb{Z}_2$  numbers  $a = (a_e, a_m)$  as  $e^{a_e} \times m^{a_m}$ . In a choice of gauge, the  $F$ -symbols are all trivial and the nontrivial  $R$ -symbols are given by

$$R^{ee} = R^{mm} = R^{\psi\psi} = R^{\psi e} = R^{m\psi} = R^{em} = (-1) \quad (4.57)$$

Here we omit the subscript of the  $R$ -symbol since the outcome of the fusion rules is unique. A  $\mathbb{Z}_2^T \times \mathbb{Z}_2^T$  symmetry fractionalization class is specified by the data  $\{\rho; U, \eta\}$ , which will be classified below.

First we consider the situation where the  $\mathbb{Z}_2^T \times \mathbb{Z}_2^T$  symmetry does not permute anyons. In this case, to satisfy Eq. (4.19) all  $U$ -symbols can be set to 1. Different symmetry fractionalization classes are then classified by

$$\mathcal{H}^2(\mathbb{Z}_2 \times \mathbb{Z}_2, \mathbb{Z}_2 \times \mathbb{Z}_2) = \mathbb{Z}_2^6, \quad (4.58)$$

Denoting a representative cocycle of an element in  $\mathcal{H}^2(\mathbb{Z}_2 \times \mathbb{Z}_2, \mathbb{Z}_2 \times \mathbb{Z}_2)$  by  $\mathbf{t}(\mathbf{g}, \mathbf{h})$  with  $\mathbf{g}, \mathbf{h} \in \mathbb{Z}_2^T \times \mathbb{Z}_2^T$ , different cohomology elements are distinguished by  $\mathbf{t}(\mathcal{T}_1, \mathcal{T}_1)$ ,  $\mathbf{t}(\mathcal{T}_2, \mathcal{T}_2)$ ,  $\mathbf{t}(\mathcal{T}_1\mathcal{T}_2, \mathcal{T}_1\mathcal{T}_2)$ . Here we use the gauge convention that  $\mathbf{t}(\mathbf{g}, \mathbf{1}) = \mathbf{t}(\mathbf{1}, \mathbf{h}) = 1$ , in order to be compatible with the gauge choice Eq. (4.27). Relatedly, we have

$$\eta_a(\mathcal{T}_1, \mathcal{T}_1) = M_{a, \mathbf{t}(\mathcal{T}_1, \mathcal{T}_1)}, \quad \eta_a(\mathcal{T}_2, \mathcal{T}_2) = M_{a, \mathbf{t}(\mathcal{T}_2, \mathcal{T}_2)}, \quad \eta_a(\mathcal{T}_1\mathcal{T}_2, \mathcal{T}_1\mathcal{T}_2) = M_{a, \mathbf{t}(\mathcal{T}_1\mathcal{T}_2, \mathcal{T}_1\mathcal{T}_2)}. \quad (4.59)$$

These three  $\eta$ -phases characterize whether anyon  $a$  is a Kramers doublet under  $\mathcal{T}_1$ , a Kramers doublet under  $\mathcal{T}_2$  and charge  $1/2$  under  $\mathcal{T}_1\mathcal{T}_2$ , respectively. In total, there are 36 inequivalent symmetry fractionalization classes in this situation (Of the 64 possible classes associated with  $\mathcal{H}^2(\mathbb{Z}_2 \times \mathbb{Z}_2, \mathbb{Z}_2 \times \mathbb{Z}_2) = (\mathbb{Z}_2)^6$ , relabeling  $e$  and  $m$  gives 36 inequivalent classes).

Substituting the UMTC data to the previously derived expressions of  $\mathcal{I}_{0,1,2,3}$ , the anomaly indicators become

$$\begin{aligned} \mathcal{I}_0 &= \frac{1}{2} \sum_a \theta_a \\ \mathcal{I}_1 &= \frac{1}{2} \sum_a \theta_a \eta_a(\mathcal{T}_1, \mathcal{T}_1) \\ \mathcal{I}_2 &= \frac{1}{2} \sum_a \theta_a \eta_a(\mathcal{T}_2, \mathcal{T}_2) \\ \mathcal{I}_3 &= \frac{1}{8} \sum_{abc} \frac{\theta_{a \times b} \theta_c}{\theta_a \theta_b} \eta_a(\mathcal{T}_1, \mathcal{T}_1) \eta_b(\mathcal{T}_2, \mathcal{T}_2) \frac{\eta_c(\mathcal{T}_2, \mathcal{T}_1)}{\eta_c(\mathcal{T}_1, \mathcal{T}_2)} \end{aligned} \quad (4.60)$$

In particular,  $\mathcal{I}_3$  simplifies dramatically in this context.

Following Ref. [119], we make Table. 4.2 to summarize the anomalies for all of the 36 inequivalent symmetry fractionalization classes. In Table. 4.2 we use the labeling convention of Ref. [54]: If an excitation carries half charge under the unitary  $\mathbb{Z}_2$  symmetry generated by  $\mathcal{T}_1\mathcal{T}_2$ , it is followed by a  $C$  in the labeling. If it carries Kramers degeneracy under  $\mathcal{T}_1$  or  $\mathcal{T}_2$ , then it is followed by a  $\mathcal{T}_1$  or  $\mathcal{T}_2$  in the labeling.<sup>11</sup>

From Table 4.2, we see that, when the symmetry fractionalization class is trivial, i.e.,  $\eta_a(\mathbf{g}, \mathbf{h}) = 1$  for all anyon  $a$  and all group elements  $\mathbf{g}, \mathbf{h}$ ,  $\mathcal{I}_0 = \mathcal{I}_1 = \mathcal{I}_2 = \mathcal{I}_3 = -1$ , signaling nontrivial anomaly. This is to be contrast to the case of the  $\mathbb{Z}_2$  toric code with the trivial symmetry fractionalization class, where  $\mathcal{I}_0 = \mathcal{I}_1 = \mathcal{I}_2 = \mathcal{I}_3 = 1$  and no anomaly is present [119].

We mention that this result can also be achieved by considering the projection  $p : \mathbb{Z}_2^T \times \mathbb{Z}_2^T \rightarrow \mathbb{Z}_2^{T0}$ , where  $\mathbb{Z}_2^{T0}$  is thought of as an anti-unitary symmetry on  $\mathcal{C}$  that does not permute anyons as well. The anomaly indicators of  $\mathbb{Z}_2^{T0}$  are already known in previous literature [94, 116] and reproduced in Eqs. (4.46) and (4.50). Notice that the trivial symmetry fractionalization class of  $\mathbb{Z}_2^T \times \mathbb{Z}_2^T$  denoted by  $efmf$  here is the ‘‘pullback’’ of the trivial symmetry fractionalization class of  $\mathbb{Z}_2^{T0}$ , denoted by  $efmf$  as well in the literature. The anomaly of  $efmf$  for  $\mathbb{Z}_2^T \times \mathbb{Z}_2^T$  is the pullback of the anomaly of  $efmf$  for  $\mathbb{Z}_2^{T0}$ . From Eqs (4.46) and (4.50), the latter anomaly is  $(w_2^{TM})^2 + t^4$  where  $t$  is the generator of  $\mathcal{H}^1(\mathbb{Z}_2^{T0}, \mathbb{Z}_2)$ , whose pullback to  $\mathbb{Z}_2^T \times \mathbb{Z}_2^T$  is  $(w_2^{TM})^2 + t_1^4 + t_2^4$ . Comparing this result with Eq. (4.56), we get the first line of Table 4.2. Based on the anomaly of this symmetry fractionalization class, the rest of the Table 4.2 can be achieved from relative anomaly as in Ref. [119].

Next consider the situation where anyons are permuted under some elements of  $\mathbb{Z}_2^T \times \mathbb{Z}_2^T$  symmetry. There are two possibilities:

- (a)  $\mathcal{T}_1$  and  $\mathcal{T}_2$  both exchange two of three nontrivial anyons.
- (b)  $\mathcal{T}_1$  and  $\mathcal{T}_1\mathcal{T}_2$  both exchange two of three nontrivial anyons.

Without loss of generality, we will take the anyons being exchanged as  $e$  and  $m$ .

In either case, if some (unitary or anti-unitary) element  $\mathbf{g} \in \mathbb{Z}_2^T \times \mathbb{Z}_2^T$  permutes  $e$  and  $m$ , to satisfy Eq. (4.19), we can demand that  $\rho_{\mathbf{g}}$  action on  $|a, b; c\rangle$  be such that

$$U_{\mathbf{g}}(a, b; c) = (-1)^{aebm}, \quad (4.61)$$

---

<sup>11</sup> $\mathcal{I}_3$  in Table II of Ref. [119] is in fact our  $\mathcal{I}_1\mathcal{I}_2\mathcal{I}_3$ .

Label	$\mathbf{t}(\mathcal{T}_1\mathcal{T}_2, \mathcal{T}_1\mathcal{T}_2), \mathbf{t}(\mathcal{T}_1, \mathcal{T}_1), \mathbf{t}(\mathcal{T}_2, \mathcal{T}_2)$	$(\mathcal{I}_1, \mathcal{I}_2, \mathcal{I}_0\mathcal{I}_3)$
$efmf$	$(1, 1, 1)$	$(-1, -1, 1)$
$efmf\mathcal{T}_2$	$(1, 1, m)$	$(-1, 1, -1)$
$ef\mathcal{T}_2mf\mathcal{T}_2$	$(1, 1, \psi)$	$(-1, 1, -1)$
$ef\mathcal{T}_1mf$	$(1, m, 1)$	$(1, -1, -1)$
$ef\mathcal{T}_1mf\mathcal{T}_2$	$(1, m, e)$	$(1, 1, 1)$
$ef\mathcal{T}_1\mathcal{T}_2mf$	$(1, m, m)$	$(1, 1, 1)$
$ef\mathcal{T}_1\mathcal{T}_2mf\mathcal{T}_2$	$(1, m, \psi)$	$(1, 1, 1)$
$ef\mathcal{T}_1mf\mathcal{T}_1$	$(1, \psi, 1)$	$(1, -1, -1)$
$ef\mathcal{T}_1\mathcal{T}_2mf\mathcal{T}_1$	$(1, \psi, m)$	$(1, 1, 1)$
$ef\mathcal{T}_1\mathcal{T}_2mf\mathcal{T}_1\mathcal{T}_2$	$(1, \psi, \psi)$	$(1, 1, 1)$
$efmfC$	$(e, 1, 1)$	$(-1, -1, -1)$
$efmfC\mathcal{T}_2$	$(e, 1, e)$	$(-1, 1, 1)$
$ef\mathcal{T}_2mfC$	$(e, 1, m)$	$(-1, 1, -1)$
$ef\mathcal{T}_2mfC\mathcal{T}_2$	$(e, 1, \psi)$	$(-1, 1, -1)$
$efmfC\mathcal{T}_1$	$(e, e, 1)$	$(1, -1, 1)$
$efmfC\mathcal{T}_1\mathcal{T}_2$	$(e, e, e)$	$(1, 1, -1)$
$ef\mathcal{T}_2mfC\mathcal{T}_1$	$(e, e, m)$	$(1, 1, 1)$
$ef\mathcal{T}_2mfC\mathcal{T}_1\mathcal{T}_2$	$(e, e, \psi)$	$(1, 1, 1)$
$ef\mathcal{T}_1mfC$	$(e, m, 1)$	$(1, -1, -1)$
$ef\mathcal{T}_1mfC\mathcal{T}_2$	$(e, m, e)$	$(1, 1, 1)$
$ef\mathcal{T}_1\mathcal{T}_2mfC$	$(e, m, m)$	$(1, 1, -1)$
$ef\mathcal{T}_1\mathcal{T}_2mfC\mathcal{T}_2$	$(e, m, \psi)$	$(1, 1, -1)$
$ef\mathcal{T}_1mfC\mathcal{T}_1$	$(e, \psi, 1)$	$(1, -1, -1)$
$ef\mathcal{T}_1mfC\mathcal{T}_1\mathcal{T}_2$	$(e, \psi, e)$	$(1, 1, 1)$
$ef\mathcal{T}_1\mathcal{T}_2mfC\mathcal{T}_1$	$(e, \psi, m)$	$(1, 1, -1)$
$ef\mathcal{T}_1\mathcal{T}_2mfC\mathcal{T}_1\mathcal{T}_2$	$(e, \psi, \psi)$	$(1, 1, -1)$
$efCmfC$	$(\psi, 1, 1)$	$(-1, -1, -1)$
$efC\mathcal{T}_2mfC$	$(\psi, 1, m)$	$(-1, 1, -1)$
$efC\mathcal{T}_2mfC\mathcal{T}_2$	$(\psi, 1, \psi)$	$(-1, 1, 1)$
$efCmfC\mathcal{T}_1$	$(\psi, e, 1)$	$(1, -1, -1)$
$efCmfC\mathcal{T}_1\mathcal{T}_2$	$(\psi, e, e)$	$(1, 1, -1)$
$efC\mathcal{T}_2mfC\mathcal{T}_1$	$(\psi, e, m)$	$(1, 1, -1)$
$efC\mathcal{T}_2mfC\mathcal{T}_1\mathcal{T}_2$	$(\psi, e, \psi)$	$(1, 1, 1)$
$efC\mathcal{T}_1mfC\mathcal{T}_1$	$(\psi, \psi, 1)$	$(1, -1, 1)$
$efC\mathcal{T}_1\mathcal{T}_2mfC\mathcal{T}_1$	$(\psi, \psi, m)$	$(1, 1, 1)$
$efC\mathcal{T}_1\mathcal{T}_2mfC\mathcal{T}_1\mathcal{T}_2$	$(\psi, \psi, \psi)$	$(1, 1, -1)$

Table 4.2: Anomalies for all-fermion  $\mathbb{Z}_2$  topological order with  $\mathbb{Z}_2^T \times \mathbb{Z}_2^T$  symmetry, where symmetries do not permute anyons.  $efmf$  refers to the trivial symmetry fractionalization class. All classes have  $\mathcal{I}_0 = -1$  and hence the beyond-cohomology anomaly.

Label	$\mathbf{t}(\mathcal{T}_1\mathcal{T}_2, \mathcal{T}_1\mathcal{T}_2), \mathbf{t}(\mathcal{T}_1, \mathcal{T}_1), \mathbf{t}(\mathcal{T}_2, \mathcal{T}_2)$	$(\mathcal{I}_1, \mathcal{I}_2, \mathcal{I}_0\mathcal{I}_3)$
$(efmf)_{\mathcal{T}_1, \mathcal{T}_2} \psi f \mathcal{T}_1 \mathcal{T}_2$	(1, 1, 1)	(1, 1, 1)
$(efCmfC)_{\mathcal{T}_1, \mathcal{T}_2} \psi f \mathcal{T}_1 \mathcal{T}_2$	( $\psi$ , 1, 1)	(1, 1, -1)

Table 4.3: Anomalies for all-fermion  $\mathbb{Z}_2$  topological order with  $\mathbb{Z}_2^T \times \mathbb{Z}_2^T$  symmetry, where  $\mathcal{T}_1$  and  $\mathcal{T}_2$  permute anyons, which is the reason for the subscripts for  $e$  and  $m$ . The meanings of the other symbols are the same as in Table 4.2. All classes have  $\mathcal{I}_0 = -1$  and hence the beyond-cohomology anomaly.

Label	$\mathbf{t}(\mathcal{T}_1\mathcal{T}_2, \mathcal{T}_1\mathcal{T}_2), \mathbf{t}(\mathcal{T}_1, \mathcal{T}_1), \mathbf{t}(\mathcal{T}_2, \mathcal{T}_2)$	$(\mathcal{I}_1, \mathcal{I}_2, \mathcal{I}_0\mathcal{I}_3)$
$(efmf)_{\mathcal{T}_1, \mathcal{T}_1\mathcal{T}_2} \psi f \mathcal{T}_1 C$	(1, 1, 1)	(1, -1, -1)
$(ef\mathcal{T}_2mf\mathcal{T}_2)_{\mathcal{T}_1, \mathcal{T}_1\mathcal{T}_2} \psi f \mathcal{T}_1 C$	(1, 1, $\psi$ )	(1, 1, 1)

Table 4.4: Anomalies for all-fermion  $\mathbb{Z}_2$  topological order with  $\mathbb{Z}_2^T \times \mathbb{Z}_2^T$  symmetry, where  $\mathcal{T}_1$  and  $\mathcal{T}_1\mathcal{T}_2$  permute anyons, which is the reason for the subscripts for  $e$  and  $m$ . The meanings of the other symbols are the same as in Table 4.2. All classes have  $\mathcal{I}_0 = -1$  and hence the beyond-cohomology anomaly.

with  $(a_e, a_m), (b_e, b_m)$  the  $\mathbb{Z}_2$  labels of  $a, b$ . For any element  $\mathbf{g}$  that does not permute anyons, we can take  $U_{\mathbf{g}}(a, b; c) = 1$ . To satisfy Eqs. (4.23) and (4.24), a specific valid choice of the  $\eta$ -symbols is

$$\eta_{\psi}^{(1)}(\mathbf{g}, \mathbf{g}) = -1 \quad (4.62)$$

where  $\mathbf{g}$  is an element that permutes anyons, while all other  $\eta$ -symbols (such as  $\eta_e^{(1)}(\mathbf{g}, \mathbf{g})$  and  $\eta_{\psi}^{(1)}(\mathbf{g}, \mathbf{g}')$  with  $\mathbf{g}' \neq \mathbf{g}$ ) are 1. To get all possible valid choices of the  $\eta$ -symbols, note that  $\mathcal{H}_{\rho}^2(\mathbb{Z}_2 \times \mathbb{Z}_2, \mathbb{Z}_2 \times \mathbb{Z}_2) \cong \mathbb{Z}_2$  for both case (a) and case (b), which means that in either case there is one more symmetry fractionalization class. Denoting the nontrivial element in  $\mathcal{H}_{\rho}^2(\mathbb{Z}_2 \times \mathbb{Z}_2, \mathbb{Z}_2 \times \mathbb{Z}_2) \cong \mathbb{Z}_2$  by  $\mathbf{t}(\mathbf{g}, \mathbf{h})$  with  $\mathbf{g}, \mathbf{h} \in \mathbb{Z}_2^T \times \mathbb{Z}_2^T$ , the other valid choice of the  $\eta$ -symbols is related to the one above via Eq. (4.28), i.e.,  $\eta_a^{(2)}(\mathbf{g}, \mathbf{h}) = \eta_a^{(1)}(\mathbf{g}, \mathbf{h})M_{a, \mathbf{t}(\mathbf{g}, \mathbf{h})}$ . Under the gauge choice  $\mathbf{t}(\mathbf{1}, \mathbf{g}) = \mathbf{t}(\mathbf{h}, \mathbf{1}) = 1$ , in both cases (a) and (b)  $\mathbf{t}(\mathbf{g}, \mathbf{h})$  is fully characterized by  $\mathbf{t}(\mathbf{g}, \mathbf{g})$  where  $\mathbf{g}$  is the nontrivial group element that does not permute anyons. Now we discuss the two cases separately in detail.

- (a) When  $\mathcal{T}_1$  and  $\mathcal{T}_2$  exchange  $e$  and  $m$ , the representative cocycle  $\mathbf{t}$  of the nontrivial element in  $\mathcal{H}_{\rho}^2(\mathbb{Z}_2 \times \mathbb{Z}_2, \mathbb{Z}_2 \times \mathbb{Z}_2) \cong \mathbb{Z}_2$  can be chosen as

$$\mathbf{t}(\mathcal{T}_1\mathcal{T}_2, \mathcal{T}_1\mathcal{T}_2) = \psi, \quad \mathbf{t}(\mathcal{T}_1, \mathcal{T}_1) = \mathbf{t}(\mathcal{T}_2, \mathcal{T}_2) = 1 \quad (4.63)$$



The physical meaning of these symmetry fractionalization classes is as follows. In both classes  $\psi$  is a Kramers doublet under both  $\mathcal{T}_1$  and  $\mathcal{T}_2$ , and both  $e$  and  $m$  carry integer charge (half charge) under  $\mathcal{T}_1\mathcal{T}_2$  in the class characterized by  $\eta^{(1)}$  ( $\eta^{(2)}$ ). So we denote the classes  $\eta^{(1)}$  and  $\eta^{(2)}$  by  $(efmf)_{\mathcal{T}_1, \mathcal{T}_2} \psi f \mathcal{T}_1 \mathcal{T}_2$  and  $(efCmfC)_{\mathcal{T}_1, \mathcal{T}_2} \psi f \mathcal{T}_1 \mathcal{T}_2$ , respectively. We see that  $(\mathcal{I}_0, \mathcal{I}_1, \mathcal{I}_2, \mathcal{I}_3) = (-1, 1, 1, -1)$  and  $(\mathcal{I}_0, \mathcal{I}_1, \mathcal{I}_2, \mathcal{I}_3) = (-1, 1, 1, 1)$  for  $(efmf)_{\mathcal{T}_1, \mathcal{T}_2} \psi f \mathcal{T}_1 \mathcal{T}_2$  and  $(efCmfC)_{\mathcal{T}_1, \mathcal{T}_2} \psi f \mathcal{T}_1 \mathcal{T}_2$ , respectively, as summarized in Table 4.3.

We mention that this result can also be achieved by considering the projection  $p : \mathbb{Z}_2^T \times \mathbb{Z}_2^T \rightarrow \mathbb{Z}_2^{T0}$ , where  $\mathbb{Z}_2^{T0}$  is now an anti-unitary symmetry on  $\mathcal{C}$  that permutes  $e$  and  $m$ . Notice that  $(efmf)_{\mathcal{T}_1, \mathcal{T}_2} \psi f \mathcal{T}_1 \mathcal{T}_2$  class of  $\mathbb{Z}_2^T \times \mathbb{Z}_2^T$  symmetry is the pullback of  $(efmf)_{\mathcal{T}} \psi f \mathcal{T}$  of  $\mathbb{Z}_2^{T0}$  symmetry (the meaning of this notation is similar to others), hence the anomaly of  $(efmf)_{\mathcal{T}_1, \mathcal{T}_2} \psi f \mathcal{T}_1 \mathcal{T}_2$  for  $\mathbb{Z}_2^T \times \mathbb{Z}_2^T$  is the pullback of the anomaly of  $(efmf)_{\mathcal{T}} \psi f \mathcal{T}$  for  $\mathbb{Z}_2^{T0}$ . From Eqs. (4.46) and (4.50), the latter anomaly is just  $(w_2^{TM})^2$  hence the former anomaly is  $(w_2^{TM})^2$  as well. Comparing this result with Eq. (4.56), we get the first line of Table 4.3. Based on the anomaly of this symmetry fractionalization class, the second line of Table 4.2 can be achieved from relative anomaly as in Ref. [119].

- (b) When  $\mathcal{T}_1$  and  $\mathcal{T}_1\mathcal{T}_2$  exchange  $e$  and  $m$ , the representative cocycle  $\mathbf{t}$  of the nontrivial element in  $\mathcal{H}_\rho^2(\mathbb{Z}_2 \times \mathbb{Z}_2, \mathbb{Z}_2 \times \mathbb{Z}_2) \cong \mathbb{Z}_2$  can be chosen as

$$\mathbf{t}(\mathcal{T}_2, \mathcal{T}_2) = \psi, \quad \mathbf{t}(\mathcal{T}_1, \mathcal{T}_1) = \mathbf{t}(\mathcal{T}_1\mathcal{T}_2, \mathcal{T}_1\mathcal{T}_2) = 1 \quad (4.64)$$

The physical meaning of these symmetry fractionalization classes is as follows. In both classes  $\psi$  is a Kramers doublet under  $\mathcal{T}_1$  and carries half charge under  $\mathcal{T}_1\mathcal{T}_2$ , and both  $e$  and  $m$  are Kramers singlets (doublets) under  $\mathcal{T}_2$  in the class characterized by  $\eta^{(1)}$  ( $\eta^{(2)}$ ).

So we denote the classes  $\eta^{(1)}$  and  $\eta^{(2)}$  by  $(efmf)_{\mathcal{T}_1, \mathcal{T}_1\mathcal{T}_2} \psi f \mathcal{T}_1 C$  and  $(ef\mathcal{T}_2mf\mathcal{T}_2)_{\mathcal{T}_1, \mathcal{T}_1\mathcal{T}_2} \psi f \mathcal{T}_1 C$ , respectively. We see that  $(\mathcal{I}_0, \mathcal{I}_1, \mathcal{I}_2, \mathcal{I}_3) = (-1, 1, -1, 1)$  and  $(\mathcal{I}_0, \mathcal{I}_1, \mathcal{I}_2, \mathcal{I}_3) = (-1, 1, 1, -1)$  for  $(efmf)_{\mathcal{T}_1, \mathcal{T}_1\mathcal{T}_2} \psi f \mathcal{T}_1 C$  and  $(ef\mathcal{T}_2mf\mathcal{T}_2)_{\mathcal{T}_1, \mathcal{T}_1\mathcal{T}_2} \psi f \mathcal{T}_1 C$ , respectively, as summarized in Table 4.4.

For this particular case, because the unitary symmetry  $\mathcal{T}_1\mathcal{T}_2$  exchanges  $e$  and  $m$ , we are aware of no other method to get the anomaly besides the complete knowledge of anomaly indicators of  $\mathbb{Z}_2^T \times \mathbb{Z}_2^T$ .

## 4.4 Generalization to connected Lie group symmetry

We believe that the construction and recipe presented in Sec. 4.2 can be generalized to arbitrary group  $G$ . Comparing general group symmetry and finite group symmetry, what concerns us the most in the calculation of the partition function  $\mathcal{Z}(\mathcal{M}, \mathcal{G})$  is how to write down the  $U$ -factors and  $\eta$ -factors. Manifestly, given a  $G$ -bundle  $\mathcal{G}$ , there is an associated map  $f : \mathcal{M} \rightarrow BG$ , with  $BG$  the classifying space of  $G$ . In particular, the map  $f$  maps a 1-chain of  $\mathcal{M}$  to a 1-chain of  $BG$ , and then assigns an element  $\rho_{\mathbf{g}}$  to this 1-chain of  $\mathcal{M}$ , which in turn gives the desired  $U$ -factors. Moreover, the map  $f$  maps a 2-chain of  $\mathcal{M}$  to a 2-chain of  $BG$ , and then assigns an element  $\rho_{\mathbf{g}} \circ \rho_{\mathbf{h}} \circ \dots$  to this 2-chain of  $\mathcal{M}$ , which gives the desired  $\eta$ -factors. This serves as a formal construction of the partition function of the TQFT with a general symmetry  $G$ . However, such a construction seems to be dependent on a specific choice of  $f$  and  $BG$ . We believe that the partition function ultimately only depends on the  $G$ -bundle itself (but not the specific choice of  $f$  and  $BG$ ), although we are unable to prove it using arguments similar to what we present in Appendix 4.C. Moreover, this construction is hard to work with for a general group  $G$ . Fortunately, for a connected Lie group  $G$ , there is a more operational method to write down the  $\eta$ -factors and eventually calculate  $\mathcal{Z}(\mathcal{M}, \mathcal{G})$ . We discuss it in this section.

Specifically, for a connected Lie group  $G$ , to calculate the partition function  $\mathcal{Z}(\mathcal{M}, \mathcal{G})$  of the manifold  $\mathcal{M}$  with a  $G$ -bundle structure  $\mathcal{G}$  on  $\mathcal{M}$ , we can still start with a handle decomposition of the manifold  $\mathcal{M}$ . Since now  $G$  cannot permute anyons, we can associate a single anyon  $a$  to the  $S^1$  boundary of each 2-handle. Moreover, no  $U$ -factors are involved. Now, given the prescribed labels, we need to calculate the correct  $\eta$ -factor, evaluate the anyon diagram from the Kirby diagram  $\langle K \rangle$  of  $\mathcal{M}$ , and assemble the result in a way similar to Eq. (4.44):

$$\mathcal{Z}(\mathcal{M}, \mathcal{G}) = D^{-\chi + 2(N_4 - N_3)} \times \sum_{\text{labels}} \left( \frac{\prod_{2 \text{ handle } i} d_{a_i}}{\prod_{1 \text{ handle } x} \left( \prod_{2 \text{ handle } j \text{ across } x} d_{a_j} \right)} \right)^{1/2} \times \left( \prod_i (\eta\text{-factors})_i \times \langle K \rangle \right) \quad (4.65)$$

Here  $N_k$  is the number of  $k$ -handles of this handle decomposition, and  $\chi \equiv N_0 - N_1 + N_2 - N_3 + N_4$  is the Euler number of  $\mathcal{M}$ .

The only nontrivial part compared with previous examples of finite group symmetry is the calculation of the  $\eta$ -factor for a 2-handle. In the presence of a connected Lie group symmetry  $G$ , we have the following prescription. For every 2-handle, there is an associated 2-chain  $[h]$ . The map  $f : \mathcal{M} \rightarrow BG$  associated to the  $G$ -bundle  $\mathcal{G}$  then gives  $f_*[h]$ , which

is a 2-chain in  $BG$ . The symmetry fractionalization class is characterized by an element  $\mathbf{w} \in \mathcal{H}^2(G, \mathcal{A}) \cong \mathcal{H}^2(BG, \mathcal{A})$ , and pairing it with  $f_*[h]$  gives an anyon  $\mathbf{w}(f_*[h]) \in \mathcal{A}$ . If we associate an anyon  $a$  to the  $S^1$  boundary of a 2-handle, the  $\eta$ -factor of this 2-handle is  $M_{a, \mathbf{w}(f_*[h])}$ , i.e., the double braid between  $a$  and  $\mathbf{w}(f_*[h])$ . Intuitively, such a phase can be viewed as the phase the anyon  $a$  experiences when traveling along the  $S^1$  boundary, given the nontrivial background  $G$ -bundle structure  $\mathcal{G}$ . Therefore, it can be written down in terms of the charge of  $a$ .

To illustrate this recipe regarding a connected Lie group symmetry  $G$ , now we go to the example of  $SO(N)$ . We will see that this recipe gives the correct partition function on manifolds with an  $SO(N)$ -bundle structure, and eventually provides us with the anomaly indicators, together with the  $SO(N)$  Hall conductance.

#### 4.4.1 Example: $SO(N)$

The relevant bordism group for symmetry group  $SO(N)$  is [120]

$$\Omega_4^{SO}(BSO(N)) = \begin{cases} (\mathbb{Z})^2, & N = 2, 3 \\ (\mathbb{Z})^3, & N = 4 \\ (\mathbb{Z})^2 \oplus \mathbb{Z}_2, & N \geq 5 \end{cases} \quad (4.66)$$

The first generating manifold is  $\mathbb{C}\mathbb{P}^2$  with a trivial  $SO(N)$  bundle. The second generating manifold is  $\mathbb{C}\mathbb{P}^2$  with a nontrivial  $SO(N)$  bundle such that the associated map  $f_1 : \mathbb{C}\mathbb{P}^2 \rightarrow BSO(N)$  is given by

$$f_1 : \mathbb{C}\mathbb{P}^2 \subset \mathbb{C}\mathbb{P}^\infty \cong BU(1) \xrightarrow{B\tilde{f}_1} BSO(N), \quad (4.67)$$

and  $\tilde{f}_1 : U(1) \rightarrow SO(N)$  is

$$e^{i\theta} \rightarrow \begin{pmatrix} \cos(\theta) & \sin(\theta) & & \\ -\sin(\theta) & \cos(\theta) & & \\ & & & \text{diag}(1, 1, \dots) \end{pmatrix} \quad (4.68)$$

Its associated vector bundle is simply the tautological line bundle of  $\mathbb{C}\mathbb{P}^2$  [69] (together with an  $(N - 2)$ -dimensional trivial bundle), and thus we denote it by  $\mathcal{A}_t$ . When  $N \geq 4$ , there exists a third generating manifold, which is  $\mathbb{C}\mathbb{P}^2$  with another nontrivial  $SO(N)$  bundle such that the associated map  $f_2 : \mathbb{C}\mathbb{P}^2 \rightarrow BSO(N)$  is given by

$$f_2 : \mathbb{C}\mathbb{P}^2 \subset \mathbb{C}\mathbb{P}^\infty \cong BU(1) \xrightarrow{B\tilde{f}_2} BSO(N), \quad (4.69)$$

and  $\tilde{f}_2 : U(1) \rightarrow SO(N)$  is

$$e^{i\theta} \rightarrow \begin{pmatrix} \cos(\theta) & \sin(\theta) & & & & & \\ -\sin(\theta) & \cos(\theta) & & & & & \\ & & \cos(\theta) & \sin(\theta) & & & \\ & & -\sin(\theta) & \cos(\theta) & & & \\ & & & & \text{diag}(1, \dots) & & \end{pmatrix} \quad (4.70)$$

Its associated vector bundle is the direct sum of two tautological line bundles of  $\mathbb{CP}^2$  (together with an  $(N - 4)$ -dimensional trivial bundle), and thus we denote it by  $\mathcal{A}_t^{\oplus 2}$ .

The partition function corresponds to an element in

$$\Omega_{SO}^4(BSO(N), U(1)) \equiv \text{Hom}(\Omega_4^{SO}(BSO(N)), U(1)) = \begin{cases} (U(1))^2, & N = 2, 3 \\ (U(1))^3, & N = 4 \\ (U(1))^2 \oplus \mathbb{Z}_2, & N \geq 5 \end{cases} \quad (4.71)$$

Similar to the case in Sec. 4.3.1, because all elements corresponding to  $U(1)$  are smoothly connected to the trivial element, the 't Hooft anomaly is absent when  $N = 2, 3, 4$  and classified by  $\mathbb{Z}_2$  when  $N \geq 5$ . Still, the partition function is not completely trivial even for  $N = 2, 3, 4$ . To evaluate the partition function on an oriented 4-dimensional manifold with an  $SO(N)$ -bundle structure, we just need to evaluate it on the generating manifolds.

Since the underlying manifold is always  $\mathbb{CP}^2$ , compared with the calculation that leads to Eq. (4.46), the calculation of the partition function of  $\mathbb{CP}^2$  with nontrivial bundle  $\mathcal{A}_t$  or  $\mathcal{A}_t^{\oplus 2}$  just requires us to add an appropriate  $\eta$ -factor for the 2-handle.

First consider  $\mathcal{A}_t$ . The extra  $\eta$ -factor can be seen as follows. The 2-handle  $[h]$  here is the generator of  $H_2(\mathbb{CP}^2, \mathbb{Z})$ , the pushforward of which under  $f_1$ , i.e.,  $f_{1*}[h]$ , gives the generator of  $H_2(BSO(N), \mathbb{Z})$ . According to the recipe, given the anyon label  $a$  in Eq. (4.45), the correct  $\eta$ -factor should be  $M_{a, \mathbf{w}([f_{1*}[h])}$ . Since  $f_{1*}[h]$  is the generator of  $H_2(BSO(N), \mathbb{Z})$ , physically this phase factor is related to the  $SO(N)$  charge  $q_a$  of anyon  $a$  by  $e^{i2\pi q_a}$ , where for  $N = 2$   $q_a \in [0, 1)$  is the (fractional)  $SO(2) \cong U(1)$  charge of  $a$ , and for  $N \geq 3$   $q_a \in \{0, \frac{1}{2}\}$  labels whether  $a$  carries linear ( $q_a = 0$ ) or spinor ( $q_a = \frac{1}{2}$ ) representation under  $SO(N)$ . Consequently, we have

$$\mathcal{Z}_{SO(N)}(\mathbb{CP}^2; \mathcal{A}_t) = \frac{1}{D} \sum_a d_a^2 \theta_a e^{i2\pi q_a} \quad (4.72)$$

Secondly, for  $\mathcal{A}_t^{\oplus 2}$ , there is no extra  $\eta$ -factor. This is simply because  $\tilde{f}_2$  defines a trivial element in  $\pi_1(SO(N)) \cong \mathbb{Z}_2$ , which suggests that  $\mathcal{A}_t^{\oplus 2}$  can be constructed from attaching a

4-handle to lower handlebody with a trivial  $SO(N)$  bundle on it. Therefore, the partition function of  $\mathbb{CP}^2$  with the  $SO(N)$  bundle  $\mathcal{A}_t^{\oplus 2}$  is identical to the partition function of  $\mathbb{CP}^2$  with a trivial  $SO(N)$  bundle, i.e.,

$$\mathcal{Z}_{SO(N), N \geq 4}(\mathbb{CP}^2; \mathcal{A}_t^{\oplus 2}) = \frac{1}{D} \sum_a d_a^2 \theta_a \quad (4.73)$$

When  $N = 2, 3, 4$ , even though there is no nontrivial 't Hooft anomaly, the partition function is still nontrivial and can be written down in terms of various theta terms. In particular, when  $N = 2$ , we have

$$\mathcal{Z}_{SO(2)}(\mathcal{M}; \mathcal{A}) = \mathcal{Z}(\mathbb{CP}^2)^{\sigma(\mathcal{M})} \cdot \left( \frac{\mathcal{Z}(\mathbb{CP}^2; \mathcal{A}_t)}{\mathcal{Z}(\mathbb{CP}^2)} \right)^{(c_1^{SO(2)})^2} \quad (4.74)$$

where  $\sigma(\mathcal{M})$  is the intersection number of  $\mathcal{M}$  and  $c_1^{SO(2)} \in \mathcal{H}^2(SO(2), \mathbb{Z})$  is the first Chern class of  $SO(2)$ . When  $N = 3$ , we have

$$\mathcal{Z}_{SO(3)}(\mathcal{M}; \mathcal{A}) = \mathcal{Z}(\mathbb{CP}^2)^{\sigma(\mathcal{M})} \cdot \left( \frac{\mathcal{Z}(\mathbb{CP}^2; \mathcal{A}_t)}{\mathcal{Z}(\mathbb{CP}^2)} \right)^{p_1^{SO(3)}} \quad (4.75)$$

where  $p_1^{SO(3)} \in \mathcal{H}^4(SO(3), \mathbb{Z})$  is the first Pontryagin class of  $SO(3)$ . When  $N = 4$ , when writing down the term corresponding to the Euler class  $e^{SO(4)}$ , pay attention that given Eq. (4.69), the pullback of Pontryagin class  $p_1^{SO(4)}$  should be twice the generator of  $\mathcal{H}^4(\mathbb{CP}^2, \mathbb{Z})$ . Therefore, we have

$$\mathcal{Z}_{SO(4)}(\mathcal{M}; \mathcal{A}) = \mathcal{Z}(\mathbb{CP}^2)^{\sigma(\mathcal{M})} \cdot \left( \frac{\mathcal{Z}(\mathbb{CP}^2; \mathcal{A}_t)}{\mathcal{Z}(\mathbb{CP}^2)} \right)^{p_1^{SO(4)}} \cdot \left( \left( \frac{\mathcal{Z}(\mathbb{CP}^2)}{\mathcal{Z}(\mathbb{CP}^2; \mathcal{A}_t)} \right)^2 \right)^{e^{SO(4)}} \quad (4.76)$$

where  $p_1^{SO(4)} \in \mathcal{H}^4(SO(4), \mathbb{Z})$  is the first Pontryagin class of  $SO(4)$ , and  $e^{SO(4)} \in \mathcal{H}^4(SO(4), \mathbb{Z})$  is the Euler class of  $SO(4)$ . When  $N \geq 5$ , similarly we have

$$\mathcal{Z}_{SO(N), N \geq 5}(\mathcal{M}; \mathcal{A}) = \mathcal{Z}(\mathbb{CP}^2)^{\sigma(\mathcal{M})} \cdot \left( \frac{\mathcal{Z}(\mathbb{CP}^2; \mathcal{A}_t)}{\mathcal{Z}(\mathbb{CP}^2)} \right)^{p_1^{SO(N)}} \cdot \left( \left( \frac{\mathcal{Z}(\mathbb{CP}^2)}{\mathcal{Z}(\mathbb{CP}^2; \mathcal{A}_t)} \right)^2 \right)^{w_4^{SO(N)}} \quad (4.77)$$

where  $p_1^{SO(N)} \in \mathcal{H}^4(SO(N), \mathbb{Z})$  is the first Pontryagin class of  $SO(N)$ , and  $w_4^{SO(N)} \in \mathcal{H}^4(SO(N), \mathbb{Z}_2)$  is the fourth Stiefel-Whitney class of  $SO(N)$ .

### Anomaly indicator for $N \geq 5$

As discussed before, there is no nontrivial  $SO(N)$  anomaly if  $N < 5$ . When  $N \geq 5$ , the  $SO(N)$  anomalies are classified by  $\mathbb{Z}_2$ , whose anomaly indicator is given by

$$\mathcal{I} = \left( \frac{\mathcal{Z}(\mathbb{CP}^2)}{\mathcal{Z}(\mathbb{CP}^2; \mathcal{A}_t)} \right)^2 = \left( \frac{\sum_a d_a^2 \theta_a}{\sum_b d_b^2 \theta_b e^{i2\pi q_b}} \right)^2 \quad (4.78)$$

As before, the general proof of the cobordism invariance and invertibility of this partition function indicates that this expression is  $\pm 1$ . The anomaly  $\mathcal{O}$  can be written as

$$\mathcal{O} = (\mathcal{I})^{w_4^{SO(N)}}, \quad (4.79)$$

where  $w_4^{SO(N)}$  is the fourth Stiefel-Whitney class belonging to  $\mathcal{H}^4(SO(N), \mathbb{Z}_2)$ .

### $SO(N)$ Hall conductance

Besides giving the anomaly indicator, the above partition functions also encode various Hall conductance in a topological order with an  $SO(N)$  symmetry. First, as discussed in Sec. 4.3.1, they reproduce the thermal Hall conductance from the chiral central charge (up to contributions from  $(2+1)$ -d invertible states). Moreover, they also yield the  $SO(N)$  Hall conductance. Concretely, let us consider threading a  $2\pi$   $SO(N)$  flux into the system, which breaks the  $SO(N)$  symmetry to  $SO(2) \times SO(N-2)$ . The Hall conductance measures the charge under  $SO(2) \times SO(N-2)$  that this flux attracts. For  $N > 4$ , the charge under  $SO(N-2)$  means the representation under  $SO(N-2)$ . For  $N = 4$ , the flux breaks the  $SO(4)$  symmetry to  $SO(2) \times SO(2)'$ , and it can attract charge under either  $SO(2)$  or  $SO(2)'$ . We will use the unit where  $\hbar = 1$  and the elementary charge of local excitations in the system under  $SO(2)$  (and also under  $SO(2)'$  when  $N = 4$ ) is 1.

Let us first consider the amount of  $SO(2)$  charge being attracted, denoted by  $\sigma_{xy}$ . We start with the case where  $N = 2$ . In the partition function, this can be read off from the factor  $\left( \frac{\mathcal{Z}(\mathbb{CP}^2; \mathcal{A}_t)}{\mathcal{Z}(\mathbb{CP}^2)} \right)^{\left( \mathcal{C}_1^{SO(2)} \right)^2}$ . Denoting  $e^{i\Theta} = \frac{\mathcal{Z}(\mathbb{CP}^2; \mathcal{A}_t)}{\mathcal{Z}(\mathbb{CP}^2)}$ , and using  $\left( \mathcal{C}_1^{SO(2)} \right)^2 = \frac{1}{4\pi^2} dA \wedge dA$  where  $A$  is the  $SO(2)$  gauge field, this factor can be written as  $e^{i\frac{\Theta}{\pi} \cdot \frac{1}{4\pi} d(A \wedge dA)}$ . The standard argument (see, e.g., Ref. [117]) then shows that

$$\sigma_{xy} = \frac{\Theta}{\pi}, \quad e^{i\Theta} \equiv \frac{\mathcal{Z}(\mathbb{CP}^2; \mathcal{A}_t)}{\mathcal{Z}(\mathbb{CP}^2)} = \frac{\sum_a d_a^2 \theta_a e^{i2\pi q_a}}{\sum_b d_b^2 \theta_b}. \quad (4.80)$$

Notice that this formula only captures the “fractional” part of the Hall conductance, and there can be extra contributions to the Hall conductance from a  $(2 + 1)$ -d invertible state, which are integral multiples of 2.

For  $N > 2$ ,  $\sigma_{xy}$  can be extracted from the factor  $\left(\frac{\mathcal{Z}(\mathbb{CP}^2; \mathcal{A}_t)}{\mathcal{Z}(\mathbb{CP}^2)}\right)^{p_1^{SO(N)}}$ . Consider the inclusion map that maps  $SO(2)$  into  $SO(N)$ , because  $p_1^{SO(N)}$  becomes precisely  $\left(\mathcal{C}_1^{SO(2)}\right)^2$  under the pullback induced by this inclusion map, using the above result for  $N = 2$  we get the  $SO(N)$  Hall conductance for  $N > 2$  with the same formula as Eq. (4.80).

For the special case of  $N = 4$ , there can be an additional  $SO(2)'$  being attracted, whose amount  $\sigma'_{xy}$  can be read off from the factor  $\left(\left(\frac{\mathcal{Z}(\mathbb{CP}^2)}{\mathcal{Z}(\mathbb{CP}^2; \mathcal{A}_t)}\right)^2\right)^{e^{SO(4)}}$ . Consider the inclusion map that maps  $SO(2) \times SO(2)'$  into  $SO(4)$ . It turns out that  $e^{SO(4)}$  becomes  $\frac{dA \wedge dA'}{4\pi^2}$  under the pullback induced by this inclusion map, where  $A$  and  $A'$  are the gauge fields for  $SO(2)$  and  $SO(2)'$ , respectively. Similar analysis as above then shows that the fractional part of this Hall conductance is

$$\sigma'_{xy} = \frac{\Theta'}{2\pi}, \quad e^{i\Theta'} = \left(\frac{\mathcal{Z}(\mathbb{CP}^2)}{\mathcal{Z}(\mathbb{CP}^2; \mathcal{A}_t)}\right)^2 = \left(\frac{\sum_a d_a^2 \theta_a}{\sum_b d_b^2 \theta_b e^{i2\pi q_b}}\right)^2 \quad (4.81)$$

There can be extra contributions to the Hall conductance from a  $(2 + 1)$ -d invertible state as well, which are integral multiples of 1.

For  $N > 4$ , the flux can also attract certain representation under  $SO(N - 2)$ , which can be read off from the factor  $\mathcal{I}^{w_4^{SO(4)}} = \left(\left(\frac{\mathcal{Z}(\mathbb{CP}^2)}{\mathcal{Z}(\mathbb{CP}^2; \mathcal{A}_t)}\right)^2\right)^{w_4^{SO(N)}}$ . Consider the inclusion map that maps  $SO(2) \times SO(N - 2)$  into  $SO(N)$ . It turns out that  $w_4^{SO(N)}$  becomes  $w_2^{SO(2)} \cup w_2^{SO(N-2)}$ . So when the topological order is anomaly-free (anomalous), i.e.,  $\mathcal{I} = 1$  ( $\mathcal{I} = -1$ ), the flux attracts a linear (spinor) representation under  $SO(N - 2)$ .

Combining the above results of the Hall conductance and the fact that  $\mathcal{I}$  takes values in  $\pm 1$ , we see that the possible values of the Hall conductance  $\sigma_{xy}$  of an  $SO(N)$  symmetric topological order with  $N > 4$  is severely constrained. In particular, if this topological order is anomaly-free, then  $\sigma_{xy} = 0$  or  $\sigma_{xy} = 1$ . If it is anomalous, then  $\sigma_{xy} = \pm \frac{1}{2}$ , which means that this topological order is incompatible with a further time reversal symmetry. This is related to the phenomenon of “symmetry-enforced gaplessness” [45, 56, 57, 121–123] discussed in the Sec. 4.5.

## 4.5 Other symmetry groups

The examples presented in Sec. 4.3 and Sec. 4.4 contain many interesting and physically relevant examples. However, for some symmetries, the calculation of the anomaly indicators may be more technically involved, whose expressions may also be more complicated. Moreover, for disconnected Lie group  $G$ , the identification of  $\eta$ -factors and  $U$ -factors is not as straightforward, and the partition function appears to explicitly depend on a specific choice of the map  $f : \mathcal{M} \rightarrow BG$  associated to a  $G$ -bundle  $\mathcal{G}$  (although we believe that the partition function actually only depends on the homotopy class of  $f$ ).

However, it turns out that even if we consider other symmetry groups, examples presented before can be very useful. Specifically, we discuss symmetries whose anomaly indicators nevertheless can be obtained by simply copying results that we have already derived without any need of further calculations. The common properties of these symmetries  $G$  are that i) they have subgroups like  $\mathbb{Z}_2^T$ ,  $\mathbb{Z}_2 \times \mathbb{Z}_2$ ,  $\mathbb{Z}_2^T \times \mathbb{Z}_2^T$  and/or  $SO(N)$ , whose anomaly indicators have already been obtained, and ii) by restricting  $G$  to its various subgroups and considering the pullbacks of its anomaly, its anomaly can be uniquely determined. Such symmetries  $G$  include  $O(N)^T$ ,  $SO(N) \times \mathbb{Z}_2^T$ ,  $\mathbb{Z}_n \times \mathbb{Z}_2^T$ ,  $\mathbb{Z}_n \times \mathbb{Z}_2^T$ ,  $\mathbb{Z}_n \times \mathbb{Z}_2$ ,  $O(N)$ , etc. Here  $O(N)^T$  means that the symmetry group is  $O(N)$ , and the superscript  $T$  denotes that elements in  $O(N)$  with determinant  $-1$  are anti-unitary. For an odd  $N$ , the groups  $O(N)^T$  and  $SO(N) \times \mathbb{Z}_2^T$  are actually the same.

In the following two subsections, we illustrate this strategy by calculating the anomaly indicators of  $O(N)^T$  and  $SO(N) \times \mathbb{Z}_2^T$ . Especially, we demonstrate that for  $O(N)^T$ ,  $N \geq 5$  and  $SO(N) \times \mathbb{Z}_2^T$ ,  $N \geq 4$ , certain 't Hooft anomaly cannot be realized by any symmetry-enriched topological order, illustrating the phenomenon of “symmetry-enforced gaplessness”, first discussed in Ref. [45]. The anomaly indicators of  $O(2)^T$  and  $SO(2) \times \mathbb{Z}_2^T$  were first proposed in Ref. [124], while the anomaly indicators of  $O(3)^T = SO(3) \times \mathbb{Z}_2^T$  were proposed in Ref. [123].

### 4.5.1 $O(N)^T$

The relevant bordism group for symmetry group  $O(N)^T$  is [120]

$$\Omega_4^{SO}((BO(N))^{q-1}) = \begin{cases} (\mathbb{Z}_2)^3, & N = 2 \\ (\mathbb{Z}_2)^4, & N = 3 \\ (\mathbb{Z}_2)^4 \oplus \mathbb{Z}, & N = 4 \\ (\mathbb{Z}_2)^5, & N \geq 5 \end{cases} \quad (4.82)$$



First consider the case where  $N = 2$  and the symmetry group is  $O(2)^T$ . The anomalies of  $O(2)^T$  in (2+1)-dimension are classified by  $(\mathbb{Z}_2)^3$ , whose basis elements can be chosen as  $(w_2^{TM})^2$ ,  $(w_1^{O(2)})^4$ ,  $(w_2^{O(2)})^2$ , where  $w_1^{O(2)}$  and  $w_2^{O(2)}$  are the first and second Stiefel-Whitney class belonging to  $\mathcal{H}^1(O(2)^T, \mathbb{Z}_2)$  and  $\mathcal{H}^2(O(2)^T, \mathbb{Z}_2)$ , respectively, and  $(w_2^{TM})^2$  is the generator of the beyond-cohomology piece of anomaly. We can write down the anomaly/partition function as

$$\mathcal{O} = (\mathcal{I}_0)^{(w_2^{TM})^2} \cdot (\mathcal{I}_1)^{(w_1^{O(2)})^4} \cdot (\mathcal{I}_0 \mathcal{I}_2)^{(w_2^{O(2)})^2} \quad (4.83)$$

Here the appearance of  $\mathcal{I}_0 \mathcal{I}_2$  is just to make the final expression nicer and match with the known literature. Denote the anti-unitary element  $\text{diag}(-1, 1)$  by  $\mathcal{T}$ . When pulled back to the  $\mathbb{Z}_2^T$  subgroup generated by  $\mathcal{T}$ , the anomaly becomes

$$\tilde{\mathcal{O}} = (\mathcal{I}_0)^{(w_2^{TM})^2} \cdot (\mathcal{I}_1)^{t^4} \quad (4.84)$$

Therefore, compared with Eq. (4.51), we immediately have  $\mathcal{I}_0 = \mathcal{Z}(\mathbb{CP}^2)$ , given by Eq. (4.46), and  $\mathcal{I}_1 = \mathcal{Z}(\mathbb{RP}^4; \mathcal{T})$ , given by Eq. (4.50). When pulled back to the subgroup  $SO(2)$ , the anomaly becomes

$$\tilde{\mathcal{O}} = (\mathcal{I}_0)^{\sigma(\mathcal{M})} \cdot (\mathcal{I}_0 \mathcal{I}_2)^{(c_1^{SO(2)})^2} \quad (4.85)$$

Therefore, compared with Eq. (4.74), we have  $\mathcal{I}_2 = \mathcal{Z}(\mathbb{CP}^2; \mathcal{A}_t)$ , given by Eq. (4.72).

Next consider  $N = 3$ . The anomalies of  $O(3)^T$  in (2+1)-dimension are classified by  $(\mathbb{Z}_2)^4$ , whose basis elements can be chosen as  $(w_2^{TM})^2$ ,  $(w_1^{O(3)})^4$ ,  $(w_1^{O(3)})^2 w_2^{O(3)}$ ,  $(w_2^{O(3)})^2$ , where  $w_1^{O(3)}$  and  $w_2^{O(3)}$  are the first and second Stiefel-Whitney class belonging to  $\mathcal{H}^1(O(3)^T, \mathbb{Z}_2)$  and  $\mathcal{H}^2(O(3)^T, \mathbb{Z}_2)$ , respectively, and  $(w_2^{TM})^2$  is the generator of the beyond-cohomology piece of anomaly. We can write down the anomaly as

$$\mathcal{O} = (\mathcal{I}_0)^{(w_2^{TM})^2} \cdot (\mathcal{I}_1)^{(w_1^{O(N)})^4} \cdot (\mathcal{I}_0 \mathcal{I}_1 \mathcal{I}_2 \mathcal{I}_3)^{w_2^{O(N)} (w_1^{O(N)})^2} \cdot (\mathcal{I}_0 \mathcal{I}_3)^{(w_2^{O(N)})^2} \quad (4.86)$$

Again, such a choice of coefficients is just to make the final expression nicer. Denote the anti-unitary element  $\text{diag}(-1, 1, 1)$  of  $O(3)^T$  by  $\mathcal{T}$ , and another anti-unitary element  $\text{diag}(-1, -1, -1)$  of  $O(3)^T$  by  $\mathcal{T}' = \mathcal{T} U_\pi$ , where  $U_\pi$  is a  $\pi$  rotation in the 2-3 plane. When pulled back to the subgroup generated by  $\mathcal{T}$ , the partition function becomes

$$\tilde{\mathcal{O}} = (\mathcal{I}_0)^{(w_2^{TM})^2} \cdot (\mathcal{I}_1)^{t^4} \quad (4.87)$$

Therefore, compared with Eq. (4.51), we immediately have  $\mathcal{I}_0 = \mathcal{Z}(\mathbb{CP}^2)$ , given by Eq. (4.46), and  $\mathcal{I}_1 = \mathcal{Z}(\mathbb{RP}^4; \mathcal{T})$ , given by Eq. (4.50). When pulled back to the subgroup generated by  $\mathcal{T}'$ , the partition function becomes

$$\tilde{\mathcal{O}} = (\mathcal{I}_0)^{(w_2^{TM})^2} \cdot (\mathcal{I}_2)^{t^4} \quad (4.88)$$

Therefore, compared with Eq. (4.51), we have  $\mathcal{I}_2 = \mathcal{Z}(\mathbb{RP}^4; \mathcal{T}')$ , again given by Eq. (4.50), which also can be written in the following form

$$\mathcal{Z}(\mathbb{RP}^4; \mathcal{T}') = \frac{1}{D} \sum_{\tau'_a} d_a \theta_a \times \eta_a(\mathcal{T}', \mathcal{T}') = \frac{1}{D} \sum_{\tau_a} d_a \theta_a \times \eta_a(\mathcal{T}, \mathcal{T}) e^{i2\pi q_a} \quad (4.89)$$

where  $q_a \in \{0, \frac{1}{2}\}$  labels the symmetry fractionalization class of anyon  $a$  under the  $SO(N)$  symmetry. Finally, when pulled back to the subgroup generated by  $SO(N)$ , the partition function becomes

$$\tilde{\mathcal{O}} = (\mathcal{I}_0)^{\sigma(\mathcal{M})} \cdot (\mathcal{I}_0 \mathcal{I}_3)^{p_1^{SO(N)}} \quad (4.90)$$

Therefore, compared with Eq. (4.75), we have  $\mathcal{I}_3 = \mathcal{Z}(\mathbb{CP}^2; \mathcal{A}_t)$ , given by Eq. (4.72).

When  $N = 4$ , the anomalies of  $O(4)^T$  in  $(2+1)$ -dimension are classified by  $(\mathbb{Z}_2)^4$ , whose basis elements can be chosen as  $(w_2^{TM})^2$ ,  $(w_1^{O(4)})^4$ ,  $(w_1^{O(4)})^2 w_2^{O(4)}$ ,  $(w_2^{O(4)})^2$ , where  $w_1^{O(N)}$  and  $w_2^{O(N)}$  are the first and second Stiefel-Whitney class belonging to  $\mathcal{H}^1(O(N)^T, \mathbb{Z}_2)$  and  $\mathcal{H}^2(O(N)^T, \mathbb{Z}_2)$ , and  $(w_2^{TM})^2$  is the generator of the beyond-cohomology piece of anomaly. There is an extra  $U(1)$  piece in the cobordism group, which is associated to  $e_4^{O(4)^T}$ , i.e., the twisted Euler class belonging to  $\mathcal{H}^4(O(N)^T, \mathbb{Z}_q)$ . We can write down the partition function as

$$\mathcal{O} = (\mathcal{I}_0)^{(w_2^{TM})^2} \cdot (\mathcal{I}_1)^{(w_1^{O(N)})^4} \cdot (\mathcal{I}_0 \mathcal{I}_1 \mathcal{I}_2 \mathcal{I}_3)^{w_2^{O(N)} (w_1^{O(N)})^2} \cdot (\mathcal{I}_0 \mathcal{I}_3)^{(w_2^{O(N)})^2} \cdot (\tilde{\mathcal{I}})^{e_4^{O(N)^T}} \quad (4.91)$$

Denote the anti-unitary element  $\text{diag}(-1, 1, 1, 1)$  of  $O(N)^T$  by  $\mathcal{T}$ , and another anti-unitary element  $\text{diag}(-1, -1, -1, 1)$  of  $O(N)^T$  by  $\mathcal{T}' = \mathcal{T} U_\pi$ , where  $U_\pi$  is a  $\pi$  rotation in the 2-3 plane. From pullback to the subgroup generated by  $\mathcal{T}$  and  $\mathcal{T}'$ , we still have  $\mathcal{I}_0 = \mathcal{Z}(\mathbb{CP}^2)$ , given by Eq. (4.46),  $\mathcal{I}_1 = \mathcal{Z}(\mathbb{RP}^4; \mathcal{T})$ , given by Eq. (4.50),  $\mathcal{I}_2 = \mathcal{Z}(\mathbb{RP}^4; \mathcal{T}')$ , given by Eq. (4.50) or (4.89). When pulled back to the subgroup generated by  $SO(4)$ , the partition function becomes

$$\tilde{\mathcal{O}} = (\mathcal{I}_0)^{\sigma(\mathcal{M})} \cdot (\mathcal{I}_0 \mathcal{I}_3)^{p_1^{SO(N)}} \cdot (\tilde{\mathcal{I}})^{e_4^{O(4)^T}} \quad (4.92)$$

Therefore, compared with Eq. (4.77), we have  $\mathcal{I}_3 = \mathcal{Z}(\mathbb{CP}^2; \mathcal{A}_t)$ , given by Eq. (4.72), and  $\tilde{\mathcal{I}} = (\mathcal{I}_0/\mathcal{I}_3)^2$ . Because both  $\mathcal{I}_0$  and  $\mathcal{I}_3$  here must take values only in  $\pm 1$ ,  $\tilde{\mathcal{I}}$  is always 1. Therefore, the (fractional part of)  $SO(4)$  Hall conductance  $\sigma'_{xy}$  as in Eq. (4.81) is always 0.

Finally, when  $N \geq 5$ , the anomalies of  $O(N)^T$  in (2+1)-dimension are classified by  $(\mathbb{Z}_2)^5$ , whose basis elements can be chosen as  $(w_2^{TM})^2$ ,  $(w_1^{O(N)})^4$ ,  $(w_1^{O(N)})^2 w_2^{O(N)}$ ,  $(w_2^{O(N)})^2$  and  $w_4^{O(N)}$ , where  $w_1^{O(N)}$ ,  $w_2^{O(N)}$  and  $w_4^{O(N)}$  are the first, second and fourth Stiefel-Whitney class belonging to  $\mathcal{H}^1(O(N)^T, \mathbb{Z}_2)$ ,  $\mathcal{H}^2(O(N)^T, \mathbb{Z}_2)$  and  $\mathcal{H}^4(O(N)^T, \mathbb{Z}_2)$ , respectively, and  $(w_2^{TM})^2$  is the generator of the beyond-cohomology piece of anomaly. We can write down the anomaly as

$$\mathcal{O} = (\mathcal{I}_0)^{(w_2^{TM})^2} \cdot (\mathcal{I}_1)^{(w_1^{O(N)})^4} \cdot (\mathcal{I}_0 \mathcal{I}_1 \mathcal{I}_2 \mathcal{I}_3)^{w_2^{O(N)} (w_1^{O(N)})^2} \cdot (\mathcal{I}_0 \mathcal{I}_3)^{(w_2^{O(N)})^2} \cdot (\tilde{\mathcal{I}})^{w_4^{O(N)}} \quad (4.93)$$

Denote the anti-unitary element  $\text{diag}(-1, 1, 1, 1, \dots)$  of  $O(N)^T$  by  $\mathcal{T}$ , and another anti-unitary element  $\text{diag}(-1, -1, -1, 1, \dots)$  of  $O(N)^T$  by  $\mathcal{T}' = \mathcal{T}U_\pi$ , where  $U_\pi$  is a  $\pi$  rotation in the 2-3 plane. From pullback to the subgroup generated by  $\mathcal{T}$  and  $\mathcal{T}'$ , we still have  $\mathcal{I}_0 = \mathcal{Z}(\mathbb{CP}^2)$ , given by Eq. (4.46),  $\mathcal{I}_1 = \mathcal{Z}(\mathbb{RP}^4; \mathcal{T})$ , given by Eq. (4.50),  $\mathcal{I}_2 = \mathcal{Z}(\mathbb{RP}^4; \mathcal{T}')$ , given by Eq. (4.50) or (4.89). When pulled back to the subgroup generated by  $SO(N)$ , the partition function becomes

$$\tilde{\mathcal{O}} = (\mathcal{I}_0)^{\sigma(\mathcal{M})} \cdot (\mathcal{I}_0 \mathcal{I}_3)^{p_1^{SO(N)}} \cdot (\tilde{\mathcal{I}})^{w_4^{SO(N)}} \quad (4.94)$$

Therefore, compared with Eq. (4.77), we have  $\mathcal{I}_3 = \mathcal{Z}(\mathbb{CP}^2; \mathcal{A}_t)$ , given by Eq. (4.72), and  $\tilde{\mathcal{I}} = (\mathcal{I}_0/\mathcal{I}_3)^2$ . Because both  $\mathcal{I}_0$  and  $\mathcal{I}_3$  here must take values only in  $\pm 1$ , we see that  $\tilde{\mathcal{I}}$  is always 1. As a result, given a (3+1)-dimensional theory with global symmetry  $O(N)^T$  and nontrivial 't Hooft anomaly involving  $w_4^{O(N)}$ , the boundary cannot be a topologically ordered state, i.e., it can either spontaneously break the  $O(N)^T$  symmetry or be a gapless state. This phenomenon is called ‘‘symmetry-enforced gaplessness’’.<sup>12</sup>

<sup>12</sup>For the reader’s convenience, we repeat the argument in Refs. [15, 21] of ‘‘symmetry-enforced gaplessness’’ discussed here. Consider an  $SO(N)$  monopole, represented as a unit  $SO(2) \subset SO(N)$  monopole in the first two components. The  $w_4^{O(N)}$  anomaly requires the monopole to carry spinor representation for the remaining  $SO(N-2)$ . For a gapped topologically ordered state, this condition can be satisfied only by attaching a gapped anyon excitation to the monopole, with the anyon carrying spinor representation under  $SO(N-2)$ . But an anyon should carry irreducible representation under the entire  $SO(N)$ , which means that the  $SO(N-2)$  spinor anyon should also carry  $SO(2)$  charge 1/2. This leads to a nontrivial Hall conductance for the  $SO(2)$ , which necessarily breaks time-reversal symmetry. This argument can also be carried over to the symmetry group  $SO(N) \times \mathbb{Z}_2^T$ ,  $N \geq 4$  with anomaly involving  $w_4^{SO(N)}$ . However, it does not apply to  $O(4)^T$ , because in that case the charge of the  $SO(4)$  monopole under  $SO(2)'$  is not quantized by time reversal.

As a summary, there are three anomaly indicators of  $O(2)^T$ :

$$\mathcal{I}_0 = \frac{1}{D} \sum_a d_a^2 \theta_a, \quad \mathcal{I}_1 = \frac{1}{D} \sum_{\tau_{a=a}^a} d_a \theta_a \eta_a(\mathcal{T}, \mathcal{T}), \quad \mathcal{I}_2 = \frac{1}{D} \sum_a d_a^2 \theta_a e^{2\pi i q_a} \quad (4.95)$$

There are four anomaly indicators of  $O(3)^T$  and  $O(4)^T$ :

$$\begin{aligned} \mathcal{I}_0 &= \frac{1}{D} \sum_a d_a^2 \theta_a, \quad \mathcal{I}_1 = \frac{1}{D} \sum_{\tau_{a=a}^a} d_a \theta_a \eta_a(\mathcal{T}, \mathcal{T}), \\ \mathcal{I}_2 &= \frac{1}{D} \sum_{\tau_{a=a}^a} d_a \theta_a \eta_a(\mathcal{T}, \mathcal{T}) e^{2\pi i q_a}, \quad \mathcal{I}_3 = \frac{1}{D} \sum_a d_a^2 \theta_a e^{2\pi i q_a} \end{aligned} \quad (4.96)$$

Here  $\mathcal{T}$  denotes the anti-unitary element  $\text{diag}(-1, 1, \dots)$ . For  $N \geq 5$ , these four expressions still give the anomaly indicators for  $O(N)^T$ , and there is one more anomaly indicator,  $\tilde{\mathcal{I}} = (\mathcal{I}_0/\mathcal{I}_3)^2$ , which is always 1 and indicates that this anomaly cannot be realized by any topological order. The full anomaly of the topological order can be written in the form of Eqs. (4.83), (4.86), (4.91) and (4.93), for  $N = 2, 3, 4$  and  $N \geq 5$ , respectively.

### 4.5.2 $SO(N) \times \mathbb{Z}_2^T$

The relevant bordism group for symmetry group  $SO(N) \times \mathbb{Z}_2^T$  is [120]

$$\Omega_4^{SO}((B(SO(N) \times \mathbb{Z}_2))^{q-1}) = \begin{cases} (\mathbb{Z}_2)^4, & N = 2, 3 \\ (\mathbb{Z}_2)^5, & N \geq 4 \end{cases} \quad (4.97)$$

When  $N = 2, 3$ , and the anomalies are classified by  $(\mathbb{Z}_2)^4$ , whose basis elements can be chosen as  $(w_2^{TM})^2$ ,  $t^4$ ,  $t^2 w_2^{SO(N)}$ ,  $(w_2^{SO(N)})^2$ , where  $t$  is the generator of  $\mathcal{H}^1(\mathbb{Z}_2^T, \mathbb{Z}_2)$  and  $w_2^{SO(N)}$  is the second Stiefel-Witney class or the generator of  $\mathcal{H}^2(SO(N), \mathbb{Z}_2)$ . We can write down the anomaly/partition function as

$$\mathcal{O} = (\mathcal{I}_0)^{(w_2^{TM})^2} \cdot (\mathcal{I}_1)^{t^4} \cdot (\mathcal{I}_0 \mathcal{I}_1 \mathcal{I}_2 \mathcal{I}_3)^{w_2^{SO(N)} t^2} \cdot (\mathcal{I}_0 \mathcal{I}_3)^{(w_2^{SO(N)})^2}, \quad (4.98)$$

Denote the anti-unitary generator of  $\mathbb{Z}_2^T$  as  $\mathcal{T}$  and a  $\pi$ -rotation of  $SO(N)$  as  $U_\pi$ . When pulled back to the subgroup generated by  $\mathcal{T}$ , the anomaly becomes

$$\tilde{\mathcal{O}} = (\mathcal{I}_0)^{(w_2^{TM})^2} \cdot (\mathcal{I}_1)^{t^4} \quad (4.99)$$

Therefore, compared with Eq. (4.51), we immediately have  $\mathcal{I}_0 = \mathcal{Z}(\mathbb{CP}^2)$ , given by Eq. (4.46),  $\mathcal{I}_1 = \mathcal{Z}(\mathbb{RP}^4; \mathcal{T})$ , given by Eq. (4.50). When pulled back to the subgroup generated by  $\mathcal{TU}_\pi$ , the anomaly becomes

$$\tilde{\mathcal{O}} = (\mathcal{I}_0)^{(w_2^{TM})^2} \cdot (\mathcal{I}_2)^{t^4} \quad (4.100)$$

Therefore, compared with Eq. (4.51), we have  $\mathcal{I}_2 = \mathcal{Z}(\mathbb{RP}^4; \mathcal{T}')$ , again given by Eq. (4.50), which can also be written in the following form

$$\mathcal{Z}(\mathbb{RP}^4; \mathcal{T}') = \frac{1}{D} \sum_{\tau'_{a=a}}^a d_a \theta_a \times \eta_a(\mathcal{T}', \mathcal{T}') = \frac{1}{D} \sum_{\tau_{a=a}}^a d_a \theta_a \times \eta_a(\mathcal{T}, \mathcal{T}) e^{i2\pi q_a} \quad (4.101)$$

where again  $q_a \in \{0, \frac{1}{2}\}$  labels the symmetry fractionalization class of anyone  $a$  under  $SO(N)$  symmetry (even for  $N = 2$ , here  $q_a$  can only take values from  $\{0, \frac{1}{2}\}$ ). When pulled back to the subgroup  $SO(N)$ , the anomaly becomes for  $N = 2$

$$\tilde{\mathcal{O}} = (\mathcal{I}_0)^{\sigma(\mathcal{M})} \cdot (\mathcal{I}_0 \mathcal{I}_3)^{(c_1^{SO(2)})^2} \quad (4.102)$$

or for  $N = 3$

$$\tilde{\mathcal{O}} = (\mathcal{I}_0)^{\sigma(\mathcal{M})} \cdot (\mathcal{I}_0 \mathcal{I}_3)^{p_1^{SO(N)}} \quad (4.103)$$

Therefore, compared with Eq. (4.74) or Eq. (4.75), we have  $\mathcal{I}_3 = \mathcal{Z}(\mathbb{CP}^2; \mathcal{A}_t)$ , given by Eq. (4.72).

When  $N \geq 4$ , the anomalies of  $SO(N) \times \mathbb{Z}_2^T$  in (2+1)-dimension are classified by  $(\mathbb{Z}_2)^5$ , whose basis elements can be chosen as  $(w_2^{TM})^2$ ,  $t^4$ ,  $t^2 w_2^{SO(N)}$ ,  $(w_2^{SO(N)})^2$  and  $w_4^{SO(N)}$ , where  $t$  is the generator of  $\mathcal{H}^1(\mathbb{Z}_2^T, \mathbb{Z}_2)$ , and  $w_2^{SO(N)}$  ( $w_4^{SO(N)}$ ) is the second (fourth) Stiefel-Witney class or the generator of  $\mathcal{H}^2(SO(N), \mathbb{Z}_2)$  ( $\mathcal{H}^4(SO(N), \mathbb{Z}_2)$ ). We can write down the anomaly/partition function as

$$\mathcal{O} = (\mathcal{I}_0)^{(w_2^{TM})^2} \cdot (\mathcal{I}_1)^{t^4} \cdot (\mathcal{I}_0 \mathcal{I}_1 \mathcal{I}_2 \mathcal{I}_3)^{w_2^{SO(N)} t^2} \cdot (\mathcal{I}_0 \mathcal{I}_3)^{(w_2^{SO(N)})^2} \cdot (\tilde{I})^{w_4^{SO(N)}}, \quad (4.104)$$

Denote the anti-unitary generator of  $\mathbb{Z}_2^T$  as  $\mathcal{T}$  and a  $\pi$ -rotation of  $SO(N)$  as  $U_\pi$ . From pullback to the subgroup generated by  $\mathcal{T}$  and  $\mathcal{TU}_\pi$ , we still have  $\mathcal{I}_0 = \mathcal{Z}(\mathbb{CP}^2)$ , given by Eq. (4.46),  $\mathcal{I}_1 = \mathcal{Z}(\mathbb{RP}^4; \mathcal{T})$ , given by Eq. (4.50),  $\mathcal{I}_2 = \mathcal{Z}(\mathbb{RP}^4; \mathcal{T}')$ , given by Eq. (4.50) or (4.101). When pulled back to the subgroup generated by  $SO(N)$ , the partition function becomes

$$\tilde{\mathcal{O}} = (\mathcal{I}_0)^{\sigma(\mathcal{M})} \cdot (\mathcal{I}_0 \mathcal{I}_3)^{p_1^{SO(N)}} \cdot (\tilde{I})^{w_4^{SO(N)}} \quad (4.105)$$

Therefore, compared with Eq. (4.76) or (4.77), we have  $\mathcal{I}_3 = \mathcal{Z}(\mathbb{CP}^2; \mathcal{A}_t)$ , given by Eq. (4.72), and  $\tilde{\mathcal{I}} = (\mathcal{I}_0/\mathcal{I}_3)^2$ . Again, because both  $\mathcal{I}_0$  and  $\mathcal{I}_3$  here must take values only in  $\pm 1$ , we see that  $\tilde{\mathcal{I}}$  is identically 1. Consequently, given a (3+1)-dimensional theory with global symmetry  $SO(N) \times \mathbb{Z}_2^T$  and nontrivial 't Hooft anomaly involving  $w_4^{SO(N)}$ , the boundary cannot be a topologically ordered state, i.e., it can either spontaneously break the  $SO(N) \times \mathbb{Z}_2^T$  symmetry or be a gapless state. We again discover the phenomenon of “symmetry-enforced gaplessness”.

In summary, there are four anomaly indicators of  $SO(N) \times \mathbb{Z}_2^T$ :

$$\begin{aligned} \mathcal{I}_0 &= \frac{1}{D} \sum_a d_a^2 \theta_a, & \mathcal{I}_1 &= \frac{1}{D} \sum_{\tau_{a=a}^a} d_a \theta_a \eta_a(\mathcal{T}, \mathcal{T}), \\ \mathcal{I}_2 &= \frac{1}{D} \sum_{\tau_{a=a}^a} d_a \theta_a \eta_a(\mathcal{T}, \mathcal{T}) e^{2\pi i q_a}, & \mathcal{I}_3 &= \frac{1}{D} \sum_a d_a^2 \theta_a e^{2\pi i q_a} \end{aligned} \tag{4.106}$$

Here  $\mathcal{T}$  denotes the generator of  $\mathbb{Z}_2^T$ . For  $N = 2, 3$ , these are all the anomaly indicators. For  $N \geq 4$ , besides these four anomaly indicators, there is another one  $\tilde{\mathcal{I}} = (\mathcal{I}_0/\mathcal{I}_3)^2$ , which is always 1 and implies that such anomaly cannot be realized by any topological order. The full anomaly of the topological order can be written in the form of Eq. (4.98) and (4.104), for  $N = 2, 3$  and  $N \geq 4$ , respectively.

## 4.A Derivation of Eq. (4.44)

For the reader's convenience, in this appendix we repeat some explicit computations of various factors in Eq. (4.42), including partition functions of various handles and inner products, which ultimately lead to the main formula Eq. (4.44). The presentation here follows Ref. [94], see also Ref. [95] for the calculation from a higher-category point of view.

### 4.A.1 Vector Spaces

First of all, in this sub-appendix, we write down  $\mathcal{V}(\mathcal{N})$ , the vector space associated to some 3-dimensional manifold  $\mathcal{N}$  which will be defined as the attaching region of some  $k$ -handle, following the diagrammatic definition in Eq. (4.38). This will serve as the starting point of our diagrammatic treatment and calculation.

A 4-handle is attached to lower handles along  $S^3$ , and it is clear that

$$\mathcal{V}(S^3) \simeq \mathbb{C} \tag{4.107}$$

is one-dimensional, spanned by the empty diagram in  $S^3$ , as all closed anyon diagrams in  $S^3$  can be reduced via local moves to a multiple of the empty diagram.

Similarly, a 3-handle is attached to lower handles along  $S^2 \times D^1$ , and we have

$$\mathcal{V}(S^2 \times D^1; \emptyset) \simeq \mathbb{C} \tag{4.108}$$

We use  $\emptyset$  to denote that we put only trivial anyon on the boundary.

A 2-handle is attached to lower handles along  $S^1 \times D^2$ . It is also clear that

$$\mathcal{V}(S^1 \times D^2; \emptyset) \simeq \mathbb{C}^{|\mathcal{C}|} \tag{4.109}$$

Here,  $|\mathcal{C}|$  denotes the number of simple anyons in  $\mathcal{C}$ . The basis vector in  $\mathcal{V}(S^1 \times D^2; \emptyset)$  associated to an anyon  $a \in \mathcal{C}$  corresponds to putting the anyon loop with label  $a$  along  $S^1 \times \{\text{pt}\} \subset S^1 \times D^2$ , where  $\{\text{pt}\}$  denotes a point in  $D^2$ .

Finally, a 1-handle is attached to lower handles along two copies of  $D^3$ , and we have

$$\mathcal{V}(D^3; (a_1, \dots; b_1, \dots)) \simeq V_{b_1, \dots}^{a_1, \dots} \tag{4.110}$$

Here  $a_1, \dots$  and  $b_1, \dots$  are used to denote anyons associated to 2-handles running out of and into the 1-handle along the boundary of  $D^3$ . And  $V_{b_1, \dots}^{a_1, \dots}$  is the fusion space of  $a_1, \dots$  into  $b_1, \dots$ . This is illustrated in the upper plane of Fig. 4.12.

## 4.A.2 Partition functions

In this sub-appendix, we compute the partition functions for different handles. Suppose for  $D^4$  we have

$$\mathcal{Z}(D^4; \emptyset) = \lambda, \tag{4.111}$$

where  $\lambda$  is a parameter to be fixed later and  $\emptyset$  denotes the empty diagram in  $\partial D^4 = S^3$ . Then if there is some anyon diagram  $K$  on  $S^3$ , we have

$$\mathcal{Z}(D^4; K) = \lambda \langle K \rangle, \tag{4.112}$$

where  $\langle K \rangle$  denotes the evaluation of the anyon diagram  $K$ .

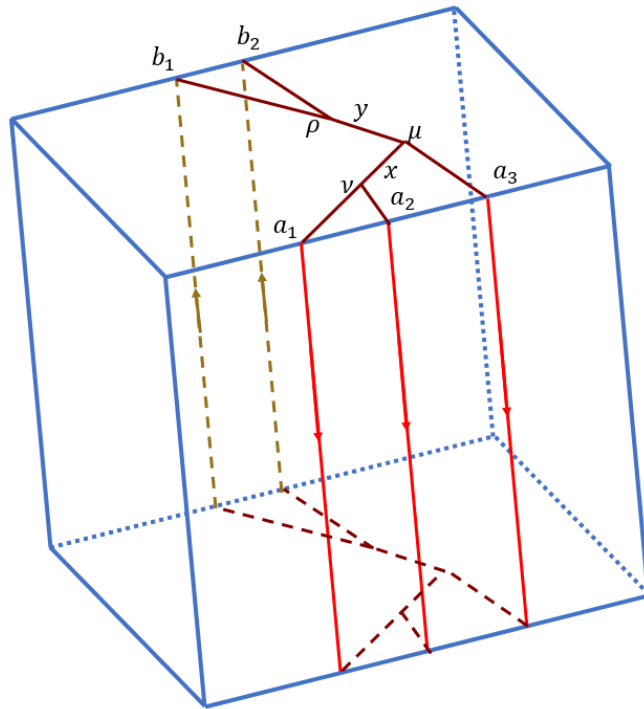


Figure 4.12: Illustration of the 1-handle, with no defect present. The 1-handle has topology of a  $D^4$  but we draw it as a  $D^3$  for illustration. The lower plane displays a vector  $(x, \nu, \mu)(y, \mu, \rho)$  that lives in the vector space associated to  $D^3$ , i.e.,  $\mathcal{V}(D^3; (a_1, \dots; b_1, \dots)) \in V_{b_1, b_2}^{a_1, a_2, a_3}$ , while the upper plane hosts a dual vector.



Specifically, first consider the situation where no defect is present. For a 2-handle, there is a loop  $l_a$  of anyon  $a$  on  $S^1$  and we have

$$\mathcal{Z}(D^4; l_a) = \lambda d_a. \quad (4.113)$$

For a 1-handle there is a  $\Theta$ -diagram as in Fig. 4.12, and if no defect is present the evaluation of the diagram gives

$$\mathcal{Z}(D^4; \Theta_{a_1, \dots; b_1, \dots}) = \lambda \sqrt{\prod_i d_{a_i} \prod_j d_{b_j}}. \quad (4.114)$$

For a 0-handle the anyon diagram  $K$  on the boundary  $S^3$  is precisely the Kirby diagram of the manifold  $\mathcal{M}$ , with correct labels on the attaching regions of 1-handles and 2-handles.

In the presence of defects, for a 2-handle the associated anyon  $a$  is acted on by successive defects, but the combination of all defects along the  $S^1$  line of a 2-handle is still a trivial defect, since this  $S^1$  is contractible. Nevertheless, the functor of successive symmetry actions is not the same as the identity functor, and they are connected to each other by some natural isomorphism, which when acting on  $a$  gives the desired  $\eta$ -factor. This is explained in detail in Sec. 4.2.4.

For a 1-handle we just need to take account of the symmetry action on the vector assigned to the boundary, and then calculate the  $\Theta$ -diagram. In particular, from the symmetry action we get the desired  $U$ -factor in Eq. (4.43).

### 4.A.3 Inner Products

Next, in this sub-appendix, we calculate the inner products in the vector spaces described in Appendix 4.A.1.

For a vector in  $|\beta\rangle \in \mathcal{V}(D^3; (a_1, \dots; b_1, \dots))$  representing the label on the boundary of Fig. 4.12, from Eq. (4.39) we see that

$$\langle \beta | \beta \rangle = \mathcal{Z}(D^4; \Theta_{a_1, \dots; b_1, \dots}) = \lambda \sqrt{\prod_i d_{a_i} \prod_j d_{b_j}} \quad (4.115)$$

Specifically, in the presence of only 2 anyons,  $\dim \mathcal{V}(D^3; (a; b)) = \delta_{ab}$ , and when  $a = b$ ,  $\mathcal{V}(D^3; (a; b))$  is 1-dimensional and spanned by an arc that we denote as  $\text{arc}_a$  connecting the two anyons. The inner product is

$$\langle \text{arc}_a | \text{arc}_b \rangle_{\mathcal{V}(D^3; (a; b))} = \mathcal{Z}(D^4; l_a) \delta_{ab} = d_a \lambda \delta_{ab}. \quad (4.116)$$

Then consider the inner product in  $\mathcal{V}(S^1 \times D^2; \emptyset)$ . Let  $|l_a\rangle$  denote the basis vector in  $\mathcal{V}(S^1 \times D^2; \emptyset)$  corresponding to anyon loop  $a$  along  $S^1$ . From Eq. (4.39), we have

$$\langle l_a | l_b \rangle_{\mathcal{V}(S^1 \times D^2; \emptyset)} = \mathcal{Z}(S^1 \times D^3; l_{\bar{a}} \cup l_b). \quad (4.117)$$

From the gluing formula Eq. (4.40),

$$\begin{aligned} & \mathcal{Z}(S^1 \times D^3; l_{\bar{a}} \cup l_b) \\ &= \sum_{|\beta\rangle \in \mathcal{V}(D^3; (a; b))} \frac{\mathcal{Z}(D^4; \text{arc}_b \cup \bar{\beta} \cup \text{arc}_a \cup \beta)}{\langle \beta | \beta \rangle_{\mathcal{V}(D^3; (a; b))}} \\ &= \delta_{ab} \frac{\mathcal{Z}(D^4; \text{arc}_a \cup \text{arc}_a \cup \text{arc}_a \cup \text{arc}_a)}{\langle \text{arc}_a | \text{arc}_a \rangle_{\mathcal{V}(D^3; (a; b))}} \\ &= \delta_{ab} \frac{\mathcal{Z}(D^4; l_a)}{\langle \text{arc}_a | \text{arc}_a \rangle_{\mathcal{V}(D^3; (a; b))}} \\ &= \delta_{ab}. \end{aligned} \quad (4.118)$$

Here we have used the fact that cutting  $l_{\bar{a}} \cup l_b$  gives rise to two arcs,  $\text{arc}_b$  and  $\text{arc}_a$ , while  $\mathcal{V}(D^3; (a; b))$  is spanned by an arc connecting  $a$  and  $b$ . Thus the combination  $\text{arc}_a \cup \text{arc}_a \cup \text{arc}_a \cup \text{arc}_a = l_a$ . This is illustrated in Fig. 4.13.

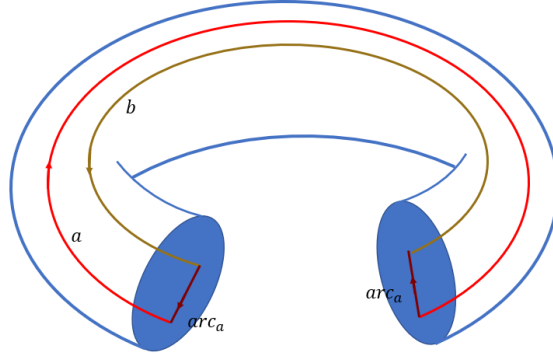


Figure 4.13: Illustration of the calculation of  $\langle l_a | l_b \rangle_{\mathcal{V}(S^1 \times D^2; \emptyset)}$  through  $\mathcal{Z}(S^1 \times D^3)[l_{\bar{a}} \cup l_b]$ .

Then let us consider the inner product in  $\mathcal{V}(S^2 \times D^1; \emptyset)$ . For  $|\emptyset\rangle \in \mathcal{V}(S^2 \times D^1; \emptyset)$

denoting the empty diagram, we have

$$\begin{aligned}
\langle \emptyset | \emptyset \rangle_{\mathcal{V}(S^2 \times D^1; \emptyset)} &= \mathcal{Z}(S^2 \times D^2; \emptyset) \\
&= \sum_{|l_a\rangle \in \mathcal{V}(S^1 \times D^2)} \frac{\mathcal{Z}(D^4; l_a) \mathcal{Z}(D^4; l_a)}{\langle l_a | l_a \rangle_{\mathcal{V}(S^1 \times D^2; \emptyset)}} \\
&= \sum_a d_a^2 \lambda^2 = D^2 \lambda^2
\end{aligned} \tag{4.119}$$

where  $D$  is the total dimension.

Finally, for  $\mathcal{V}(S^3)$  and a basis vector  $|\emptyset\rangle$  denoting the empty diagram, we have

$$\begin{aligned}
\langle \emptyset | \emptyset \rangle_{\mathcal{V}(S^3)} &= \mathcal{Z}(D^1 \times S^3; \emptyset) \\
&= \frac{\mathcal{Z}(D^4; \emptyset) \mathcal{Z}(D^4; \emptyset)}{\langle \emptyset | \emptyset \rangle_{\mathcal{V}(S^2 \times D^1; \emptyset)}} \\
&= \frac{1}{D^2}.
\end{aligned} \tag{4.120}$$

#### 4.A.4 Requirement from Invertibility

A further constraint comes from our wish to define an invertible TQFT [99, 100], given a suitable choice of  $\lambda$ . This means that on every closed 3-manifold  $\mathcal{N}$  the associated vector space  $\mathcal{V}(\mathcal{N})$  is one-dimensional, and on every closed 4-manifold the partition function is a pure phase factor.

Consider  $\mathcal{Z}(S^4)$ , the gluing formula Eq. (4.40) gives

$$\mathcal{Z}(S^4) = \frac{\mathcal{Z}(D^4; \emptyset) \mathcal{Z}(D^4; \emptyset)}{\langle \emptyset | \emptyset \rangle_{\mathcal{V}(S^3)}} = \lambda^2 D^2 \tag{4.121}$$

In order for  $|\mathcal{Z}(S^4)| = 1$ , we must choose  $|\lambda| = \frac{1}{D}$ .

Furthermore, we have found in Eq. (4.116) that the norm of the state  $|\text{arc}_0\rangle$  is  $\lambda$ . In a unitary TQFT, norms are always positive definite, so  $\lambda > 0$ . Therefore we have determined

$$\lambda = \frac{1}{D}. \tag{4.122}$$

As a result we also have  $\mathcal{Z}(S^4) = 1$ .

Assembling all these factors together, we finally arrive at Eq. (4.44).

## 4.B An explicit expression of the $\eta$ -factor

In Remark g of Sec. 4.2.4, we have explained that, for a finite group symmetry  $G$ , the  $\eta$ -factor associated with a 2-handle comes from the natural isomorphism connecting the functor  $\rho_{\mathbf{g}_1}^{s_1} \circ \rho_{\mathbf{g}_2}^{s_2} \circ \dots$  and the identity functor, where  $\mathbf{g}_{1,2,\dots}$  are defects the  $S^1$  line of this 2-handle crosses, starting from a segment with anyon label  $a$ , and  $s_{1,2,\dots}$  are determined by whether the  $S^1$  crosses the defect upward or downward, according to the convention in Remark f. In this appendix, we give an explicit expression of this  $\eta$ -factor. We stress again that the expression of this  $\eta$ -factor is not unique, and different expressions can be converted into each other via Eq. (4.24). The expression presented here is obtained by “combining from left to right” of the functor  $\rho_{\mathbf{g}_1}^{s_1} \circ \rho_{\mathbf{g}_2}^{s_2} \circ \dots$ .

To describe this expression, we first write down the  $\eta$ -factor we get after connecting  $\rho_{\mathbf{g}_1}^{s_1} \circ \rho_{\mathbf{g}_2}^{s_2}$  to a single functor  $\rho_{\mathbf{g}_{12}}^{s_{12}}$ , i.e.,

$$H_{12} : \quad \rho_{\mathbf{g}_1}^{s_1} \circ \rho_{\mathbf{g}_2}^{s_2} \implies \rho_{\mathbf{g}_{12}}^{s_{12}} \quad (4.123)$$

where  $\mathbf{g}_{12}$  and  $s_{12}$  are defined as follows

$$\mathbf{g}_{12} \equiv \begin{cases} \mathbf{g}_2 \mathbf{g}_1, & s_1 = s_2 = -1 \\ \mathbf{g}_1^{s_1} \mathbf{g}_2^{s_2}, & \text{else} \end{cases} \quad (4.124)$$

$$s_{12} \equiv \begin{cases} -1, & s_1 = s_2 = -1 \\ 1, & \text{else} \end{cases} \quad (4.125)$$

and  $H_{12}$  acting on anyon  $a$  gives the following  $\eta$ -factor

$$(H_{12})_a = \begin{cases} \eta_a(\mathbf{g}_1, \mathbf{g}_2), & s_1 = s_2 = 1 \\ \eta_{\mathbf{g}_2 \mathbf{g}_1 a}(\mathbf{g}_2, \mathbf{g}_1)^{-\sigma(\mathbf{g}_2 \mathbf{g}_1)}, & s_1 = s_2 = -1 \\ \eta_a(\mathbf{g}_1 \mathbf{g}_2^{-1}, \mathbf{g}_2)^{-1}, & s_1 = 1, s_2 = -1 \\ \eta_{\mathbf{g}_1 a}(\mathbf{g}_1, \mathbf{g}_1^{-1} \mathbf{g}_2)^{-\sigma(\mathbf{g}_1)}, & s_1 = -1, s_2 = 1 \end{cases} \quad (4.126)$$

Then we have an expression of the form  $\rho_{\mathbf{g}_{12}}^{s_{12}} \circ \rho_{\mathbf{g}_3}^{s_3} \circ \dots$ , and we can iterate the above process until we get the identity functor. Finally, simply multiplying all individual  $\eta$ -factors we get the  $\eta$ -factor associated with the 2-handle,

$$(H_{1,2})_a \cdot (H_{12,3})_a \cdot (H_{123,4})_a \cdot \dots \quad (4.127)$$

## 4.C Consistency check of TQFT

There are multiple consistency checks that we need to perform in order to confirm that, for finite group symmetry  $G$ , the recipe in Sec. 4.2.4, especially Eq. (4.44), indeed gives rise to a well-defined partition function  $\mathcal{Z}(\mathcal{M}, \mathcal{G})$ , defined on a target manifold  $\mathcal{M}$  together with a  $G$ -bundle structure  $\mathcal{G}$  on it. In this appendix we explicitly perform the consistency checks and prove that the recipe in Sec. 4.2.4 does give rise to a well-defined partition function, in the sense that we will make explicit in the following subsections. Most of our exposition will utilize similar proofs for the Crane-Yetter model, as in Refs. [94, 95, 101, 125] for example. However, we need to understand the roles played by symmetry defects. These checks provide further evidence that the partition function  $\mathcal{Z}(\mathcal{M}, \mathcal{G})$  constructed in Sec. 4.2.4 is indeed exactly the same partition function of the TQFT described in Sec. 4.2.2.

The checks we perform include:

1. Independence of the partition function on the handle decomposition in Appendix 4.C.1.
2. Invariance of the partition function under changes of defects in Appendix 4.C.2.
3. Gauge invariance of the partition function in Appendix 4.C.3.
4. Cobordism invariance of the partition function in Appendix 4.C.4.
5. Invertibility of the partition function in Appendix 4.C.5.

For connected Lie group symmetry  $G$ , we also need to prove that Eq. (4.65) gives rise to a well-defined partition function. Such a proof follows closely the proof for a finite group symmetry  $G$  but is much easier, since we just need to focus on  $\eta$ -factors. This proof is presented in Appendix 4.C.6.

### 4.C.1 Independence on the handle decomposition

First of all, our construction explicitly uses a handle decomposition of the target manifold  $\mathcal{M}$ . In this sub-appendix, we prove that the partition function  $\mathcal{Z}(\mathcal{M}, \mathcal{G})$  we get in Eq. (4.44) is in fact independent of the handle decomposition.

Two different handle decompositions of a given manifold are related to each other by the following handle moves: isotopies, handle slides and creating/annihilating cancelling

handle pairs [111]. In order to prove the independence of the partition function on the handle decomposition, we just need to show its invariance under all handle moves. Fortunately, most handle moves do not involve  $G$ -defects, and therefore the partition function is automatically invariant under these handle moves, according to our knowledge of the Crane-Yetter model [95, 101]. Here we just need to analyze handle moves which do explicitly involve  $G$ -defects, and they are either 1-1 handle slides (see Fig. 4.14), isotopies where some 2-handles cross some defects (see Fig. 4.15) or 2-2 handle slides (see Fig. 4.16).

- 1-1 handle slide.

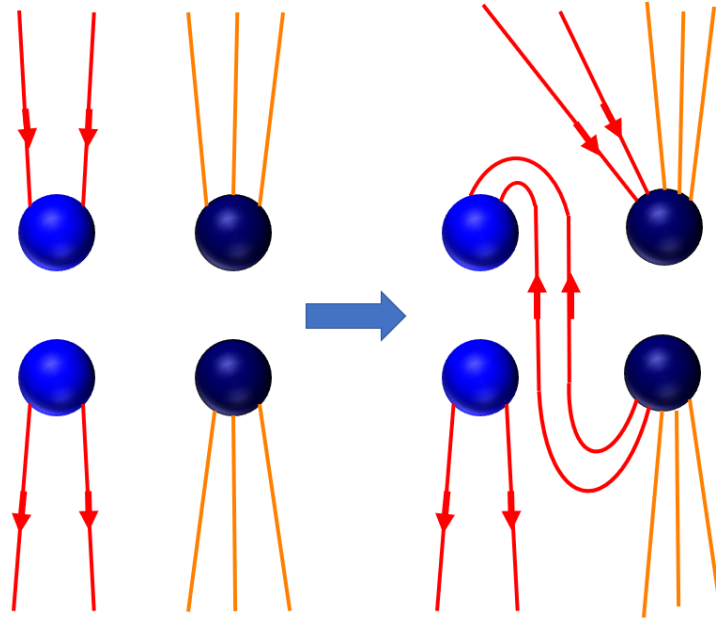


Figure 4.14: An illustration of the effect of 1-1 handle slide on the Kirby diagram, where the blue 1-handle slides past the darkblue 1-handle. On the anyon diagram the two red lines running upward become a bubble.

The effect of a 1-1 handle slide on a Kirby diagram is explicitly shown in Fig. 4.14. Suppose that before the handle slide, a  $\mathbf{g}$ -defect is present across the blue 1-handle, and an  $\mathbf{h}$ -defect is present across the darkblue 1-handle. Then after the handle slide, an  $\mathbf{h}^{-1}\mathbf{g}$  defect is present across the blue 1-handle while an  $\mathbf{h}$  defect is still present across the darkblue 1-handle. We wish to prove the invariance of the partition function  $\mathcal{Z}(\mathcal{M}, \mathcal{G})$  by proving the invariance of each individual summand of Eq. (4.44), which has a given set of labels  $\beta$ .

Suppose anyons labeled by  $\{a_i\}$  cross the blue 1-handle before the handle slide. Without loss of generality, suppose that they are running downward in the blue 1-handle of the Kirby diagram as in Fig. 4.14. After the handle slide, anyons  $\{a_i\}$  cross both the blue 1-handle and the darkblue 1-handle. Accordingly, the prefactor of quantum dimension in the individual summand of Eq. (4.44) is modified by an extra  $1/\sqrt{\prod_i d_{a_i}}$  after the handle slide. This is canceled by the contribution from the extra bubble in the Kirby diagram, formed e.g., by the two red lines running upward in Fig. 4.14, as can be seen by using Eq. (4.4). After accounting for this extra bubble, the contribution of the Kirby diagram is invariant before and after the handle move. Then we just need to analyze the change of the  $\eta$ -factors and  $U$ -factors. For the sake of presentation, let us first assume that all symmetry defects involved are unitary. Now consider the change of the  $\eta$ -factors. Before the handle slide,  $\{a_i\}$  are acted upon by  $\rho_{\mathbf{g}}^{-1}$  while after the handle slide,  $\{a_i\}$  are acted upon by  $\rho_{\mathbf{h}^{-1}\mathbf{g}}^{-1} \circ \rho_{\mathbf{h}}^{-1}$ . This gives an extra  $\eta$ -factor

$$\prod_i (\eta_{a_i}(\mathbf{h}, \mathbf{h}^{-1}\mathbf{g}))^{-1} \quad (4.128)$$

Next we consider the change of  $U$ -factors. Before the handle slide, the vector and the dual vector assigned to the two disconnected  $D^3$  balls of the blue 1-handle are  $|a_i, \dots; 1\rangle_{\tilde{\mu}\dots}$  and  $\langle \bar{\mathbf{g}}a_i, \dots; 1|_{\mu\dots}$ , respectively, which give the  $U$ -factor from the red lines

$$\langle \bar{\mathbf{g}}a_i, \dots; 1|_{\mu\dots} \rho_{\mathbf{g}}^{-1} |a_i, \dots; 1\rangle_{\tilde{\mu}\dots} = U_{\mathbf{g}}^{-1}(a_i, \dots; 1)_{\tilde{\mu}\dots, \mu\dots} \quad (4.129)$$

After the handle slide, the vector assigned to the upper ball of the darkblue 1-handle is the tensor product of  $|a_i, \dots; 1\rangle_{\tilde{\mu}\dots}$  and the original vector corresponding to the orange lines. The dual vector assigned to the lower ball of the darkblue 1-handle is the tensor product of  $\langle \bar{\mathbf{h}}a_i, \dots; 1|_{\tilde{\mu}\dots}$  and the original dual vector corresponding to orange lines. The vector assigned to the upper ball of the blue 1-handle is  $|\bar{\mathbf{h}}a_i, \dots; 1\rangle_{\tilde{\mu}\dots}$ , and finally the dual vector assigned to the lower ball of the blue 1-handle is still  $\langle \bar{\mathbf{g}}a_i, \dots; 1|_{\mu\dots}$ . Then the  $U$ -factor relevant to the red lines after the handle slide becomes

$$\begin{aligned} & \sum_{\tilde{\mu}\dots} \langle \bar{\mathbf{g}}a_i, \dots; 1|_{\mu\dots} \rho_{\mathbf{h}^{-1}\mathbf{g}}^{-1} |\bar{\mathbf{h}}a_i, \dots; 1\rangle_{\tilde{\mu}\dots} \cdot \langle \bar{\mathbf{h}}a_i, \dots; 1|_{\tilde{\mu}\dots} \rho_{\mathbf{h}}^{-1} |a_i, \dots; 1\rangle_{\tilde{\mu}\dots} \\ &= \sum_{\tilde{\mu}\dots} U_{\mathbf{h}}^{-1}(a_i, \dots; 1)_{\tilde{\mu}\dots, \tilde{\mu}\dots} \cdot U_{\mathbf{h}^{-1}\mathbf{g}}^{-1} \left( \bar{\mathbf{h}}a_i, \dots; 1 \right)_{\tilde{\mu}\dots, \mu\dots} \end{aligned} \quad (4.130)$$

According to Eq. (4.23), the product of Eq. (4.128) and Eq. (4.130) is precisely Eq. (4.129), which means that the changes of the  $\eta$ -factors and  $U$ -factors cancel each other, and each individual summand in Eq. (4.44) is invariant under 1-1 handle slides.

To account for anti-unitary symmetry, we need to pay attention to two special effects: i) some anyons will change their directions of flow compared with the Kirby diagram; ii) we need to add proper factors of  $K^{q(\mathbf{h})}$  in front of some vectors to account for  $\mathbb{C}$ -anti-linear functor. Without loss of generality, we can still suppose that anyons labeled by  $\{a_i\}$  are running downward in the blue 1-handle of the Kirby diagram. Yet we should give these anyons an extra label  $\{s_i\}$ , according to whether the segment corresponding to labels  $\{a_i\}$  has flipped the direction of the flow or not:

$$s_i = \begin{cases} +1 & \text{if } a_i \text{ does not flip} \\ -1 & \text{if } a_i \text{ does flip} \end{cases} \quad (4.131)$$

Then after carefully counting the extra contribution from anti-unitary symmetry, the change of  $\eta$ -factor becomes

$$\prod_i (\eta_{a_i}(\mathbf{h}, \mathbf{h}^{-1}\mathbf{g}))^{-s_i} \quad (4.132)$$

Before the handle slide, the vector and the dual vector assigned to the two disconnected  $D^3$  balls of the blue 1-handle are  $|a_i, \dots, \{s_i = +1\}; a_{\tilde{i}}, \dots, \{s_{\tilde{i}} = -1\}\rangle_{\tilde{\mu}\dots}$  and  $\langle \bar{\mathbf{g}} a_i, \dots, \{s_i = +1\}; \bar{\mathbf{g}} a_{\tilde{i}}, \dots, \{s_{\tilde{i}} = -1\} |_{\mu\dots} K^{q(\mathbf{g})}$ , which gives the  $U$ -factor from the red lines

$$\langle \bar{\mathbf{g}} a_i, \dots; \bar{\mathbf{g}} a_{\tilde{i}}, \dots |_{\mu\dots} K^{q(\mathbf{g})} \rho_{\mathbf{g}}^{-1} | a_i, \dots; a_{\tilde{i}}, \dots \rangle_{\tilde{\mu}\dots} = U_{\mathbf{g}}^{-1}(a_i, \dots; a_{\tilde{i}}, \dots)_{\tilde{\mu}\dots, \mu\dots} \quad (4.133)$$

where  $i$  and  $\tilde{i}$  are indices to label anyons with  $s_i = +1$  or  $s_i = -1$ , respectively. After the handle slide, the  $U$ -factor relevant to the red lines after the handle slide becomes

$$\begin{aligned} & \sum_{\tilde{\mu}\dots} \langle \bar{\mathbf{g}} a_i, \dots; \bar{\mathbf{g}} a_{\tilde{i}}, \dots |_{\mu\dots} K^{q(\mathbf{g})} \rho_{\mathbf{h}^{-1}\mathbf{g}}^{-1} K^{q(\mathbf{h})} | \bar{\mathbf{h}} a_i, \dots; \bar{\mathbf{h}} a_{\tilde{i}}, \dots \rangle_{\tilde{\mu}\dots} \langle \bar{\mathbf{h}} a_i, \dots; \bar{\mathbf{h}} a_{\tilde{i}}, \dots |_{\tilde{\mu}\dots} K^{q(\mathbf{h})} \rho_{\mathbf{h}}^{-1} | a_i, \dots; a_{\tilde{i}}, \dots \rangle_{\tilde{\mu}\dots} \\ & = \sum_{\tilde{\mu}\dots} U_{\mathbf{h}^{-1}\mathbf{g}}^{-1}(a_i, \dots; a_{\tilde{i}}, \dots)_{\tilde{\mu}\dots, \tilde{\mu}\dots} \cdot U_{\mathbf{h}^{-1}\mathbf{g}}^{-1}(\bar{\mathbf{h}} a_i, \dots; \bar{\mathbf{h}} a_{\tilde{i}}, \dots)_{\tilde{\mu}\dots, \mu\dots}^{\sigma(\mathbf{h})} \end{aligned} \quad (4.134)$$

Again, according to Eq. (4.23), the product of Eq. (4.132) and Eq. (4.134) is precisely Eq. (4.133), which means that the changes of the  $\eta$ -factors and  $U$ -factors cancel each other, and each individual summand in Eq. (4.44) is invariant under 1-1 handle slides.

Therefore, we have established that the partition function  $\mathcal{Z}(\mathcal{M}, \mathcal{G})$  is invariant under the 1-1 handle slide.



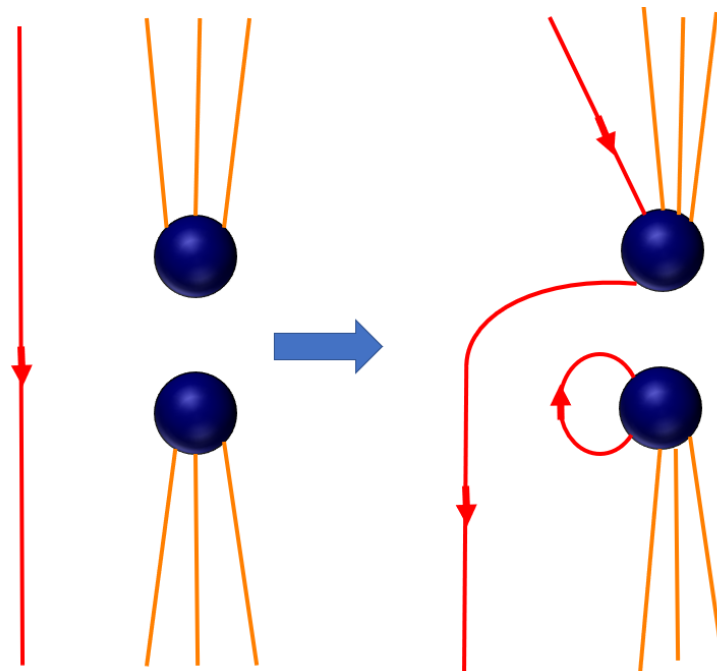


Figure 4.15: An illustration of the effect of isotopies where the red 2-handle crosses some defect on the darkblue 1-handle. On the anyon diagram the red line connecting the lower darkblue ball to itself becomes a red bubble.

- Isotopy.

The invariance of the partition function  $\mathcal{Z}(\mathcal{M}, \mathcal{G})$  under an isotopy where a 2-handle crosses a defect is relatively easy. Suppose that a  $\mathfrak{g}$ -defect is present across the darkblue 1-handle (see Fig. 4.15). We wish to prove the invariance of the partition function  $\mathcal{Z}(\mathcal{M}, \mathcal{G})$  by proving the invariance of each individual summand of Eq. (4.44). Label the red 2-handle by an anyon  $a$ . After this isotopy, the prefactor of quantum dimension in the individual summand of Eq. (4.44) is modified by an extra  $1/d_a$ . This is canceled by the contribution from the extra bubble in the Kirby diagram. There is no change in  $\eta$ -factors and  $U$ -factors. Therefore, we see that  $\mathcal{Z}(\mathcal{M}, \mathcal{G})$  is invariant under the isotopy.

- 2-2 handle slide.

The effect of a 2-2 handle slide on a Kirby diagram is explicitly shown in Fig. 4.16. We wish to prove the invariance of the partition function  $\mathcal{Z}(\mathcal{M}, \mathcal{G})$  by proving the invariance of each individual summand of Eq. (4.44).

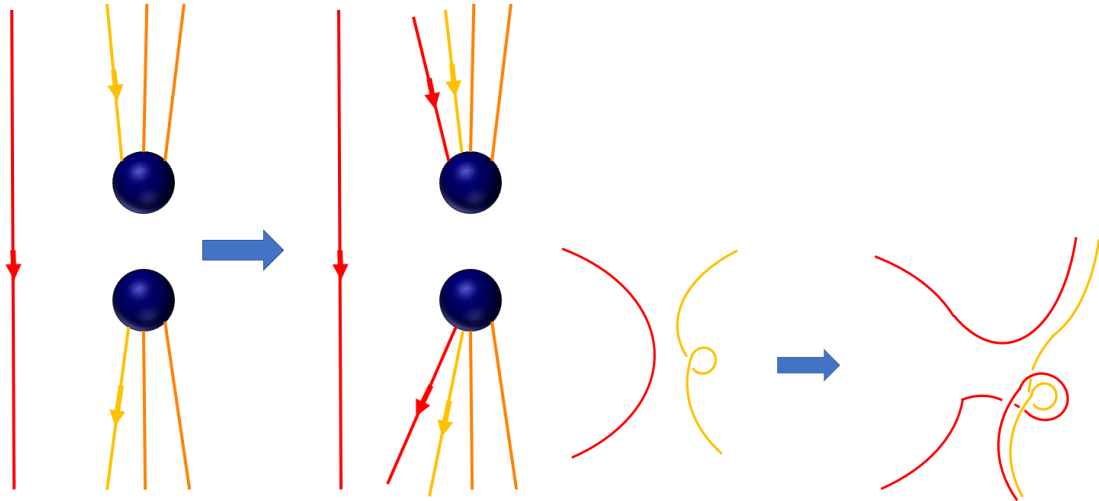


Figure 4.16: Upper: An illustration of the effect of a 2-2 handle slide on the Kirby diagram, where the red 2-handle slides past the yellow 2-handle. Lower: An illustration of the change of framing after 2-2 handle slide.

Let us put anyon  $a$  on (a segment of) the red 2-handle and anyon  $b$  on the yellow 2-handle. The strategy is to fuse  $a$  and  $b$  into another anyon  $c$ , such that the expression involving  $a$  and  $b$  can be transformed to an expression involving  $a$  and  $c$ , which turns out to be manifestly the same as the expression before the 2-2 handle slide.

First of all, at every 1-handle that the yellow 2-handle crosses, the relevant prefactor involving quantum dimensions is shifted from  $\frac{1}{\sqrt{d_b}}$  to  $\frac{1}{\sqrt{d_a d_b}}$ . Yet when we fuse  $a$  and  $b$  into another anyon  $c$ , there is an extra bubble as in Eq. (4.4) which gives  $\sqrt{\frac{d_a d_b}{d_c}}$ . Multiplying them together gives  $\frac{1}{\sqrt{d_c}}$ . Therefore, the factors regrading quantum dimensions match before and after the handle slide.

Next, we should consider the effect of the change of framing, as illustrated in the lower figure of Fig. 4.16. Suppose that before the handle slide  $b$  has framing  $n$ . This contributes a  $\theta_b^n$  term in  $\mathcal{Z}(\mathcal{M}, \mathcal{G})$ . After the handle slide, the red 2-handle should have an additional framing  $n$ , the yellow 2-handle should still have framing  $n$ , and the red 2-handle should wind around the yellow 2-handle  $(-n)$ -times, contributing an extra factor of

$$\theta_a^n \theta_b^n \times \frac{\theta_c^n}{\theta_a^n \theta_b^n} = \theta_c^n, \quad (4.135)$$

consistent with the expression before the handle slide.

Now we consider  $U$ - and  $\eta$ -factors. Suppose that starting with the segment of the yellow 2-handle labeled by  $b$ , the yellow 2-handle begins crossing some 1-handles, and the symmetry defects these 1-handles host are  $\mathbf{g}, \mathbf{h}, \dots$ . Moreover, without loss of generality suppose that on the Kirby diagram the yellow 2-handle runs downward in these 1-handles. Then consider two consecutive 1-handles that the yellow 2-handle crosses with  $\mathbf{g}, \mathbf{h}$ -defects on them, the extra  $U$ -factor involved is

$$U_{\mathbf{g}}^{-1}(a, b; c)_{\mu\mu'} U_{\mathbf{h}}^{-1}(\bar{\mathbf{g}}a, \bar{\mathbf{g}}b; \bar{\mathbf{g}}c)_{\mu''\mu'}^{\sigma(\mathbf{g})} \quad (4.136)$$

The  $\eta$ -factor coming from composing  $\rho_{\mathbf{h}}^{-1}$  and  $\rho_{\mathbf{g}}^{-1}$  to  $\rho_{\mathbf{gh}}^{-1}$ , is

$$\eta_a(\mathbf{g}, \mathbf{h})^{-1} \eta_b(\mathbf{g}, \mathbf{h})^{-1} \quad (4.137)$$

Multiplying Eq. (4.136) and Eq. (4.137) and using Eq. (4.23), we get

$$\eta_c(\mathbf{g}, \mathbf{h})^{-1} U_{\mathbf{gh}}^{-1}(a, b; c)_{\mu\mu'} \quad (4.138)$$

It is then straightforward to see that, after accounting for all 1-handles that the yellow 2-handle crosses, such manipulation will cancel all extra  $U$ -factors while reproducing the correct  $\eta$ -factor from the natural isomorphism for anyon  $c$ .

Therefore, we have established that the partition function  $\mathcal{Z}(\mathcal{M}, \mathcal{G})$  is invariant under the 2-2 handle slide.

## 4.C.2 Invariance under change of defects

The partition function  $\mathcal{Z}(\mathcal{M}, \mathcal{G})$  is also dependent on a specific choice of the defect network defined on  $\mathcal{M}$  to reflect the  $G$ -bundle structure  $\mathcal{G}$ . There are two important choices that we have made during calculation in Eq. (4.44). The first choice is that, for a 1-handle hosting a  $\mathfrak{g}$ -defect, there are two  $D^3$  balls on the attaching region, and we need to choose one  $D^3$  ball out of the two to be “above” another one, as in Remark e in Sec. 4.2.4. It amounts to choosing an orientation of the defect, i.e., whether this defect is  $\mathfrak{g}$  or  $\bar{\mathfrak{g}}$ . Another choice is that even for the same  $G$ -bundle  $\mathcal{G}$  on  $\mathcal{M}$ , we can choose a different set of defects put across 1-handles by changing each defect  $\mathfrak{g}$  to  $\mathbf{h}\mathfrak{g}\mathbf{h}^{-1}$ , where  $\mathbf{h}$  is an arbitrary fixed element in  $G$ . Remember that  $G$ -bundles on  $\mathcal{M}$  are classified by

$$\text{Hom}(\pi_1(\mathcal{M}), G) / G \quad (4.139)$$

Here  $\text{Hom}(\pi_1(\mathcal{M}), G)$  is nothing but identifying the holonomy we put on noncontractible cycles, yet there is an equivalence relation due to  $G$ -action by conjugation on the holonomy. Therefore, we need to prove that the partition function  $\mathcal{Z}(\mathcal{M}, \mathcal{G})$  is the same if the defect we put on 1-handles are conjugated by elements in  $G$ . This amounts to showing the gauge invariance of the partition function under gauge transformation of  $G$ .

Let us start by considering the first choice, i.e., the choice of the orientation of the defect. Again, we wish to prove the invariance of the partition function  $\mathcal{Z}(\mathcal{M}, \mathcal{G})$  by proving the invariance of each individual summand of Eq. (4.44). Suppose anyons labeled by  $\{a_i\}$  cross the blue 1-handle which hosts a defect labeled by  $\mathfrak{g}$ . Without loss of generality suppose that at the beginning they are all running downward in the blue 1-handle of the Kirby diagram. Now we flip the relative position of the two balls. Then anyons crossing the 1-handles upwards are acted upon by  $\rho_{\bar{\mathfrak{g}}}$  instead of  $\rho_{\mathfrak{g}}^{-1}$ , which gives the extra  $\eta$ -factor

$$\prod_i (\eta_{a_i}(\mathfrak{g}, \bar{\mathfrak{g}}))^{s_i} \quad (4.140)$$

Again, to account for the fact that some anyons will flip the direction of the flow, we introduce an extra factor  $s_i$  as in Eq. (4.131). Before the flip, the vector and the dual vector assigned to the two disconnected  $D^3$  balls of the blue 1-handle are  $|a_i, \dots, \{s_i = +1\}; a_{\tilde{i}}, \dots, \{s_{\tilde{i}} = -1\}\rangle_{\tilde{\mu}\dots}$  and  $\langle \bar{\mathfrak{g}}a_i, \dots, \{s_i = +1\}; \bar{\mathfrak{g}}a_{\tilde{i}}, \dots, \{s_{\tilde{i}} = -1\} |_{\mu\dots} K^{q(\mathfrak{g})}$ , which gives the  $U$ -factor

$$\langle \bar{\mathfrak{g}}a_i, \dots; \bar{\mathfrak{g}}a_{\tilde{i}}, \dots |_{\mu\dots} K^{q(\mathfrak{g})} \rho_{\mathfrak{g}}^{-1} |a_i, \dots; a_{\tilde{i}}, \dots \rangle_{\tilde{\mu}\dots} = U_{\mathfrak{g}}^{-1}(a_i, \dots; a_{\tilde{i}}, \dots)_{\tilde{\mu}\dots, \mu\dots}, \quad (4.141)$$

where again  $i$  and  $\tilde{i}$  are indices to label anyons with  $s_i = +1$  or  $s_i = -1$ , respectively. After the flip, the vector and the dual vector assigned to the two disconnected  $D^3$  balls of

the blue 1-handle are  $K^{q(\mathfrak{g})}|\bar{\mathfrak{g}}a_{\bar{i}}, \dots, \{s_{\bar{i}} = -1\}; \bar{\mathfrak{g}}a_i, \dots, \{s_i = +1\}\rangle_{\mu\dots}$  and  $\langle a_{\bar{i}}, \dots, \{s_{\bar{i}} = -1\}; a_i, \dots, \{s_i = +1\}\rangle_{\tilde{\mu}\dots}$ , which gives the  $U$ -factor

$$\begin{aligned} \langle a_{\bar{i}}, \dots; a_i, \dots \dots |_{\tilde{\mu}\dots} \rho_{\bar{\mathfrak{g}}}^{-1} K^{q(\mathfrak{g})} |\bar{\mathfrak{g}}a_{\bar{i}}, \dots; \bar{\mathfrak{g}}a_i, \dots \rangle_{\mu\dots} &= U_{\bar{\mathfrak{g}}}^{-1} (\bar{\mathfrak{g}}a_{\bar{i}}, \dots; \bar{\mathfrak{g}}a_i, \dots)_{\mu\dots, \tilde{\mu}\dots}^{\sigma(\mathfrak{g})} \\ &= U_{\bar{\mathfrak{g}}} (\bar{\mathfrak{g}}a_i, \dots; \bar{\mathfrak{g}}a_{\bar{i}}, \dots)_{\tilde{\mu}\dots, \mu\dots}^{\sigma(\mathfrak{g})} \end{aligned} \quad (4.142)$$

According to Eq. (4.23), the product of Eq. (4.140) and Eq. (4.142) is precisely Eq. (4.141). Therefore, we have established that the partition function  $\mathcal{Z}(\mathcal{M}, \mathcal{G})$  is independent of the first choice.

Now consider the second choice. Suppose that all defects are conjugated by an element  $\mathbf{h}$  in  $G$ , i.e., all  $\mathfrak{g}$ -defects become  $\mathbf{h}\mathfrak{g}\mathbf{h}^{-1}$ . We need to consider the case where  $\mathbf{h}$  is unitary or anti-unitary separately.

Suppose that  $\mathbf{h}$  is unitary. First we change the labels  $\{a_i\}$  of all anyons to  $\{\mathbf{h}a_i\}$ . Then we wish to prove the invariance of the partition function  $\mathcal{Z}(\mathcal{M}, \mathcal{G})$  by proving the invariance of each individual summand of Eq. (4.44). First consider the Kirby diagram, whose evaluation schematically takes the form

$$\left( F \cdot R \cdot F \cdot R \dots \right)_{\mu_1 \dots \mu_2 \dots, \tilde{\mu}_1 \dots \tilde{\mu}_2 \dots} \quad (4.143)$$

where  $\mu_1 \dots$  and  $\tilde{\mu}_1 \dots$  are indices corresponding to vectors and dual vectors on the anyon diagram associated to the Kirby diagram, respectively. After relabeling, according to Eq. (4.19) the Kirby diagram changes to

$$\sum_{\mu'_1 \dots \tilde{\mu}'_1 \dots} U_{\mu_1 \mu'_1}^{-1} \dots U_{\mu_2 \mu'_2}^{-1} \dots \left( F \cdot R \cdot F \cdot R \dots \right)_{\mu'_1 \dots \mu'_2 \dots, \tilde{\mu}'_1 \dots \tilde{\mu}'_2 \dots} \cdot U_{\tilde{\mu}'_1 \tilde{\mu}_1} \dots U_{\tilde{\mu}'_2 \tilde{\mu}_2} \dots \quad (4.144)$$

We have suppressed all anyon labels, but pay attention that in the above formula anyon labels in  $F$ - and  $R$ - symbols are from  $\{a_i\}$  while anyon labels in  $U$ -symbols are from  $\{\mathbf{h}a_i\}$ .

Now we focus on a single 1-handle. Suppose anyons labeled by  $\{a_i\}$  cross the 1-handle which hosts a defect labeled by  $\mathfrak{g}$ , and without loss of generality suppose that they are all running downward in the Kirby diagram. Before the change of defects, the vector and the dual vector assigned to the two disconnected  $D^3$  balls are  $|a_i, \dots, \{s_i = +1\}; a_{\bar{i}}, \dots, \{s_{\bar{i}} = -1\}\rangle_{\tilde{\mu}\dots}$  and  $\langle \bar{\mathfrak{g}}a_i, \dots, \{s_i = +1\}; \bar{\mathfrak{g}}a_{\bar{i}}, \dots, \{s_{\bar{i}} = -1\}\rangle_{\mu\dots} K^{q(\mathfrak{g})}$ , which gives the  $U$ -factor

$$\langle \bar{\mathfrak{g}}a_i, \dots; \bar{\mathfrak{g}}a_{\bar{i}}, \dots \dots |_{\mu\dots} K^{q(\mathfrak{g})} \rho_{\mathfrak{g}}^{-1} |a_i, \dots; a_{\bar{i}}, \dots \rangle_{\tilde{\mu}\dots} = U_{\mathfrak{g}}^{-1} (a_i, \dots; a_{\bar{i}}, \dots)_{\tilde{\mu}\dots, \mu\dots}, \quad (4.145)$$

where again  $i$  and  $\tilde{i}$  are indices to label anyons with  $s_i = +1$  or  $s_i = -1$ , respectively. After the change of defects (and relabeling), the vector and the dual vector assigned to the two disconnected  $D^3$  balls are  $|\mathbf{h}_{a_i, \dots, \{s_i = +1\}}; \mathbf{h}_{a_{\tilde{i}}, \dots, \{s_{\tilde{i}} = -1\}}\rangle_{\tilde{\mu} \dots}$  and  $\langle \mathbf{h}\bar{\mathbf{g}}_{a_i, \dots, \{s_i = +1\}}; \mathbf{h}\bar{\mathbf{g}}_{a_{\tilde{i}}, \dots, \{s_{\tilde{i}} = -1\}} |_{\mu \dots} K^{q(\mathbf{g})}$ , which gives the  $U$ -factor

$$\langle \mathbf{h}\bar{\mathbf{g}}_{a_i, \dots; \mathbf{h}\bar{\mathbf{g}}_{a_{\tilde{i}}, \dots} |_{\mu \dots} K^{q(\mathbf{g})} \rho_{\mathbf{h}\mathbf{g}\mathbf{h}^{-1}}^{-1} | \mathbf{h}_{a_i, \dots; \mathbf{h}_{a_{\tilde{i}}, \dots} \rangle_{\tilde{\mu} \dots} = U_{\mathbf{h}\mathbf{g}\mathbf{h}^{-1}}^{-1} (\mathbf{h}_{a_i, \dots; \mathbf{h}_{a_{\tilde{i}}, \dots})_{\tilde{\mu} \dots, \mu \dots} \quad (4.146)$$

Together with the extra  $U$ -factor in Eq. (4.144), we have

$$\sum_{\mu' \tilde{\mu}'} U_{\mathbf{h}} (\mathbf{h}_{a_i, \dots; \mathbf{h}_{a_{\tilde{i}}, \dots})_{\tilde{\mu} \tilde{\mu}'} \cdot U_{\mathbf{h}\mathbf{g}\mathbf{h}^{-1}}^{-1} (\mathbf{h}_{a_i, \dots; \mathbf{h}_{a_{\tilde{i}}, \dots})_{\tilde{\mu}' \mu'} \cdot U_{\mathbf{h}}^{-1} (\mathbf{h}\bar{\mathbf{g}}_{a_i, \dots; \mathbf{h}\bar{\mathbf{g}}_{a_{\tilde{i}}, \dots})_{\mu' \mu}^{\sigma(\mathbf{g})} \quad (4.147)$$

Finally, after conjugation by  $\mathbf{h}$ , anyons are now labeled by  $\{\mathbf{h}_{a_i}\}$ , and acted by  $\rho_{\mathbf{h}\mathbf{g}\mathbf{h}^{-1}}^{-1}$ . Comparing with  $\rho_{\mathbf{h}} \circ \rho_{\mathbf{g}}^{-1} \circ \rho_{\mathbf{h}}^{-1}$ , this gives an extra  $\eta$ -factor to be

$$\prod_i \left( \frac{\eta_{\mathbf{h}_{a_i}}(\mathbf{h}, \mathbf{g})}{\eta_{\mathbf{h}_{a_i}}(\mathbf{h}\mathbf{g}\mathbf{h}^{-1}, \mathbf{h})} \right)^{s_i} \quad (4.148)$$

According to Eq. (4.23), the product of Eq. (4.148) and Eq. (4.147) is precisely Eq. (4.145), which means that each individual summand in Eq. (4.44) is invariant.

Finally, suppose that  $\mathbf{h}$  is anti-unitary. Then conjugation by  $\mathbf{h}$  needs to be accompanied by change of orientation of the manifold  $\mathcal{M}$ .<sup>13</sup> Then the partition function  $\mathcal{Z}(\mathcal{M}, \mathcal{G})$  is complex conjugated under the change of orientation. The rest analysis is similar to the case where  $\mathbf{h}$  is unitary. Compared with Eq. (4.143) and according to Eq. (4.19), after relabeling the Kirby diagram changes to

$$\sum_{\mu'_1 \dots \tilde{\mu}'_1 \dots} \left( U_{\mu_1 \mu'_1}^{-1} \dots U_{\mu_2 \mu'_2}^{-1} \dots \right)^* \cdot \left( F \cdot R \cdot F \cdot R \dots \right)_{\mu'_1 \dots \mu'_2 \dots, \tilde{\mu}'_1 \dots \tilde{\mu}'_2 \dots} \cdot \left( U_{\tilde{\mu}'_1 \tilde{\mu}_1} \dots U_{\tilde{\mu}'_2 \tilde{\mu}_2} \dots \right)^* \quad (4.149)$$

Again pay attention that in the above formula anyon labels in  $F$ - and  $R$ - symbols are from  $\{a_i\}$  while anyon labels in  $U$ - symbols are from  $\{\mathbf{h}_{a_i}\}$ . Then focus on a single 1-handle. Again suppose anyons labeled by  $\{a_i\}$  cross the 1-handle which hosts a defect labeled by  $\mathbf{g}$ , and without loss of generality suppose that they are all running downward in the Kirby

<sup>13</sup>For  $\mathcal{M}$  orientable the meaning is clear. For  $\mathcal{M}$  non-orientable note that since we have cut across crosscaps, we also choose an orientation of  $\mathcal{M}$  except at the cut, where two orientations on two faces of the cut are opposite to each other, and this is reflected in the change of the direction of the flow of anyons. A more formal way of thinking it is via a more precise definition of  $G$ -bordism in terms of the associated vector bundle  $\xi$  of the gauge bundle  $\mathcal{G}$  [98], and we need to choose an orientation of  $T\mathcal{M} \oplus \xi$ , where  $T\mathcal{M}$  is the tangent bundle of  $\mathcal{M}$ , as mentioned in Footnote 3.

diagram. After the change of defects (and relabeling), together with the extra  $U$ -factor in Eq. (4.149), the  $U$ -factor relevant to the 1-handle becomes

$$\sum_{\mu' \tilde{\mu}'} U_{\mathbf{h}}(\mathbf{h}a_i, \dots; \mathbf{h}a_{\tilde{i}}, \dots)_{\tilde{\mu}' \mu'}^* \cdot U_{\mathbf{hgh}^{-1}}^{-1}(\mathbf{h}a_i, \dots; \mathbf{h}a_{\tilde{i}}, \dots)_{\tilde{\mu}' \mu'}^* \cdot U_{\mathbf{h}}^{-1}(\mathbf{h}\bar{\mathbf{g}}a_i, \dots; \mathbf{h}\bar{\mathbf{g}}a_{\tilde{i}}, \dots)_{\mu' \mu}^{*\sigma(\mathbf{g})} \quad (4.150)$$

Finally, after conjugation by  $\mathbf{h}$ , anyons are now labeled by  $\{\mathbf{h}a_i\}$ , and acted by  $\rho_{\mathbf{hgh}^{-1}}^{-1}$ . Comparing with  $\rho_{\mathbf{h}} \circ \rho_{\mathbf{g}}^{-1} \circ \rho_{\mathbf{h}}^{-1}$ , this gives an extra  $\eta$ -factor to be

$$\prod_i \left( \frac{\eta_{\mathbf{h}a_i}(\mathbf{h}, \mathbf{g})}{\eta_{\mathbf{h}a_i}(\mathbf{hgh}^{-1}, \mathbf{h})} \right)^{-s_i} \quad (4.151)$$

According to Eq. (4.23), the product of Eq. (4.151) and Eq. (4.150) is precisely Eq. (4.145), which means that each individual summand in Eq. (4.44) is invariant.

Therefore, we have established that the partition function  $\mathcal{Z}(\mathcal{M}, \mathcal{G})$  is invariant under the change of defects.

### 4.C.3 Gauge invariance

Another important check we need to perform is the ‘‘gauge invariance’’ of Eq. (4.44). Specifically, we need to prove that Eq. (4.44) is invariant under vertex basis transformation Eqs. (4.10) and (4.18), as well as symmetry action gauge transformation Eq. (4.26). In this sub-appendix, we explicitly perform this check.

To show the invariance under vertex basis transformation, we can think of the result of the Kirby diagram as a giant matrix, which schematically takes the form

$$\left( F \cdot R \cdot F \cdot R \cdots \right)_{\mu_1 \dots \mu_2 \dots \dots, \tilde{\mu}_1 \dots \tilde{\mu}_2 \dots \dots} \quad (4.152)$$

where  $\mu_1 \dots$  and  $\tilde{\mu}_1 \dots$  are indices corresponding to vectors and dual vectors on the anyon diagram associated to the Kirby diagram, respectively. Then we can schematically write down what the giant matrix Eq. (4.152) becomes after vertex basis transformation Eq. (4.10), which is

$$(\Gamma^{\cdot})_{\mu_1 \mu'_1} \cdots (\Gamma^{\cdot})_{\mu_2 \mu'_2} \cdots \times \left( F \cdot R \cdot F \cdot R \cdots \right)_{\mu'_1 \dots \mu'_2 \dots \dots, \tilde{\mu}'_1 \dots \tilde{\mu}'_2 \dots \dots} \times (\Gamma^{\cdot})_{\tilde{\mu}'_1 \tilde{\mu}_1}^\dagger \cdots (\Gamma^{\cdot})_{\tilde{\mu}'_2 \tilde{\mu}_2}^\dagger \cdot (4.153)$$

On the 1-handles, we have  $U$ -factors  $U_{\mathbf{g}}^{-1}(\dots)_{\tilde{\mu}_1, \dots, \mu_1, \dots}$ , which under vertex basis transformation transforms according to Eq. (4.18), i.e., it becomes

$$(\Gamma^\cdot)_{\tilde{\mu}_1 \tilde{\mu}'_1} \cdots \times U_{\mathbf{g}}^{-1}(\dots)_{\tilde{\mu}'_1, \dots, \mu'_1, \dots} \times \left( (\Gamma^\cdot)_{\mu'_1 \mu_1}^\dagger \right)^* \quad (4.154)$$

Here we substitute all anyon labels by  $\cdot$  and hopefully they will be clear in specific contexts. Now we immediately see that after multiplying  $\Gamma$ -matrices and summing over  $\mu, \tilde{\mu}$  indices, we have  $\delta_{\mu'_1 \mu''_1} \cdots \delta_{\tilde{\mu}'_1 \tilde{\mu}''_1} \cdots$  and the expression becomes the original expression.

Next consider symmetry action gauge transformation. Again let us focus on a single 1-handle, and without loss of generality suppose that all anyons  $\{a_i\}$  crossing the 1-handle are running downward in the Kirby diagram. Again, to account for the fact that some anyons will flip the direction of the flow, we introduce an extra factor  $s_i$  as in Eq. (4.131). The vector and the dual vector assigned to the two disconnected  $D^3$  balls are  $|a_i, \dots, \{s_i = +1\}; a_{\tilde{i}}, \dots, \{s_{\tilde{i}} = -1\}\rangle_{\tilde{\mu} \dots}$  and  $\bar{\mathfrak{g}}\langle a_i, \dots, \{s_i = +1\}; \bar{\mathfrak{g}}a_{\tilde{i}}, \dots, \{s_{\tilde{i}} = -1\} |_{\mu \dots} K^{q(\mathfrak{g})}$ , which gives the  $U$ -factor

$$\langle \bar{\mathfrak{g}}a_i, \dots; \bar{\mathfrak{g}}a_{\tilde{i}}, \dots \dots |_{\mu \dots} K^{q(\mathfrak{g})} \rho_{\mathbf{g}}^{-1} |a_i, \dots; a_{\tilde{i}}, \dots \rangle_{\tilde{\mu} \dots} = U_{\mathbf{g}}^{-1}(a_i, \dots; a_{\tilde{i}}, \dots)_{\tilde{\mu} \dots, \mu \dots}, \quad (4.155)$$

where  $i$  and  $\tilde{i}$  are indices to label anyons with  $s_i = +1$  or  $s_i = -1$ , respectively. Under the transformation in Eq. (4.26), it becomes

$$\prod_i (\gamma_{a_i}(\mathfrak{g}))^{-s_i} U_{\mathbf{g}}^{-1}(a_i, \dots; a_{\tilde{i}}, \dots)_{\tilde{\mu} \dots, \mu \dots} \quad (4.156)$$

All  $\{a_i\}$  crossing the 1-handle are acted by  $\rho_{\mathbf{g}}^{-1}$ , and therefore following Eq. (4.25) under symmetry action gauge transformation we have extra  $\gamma$  parts:

$$\prod_i (\gamma_{a_i}(\mathfrak{g}))^{s_i} \quad (4.157)$$

Then we immediately see that the extra  $\gamma$  part in Eq. (4.157) exactly cancels the extra  $\gamma$  part in Eq. (4.156).

Therefore, we have established that the partition function  $\mathcal{Z}(\mathcal{M}, \mathcal{G})$  is invariant under vertex basis transformation Eqs. (4.10), (4.18) and symmetry action gauge transformation Eq. (4.26).

#### 4.C.4 Cobordism invariance

In order to demonstrate that the construction gives the TQFT that reflects the anomaly of the symmetry-enriched topological order, in this sub-appendix we prove that the partition



function in Eq. (4.44) on a closed 4-manifold  $\mathcal{M}$  with  $G$ -bundle structure  $\mathcal{G}$  is in fact a cobordism invariant.

Two closed, oriented  $n$ -dimensional manifolds  $\mathcal{M}$  and  $\tilde{\mathcal{M}}$  are cobordant if and only if they are related to each other by a sequence of surgeries [111]. In 4 dimensions, cobordisms of 4-manifolds can be generated by the following types of surgery moves:

- Removing or adding an  $S^4$ .
- Replacing an  $S^1 \times D^3$  by  $S^2 \times D^2$  and vice versa. Note that they have the same boundary  $S^1 \times S^2$ .
- Replacing  $S^0 \times D^4$  by  $D^1 \times S^3$  and vice versa. Note that they have the same boundary  $S^0 \times S^3$ .

In the Crane-Yetter model, in order to prove that the partition function is a cobordism invariant, we need to prove that the partition function  $\mathcal{Z}(\mathcal{M})$  is invariant under these three surgery moves.

Now in the presence of  $G$ -bundle structure  $\mathcal{G}$ , we need to consider  $G$ -bordism [69, 99], and therefore we need to pay special attention to whether defects can be extended or not during the surgery. Let us enumerate the effect of the three surgery moves one by one.

- Removing or adding an  $S^4$ .

This surgery move will not involve  $G$ -defects because  $S^4$  is simply connected (i.e.,  $\pi_1(S^4) = 0$ ) and a  $G$ -bundle on it must be trivial. Then the partition function is invariant because we can directly see from Eq. (4.44) that  $\mathcal{Z}(S^4) = 1$ .

- Replacing an  $S^1 \times D^3$  by  $S^2 \times D^2$  and vice versa.

We can interpret this surgery move as “trading” a 1-handle with a 2-handle as follows. Decompose  $S^1$  into  $S^1_+$  and  $S^1_-$  which are both homeomorphic to  $D^1$ . Interpret the  $S^1_+ \times D^3$  part as a 1-handle that is attached to  $S^1_- \times D^3$  which is interpreted as a 0-handle. (Now we do not assume that there is only 1 0-handle.) Similarly, decompose  $S^2$  into  $S^2_+$  and  $S^2_-$  which are all homeomorphic to  $D^2$ . Interpret the  $S^2_+ \times D^2$  part as a 2-handle that is attached to  $S^2_- \times D^2$  which is interpreted as a 0-handle. Then before and after the surgery move that replaces an  $S^1 \times D^3$  by  $S^2 \times D^2$ , a 1-handle is removed and a 2-handle is added.

An important observation is that for a  $G$ -bordism, there can be no  $G$ -defect that is put on the 1-handle before the trading. This fact can be proven as follows. Consider

$S^1 \times \{pt\} \subset S^1 \times \partial(D^3) \cong S^1 \times S^2$ , which is a loop that survives before and after the trading. Even though it can be a noncontractible loop before the trading, it is a contractible loop after the trading, because we can shrink it to a point as it lives on the boundary of the 2-handle  $D^2 \times D^2$ . Therefore,  $G$ -bordism demands that no  $\mathfrak{g}$ -defect can be present on such  $S^1$  loop.

It is immediate that now we can carry over the proof of the invariance in the Crane-Yetter model [95] to prove the invariance of  $\mathcal{Z}(\mathcal{M}, \mathcal{G})$  under the surgery move.

- Replacing  $S^0 \times D^4$  by  $D^1 \times S^3$  and vice versa.

We can interpret this surgery move as adding a 1-handle and removing a 4-handle. Note that we can introduce some  $G$ -defect as well, including crosscap, to the newly introduced non-contractible cycle.

To consider the effect of this surgery move, we can choose a handle decomposition such that  $S^0 \times D^4$  before the surgery move are two 4-handles. Then  $D^1 \times S^3$  can be thought of as a 1-handle and a 4-handle. In particular, no 2-handle is attached to the newly introduced 1-handle. We can also directly see this by noting that the cycle corresponding to the newly introduced 1-handle is a free generator in  $\pi_1(\tilde{\mathcal{M}})$ , therefore we can make handle moves such that no 2-handle touches the 1-handle. It is then straightforward to see that the partition function is invariant under the handle move just by inspecting Eq. (4.44). Namely, after replacing  $S^0 \times D^4$  by  $D^1 \times S^3$ ,  $N_4$  is decreased by 1 while  $N_1$  is increased by 1. Moreover, all other factors do not change. Therefore, the partition function  $\mathcal{Z}(\mathcal{M}, \mathcal{G})$  is invariant under the surgery move.

Therefore, we have established that the partition function  $\mathcal{Z}(\mathcal{M}, \mathcal{G})$  is invariant under  $G$ -bordism.

### 4.C.5 Invertibility

A TQFT is invertible if on every closed 4-manifold the partition function is a pure phase factor, and on every closed 3-manifold  $\mathcal{N}$  the associated vector space  $\mathcal{V}(\mathcal{N})$  is one-dimensional. We prove that Eq. (4.44) is indeed a pure phase factor on closed 4-manifolds, due to the cobordism invariance proved previously. To see it, first note that there is a  $\mathbb{Z}$  piece in  $\Omega_4^{SO}(BG)$  when  $G$  contains unitary symmetry only, the generator of which is  $\mathbb{C}\mathbb{P}^2$  with trivial  $G$ -bundle structure on it. Moreover, the partition function  $\mathcal{Z}(\mathbb{C}\mathbb{P}^2)$  is a pure phase factor (see Eq. (4.47)). If  $G$  is finite, besides the  $\mathbb{Z}$  piece in  $\Omega_4^{SO}(BG)$  when  $G$  contains

unitary symmetry only, all elements in the relevant bordism group are torsion elements. Accordingly, several copies of  $\mathcal{M}$  together with  $G$ -bundle structure  $\mathcal{G}$  on it have to be bordant to  $S^4$  with trivial  $G$ -bundle structure on it. Since  $\mathcal{Z}(S^4) = 1$  from Appendix 4.A.4, the norm of  $\mathcal{Z}(\mathcal{M}, \mathcal{G})$  has to be 1. This further means that the anomaly indicators we calculate have norm 1, which is not at all obvious from the explicit formulae, as given by, for example, Eqs. (4.50),(4.53),(4.55). Now we see that they actually take values only in  $\pm 1$ .

As a side remark, according to a theorem by Freed and Teleman from Ref. [126] (see footnote 10 therein), in order for a fully-extended TQFT to be invertible, we just need to prove that  $\mathcal{Z}(S^4)$  is nonzero and  $\mathcal{V}(S^1 \times S^2)$  as well as  $\mathcal{V}(S^3)$  are all 1-dimensional. They are all straightforward to check for the theory proposed in Sec. 4.2.2.

### 4.C.6 Generalization to connected Lie groups

In this sub-appendix, we generalize the consideration to connected Lie groups  $G$ , and prove that the partition function  $\mathcal{Z}(\mathcal{M}, \mathcal{G})$  in Eq. (4.65), defined on a target manifold  $\mathcal{M}$  together with a  $G$ -bundle structure  $\mathcal{G}$  on it with associated map  $f : \mathcal{M} \rightarrow BG$ , is a well-defined partition function as well. Given the results from the Crane-Yetter model, we just need to focus on  $\eta$ -factors, which greatly simplifies the analysis.

- Independence on the handle decomposition

In order to prove the independence of the partition function  $\mathcal{Z}(\mathcal{M}, \mathcal{G})$  on the handle decomposition, again we just need to show its invariance under all handle moves. Moreover, we also just need to focus on the handle moves that explicitly alter  $\eta$ -factors. Such handle moves contain 2-2 handle slides only, which are illustrated in Fig. 4.16.

Let us put anyon  $a$  on the red 2-handle and anyon  $b$  on the yellow 2-handle. Suppose that the yellow 2-handle corresponds to a 2-chain  $[h]$  of  $\mathcal{M}$ . Then if we fuse  $a$  and  $b$  into another anyon  $c$ , the extra  $\eta$ -factors for the red 2-handle and the yellow 2-handle become

$$M_{a, \mathbf{w}(f_*[h])} M_{b, \mathbf{w}(f_*[h])} = M_{c, \mathbf{w}(f_*[h])}, \quad (4.158)$$

consistent with the expression before the handle slide.

- Independence on the choice of  $f : \mathcal{M} \rightarrow BG$

The prescription to write down the  $\eta$ -factors explicitly uses a specific choice of  $f : \mathcal{M} \rightarrow BG$ . Yet two maps  $f : \mathcal{M} \rightarrow BG$  and  $\tilde{f} : \mathcal{M} \rightarrow BG$  that are homotopic to each other should give rise to a topologically equivalent bundle  $\mathcal{G}$ . Because  $f$  and  $\tilde{f}$  are homotopic to each other, for a 2-handle with its associated 2-chain  $[h]$ ,  $f_*[h]$  and  $\tilde{f}_*[h]$  should be related to each other by some 3-chain  $v$ , i.e.,  $f_*[h] = \tilde{f}_*[h] + \partial v$ . Therefore, given the symmetry fractionalization class  $\mathbf{w} \in \mathcal{H}^2(G, \mathcal{A})$ ,  $\mathbf{w}(f_*[h]) = \mathbf{w}(\tilde{f}_*[h])$  and  $\eta$ -factors are indeed independent of the specific choice of  $f : \mathcal{M} \rightarrow BG$ .

- Cobordism invariance

To prove that the partition function is a cobordism invariant, we also need to prove that the partition function  $\mathcal{Z}(\mathcal{M}, \mathcal{G})$  is invariant under the three surgery moves. Especially, the first surgery move, i.e., removing or adding an  $S^4$ , does not change the partition function because we can directly see from Eq. (4.65) that  $\mathcal{Z}(S^4, \mathcal{G}) = 1$ , no matter what  $G$ -bundle  $\mathcal{G}$  we put on  $S^4$ . The third surgery move does not involve any 2-handles. The second surgery move, i.e., replacing an  $S^1 \times D^3$  by  $S^2 \times D^2$  and vice versa, involves a 2-handle. Now consider  $S^2 \times \{pt\} \subset S^2 \times \partial(D^2) \cong S^2 \times S^1$ . Such an  $S^2$  lives on the boundary of  $D^3$  before the surgery, hence the  $G$ -bundle on this  $S^2$  can be thought of as trivial. Denoting the 2-chain associated to the 2-handle by  $[h]$ , we then see that  $f_*[h]$  is accordingly also trivial and thus no  $\eta$ -factor is involved. This argument is in a similar spirit to the argument presented in Appendix 4.C.4. Now we can carry over the proof of cobordism invariance in the Crane-Yetter model to prove cobordism invariance of  $\mathcal{Z}(\mathcal{M}, \mathcal{G})$  under the surgery moves.

- Invertibility

For torsion elements in  $\Omega_4^{SO}((BG)^{q-1})$ , cobordism invariance and the fact that  $\mathcal{Z}(S^4) = 1$  from Eq. (4.65) also dictate that the norm of the partition function  $\mathcal{Z}(\mathcal{M}, \mathcal{G})$  on such manifolds is 1. However, for a connected Lie group  $G$ , there can be many  $\mathbb{Z}$  pieces in  $\Omega_4^{SO}((BG)^{q-1})$  which do not correspond to  $\mathbb{C}\mathbb{P}^2$  with trivial  $G$ -bundle structure. We conjecture that partition functions of these manifolds according to the construction in Eq. (4.65) still have norm 1, but we do not have a direct proof (but see Appendix 4.C.5 for an argument based on properties of a fully-extended TQFT).

## 4.D Identifying the manifold $\mathcal{M}$ from bordism

In this appendix, we say more about which  $(3+1)D$  manifolds  $\mathcal{M}$  concern us, given a symmetry group  $G$  equipped with a  $\mathbb{Z}_2$  grading  $q : G \rightarrow \mathbb{Z}_2$  to denote anti-unitary elements as in Eq. (4.15).

First of all, the manifolds  $\mathcal{M}$  should be the generating manifolds of  $\Omega_4^{SO}((BG)^{q-1})$  [69, 98], which we define in detail below by identifying its tangential structure.

Let  $H$  be the tangential structure that concerns us, given the symmetry group  $G$  together with a  $\mathbb{Z}_2$  grading  $q$  to denote anti-unitary symmetries. Then for any integer  $n$  we have

$$\begin{array}{ccccccc} 1 & \longrightarrow & G/\mathbb{Z}_2 & \longrightarrow & H_n & \longrightarrow & O_n \longrightarrow 1 \\ & & \downarrow \cong & & \downarrow & & \downarrow \det \\ 1 & \longrightarrow & G/\mathbb{Z}_2 & \longrightarrow & G & \xrightarrow{q} & \mathbb{Z}_2 \longrightarrow 1 \end{array} \quad (4.159)$$

where  $\det$  denotes the determinant map. Here  $H$  is a nontrivial extension of  $O$  by  $G/\mathbb{Z}_2$ , and  $H_n \rightarrow G$  is the pullback of the determinant map  $\det : O_n \rightarrow \mathbb{Z}_2$  by the  $\mathbb{Z}_2$  grading  $q : G \rightarrow \mathbb{Z}_2$ . In this paper we use  $\Omega_4^{SO}((BG)^{q-1})$  to denote the bordism group with this tangential structure  $H$ .

An informative example is when  $G$  is  $\mathbb{Z}_4^T$  with the generator of  $\mathbb{Z}_4$  an anti-unitary symmetry. Then  $q : \mathbb{Z}_4^T \rightarrow \mathbb{Z}_2$  is just the projection from  $\mathbb{Z}_4$  to  $\mathbb{Z}_2$ . According to Eq. (4.159), we see that  $H$  is a nontrivial extension of  $O$  by  $\mathbb{Z}_2$ . But pay attention that  $H$  is not the same as  $\text{Pin}^+$  or  $\text{Pin}^-$ , because the extension for  $H$  corresponds to  $w_1^2$  in  $\mathcal{H}^2(O_n, \mathbb{Z}_2)$ , while the extension for  $\text{Pin}^+$  or  $\text{Pin}^-$  corresponds to  $w_2$  or  $w_2 + w_1^2$  in  $\mathcal{H}^2(O_n, \mathbb{Z}_2)$ , respectively. Accordingly, for  $G = \mathbb{Z}_4^T$  the manifold  $\mathcal{M}$  as the generator of the bordism group  $\Omega_4^{SO}((BG)^{q-1})$  should have  $w_1^2 = 0$ . It is also straightforward to see that when  $G$  is  $\mathbb{Z}_2^T \times \mathbb{Z}_2^T$ ,  $H$  is a trivial extension of  $O$  by  $\mathbb{Z}_2$ . Given  $\mathcal{H}^2(O_n, \mathbb{Z}_2) \cong \mathbb{Z}_2 \times \mathbb{Z}_2$ , we have listed all tangential structures associated to the four extensions of  $O_n$  by  $\mathbb{Z}_2$ .

From the right box in Eq. (4.159), we also see that  $H$ -tangential structure is equivalent to a  $(BG, q)$ -twisted orientation of  $\mathcal{M}$ , hence the notation  $\Omega_4^{SO}((BG)^{q-1})$ . Namely, to identify some  $H$ -structure on  $\mathcal{M}$ , we can first put a principal  $G$  bundle  $\mathcal{G}$  on  $\mathcal{M}$ . The map  $q : G \rightarrow \mathbb{Z}_2$  induces an associated 1-dimensional line bundle on  $\mathcal{M}$  that we denote by  $\xi$ , then we must have  $w_1(\xi) = w_1(\mathcal{M})$  and we need to choose an orientation of  $\xi \oplus T\mathcal{M}$ , where  $T\mathcal{M}$  is the tangent bundle of  $\mathcal{M}$ .

Secondly, it turns out that most elements in the group are “in-cohomology” in the following sense. When  $G$  only contains unitary symmetry,  $\Omega_4^{SO}(BG)$  contains a special  $\mathbb{Z}$  piece, generated by  $\mathbb{C}\mathbb{P}^2$ . When  $G$  also contains anti-unitary symmetry,  $\Omega_4^{SO}((BG)^{q-1})$  contains a special  $\mathbb{Z}_2$  piece, also generated by  $\mathbb{C}\mathbb{P}^2$ . The rest elements are (Pontraygin) dual to the image of the natural map from group cohomology to cobordism group, i.e.,

$$\mathcal{H}^4(BG, U(1)_q) \longrightarrow \Omega_{SO}^4((BG)^{q-1}), \quad (4.160)$$

where  $q$  as subscript of  $U(1)$  denotes the nontrivial  $G$  action on  $U(1)$  associated with  $q$ . Therefore, we call the  $\mathbb{Z}$  piece or  $\mathbb{Z}_2$  piece “beyond-cohomology”, while the rest piece “in-cohomology” [27].

Therefore, as an easier step to identify a complete list of  $(3+1)D$  manifolds needed for the calculation, first we calculate  $\mathcal{H}^4(BG, U(1)_q)$  and identify a set of generators  $\mathcal{O}_i$ . For  $G$  containing unitary symmetry only, we proceed by searching for some oriented manifold  $\mathcal{M}_i$  together with a map  $f_i : \mathcal{M}_i \rightarrow BG$  corresponding to some  $G$ -bundle for each  $i$ , such that  $f^*(\mathcal{O}_i)$  is dual to the fundamental cycle  $[\mathcal{M}_i] \in H_4(\mathcal{M}_i, \mathbb{Z})$ .

For  $G$  containing anti-unitary symmetry, we also need to search for some manifold  $\mathcal{M}_i$  together with a map  $f_i : \mathcal{M}_i \rightarrow BG$  corresponding to some  $G$ -bundle for each  $i$ , with the following two constraints:

1. The following diagram commute

$$\begin{array}{ccc}
 \mathcal{M}_i & \xrightarrow{f_i} & BG \\
 & \searrow w & \downarrow q \\
 & & B\mathbb{Z}_2
 \end{array} \tag{4.161}$$

where  $w$  is the map corresponding to the orientation bundle. In particular, we allow  $\mathcal{M}_i$  to be non-orientable.

2.  $f^*(\mathcal{O}_i)$  is dual to the twisted fundamental cycle  $[\mathcal{M}_i] \in H_4(\mathcal{M}_i, \mathbb{Z}_w)$  twisted by the orientation character  $w$  [69].

We call such a manifold  $\mathcal{M}_i$  (together with a  $G$ -bundle structure  $\mathcal{G}_i$  on it) a *representative manifold* of  $\mathcal{O}_i$ . Moreover, we also need  $\mathbb{C}\mathbb{P}^2$  for the “beyond-cohomology” piece of the bordism group.

Finally, we refer the reader to Ref. [92] for an algorithm to get the cellulation of the representative manifolds given a finite symmetry group  $G$ .

## 4.E More information about handle decomposition of manifolds

In this appendix, we give more information about the handle decomposition of various manifolds that appear in the main text, i.e., those manifolds listed in Table 4.1. More information about them can be found in Refs. [111, 112].

### 4.E.1 $\mathbb{C}\mathbb{P}^2$

Let us start with  $\mathbb{C}\mathbb{P}^2$ . The manifolds  $\mathbb{C}\mathbb{P}^n$  have a handle decomposition with  $n+1$  handles. There is one handle of each even index from 0 to  $2n$ . Such a decomposition for  $\mathbb{C}\mathbb{P}^n$  can be constructed as follows. Recall that each point  $p \in \mathbb{C}\mathbb{P}^n$  has homogeneous coordinates  $[z_0 : \cdots : z_n]$ ,  $z_i \in \mathbb{C}$ , which we can normalize so that  $\max_i |z_i| = 1$ . Let  $\mathcal{D}$  be the closed unit disk in  $\mathbb{C}$ , which is homeomorphic to  $D^2 = [-1, 1]^2$ . Then  $\mathbb{C}\mathbb{P}^n$  can be covered by  $n+1$  balls  $\mathcal{D}^n$  through the following map

$$\psi_i : \mathcal{D}^n \rightarrow \mathbb{C}\mathbb{P}^n, i = 0, \dots, n, \quad (4.162)$$

where

$$\psi_i(z_1, \dots, z_n) = [z_1 : \cdots : z_i : 1 : z_{i+1} : \cdots : z_n] \quad (4.163)$$

Let the image of  $\mathcal{D}^n$  under the map  $\psi_i$  be  $B_{2i}$ . Then  $p \in B_{2i}$  if and only if  $|z_i| = 1$ , and  $p \in \text{int } B_{2i}$  if and only if  $|z_j| < 1$  for all  $j \neq i$ . It follows immediately that the balls  $B_{2i}$  cover  $\mathbb{C}\mathbb{P}^n$ , and that they only intersect along their boundaries. Moreover,  $B_{2k}$  intersects  $\cup_{i < k} B_{2i}$  precisely on  $\psi_k(\partial(\mathcal{D}^k) \times \mathcal{D}^{n-k})$ . Therefore, we can interpret  $B_{2k}$  as a  $2k$ -handle attached to  $\cup_{i < k} B_{2i}$ , exhibiting the required handle decomposition.

Now specialize to  $\mathbb{C}\mathbb{P}^2$ . To draw the Kirby diagram as in Eq. (4.45) we just need to understand the appearance of the topological twist reflecting the self-intersection number  $+1$ . We can see the fact from the intersection form of  $\mathbb{C}\mathbb{P}^2$ , which is  $[+1]$ . We can also directly determine the attaching region of the 2-handle. A point  $p$  in  $B_0 \cap B_2$  can be written in two ways:  $p = \psi_0(w_1, w_2) = [1 : w_1 : w_2]$  and  $p = \psi_1(z_1, z_2) = [z_1 : 1 : z_2]$ . Comparing homogeneous coordinates, we find that  $w_1 = z_1^{-1}$  and  $w_2 = z_1^{-1}z_2$ , so  $\varphi(z_1, z_2) = (z_1^{-1}, z_1^{-1}z_2)$  defines the attaching map  $\varphi : \partial\mathcal{D} \times \mathcal{D} \rightarrow \partial\mathcal{D} \times \mathcal{D} \subset \partial B_0$ . Parametrize  $z_1 = e^{2\pi it}$ ,  $0 \leq t \leq 1$ , as we travel once around  $\partial\mathcal{D}$ ,  $t$  goes from 0 to 1 while the identification of the fibers ( $z_2 \mapsto e^{-2\pi it}z_2$ ) rotates once, realizing a generator of  $\pi_1(O(2)) \cong \mathbb{Z}$ . As a result, there is a  $+1$  framing of the 2-handle, reflecting the self-intersection number  $+1$ .

### 4.E.2 $\mathbb{R}\mathbb{P}^4$

The handle decomposition of manifolds  $\mathbb{R}\mathbb{P}^n$  is very similar to  $\mathbb{C}\mathbb{P}^n$ . The manifolds  $\mathbb{R}\mathbb{P}^n$  have a handle decomposition with  $n+1$  handles. There is one handle of each index from 0 to  $n$ . A decomposition for  $\mathbb{R}\mathbb{P}^n$  can be constructed from the construction of  $\mathbb{C}\mathbb{P}^n$  simply by changing  $\mathbb{C}$  to  $\mathbb{R}$  and  $\mathcal{D}$  to  $D$ . More specifically, recall that each point  $p \in \mathbb{R}\mathbb{P}^n$

has homogeneous coordinates  $[x_0 : \cdots : x_n]$ ,  $x_i \in \mathbb{R}$ , which we can normalize so that  $\max_i |x_i| = 1$ . Then  $\mathbb{R}P^n$  can be covered by  $n + 1$  balls  $D^n$  through the following map

$$\psi_i : D^n \rightarrow \mathbb{R}P^n, i = 0, \dots, n, \quad (4.164)$$

where

$$\psi_i(x_1, \dots, x_n) = [x_1 : \cdots : x_i : 1 : x_{i+1} : \cdots : x_n] \quad (4.165)$$

Let the image of  $D^n$  under the map  $\psi_i$  be  $B_i$ . Then we see that  $B_i$  as an  $i$ -handle is the required handle decomposition.

Now specialize to  $\mathbb{R}P^4$ . To draw the Kirby diagram as in Fig. 4.7 we need to determine the self-intersection number of the line reflecting the 2-handle. We can see this from the mod-2 intersection form of  $\mathbb{R}P^4$ , which is  $[+1]$ . We can also directly determine the attaching region of the 2-handle. A point  $p$  in  $\partial(D^2) \times D^2 \subset \partial B_2$  can be written as:  $p = \psi_2(x_1, x_2, x_3, x_4) = [x_1 : x_2 : 1 : x_3 : x_4]$  and either  $|x_1| = 1$ ,  $p \in \partial B_0$  or  $|x_2| = 1$ ,  $p \in \partial B_1$ . Comparing the fibre  $(x_3, x_4)$ , we see that when we travel along the boundary  $\partial(D^2)$ ,  $(x_3, x_4)$  changes sign twice after the identification. As a result, there is a  $+1$  framing of the 2-handle as well.

Notice that when attaching a 2-handle to a 1-handle, the framing may not be a well-defined integer because some isotopy involving the 1-handle may change the framing. But it is a well-defined integer mod-2 [112].

### 4.E.3 $\mathbb{R}P^3 \times S^1$

The handle decomposition of a product manifold  $\mathcal{A} \times \mathcal{B}$  is easy to achieve if we know the handle decomposition of  $\mathcal{A}$  and  $\mathcal{B}$  individually. In this way, we can get the handle decomposition of  $\mathbb{R}P^3 \times S^1$  and  $\mathbb{R}P^2 \times \mathbb{R}P^2$  that concerns us in this thesis.

For  $\mathbb{R}P^3 \times S^1$ , the handle decomposition of  $\mathbb{R}P^3$  has been worked out in Appendix 4.E.2, which consists of 1 0-handle, 1 1-handle, 1 2-handle and 1 3-handle, and the handle decomposition of  $S^1$  can just consist of 1 0-handle  $D^1$  and 1 1-handle  $D^1$  attached along the two end points. Therefore, the handle decomposition of  $\mathbb{R}P^3 \times S^1$  consists of 1 0-handle, 2 1-handle, 2 2-handle, 2 3-handle and 1 4-handle, and the Kirby diagram is drawn in Fig. 4.7. The blue 1-handle comes from the product of 0-handle of  $S^1$  and 1-handle of  $\mathbb{R}P^3$ , and the darkblue 1-handle comes from the product of 0-handle of  $\mathbb{R}P^3$  and 1-handle of  $S^1$ . The orange 2-handle comes from the product of 0-handle of  $S^1$  and 2-handle of  $\mathbb{R}P^3$ , and we can determine its framing either by mod-2 intersection form or from the Heegard



diagram of  $\mathbb{RP}^3$ . Finally, the red 2-handle comes from the product of 1-handle of  $S^1$  and 1-handle of  $\mathbb{RP}^1$ . The explicit ways of drawing the 2-handles on the Kirby diagram can be worked out by following closely the construction of the handle decomposition.

#### 4.E.4 $\mathbb{RP}^2 \times \mathbb{RP}^2$

The handle decomposition of  $\mathbb{RP}^2 \times \mathbb{RP}^2$  can be achieved in a similar manner to  $\mathbb{RP}^3 \times S^1$ . Specifically, the handle decomposition of  $\mathbb{RP}^2$  has been worked out in Appendix 4.E.2, which consists of 1 0-handle, 1 1-handle and 1 2-handle. Therefore, the handle decomposition of  $\mathbb{RP}^2 \times \mathbb{RP}^2$  consists of 1 0-handle, 2 1-handle, 3 2-handle, 2 1-handle and 1 4-handle, and the Kirby diagram is drawn in Fig. 4.10. The blue 1-handle and the red 2-handle come from one  $\mathbb{RP}^2$  piece while the darkblue 1-handle and the orange 2-handle come from the other  $\mathbb{RP}^2$  piece. There is another sanddune 2-handle, coming from the product of 2 1-handles of two  $\mathbb{RP}^2$  pieces. The explicit ways of drawing the 2-handles on the Kirby diagram can be worked out by following closely the construction of the handle decomposition.

# Chapter 5

## Emergibility of Symmetry-Enriched Quantum Criticality

Motivated by the study of quantum magnetism, we collect the results in Chapter 2 and Chapter 3 to study the emergibility of Stiefel Liquids in  $(2+1)$ -d lattice systems, utilizing the hypothesis of emergibility. We will focus on lattice systems with  $G_{UV} = G_s \times G_{int}$  symmetry, where  $G_s$  is  $p4m$  or  $p6m$ , and  $G_{int} = O(3)^T \equiv SO(3) \times \mathbb{Z}_2^T$ , the product of spin rotation and time reversal symmetries. We further demand that the PR type of the system correspond to half-integer spin, i.e., spinor under  $SO(3)$  while Kramers doublet under  $\mathbb{Z}_2^T$ , which implies that the  $(1+1)$ -d SPT related to the LSM constraints has a TPF  $\exp\left(i\pi \int_{M_2} (w_2^{SO(3)} + t^2)\right) = \exp\left(i\pi \int_{M_2} w_2^{O(3)^T}\right)$ . For the IR effective theory, we focus on DQCP, DSL, and the simplest non-Lagrangian SL, denoted by  $SL^{(7)}$ . We will exhaustively search SEP that can match the anomalies of these IR theories with the LSM anomalies on these lattices, assuming that the IR theories can emerge as a consequence of the competition between a magnetic state (a state that breaks the  $SO(3)$  spin rotational symmetry, e.g., a Neel state) and a non-magnetic state (an  $SO(3)$  symmetric state, e.g., a valance bond solid (VBS)). We will utilize the hypothesis of emergibility discussed in Section 1.3 to obtain various realizations.

This chapter is adapted from Ref. [1].

## 5.1 Methods of Calculation

The IR theory we want to analyze is SL proposed in Ref. [15] and discussed in Chapter 3. For the reader's convenience, first we collect the symmetry and anomaly of SLs relevant to our calculation. See Chapter 3 and Ref. [15] for more details.

The DOF of  $\text{SL}^{(N)}$  is represented by an  $N \times (N-4)$  matrix  $n$  with orthonormal columns. The symmetry  $G_{\text{IR}}$  of  $\text{SL}^{(N)}$  includes Poincaré symmetry and

$$\frac{O(N)^T \times O(N-4)^T}{\mathbb{Z}_2} \quad (5.1)$$

The  $O(N)$  acts as  $n \rightarrow Ln$  with  $L \in O(N)$ , and the  $O(N-4)$  acts as  $n \rightarrow nR$  with  $R \in O(N-4)$ . The superscript ‘‘T’’ represents the locking between an improper rotation of either  $O(N)$  or  $O(N-4)$  and a spacetime orientation reversal action. The  $\mathbb{Z}_2$  subgroup that is modded out is generated by  $(-I_N, -I_{N-4}) \in O(N) \times O(N-4)$  since they have no action on  $n$ .

The anomaly of  $\text{SL}^{(N)}$  is captured by  $\Omega_{\text{IR}}$ , an element in  $H^4(G_{\text{IR}}, \text{U}(1)_\rho)$ . It is useful to consider the projection from  $\tilde{G}_{\text{IR}} \equiv O(N)^T \times O(N-4)^T$  to  $G_{\text{IR}}$ , and the pullback of  $\Omega_{\text{IR}}$  induced by the projection is given by  $\tilde{\Omega}_{\text{IR}} = e^{i\pi \tilde{L}_{\text{IR}}} \in H^4(\tilde{G}_{\text{IR}}, \text{U}(1)_\rho)$ , where

$$\tilde{L}_{\text{IR}} = w_4^{O(N)} + w_4^{O(N-4)} + \left[ w_2^{O(N-4)} + \left( w_1^{O(N-4)} \right)^2 \right] \left( w_2^{O(N)} + w_2^{O(N-4)} \right) + \left( w_1^{O(N-4)} \right)^4 \quad (5.2)$$

supplemented with a constraint  $w_1^{TM} + w_1^{O(N)} + w_1^{O(N-4)} = 0 \pmod{2}$ , which originates from the locking condition. Here  $w_i^{O(N)}$ ,  $w_i^{O(N-4)}$  and  $w_i^{TM}$  are the  $i$ -th Stiefel-Whitney classes of the  $O(N)$ ,  $O(N-4)$  gauge bundles and the tangent bundle of the spacetime manifold, respectively. Again, for even  $N$ ,  $\tilde{\Omega}_{\text{IR}}$  misses some important information. Fortunately, it turns out that  $\tilde{\Omega}_{\text{IR}}$  is still adequate for the following discussion, even for the case with  $N = 6$  (see Appendix 5.A.2 and discussions below Eq. (5.44)). Below we will view  $\tilde{\Omega}_{\text{IR}}$  as the IR anomaly of SLs and omit the tilde symbol, i.e., we rewrite  $\tilde{\Omega}_{\text{IR}}$  and  $\tilde{L}_{\text{IR}}$  as  $\Omega_{\text{IR}}$  and  $L_{\text{IR}}$  for simplicity.

We are interested in the stability of these states in a specific lattice realization, whose symmetry is  $G_{\text{UV}}$ . Some perturbations that are not  $G_{\text{IR}}$ -symmetric can be  $G_{\text{UV}}$ -symmetric and drive the states unstable. For a realization to be stable, we demand that  $G_{\text{UV}}$  forbid all the relevant perturbations mentioned in Section 3.4 that change the emergent order of the state.

Now we sketch a streamlined method to check the emergibility condition Eq. (1.2), for a given symmetry embedding pattern (SEP)  $\varphi$ . This method crucially relies on the fact that  $H^4(G_{UV}, U(1)_\rho) = \mathbb{Z}_2^k$  with some  $k \in \mathbb{N}$ , which always holds if  $G_{UV} = G' \times \mathbb{Z}_2^T$  with some group  $G'$ . In our case,  $G' = G_s \times SO(3)$ . More generally, as long as  $G_{UV} = G' \times \mathbb{Z}_2^T$  for any  $G'$ , we expect this method to be useful in matching the LSM anomaly of a lattice system with the anomaly of any IR effective theories. This subsection is relatively formal and abstract, and readers more interested in the physical results can skip to the next section.

To motivate this method, first note that  $\Omega_{UV}$  and  $\varphi^*(\Omega_{IR})$  are elements in  $H^4(G_{UV}, U(1)_\rho)$ . To compare two elements in  $H^4(G_{UV}, U(1)_\rho)$ , generically we need a complete set of topological invariants (or some equivalents) for  $H^4(G_{UV}, U(1)_\rho)$ , which is often difficult to obtain. This difficulty comes from the fact that we are considering cohomology with  $U(1)$  coefficients.

Nevertheless, simplification occurs when  $G_{UV} = G' \times \mathbb{Z}_2^T$  and hence  $H^4(G_{UV}, U(1)_\rho) = \mathbb{Z}_2^k$  with some  $k \in \mathbb{N}$ . This enables us to connect  $\Omega_{UV}$  and  $\varphi^*(\Omega_{IR})$  to elements in  $H^*(G_{UV}, \mathbb{Z}_2)$ , which simplifies the analysis due to the salient features of cohomologies with  $\mathbb{Z}_2$  coefficients.

To see the connection to  $H^*(G_{UV}, \mathbb{Z}_2)$ , first recall that  $\Omega_{UV}$  takes the form of Eq. (2.1). We can view  $\lambda$  and  $\eta$  as elements in  $H^2(G_s, \mathbb{Z}_2)$  and  $H^2(G_{int}, \mathbb{Z}_2)$ , respectively. Then  $\lambda(l_1, l_2)\eta(a_3, a_4)$  is in fact the cup product  $\lambda \cup \eta$ <sup>1</sup>, which is an element in  $H^4(G_{UV}, \mathbb{Z}_2)$  that we denote by  $L_{UV}$ . As a group, here the group operation of two elements in  $H^4(G_{UV}, \mathbb{Z}_2)$  is realized as the mod 2 addition of the representative cochains of these elements, which take values in  $\mathbb{Z}_2 = \{0, 1\}$ . Then  $\Omega_{UV}$  can be written as  $e^{i\pi L_{UV}}$ , or more formally as  $\tilde{i}(L_{UV})$ , where  $\tilde{i}$  is a map induced by the inclusion  $i : \mathbb{Z}_2 \rightarrow U(1)$  introduced in Eq. (A.13). That is, the LSM anomaly  $\Omega_{UV}$  can be expressed as an image of an element  $L_{UV} \in H^4(G_{UV}, \mathbb{Z}_2)$  under  $\tilde{i}$ .<sup>2</sup>

Furthermore, there is an *injective* map from  $H^4(G_{UV}, U(1)_\rho)$  to  $H^5(G_{UV}, \mathbb{Z}_2)$ , given by  $\tilde{p} \circ \beta$ , i.e., the combination of the Bockstein homomorphism  $\beta : H^4(G_{UV}, U(1)_\rho) \rightarrow H^5(G_{UV}, \mathbb{Z}_\rho)$  and an injective map  $\tilde{p} : H^5(G_{UV}, \mathbb{Z}_\rho) \rightarrow H^5(G_{UV}, \mathbb{Z}_2)$  (see Appendix A.2 for a brief introduction of these maps). Here the fact that  $\tilde{p}$  is injective is again guaranteed by  $H^4(G_{UV}, U(1)_\rho) = \mathbb{Z}_2^k$ , which is crucial for this method. This means that checking Eq. (1.2) is equivalent to checking

$$(\tilde{p} \circ \beta)\Omega_{UV} = (\tilde{p} \circ \beta)\varphi^*(\Omega_{IR}) \quad (5.3)$$

<sup>1</sup>More specifically, the cross product  $\lambda \times \eta$ , defined in Eq. (A.23) in Appendix A.3.

<sup>2</sup>In fact, since  $G_{UV} = G' \times \mathbb{Z}_2^T$ , which implies that  $H^n(G_{UV}, U(1)_\rho) = \mathbb{Z}_2^k$  for any  $n \in \mathbb{N}$ , any element in  $H^n(G_{UV}, U(1)_\rho)$  can be written as the image of an element in  $H^n(G_{UV}, \mathbb{Z}_2)$  under  $\tilde{i}$ .

where both sides are elements in  $H^5(G_{UV}, \mathbb{Z}_2)$ .

Now we discuss the relevant simplifying features of cohomology with  $\mathbb{Z}_2$  coefficient. First, for any group  $G$ ,  $H^*(G, \mathbb{Z}_2)$  has a *ring structure*, where the addition is the mod 2 addition as above, and the multiplication between two elements is realized as their cup product. The entire cohomology ring  $H^*(G, \mathbb{Z}_2)$  can be presented by generators and relations, such that any of its elements can be written as sum of cup products of these generators, while the relations dictate that some sums are in fact the trivial element.

Moreover,  $H^*(G_s \times G_{int}, \mathbb{Z}_2) \cong H^*(G_s, \mathbb{Z}_2) \otimes H^*(G_{int}, \mathbb{Z}_2)$  for any  $G_s$  and  $G_{int}$ , which allows us to understand  $H^*(G_s \times G_{int}, \mathbb{Z}_2)$  by understanding  $H^*(G_s, \mathbb{Z}_2)$  and  $H^*(G_{int}, \mathbb{Z}_2)$  separately.

We are interested in the case with  $G_{int} = O(3)^T \equiv SO(3) \times \mathbb{Z}_2^T$ . The cohomology ring  $H^*(O(3)^T, \mathbb{Z}_2)$  is generated by the Stiefel-Whitney classes of  $O(3)^T$ , i.e.,  $w_1^{O(3)^T} \in H^1(O(3)^T, \mathbb{Z}_2)$ ,  $w_2^{O(3)^T} \in H^2(O(3)^T, \mathbb{Z}_2)$  and  $w_3^{O(3)^T} \in H^3(O(3)^T, \mathbb{Z}_2)$ , with no relation among the generators. Sometimes we also need to write  $H^*(O(3)^T, \mathbb{Z}_2)$  as  $H^*(SO(3), \mathbb{Z}_2) \otimes H^*(\mathbb{Z}_2^T, \mathbb{Z}_2)$ , where  $H^*(SO(3), \mathbb{Z}_2)$  is generated by the Stiefel-Whitney classes  $w_2^{SO(3)}$  and  $w_3^{SO(3)}$  of  $SO(3)$ , and  $H^*(\mathbb{Z}_2^T, \mathbb{Z}_2)$  is generated by  $t \in H^1(\mathbb{Z}_2^T, \mathbb{Z}_2)$ . These two sets of generators are related by

$$\begin{aligned} w_1^{O(3)^T} &= t \\ w_2^{O(3)^T} &= w_2^{SO(3)} + t^2 \\ w_3^{O(3)^T} &= w_3^{SO(3)} + tw_2^{SO(3)} + t^3 \end{aligned} \tag{5.4}$$

As for  $H^*(G_s, \mathbb{Z}_2)$ , we have calculated the  $\mathbb{Z}_2$  cohomology ring, i.e., the generators and relations, of all 17 wallpaper groups (see Appendix 2.D). It turns out that for all wallpaper groups  $G_s$  except  $p4g$ , all generators belong to  $H^1(G_s, \mathbb{Z}_2)$  and  $H^2(G_s, \mathbb{Z}_2)$ . For  $p4g$ , besides elements in  $H^1(p4g, \mathbb{Z}_2)$  and  $H^2(p4g, \mathbb{Z}_2)$ , another element in  $H^3(p4g, \mathbb{Z}_2)$  is also needed to form a complete set of generators.

The above observations motivate us to consider the following diagram, where each

rectangular sub-diagram is commuting <sup>3</sup>:

$$\begin{array}{ccccccc}
H^4(G_{\text{IR}}, \mathbb{Z}_2) & \overset{\tilde{i}}{\dashrightarrow} & H^4(G_{\text{IR}}, \text{U}(1)_\rho) & \xrightarrow{\beta} & H^5(G_{\text{IR}}, \mathbb{Z}_\rho) & \xrightarrow{\tilde{p}} & H^5(G_{\text{IR}}, \mathbb{Z}_2) \\
\downarrow \varphi^* & & \downarrow \varphi^* & & \downarrow \varphi^* & & \downarrow \varphi^* \\
H^4(G_{\text{UV}}, \mathbb{Z}_2) & \xrightarrow{\tilde{i}} & H^4(G_{\text{UV}}, \text{U}(1)_\rho) & \xrightarrow{\beta} & H^5(G_{\text{UV}}, \mathbb{Z}_\rho) & \xrightarrow{\tilde{p}} & H^5(G_{\text{UV}}, \mathbb{Z}_2)
\end{array} \tag{5.5}$$

From the commutativity of the diagram, checking Eq. (5.3) is equivalent to checking

$$\mathcal{S}Q^1(L_{\text{UV}}) = \varphi^*(\tilde{p} \circ \beta)(\Omega_{\text{IR}}) \tag{5.6}$$

in  $H^5(G_{\text{UV}}, \mathbb{Z}_2)$ , where

$$\mathcal{S}Q^1 \equiv \tilde{p} \circ \beta \circ \tilde{i}. \tag{5.7}$$

Some important properties and calculations of  $\mathcal{S}Q^1$  are given in Appendix A.4. Because of the salient features of cohomologies with  $\mathbb{Z}_2$  coefficients, checking Eq. (5.6) is expected to be simpler than directly checking Eq. (1.2) for a generic IR effective theory.

For SLs, a further simplification takes place since  $\Omega_{\text{IR}} = e^{i\pi L_{\text{IR}}} \in H^4(G_{\text{IR}}, \text{U}(1)_\rho)$  for SLs. Here  $L_{\text{IR}}$  can also be viewed as an element in  $H^4(G_{\text{IR}}, \mathbb{Z}_2)$ , in a way similar to  $L_{\text{UV}} \in H^4(G_{\text{UV}}, \mathbb{Z}_2)$ . Then  $\Omega_{\text{IR}}$  is the image of  $L_{\text{IR}}$  under the map  $\tilde{i} : H^4(G_{\text{IR}}, \mathbb{Z}_2) \rightarrow H^4(G_{\text{IR}}, \text{U}(1)_\rho)$ . Therefore, Eq. (5.6) becomes

$$\mathcal{S}Q^1(L_{\text{UV}}) = \varphi^*(\mathcal{S}Q^1(L_{\text{IR}})) \tag{5.8}$$

Below we will use this equation to check the emergibility of various SLs. We remark that to check Eq. (1.2), one may attempt to check if  $L_{\text{UV}} = \varphi^*(L_{\text{IR}})$ . However, since  $\tilde{i}$  is not injective, this is just a sufficient but unnecessary condition of Eq. (1.2). As we have checked,  $L_{\text{UV}} \neq \varphi^*(L_{\text{IR}})$  in many examples where Eq. (5.8) holds.

### 5.1.1 Example: anomaly matching for DQCP

To make this discussion more concrete, we showcase this method in a concrete example in detail (see Appendix 5.A for more examples, including an example in (1 + 1)-d).

---

<sup>3</sup>The reason to use dashed lines to connect the left corner of the diagram to the rest is because  $H^4(G_{\text{IR}}, \mathbb{Z}_2)$  is relevant in this analysis only for theories like SLs, where  $\Omega_{\text{IR}}$  is the image of an element in  $H^4(G_{\text{IR}}, \mathbb{Z}_2)$  under  $\tilde{i}$ . For a generic IR effective theory, the left corner is irrelevant to the analysis of anomaly-matching. See Appendix 5.A.1 for an IR effective theory (the  $SU(2)_1$  CFT) where this is the case.

Consider the classic realization of DQCP ( $SL^{(5)}$ ) on a square lattice [18, 19, 21]. For DQCP,  $G_{\text{IR}} = O(5)^T$  and Eq. (5.2) becomes

$$\Omega_{\text{IR}} \equiv \exp(i\pi L_{\text{IR}}) = \exp\left(i\pi w_4^{O(5)}\right). \quad (5.9)$$

In this realization,  $G_{\text{UV}} = p4m \times O(3)^T$  and the SEP  $\varphi$  reads [15, 21],

$$\begin{aligned} T_1 &\rightarrow \begin{pmatrix} -I_3 & & \\ & -1 & \\ & & 1 \end{pmatrix}, & T_2 &\rightarrow \begin{pmatrix} -I_3 & & \\ & 1 & \\ & & -1 \end{pmatrix}, \\ C_4 &\rightarrow \begin{pmatrix} I_3 & & \\ & & 1 \\ & -1 & \end{pmatrix}, & M &\rightarrow \begin{pmatrix} I_3 & & \\ & -1 & \\ & & 1 \end{pmatrix}, \\ O(3)^T &\rightarrow \begin{pmatrix} O(3)^T & & \\ & & \\ & & I_2 \end{pmatrix}, \end{aligned} \quad (5.10)$$

where  $I_k$  denotes the  $k \times k$  identity matrix. Note that the locking between the spacetime orientation reversals and improper rotations of  $O(5)$  is satisfied above. The LSM anomaly Eqs. (2.1) or (2.2) in this case can be written as

$$\Omega_{\text{UV}} \equiv \exp(i\pi L_{\text{UV}}) = \exp\left(i\lambda_1 w_2^{O(3)^T}\right) \quad (5.11)$$

where  $\lambda_1 \in H^2(p4m, \mathbb{Z}_2)$  triggers  $\alpha_1^{p4m}$  in Eq. (2.7), i.e., define  $\omega_1 \equiv \tilde{i}(\lambda_1) = e^{i\pi\lambda_1}$ , then  $\alpha_1^{p4m}[\omega_1] = -1$  while  $\alpha_i^{p4m}[\omega_1] = 1$  for  $i = 2, \dots, 6$ . As a concrete realization of the DQCP, Eq. (1.2) must hold. Below we check it by checking its equivalent form, Eq. (5.8).

According to Appendix A.2,

$$\mathcal{S}\mathcal{Q}^1(L_{\text{IR}}) = w_5^{O(5)}, \quad (5.12)$$

and

$$\mathcal{S}\mathcal{Q}^1(L_{\text{UV}}) = \lambda_1 w_3^{O(3)^T}, \quad (5.13)$$

where  $w_3^{O(3)^T} = w_3^{SO(3)} + t w_2^{SO(3)} + t^3$  and  $t \in H^1(\mathbb{Z}_2^T, \mathbb{Z}_2)$  corresponds to the gauge field of time reversal symmetry  $\mathbb{Z}_2^T$ , when pulled back to the spacetime manifold  $\mathcal{M}_4$ .

It remains to calculate the pullback  $\varphi^*(\mathcal{S}\mathcal{Q}^1(L_{\text{IR}}))$ . Since the embedding  $\varphi$  is block-diagonal with a  $3 \times 3$  block and a  $2 \times 2$  block, invoking the Whitney product formula,

$w_5^{O(5)} = w_3^{O(3)} w_2^{O(2)}$ <sup>4</sup>, we get

$$\varphi^* (\mathcal{SQ}^1(L_{\text{IR}})) = \varphi^* (w_3^{O(3)}) \cup \varphi^* (w_2^{O(2)}) \quad (5.14)$$

Hence we just need to calculate  $\varphi^*(w_3^{O(3)})$  and  $\varphi^*(w_2^{O(2)})$ . The calculation of  $\varphi^*(w_3^{O(3)})$  is straightforward,

$$\varphi^* (w_3^{O(3)}) = w_3^{SO(3)} + (t + A_{x+y}) w_2^{SO(3)} + (t + A_{x+y})^3, \quad (5.15)$$

where  $A_{x+y} \in H^1(p4m, \mathbb{Z}_2)$  corresponds to the sum of gauge fields of  $T_1$  and  $T_2$ , when pulled back to the spacetime manifold  $\mathcal{M}_4$  (see Appendix 2.D).

The pullback of  $w_2^{O(2)}$  needs more consideration. As  $\varphi^* (w_2^{O(2)}) \in H^2(p4m, \mathbb{Z}_2)$ , it is completely determined by its action on the 6 topological invariants identified in Eqs. (2.7) and (2.8), i.e.,  $\alpha_i^{p4m}[\omega]$  with  $\omega = \tilde{i}(\varphi^*(w_2^{O(2)}))$ , for  $i = 1, \dots, 6$ . To obtain  $\alpha_i^{p4m}[\omega]$ , consider the six  $\mathbb{Z}_2$  subgroups, denoted by  $\mathbb{Z}_2^{(i)}$  with  $i = 1, \dots, 6$ , generated by  $C_2, T_1 C_2, T_1 T_2 C_2, M, T_1 M$  and  $C_4 M$ , respectively. Their embedding into  $O(2)$  reads:

$$\begin{aligned} C_2 &\rightarrow \begin{pmatrix} -1 & \\ & -1 \end{pmatrix}, & T_1 T_2 C_2 &\rightarrow \begin{pmatrix} 1 & \\ & 1 \end{pmatrix} \\ T_1 C_2 &\rightarrow \begin{pmatrix} 1 & \\ & -1 \end{pmatrix}, & M &\rightarrow \begin{pmatrix} -1 & \\ & 1 \end{pmatrix} \\ T_1 M &\rightarrow \begin{pmatrix} 1 & \\ & 1 \end{pmatrix}, & C_4 M &\rightarrow \begin{pmatrix} & 1 \\ 1 & \end{pmatrix}. \end{aligned}$$

The pullback under the embedding  $\mathbb{Z}_2^{(i)} \rightarrow O(2)$  results in an element in  $H^2(\mathbb{Z}_2^{(i)}, \mathbb{Z}_2) = \mathbb{Z}_2$ , which is precisely detected by the topological invariant  $\alpha_i^{p4m}[\omega]$ . Calculating these six pullbacks via the Whitney product formula, we find  $\alpha_1^{p4m}[\omega] = -1$ , while other topological invariants are  $+1$ . Hence, we establish that<sup>5</sup>

$$\varphi^*(w_2^{O(2)}) = \lambda_1 \quad (5.16)$$

---

<sup>4</sup>Technically speaking, what we are doing is factorizing  $\varphi$  into an embedding  $\tilde{\varphi} : G_{\text{UV}} \rightarrow O(3) \times O(2)$  composed with an embedding  $\varphi_0 : O(3) \times O(2) \rightarrow O(5)$ . Then this equation should be thought of as the pullback of  $w_5^{O(5)}$  under  $\varphi_0$ , which can be proven by considering the diagonal  $\mathbb{Z}_2^5$  symmetry. In this thesis we will omit this fine detail for simplicity.

<sup>5</sup>In practice, to obtain this result, it suffices to only consider the  $pmm$  subgroup and  $\mathbb{Z}_2$  subgroup generated by  $C_4 M$ , as argued in Section 2.2.2. Since the embedding of  $pmm$  is also in the diagonal form, the calculation is as straightforward.



Finally, combining Eqs. (5.13-5.16) and  $\lambda_1 A_{x+y} = 0$ , a relation among the cohomology generators in  $H^*(p4m, \mathbb{Z}_2)$  (see Appendix 2.D), we establish that Eq. (5.8) indeed holds, as expected.

We mention that some previous works have performed anomaly-matching for this example, but some of them only did it by restricting both  $G_{UV}$  and  $G_{IR}$  to a few subgroups [38], and some used non-rigorous method [15]. To the best of our knowledge, the analysis above is the first that performs this anomaly-matching via a rigorous method, while keeping track of the full  $G_{UV}$  and  $G_{IR}$ . When checking emergibility below, we always maintain such completeness and rigor.

## 5.2 Deconfined quantum critical point and quantum critical spin liquids

With the formalism developed in the previous sections, we perform an exhaustive search of realizations of  $SL^{(N=5,6,7)}$  that can match certain LSM constraints on lattice spin systems with  $p6m \times O(3)^T$  or  $p4m \times O(3)^T$  symmetry, if this realization is adjacent to a magnetic state and a non-magnetic state (this means that the  $SO(3)$  symmetry acts on some but not all entries of  $n$ , the  $N \times (N - 4)$  matrix representing the DOF of  $SL^{(N)}$ ). This search can be efficiently done using a computer, and the complete results can be found in the attached codes [127] with the help of Appendix 5.B. The numbers of different types of realizations are in Table 5.1, where each row represents a distinct LSM constraint, or lattice homotopy class, labeled by the IWP that hosts half-integer spins (see Figs. 2.1 and 2.2 for the symbols of IWP), and 0 means there is no nontrivial LSM constraint, which applies to systems with integer-spin moments or honeycomb lattice half-integer spin systems. Note that for  $p4m$ , situations  $a$  and  $b$  always have the same number of realizations in each case, since they both correspond to square lattice half-integer spin systems and they are related to each other via a redefinition of the  $C_4$  center. However, these two situations should still be viewed as distinct, because they cannot be smoothly deformed into each other once the  $p4m$  symmetry is specified, which means, in particular, the  $C_4$  centers are fixed. The same holds for situations  $a\&c$  and  $b\&c$ . In terms of symmetry-enriched quantum criticality, we have found 12 different  $p6m \times O(3)^T$  symmetry-enriched DQCP,  $105 + 1 = 106$  different  $p6m \times O(3)^T$  symmetry-enriched DSL,  $705 + 14 = 719$  different  $p6m \times O(3)^T$  symmetry-enriched  $SL^{(7)}$ , 26 different  $p4m \times O(3)^T$  symmetry-enriched DQCP,  $372 + 1 = 373$  different  $p4m \times O(3)^T$  symmetry-enriched DSL, and  $3819 - 27 + 29 = 3821$  different  $p4m \times O(3)^T$  symmetry-enriched  $SL^{(7)}$ . The reason for subtracting 27 in the last case is explained at the

end of this section. Many of these realizations are unstable, in the sense that they require fine-tuning due to the existence of one or more microscopic symmetry allowed relevant operators (see Appendix 5.C for all stable realizations on various systems).

Below we present some interesting examples. To the best of our knowledge, none of these examples has been discussed before. When we discuss a realization of a SL, we will also comment on its nearby phases, which are often (but not always) some simple ordered states and relatively easy to detect. This provides useful guide for the search of an SL, since if such an ordered state can be found in a material or model, perturbing this ordered state may result in an SL. A smoking-gun signature of the SLs is their large emergent symmetries, which can manifest themselves in a set of singular correlation functions with the same critical exponent. Moreover, for all classical regular magnetic orders [128], i.e., classical magnetic orders in which any broken lattice symmetry can be compensated by a spin operation (see Appendix 5.D for their spin configurations), we identify the numbers of realizations of SLs adjacent to them (see Table 5.2).

In this section, we focus on realizations where the most relevant spinful excitations have spin-1. In particular, we describe examples of realizations of DQCP as a (pseudo-)critical point, which has a single relevant perturbation allowed by the microscopic symmetries, and stable realizations of DSL, which has no relevant perturbation allowed by the microscopic symmetries. For  $SL^{(7)}$ , we discuss a realization without symmetry-allowed relevant perturbation, and another example with a single symmetry-allowed relevant perturbation that nevertheless does not change the state. We view both realizations of  $SL^{(7)}$  as stable.

### 5.2.1 DQCP

It is known that there are two types of DQCPs proximate to classical regular magnetic orders [19], both are transitions from an anti-ferromagnetic state to a VBS state, i.e., the columnar VBS for square spin-1/2 systems [129, 130] and the Kekule VBS for honeycomb spin-1/2 systems [131]. Interestingly, we find another realization of DQCP on a honeycomb lattice spin-1/2 system, as a transition between a ferromagnetic state and a staggered VBS

$$G_s = p6m$$

spin-1/2 position	DQCP	DSL	SL <sup>(7)</sup>	DSL <sub>quad</sub>	SL <sub>quad</sub> <sup>(7)</sup>
0	10(2)	76(1)	453(0)	1(1)	12(2)
<i>a</i>	0	3(3)	41(8)	0	0
<i>c</i>	0	3(3)	35(9)	0	0
<i>a&amp;c</i>	2(1)	23(5)	176(2)	0	2(0)
total	12 (3)	105 (12)	705 (19)	1 (1)	14 (2)

$$G_s = p4m$$

spin-1/2 position	DQCP	DSL	SL <sup>(7)</sup>	SL <sub>incom</sub> <sup>(7)</sup>	DSL <sub>quad</sub>	SL <sub>quad</sub> <sup>(7)</sup>
0	19(0)	217(0)	1849(0)	2(0)	1(1)	22(4)
<i>a</i>	1(1)	23(3)	299(2)	3(2,1)	0	1(1)
<i>b</i>	1(1)	23(3)	299(2)	3(2,1)	0	1(1)
<i>c</i>	3(0)	56(4)	632(0)	2(2)	0	3(1)
<i>a&amp;b</i>	1(1)	22(0)	279(0)	11(11)	0	1(0)
<i>a&amp;c</i>	0	6(6)	117(6)	0	0	0
<i>b&amp;c</i>	0	6(6)	117(6)	0	0	0
<i>a&amp;b&amp;c</i>	1(1)	19(2)	227(0)	6(6)	0	1(0)
total	26 (4)	372 (24)	3819 (16)	27 (23,2)	1 (1)	29 (7)

Table 5.1: Numbers of realizations for DQCP, DSL and SL<sup>(7)</sup> in spin systems with a  $p6m$  (upper) or  $p4m$  (lower) lattice symmetry. Two realizations with symmetry actions related by a similarity transformation are considered as a single realization. The columns without (with) subscript “quad” represent realizations where the most relevant spinful excitations, i.e., the  $n$  modes that transform nontrivially under the  $SO(3)$  spin rotational symmetry, carry spin-1 (spin-2). No realization of DQCP has the  $n$  modes carrying spin-2. The numbers in parenthesis are the numbers of *stable* realizations. Here a stable DQCP means a realization that has a single relevant perturbation allowed by the microscopic symmetry, and a stable DSL, SL<sup>(7)</sup>, DSL<sub>quad</sub> and SL<sub>quad</sub><sup>(7)</sup> means a realization that has no relevant perturbation allowed by the microscopic symmetry. For all columns except SL<sub>incom</sub><sup>(7)</sup>, the  $n$  modes are at high-symmetry momenta in the Brillouin zone. For SL<sup>(7)</sup> realized on  $p4m$  symmetric lattices, there are realizations with some  $n$  modes at incommensurate momenta, and the column SL<sub>incom</sub><sup>(7)</sup> documents the numbers of families of these realizations, where each family includes infinitely many realizations labeled by a momentum, which continuously interpolate between two realizations in the column SL<sup>(7)</sup>. Two continuous families of realizations may share a common high-symmetry momentum, at which these two realizations turn out to be always distinct, in that symmetries other than translation are implemented distinctly. (23, 2) means that there are 23 families of realizations, such that as long as a given realization is in the “interiors” of the family (i.e., not all  $n$  modes are at high-symmetry momenta), the only symmetric relevant perturbation is the one that shifts the momenta of  $n$  modes, and there are 2 other families, such that this is still the case except at two exceptional points in the interior, where there is an additional symmetric relevant perturbation that changes the emergent order. The symmetry actions of the stable realizations are explicitly listed in *ReadMe.nb*.

Lattice	Colinear order	spin-1/2	spin-1
Triangular	F	0	2(1)
Kagome	F	0	2(1)
Honeycomb	F	2(1)	2(1)
	AF	2(1)	2(1)
Square	F	0	2(0)
	AF (Neel)	1(1)	2(0)

Lattice	Coplanar order	spin-1/2	spin-1
Triangular	120°	1(1)	3(0)
Kagome	$\mathbf{q} = 0$	1(1)	2(0)
	$\sqrt{3} \times \sqrt{3}$	0	3(0)
Honeycomb	V	3(0)	3(0)
Square	V	1(0)	3(0)
	Orthogonal	1(0)	1(0)

Lattice	Non-Coplanar order	spin-1/2	spin-1
Triangular	Tetrahedral	8(4)	2(0)
	F umbrella	1(0)	4(0)
Kagome	Octahedral	0	2(0)
	Cuboc1	3(2)	1(0)
	Cuboc2	4(3)	1(0)
	$\mathbf{q} = 0$ umbrella	2(1)	3(0)
	$\sqrt{3} \times \sqrt{3}$ umbrella	1(1)	4(0)
Honeycomb	Tetrahedral	2(0)	2(0)
	Cubic	1(0)	1(0)
Square	Tetrahedral umbrella	1 Incom	2(0)
	F umbrella	2(0)	2(0)

Table 5.2: Numbers of realizations for DQCP (top), DSL (middle) and  $SL^{(7)}$  (bottom) adjacent to some colinear, coplanar and non-coplanar magnetic orders, respectively, of triangular, kagome, honeycomb and square lattice spin-1/2 (or general half-integer-spin) systems (third column) and spin-1 (or general integer-spin) systems (fourth column). The numbers in parenthesis are the numbers of stable realizations (defined in the same way as in Table 5.1). F stands for Ferromagnetic while AF stands for Anti-ferromagnetic. “1 Incom” means that realizations of  $SL^{(7)}$  adjacent to tetrahedral umbrella order on the square lattice spin-1/2 systems belong to a continuous family of realizations, where the non-magnetic components of  $n$  can have continuously changing momenta. See Appendix 5.D for the spin configurations of these magnetic orders, and the attached code *ReadMe.nb* for the explicit symmetry actions.

state.<sup>6</sup> The symmetries are realized as

$$\begin{aligned}
T_{1,2} &: n \rightarrow n \\
C_6 &: n \rightarrow \begin{pmatrix} I_3 & & \\ & -\frac{1}{2} & \frac{\sqrt{3}}{2} \\ & -\frac{\sqrt{3}}{2} & -\frac{1}{2} \end{pmatrix} n \\
M &: n \rightarrow \begin{pmatrix} I_3 & & \\ & -1 & \\ & & 1 \end{pmatrix} n \\
O(3)^T &: n \rightarrow \begin{pmatrix} O(3)^T & & \\ & & \\ & & I_2 \end{pmatrix} n
\end{aligned} \tag{5.17}$$

The components of  $n$  can be identified with microscopic operators that transform identically under the above symmetries. Denote the microscopic spin-1/2 operator on the  $A$  and  $B$  sublattices as  $\mathbf{S}_A(\mathbf{r}) \equiv \mathbf{S}(\mathbf{r} + \frac{2\mathbf{T}_1 + \mathbf{T}_2}{3})$  and  $\mathbf{S}_B(\mathbf{r}) \equiv \mathbf{S}(\mathbf{r} + \frac{\mathbf{T}_1 - \mathbf{T}_2}{3})$ , respectively, where  $\mathbf{r}$  is the position of the  $C_6$  center of each unit cell, and  $\mathbf{T}_{1,2}$  is the translation vector of  $T_{1,2}$ . Then  $\mathbf{S}_{A,i}(\mathbf{r}) = \mathbf{S}_{B,i}(\mathbf{r}) \sim n_i$  for  $i = 1, 2, 3$ . Denote the dimer operators as  $D_x(\mathbf{r}) \equiv \mathbf{S}(\mathbf{r} + \frac{-\mathbf{T}_1 + \mathbf{T}_2}{3}) \cdot \mathbf{S}(\mathbf{r} + \frac{\mathbf{T}_1 + 2\mathbf{T}_2}{3})$ ,  $D_y(\mathbf{r}) \equiv \mathbf{S}(\mathbf{r} + \frac{\mathbf{T}_1 + 2\mathbf{T}_2}{3}) \cdot \mathbf{S}(\mathbf{r} + \frac{2\mathbf{T}_1 + \mathbf{T}_2}{3})$ , and  $D_z(\mathbf{r}) \equiv \mathbf{S}(\mathbf{r} + \frac{2\mathbf{T}_1 + \mathbf{T}_2}{3}) \cdot \mathbf{S}(\mathbf{r} + \frac{\mathbf{T}_1 - \mathbf{T}_2}{3})$ . Then  $D_x(\mathbf{r}) + e^{i\frac{2\pi}{3}} D_y(\mathbf{r}) + e^{i\frac{4\pi}{3}} D_z(\mathbf{r}) \sim e^{-i\frac{5\pi}{6}} (n_4 - in_5)$ . So  $n_{1,2,3}$  and  $n_{4,5}$  can be identified as the order parameters of a ferromagnet and a stacked VBS, respectively. For examples below, one can perform similar analysis to identify components of  $n$  with microscopic operators, but we will not explicitly showcase them.

Since this ferromagnetic DQCP is the simplest example of new states discovered using our approach, it will be reassuring to also have a traditional parton-based construction [7]. Indeed this DQCP can be constructed using Schwinger bosons  $\mathbf{S} = \frac{1}{2} b_\alpha^\dagger \boldsymbol{\sigma}_{\alpha\beta} b_\beta$ , where the bosonic spinons  $b_\alpha$  couple to a dynamical U(1) gauge field  $a_\mu$ . To realize the staggered VBS, we put the Schwinger bosons into the “featureless Mott insulator” discussed in Ref. [47] – effectively this state is constructed by putting a spin-singlet, gauge-charge  $Q = 2$  spinon “Cooper pair” at each  $C_6$  center. When coupled to the dynamical U(1) gauge field, the monopole operator acquires nontrivial lattice symmetry quantum numbers due to the charged insulating background. For example, the gauge charge  $Q = 2$  at each  $C_6$  rotation center gives the monopole a  $C_6$  angular momentum  $e^{i2\pi/3}$  from the Aharonov-Bohm effect. Other lattice symmetry quantum-numbers can be analyzed in a similar fashion, following methods developed in Ref. [81]. It turns out that the monopole carries exactly the symmetry

---

<sup>6</sup>Due to the fact that a fully polarized ferromagnetic state is always an exact eigenstate of any  $SO(3)$  symmetric Hamiltonian, the ferromagnetic state immediately adjacent to this DQCP, which is partially polarized, must be separated from a fully polarized one by a level crossing, i.e., first-order transition.

quantum numbers of the staggered VBS. At low energies the monopole will spontaneously condense and confine the gauge theory, resulting in the staggered VBS phase. To access the magnetically ordered phase, we drive the spinons  $b_\alpha$  through an insulator-superfluid transition and Higgs the U(1) gauge field. The fact that  $b_\alpha$  do not carry any nontrivial projective representation in this construction means that they can be condensed without breaking any lattice symmetry, which means that the magnetically ordered phase obtained this way is a ferromagnet. The effective field theory at the phase transition is the standard (non-compact)  $CP^1$  theory for DQCP [18], described by an  $SU(2)$ -fundamental complex Wilson-Fisher boson coupled to a dynamical U(1) gauge field  $a_\mu$ .

We remark that, compared to the standard DQCP realization where the magnetic side is anti-ferromagnetic, in this realization there is one more perturbation that is likely irrelevant at the transition, but relevant in the ferromagnetic phase and responsible for making the dispersion of the magnon quadratic. In the  $CP^1$  formulation of the DQCP with Schwinger bosons  $b$  [18, 19], this operator is  $(ib^\dagger \boldsymbol{\sigma} \partial_t b) \cdot (b^\dagger \boldsymbol{\sigma} b)$ . In the  $CP^N$  generalization of this theory, this operator is indeed dangerously irrelevant in the large- $N$  limit.

The simple nature of the magnetic and VBS phases here suggests that this DQCP may be realizable in relatively simple spin models. It will be interesting to find a sign-problem-free lattice model and simulate this transition with the quantum Monte Carlo approach.

### 5.2.2 DSL

DSLs have been constructed for various lattices using the parton construction. There are two widely studied DSLs: one is on the kagome lattice spin-1/2 system proximate to the  $\mathbf{q} = 0$  coplanar magnetic order [24, 132–135]; the other is on the triangular spin-1/2 lattice proximate to the  $120^\circ$  coplanar order [81, 83, 136–140]. On the other hand, the previously constructed DSLs on the honeycomb and square lattices are unstable due to the presence of  $G_{UV}$ -symmetric monopole (i.e., the  $n$  modes) [81, 83, 141, 142]. Interestingly, we find new stable DSLs on square and honeycomb lattices. Our complete classification also shows that there is no DSL proximate to the  $\sqrt{3} \times \sqrt{3}$  coplanar order on the kagome spin-1/2 system.

For the honeycomb lattice spin-1/2 system, the symmetries act as:

$$\begin{aligned}
T_{1,2} : n &\rightarrow \begin{pmatrix} I_3 & & & \\ & -\frac{1}{2} & \frac{\sqrt{3}}{2} & \\ & -\frac{\sqrt{3}}{2} & -\frac{1}{2} & \\ & & & 1 \end{pmatrix} n \\
C_6 : n &\rightarrow \begin{pmatrix} I_3 & & & \\ & 1 & & \\ & & -1 & \\ & & & -1 \end{pmatrix} n \begin{pmatrix} \frac{1}{2} & -\frac{\sqrt{3}}{2} \\ \frac{\sqrt{3}}{2} & \frac{1}{2} \end{pmatrix} \\
M : n &\rightarrow \begin{pmatrix} I_3 & & & \\ & -1 & & \\ & & -1 & \\ & & & 1 \end{pmatrix} n \begin{pmatrix} -1 & \\ & 1 \end{pmatrix} \\
O(3)^T : n &\rightarrow \begin{pmatrix} O(3)^T & \\ & I_3 \end{pmatrix} n
\end{aligned} \tag{5.18}$$

The magnetic order adjacent to this DSL is a regular magnetic order, i.e., a magnetic order in which any broken lattice symmetry can be compensated by a spin operation [128]. However, the magnetic order here appears missing in the classification in Ref. [128], which is possibly because all magnetic orders in Ref. [128] are assumed to be realizable by product states. It is known that some SRE states in a honeycomb lattice spin-1/2 system cannot be realized by product states, so we do not make this assumption [47–50]. This DSL should also be emergible in a triangular or kagome lattice integer-spin system. In these cases, the adjacent magnetic orders are also regular but not realizable by product states. See Ref. [143] for a recent study of these *entanglement-enabled symmetry-breaking orders*.

For the square lattice spin-1/2 system, the symmetries act as:

$$\begin{aligned}
T_1 : n &\rightarrow \begin{pmatrix} I_3 & & & \\ & -1 & & \\ & & 1 & \\ & & & -1 \end{pmatrix} n \begin{pmatrix} -1 & \\ & -1 \end{pmatrix}, \\
T_2 : n &\rightarrow \begin{pmatrix} I_3 & & & \\ & 1 & & \\ & & -1 & \\ & & & -1 \end{pmatrix} n \begin{pmatrix} -1 & \\ & -1 \end{pmatrix}, \\
C_4 : n &\rightarrow \begin{pmatrix} I_3 & & & \\ & & 1 & \\ & -1 & & \\ & & & 1 \end{pmatrix} n \begin{pmatrix} -1 & \\ & -1 \end{pmatrix}, \\
M : n &\rightarrow \begin{pmatrix} I_3 & & & \\ & 1 & & \\ & & -1 & \\ & & & -1 \end{pmatrix} n \begin{pmatrix} -1 & \\ & 1 \end{pmatrix}, \\
O(3)^T : n &\rightarrow \begin{pmatrix} O(3)^T & \\ & I_3 \end{pmatrix} n,
\end{aligned} \tag{5.19}$$

The magnetic order adjacent to this DSL is also an entanglement-enabled regular magnetic order.

One interesting aspect of these realizations is that all perturbations proportional to the entries of  $n$  are forbidden by symmetries, and the lack of this property is the reason why the previous constructions on these systems are unstable [81, 83, 141, 142]. This property implies that these realizations cannot be obtained as a descendent state of an  $SU(2)$  DSL [81], which is described by 2 flavors of Dirac fermions coupled to an emergent  $SU(2)$  gauge field (including the 2 colors, there are in total 4 Dirac fermions). To see it, note that the emergent symmetry of the  $SU(2)$  DSL is just  $O(5)^T$ , so if a U(1) DSL is its descendent, all microscopic symmetries will be embedded into the  $O(5)^T$  symmetry, which necessarily leaves some components of  $n$  symmetry-allowed. The previous constructions of the U(1) DSL on a square and honeycomb lattice spin-1/2 systems are indeed descendants of an  $SU(2)$  DSL, and it would be interesting to find a parton construction of our new realizations.





actions:

$$\begin{aligned}
T_1 : n &\rightarrow \begin{pmatrix} I_3 & & \\ & \exp(-i\sigma_y k) & \\ & & -I_2 \end{pmatrix} n \begin{pmatrix} -1 & & \\ & 1 & \\ & & -1 \end{pmatrix} \\
T_2 : n &\rightarrow \begin{pmatrix} I_3 & & \\ & -I_2 & \\ & & \exp(i\sigma_y k) \end{pmatrix} n \begin{pmatrix} 1 & & \\ & -1 & \\ & & -1 \end{pmatrix} \\
C_4 : n &\rightarrow \begin{pmatrix} I_3 & & & \\ & & 1 & \\ & & & 1 \\ & & & & 1 \\ & & & & & 1 \end{pmatrix} n \begin{pmatrix} & & 1 & \\ & & & 1 \\ & & & & 1 \\ & & & & & 1 \end{pmatrix} \\
M : n &\rightarrow \begin{pmatrix} I_3 & & & \\ & & 1 & \\ & & & 1 \\ & & & & 1 \\ & & & & & 1 \end{pmatrix} n \\
O(3)^T : n &\rightarrow \begin{pmatrix} O(3)^T & \\ & I_4 \end{pmatrix} n
\end{aligned} \tag{5.21}$$

where  $k \in [-\pi, \pi)$  is a generic momentum. The magnetic order adjacent to this realization is the tetrahedral umbrella order [128].

The above represents an infinite family of realizations, where the momenta of some  $n$  modes continuously change in the Brillouin zone. Among the relevant operators discussed in Sec. 3.4.3, there is only a single one allowed by the microscopic symmetries in this family of realizations, i.e., the  $SO(7)$  current  $\sim (n_{4i}\partial_x n_{5i} + n_{6i}\partial_y n_{7i})$ . We believe all these realizations can actually be smoothly connected without encountering a phase transition, so they all represent the same symmetry-enriched SL. This also imposes some constraints on the low-energy dynamics of  $SL^{(7)}$ , i.e., although the above  $SO(7)$  conserved current is relevant, it can merely shift the “zero momentum”, but not really change the state (see Appendix 3.A for more discussions).

### 5.3 Quantum critical spin-quadrupolar liquids

Besides the previous case, we also find realizations where the most relevant spinful excitations carry spin-2. We dub these states quantum critical spin-quadrupolar liquids.

We have identified an interesting realization of the DSL as a quantum critical spin-quadrupolar liquid. This realization can actually be realized on any lattice that has no nontrivial LSM constraint, including spin-1 systems on any lattice, spin-1/2 systems on honeycomb lattice, etc. If the lattice has a  $p6m$  or  $p4m$  symmetry, this is the only spin-quadrupolar realization of DSL. The lattice translation and rotation symmetries leave  $n$  invariant, and  $SO(3)$ , time reversal  $\mathcal{T}$  and lattice reflection  $M$  (if any) act as

$$\begin{aligned} SO(3) : n &\rightarrow \begin{pmatrix} \varphi_5(SO(3)) & \\ & 1 \end{pmatrix} n, \\ \mathcal{T} : n &\rightarrow \begin{pmatrix} I_5 & \\ & -1 \end{pmatrix} n \\ M : n &\rightarrow \begin{pmatrix} I_5 & \\ & -1 \end{pmatrix} n \end{aligned} \tag{5.22}$$

where  $\varphi_5(SO(3))$  represents the spin-2 representation of  $SO(3)$ . For this realization, if  $SO(3) \times \mathbb{Z}_2^T$  and an arbitrary lattice rotational symmetry are preserved, all relevant perturbations listed in Sec. 3.4.2 are forbidden. Even if only  $SO(3) \times \mathbb{Z}_2^T$  is preserved while all lattice symmetries are broken, the only symmetry-allowed relevant perturbations are the spatial components of the conserved current associated with the  $SO(2)$  emergent symmetry, which are expected to retain the emergent order (see Appendix 3.A). So this realization represents a rare example of quantum critical liquid that requires only internal symmetry (but not lattice symmetry) to be stable. The magnetic state adjacent to this DSL is a spin-quadrupolar order where the Goldstone modes are at the  $\Gamma$  point of the Brillouin zone. For the non-magnetic state, it is possible to have  $\langle n_{61} \rangle \neq 0$  while all other entries of  $n$  have zero expectation value. This is a spin-quadrupolar realization of the DQCP, and the only possible relevant perturbation is an  $SO(5)$  singlet that breaks time reversal, which may drive the system to forming a chiral spin liquid.

Usually, a DSL is constructed by fermionic partons that have a non-interacting mean field with 4 Dirac cones, which are coupled to an emergent  $U(1)$  gauge field. Below we show that the realization above cannot be constructed in this way, which may be its most interesting property.

To see it, let us consider how the Dirac fermions transform under the  $SO(3)$  spin rotational symmetry. Denote the Dirac fermion operator as  $\psi_i$  with  $i = 1, \dots, 4$ , which

transforms in the fundamental representation of the emergent  $SU(4)$  flavor symmetry. It is known that  $\bar{\psi}_i\psi_j - \frac{1}{4}\bar{\psi}\psi\delta_{ij}$ , which is the fermion mass in the  $SU(4)$  adjoint representation, is identified with  $A_{i_1i_2}\epsilon_{j_1j_2}n_{i_1j_1}n_{i_2j_2}$ , with  $A$  and  $\epsilon$  an anti-symmetric  $6 \times 6$  and  $2 \times 2$  real matrix, respectively [15, 81, 83]. Because under  $SO(3)$  spin rotational symmetry, part of the latter operators transforms in the spin-3 representation, the former operator must also contain components in the spin-3 representation, which implies that the Dirac fermions must transform in the spin-3/2 representation of the  $SO(3)$  symmetry, i.e., all 4 flavors of Dirac fermions together form this spin-3/2 object.

Now suppose this state can be realized by a *non-interacting* parton mean field with 4 Dirac cones (coupled to an emergent  $U(1)$  gauge field), the mean-field Hamiltonian of the partons must have an *on-site*  $U(4)$  symmetry. In the presence of this  $U(4)$  and time reversal symmetries, there must be at least 8 Dirac cones in the mean field. To see it, it suffices to consider one of the 4 flavors, whose mean field has on-site  $U(1)$  and time reversal symmetries. To avoid the parity anomaly, there are necessarily an even number of Dirac cones. So taken 4 flavors together, there are at least 8 Dirac cones, which contradicts our starting point, i.e., the mean field has only 4 Dirac cones.

The above argument shows that this realization is beyond the simplest parton mean fields. However, it is still possible to realize it if the partons are strongly interacting (even without considering their coupling to the emergent gauge field), so that at low energies 4 flavors of Dirac fermions emerge out of the strong interactions. This might be theoretically described, say, by a further parton decomposition of the partons themselves. This is possible because if besides time reversal the on-site symmetry is only  $SO(3)$  but not  $U(4)$ , there is no anomaly, and hence no contradiction with having 4 Dirac cones while realizing these symmetries in an on-site fashion.<sup>7</sup> It is an interesting challenge to find such a concrete construction in the future. This situation is similar to the Standard Model in particle physics: the Standard Model cannot be realized through lattice free fermions coupled to gauge fields due to fermion doubling, but it is believed to be realizable using strongly interacting fermions since all the quantum anomalies vanish [145–152].

Finally, we give an interesting realization of  $SL^{(7)}$  as a quantum critical spin-quadrupolar liquid, on a honeycomb lattice half-integer-spin system or any integer-spin system with  $p6m$

---

<sup>7</sup>One can in principle also try to implement some of these symmetries on the partons in a non-on-site fashion, but then it is challenging to have all on-site symmetries acting on the physical operators in an on-site fashion.

symmetry. The symmetries act as follows:

$$\begin{aligned}
SO(3) : n &\rightarrow \begin{pmatrix} \varphi_5(SO(3)) & & \\ & I_2 & \\ & & \end{pmatrix} n \\
\mathcal{T} : n &\rightarrow \begin{pmatrix} I_5 & & \\ & -1 & \\ & & 1 \end{pmatrix} n \\
T_1 : n &\rightarrow n \begin{pmatrix} -\frac{1}{2} & -\frac{\sqrt{3}}{2} & \\ \frac{\sqrt{3}}{2} & -\frac{1}{2} & \\ & & 1 \end{pmatrix} \\
T_2 : n &\rightarrow n \begin{pmatrix} -\frac{1}{2} & -\frac{\sqrt{3}}{2} & \\ \frac{\sqrt{3}}{2} & -\frac{1}{2} & \\ & & 1 \end{pmatrix} \\
C_6 : n &\rightarrow \begin{pmatrix} I_5 & & \\ & 1 & \\ & & -1 \end{pmatrix} n \begin{pmatrix} 1 & & \\ & -1 & \\ & & 1 \end{pmatrix} \\
M : n &\rightarrow \begin{pmatrix} I_5 & & \\ & -1 & \\ & & 1 \end{pmatrix} n
\end{aligned} \tag{5.23}$$

The nearby phases of this  $SL^{(7)}$  can be very interesting. It is possible to have  $\langle n_{73} \rangle \neq 0$  while all other entries of  $n$  have zero expectation value. This results in the spin-quadrupolar DSL (see Eq. (5.22)), except that the  $C_2 \equiv C_6^3$  symmetry is broken, while all other symmetries (including  $C_3 \equiv C_6^2$ ) are intact. We can also view the above realization of  $SL^{(7)}$  as an unnecessary phase transition in a  $p31m \times O(3)^T$  symmetric DSL phase. This DSL is still stable, but the  $n$  modes are at the  $\pm K$  points. It is also possible to have  $\langle n_{13} \rangle \neq 0$  while all other entries of  $n$  have zero expectation value, where our choice of basis is such that this condensation pattern breaks the  $SO(3)$  symmetry to  $U(1)$ . This results in a stable  $p6m \times \mathbb{Z}_2^T \times U(1)$  symmetric DSL that simultaneously has a spin-quadrupolar order. Again, the above realization of  $SL^{(7)}$  can be regarded as an unnecessary phase transition in a  $p6m \times \mathbb{Z}_2^T \times U(1)$  symmetric DSL phase.<sup>8</sup>

---

<sup>8</sup>Strictly speaking, the DSL states on the two sides of this  $SL^{(7)}$  are slightly different, since they have different quantum anomalies if the entire emergent symmetry is taken into account. In Ref. [15], these two DSLs are denoted by  $SL^{(6,1)}$  and  $SL^{(6,-1)}$ , respectively. However, if we only look at the remaining exact symmetries, there is no difference between them. Furthermore, even if the entire emergent symmetry is considered, all correlation functions in these two cases are simply related by a unitary transformation

## 5.4 Stability under symmetry breaking

In this section we demonstrate how to use the SEP to analyse the stability of these realizations under symmetry-breaking perturbations. As a concrete example, we focus on a realization of DSL on a triangular lattice spin-1/2 system that is perturbed by spin-orbit coupling (SOC), which may be relevant to NaYbO<sub>2</sub>. In Appendix 5.E, we give a few other examples of such analysis, which may be relevant to twisted bilayer WSe<sub>2</sub>, a recently realized quantum simulator for triangular lattice spin-1/2 models [153–155].

Without considering the SOC, the triangular lattice spin-1/2 system has a  $p6m \times O(3)^T$  symmetry, which acts on this DSL as:

$$\begin{aligned}
 T_1 : n &\rightarrow \begin{pmatrix} I_3 & & & \\ & 1 & & \\ & & -1 & \\ & & & -1 \end{pmatrix} n \begin{pmatrix} -\frac{1}{2} & -\frac{\sqrt{3}}{2} \\ \frac{\sqrt{3}}{2} & -\frac{1}{2} \end{pmatrix} \\
 T_2 : n &\rightarrow \begin{pmatrix} I_3 & & & \\ & -1 & & \\ & & 1 & \\ & & & -1 \end{pmatrix} n \begin{pmatrix} -\frac{1}{2} & -\frac{\sqrt{3}}{2} \\ \frac{\sqrt{3}}{2} & -\frac{1}{2} \end{pmatrix} \\
 C_6 : n &\rightarrow \begin{pmatrix} I_3 & & & \\ & 1 & & \\ & & 1 & \\ & & & -1 \end{pmatrix} n \begin{pmatrix} 1 & \\ & -1 \end{pmatrix} \\
 M : n &\rightarrow \begin{pmatrix} I_3 & & & \\ & & -1 & \\ & -1 & & \\ & & & 1 \end{pmatrix} n \\
 O(3)^T : n &\rightarrow \begin{pmatrix} O(3)^T & & & \\ & & & \\ & & & \\ & & & I_3 \end{pmatrix} n
 \end{aligned} \tag{5.24}$$

This realization was discussed in Refs. [15, 81, 83, 136–140], and it is shown in Appendix 5.A.2 that the anomaly-matching condition Eq. (1.2) is indeed satisfied. From this symmetry action, it is straightforward to check that all the relevant operators listed in Sec. 3.4.2 are symmetry-forbidden, so this realization is expected to be stable if the full  $p6m \times O(3)^T$  symmetry is preserved.

---

(which is not a symmetry of the DSL), so practically the DSL in the two sides can be viewed as in the same phase [15]. The same is true for the  $p31m \times O(3)^T$  symmetric DSL.

Recently, a quantum disordered liquid was reported in NaYbO<sub>2</sub> [156–160] (similar phenomena were reported in related materials including NaYbS<sub>2</sub> and NaYbSe<sub>2</sub> [161–165]). In particular, there is evidence that this state is gapless with a low-temperature specific heat scaling as temperature squared, and that it has a critical mode located at the  $\pm K$  points in the Brillouin zone, which are consistent with the above DSL realization. So it was proposed that a DSL may be realized in NaYbO<sub>2</sub>. However, due to SOC, the symmetry of NaYbO<sub>2</sub> is smaller than  $p6m \times O(3)^T$ , and an important question is whether there is symmetry-allowed relevant perturbation that would destabilize a DSL in NaYbO<sub>2</sub>.

NaYbO<sub>2</sub> is a layered material with space group symmetry  $R\bar{3}m$ . Restricted to a single layer, the remaining symmetries are [166]

$$T_{1,2}, C_6^* \equiv S_3 \cdot C_6, M^* \equiv S_M \cdot M, \mathcal{T} \quad (5.25)$$

where  $S_3$  and  $S_M$  act in the spin space:

$$\begin{aligned} S_3 : \begin{pmatrix} S_x \\ S_y \\ S_z \end{pmatrix} &\rightarrow \begin{pmatrix} -\frac{1}{2} & \frac{\sqrt{3}}{2} & \\ -\frac{\sqrt{3}}{2} & -\frac{1}{2} & \\ & & 1 \end{pmatrix} \begin{pmatrix} S_x \\ S_y \\ S_z \end{pmatrix} \\ S_M : \begin{pmatrix} S_x \\ S_y \\ S_z \end{pmatrix} &\rightarrow \begin{pmatrix} -\frac{1}{2} & \frac{\sqrt{3}}{2} & \\ \frac{\sqrt{3}}{2} & \frac{1}{2} & \\ & & -1 \end{pmatrix} \begin{pmatrix} S_x \\ S_y \\ S_z \end{pmatrix} \end{aligned} \quad (5.26)$$

with  $S_{x,y,z}$  the microscopic (effective) spin-1/2 operators.

Using Eq. (5.24), it is straightforward to extract the actions of the remaining symmetry Eq. (5.25), from which one can see that all relevant operators in Sec. 3.4.2 are still symmetry-forbidden. This means that the DSL can be stably realized on NaYbO<sub>2</sub>. Of course, whether NaYbO<sub>2</sub> actually realizes a DSL requires further investigation.

## 5.A More examples of the calculation of pullback

In this appendix, we give three more examples of the analysis of anomaly matching, for  $SU(2)_1$ , DSL and  $SL^{(7)}$ . In Appendix 5.A.4, we also provide relevant formula for the calculation of pullback involving 5-dimensional representation of  $SO(3)$ .

### 5.A.1 $SU(2)_1$ and emergent anomaly

First let us consider a representative  $(1+1)$ -d quantum critical state, i.e., the  $(1+1)$ -d  $SU(2)_1$  conformal field theory, which describes the spin-1/2 antiferromagnetic Heisenberg chain at low energies [167–169]. The IR symmetry of the theory is  $\frac{SU(2) \times SU(2)}{\mathbb{Z}_2} \rtimes \mathbb{Z}_2^T \cong O(4)$ .

Ref. [170] works out the anomaly term of  $SU(2)_1$  after gauging the  $SO(4)$  part of  $G_{\text{IR}} = O(4)$ , which corresponds to the interger Euler class of  $SO(4)$ ,  $e \in H^4(SO(4), \mathbb{Z})$ . The bulk topological partition function capturing this anomaly is the Chern-Simons theory at level  $(+1, -1)$  for the two  $su(2)$  factors of  $so(4) \cong su(2) \times su(2)$ , which can be written in terms of two  $su(2)$  gauge fields  $A^{(1)}, A^{(2)}$  as follows

$$S = \frac{i}{4\pi} \int \text{tr} \left( A^1 \wedge dA^{(1)} + \frac{2}{3} A^{(1)} \wedge A^{(1)} \wedge A^{(1)} \right) - \text{tr} \left( A^{(2)} \wedge dA^{(2)} + \frac{2}{3} A^{(2)} \wedge A^{(2)} \wedge A^{(2)} \right) \quad (5.27)$$

It is straightforward to inspect that after gauging the  $\mathbb{Z}_2^T$  part of  $G_{\text{IR}}$ , the anomaly term should correspond to the twisted Euler class of  $O(4)$ , and we denote it by  $\tilde{e} \in H^4(O(4), \mathbb{Z}_\rho)$ . Note that this anomaly does not correspond to any element in  $H^3(G_{\text{IR}}, U(1)_\rho)$ , i.e., the group cohomology (not the Borel cohomology in Ref. [26]) of  $G_{\text{IR}}$  acting nontrivially on the  $U(1)$  coefficient – this is the only example in this thesis where the Bockstein homomorphism in Eq. (A.18) is not an isomorphism. Hence we need some special care to write down the TPF of the bulk SPT theory.<sup>9</sup>

<sup>9</sup>In this footnote we briefly review how to write down the TPF worked out in Ref. [51]. Suppose a  $(2+1)$ -d IR theory has gauge symmetry  $G$  and is defined on the manifold  $\mathcal{M}_3$ , which serves as the base space of some principal bundle of  $G$ . Given an element  $\omega \in H^4(G, \mathbb{Z})$ , it is possible to define a 3d topological gauge theory of  $G$  as follows

$$S = \frac{1}{n} \left( \int_{\mathcal{B}_4} \Omega - \langle \gamma^* \omega, [\mathcal{B}_4] \rangle \right) \quad \text{mod } 1, \quad (5.28)$$

where  $\Omega$  is the de Rham representative of the image of  $\omega$  in  $H^4(BG, \mathbb{R})$ ,  $[\mathcal{B}_4] \in H_4(\mathcal{B}_4, \mathbb{Z})$  is the fundamental class of the manifold  $\mathcal{B}_4$  that bounds  $n$  copies of the manifold  $\mathcal{M}_3$  with some extension of the principle bundle of  $G$ , and  $\gamma$  is the classifying map of the extension. When  $\omega$  is a torsion element,  $\Omega = 0$ , and we retrieve the more familiar form of TPF

$$S = \langle \gamma^*(\beta^{-1}(\omega)), [\mathcal{M}_3] \rangle, \quad (5.29)$$

where  $\beta$  is the Bockstein homomorphism associated to the short exact sequence  $1 \rightarrow \mathbb{Z} \rightarrow \mathbb{R} \rightarrow U(1) \rightarrow 1$ . In particular, when  $G = SO(4)$  and  $\omega$  corresponds to the Euler class  $e$ ,  $\Omega$  can be explicitly written as follows,

$$\Omega = \frac{1}{8\pi^2} \left( \text{tr} \left( F^{(1)} \wedge F^{(1)} \right) - \text{tr} \left( F^{(2)} \wedge F^{(2)} \right) \right). \quad (5.30)$$



Consider the following homomorphism  $\varphi$  from  $G_{\text{UV}} = p1m \times O(3)$  to  $G_{\text{IR}} = O(4)$ ,

$$T \rightarrow \begin{pmatrix} -I_3 & \\ & -1 \end{pmatrix}, \quad M \rightarrow \begin{pmatrix} I_3 & \\ & -1 \end{pmatrix}, \quad O(3) \rightarrow \begin{pmatrix} O(3)^T & \\ & 1 \end{pmatrix} \quad (5.31)$$

The LSM anomaly of a 1D chain has been worked out in Appendix 2.F, i.e.,

$$\Omega_{\text{UV}} \equiv \exp(i\pi L_{\text{UV}}) = \exp\left(i\pi(x+m)w_2^{O(3)^T}\right). \quad (5.32)$$

We aim to prove that under the homomorphism  $\varphi$ , the pullback of the IR theory is the UV theory. Specifically, we need to prove that <sup>10</sup>

$$\beta(\Omega_{\text{UV}}) = \varphi^*(\tilde{e}), \quad (5.33)$$

where  $\beta$  is the Bockstein homomorphism associated to the short exact sequence  $1 \rightarrow \mathbb{Z} \rightarrow \mathbb{R} \rightarrow \text{U}(1) \rightarrow 1$ .

From the commutativity of the square in the diagram below

$$\begin{array}{ccccccc} & & & & H^4(G_{\text{IR}}, \mathbb{Z}_\rho) & \xrightarrow{\tilde{p}} & H^4(G_{\text{IR}}, \mathbb{Z}_2) \\ & & & & \downarrow \varphi^* & & \downarrow \varphi^* \\ H^3(G_{\text{UV}}, \mathbb{Z}_2) & \xrightarrow{\tilde{i}} & H^3(G_{\text{UV}}, \text{U}(1)_\rho) & \xrightarrow{\beta} & H^4(G_{\text{UV}}, \mathbb{Z}_\rho) & \xrightarrow{\tilde{p}} & H^4(G_{\text{UV}}, \mathbb{Z}_2) \end{array} \quad (5.34)$$

we just need to prove that

$$\mathcal{S}\mathcal{Q}^1(L_{\text{UV}}) = \varphi^*(\tilde{p}(\tilde{e})). \quad (5.35)$$

In particular, on the left hand side we have

$$\mathcal{S}\mathcal{Q}^1(L_{\text{UV}}) = (x+m)w_3^{O(3)^T} \quad (5.36)$$

according to Appendix A.4, where  $w_3^{O(3)^T} = w_3^{SO(3)} + tw_2^{SO(3)} + t^3$  and  $t \in H^1(\mathbb{Z}_2^T, \mathbb{Z}_2)$  corresponds to the gauge field of time-reversal symmetry when pulled back to the spacetime manifold  $\mathcal{M}_3$ . On the right hand side we have  $\tilde{p}(\tilde{e}) = w_4^{O(4)}$ , and

$$\varphi^*\left(w_4^{O(4)}\right) = (x+m)\left(w_3^{SO(3)} + (t+x)w_2^{SO(3)} + (t+x)^3\right) \quad (5.37)$$

In the presence of anti-unitary symmetries, the manifold  $\mathcal{M}_3$  is assumed to be non-orientable. Then we have to choose  $\mathcal{B}_4$  to be non-orientable as well, and demand  $[\mathcal{B}_4] \in H^4(\mathcal{B}_4, \mathbb{Z}_w)$  to be the fundamental class of the non-orientable manifold  $\mathcal{B}_4$  twisted by the orientation character  $w$  [69].

<sup>10</sup>There are two terms in Eq. (5.28). The first term will become 0 when pulled back to  $G_{\text{UV}}$ , which can be explicitly checked by considering the diagonal embedding of the Lie-algebra of  $so(3) \cong su(2)$  into  $so(4) \cong su(2) \times su(2)$ . Then we just need to consider the pullback of the second term.

Finally, using the cohomology relation  $x^2 = xm$ , we see that both sides are equal to each other. Hence we establish that the pullback of the anomaly of IR CFT  $SU(2)_1$  under the homomorphism  $\varphi$  as in Eq. (5.31) is the LSM anomaly of (1+1)-d spin chain.

Below we discuss the phenomenon of emergent anomalies. Following Ref. [38], by imposing an extra constraint  $T^2 = 1$ , we can factorize  $\varphi$  acting on  $p1m$  into two pieces, i.e., a projection  $p$  on  $\mathbb{Z}_2 \times \mathbb{Z}_2$  generated by  $\tilde{T}$  or  $M$ , where  $\tilde{T}$  acts trivially on  $U(1)$  or  $\mathbb{Z}$  while  $M$  acts nontrivially on  $U(1)$  or  $\mathbb{Z}$ , composed with an embedding  $\tilde{\varphi}$  of the  $\mathbb{Z}_2 \times \mathbb{Z}_2$  into  $O(4)$ .

$$\varphi = \tilde{\varphi} \circ p : \quad p1m = \mathbb{Z} \rtimes \mathbb{Z}_2 \xrightarrow{p} \mathbb{Z}_2 \times \mathbb{Z}_2 \xrightarrow{\tilde{\varphi}} O(4) \quad (5.38)$$

With slight abuse of notation, we denote the gauge field of  $\tilde{T}$  as  $x$  as well. Then we have

$$\begin{aligned} \tilde{\varphi}^* \left( w_4^{O(4)} \right) &= (x+m) \left( w_3^{SO(3)} + (t+x)w_2^{SO(3)} + (t+x)^3 \right) \\ &= \mathcal{S}\mathcal{Q}^1 \left( (x+m)w_2^{O(3)^T} + (x+m)x^2 \right) \end{aligned} \quad (5.39)$$

in  $H^4(\mathbb{Z}_2 \times \mathbb{Z}_2 \times O(3)^T, \mathbb{Z}_2)$ . According to the terminology in Ref. [38], the first term  $(x+m)w_2^{O(3)^T}$  as in Eq. (5.32) is the intrinsic anomaly, while the second term  $(x+m)x^2$  is identified as the emergent anomaly. The emergent anomaly should be absent when pulled back to  $p1m$ , which is guaranteed by the relation  $(x+m)x = 0$  present in  $p1m$ . As a sanity check, in the absence of mirror symmetry, i.e., in the line group  $p1$ , the intrinsic anomaly becomes  $xw_2^{O(3)^T}$  and the emergent anomaly becomes  $x^3$ , consistent with the example in Ref. [38].

We envision that similar emergent anomaly will be present in IR theories emerging from a 2d lattice system with wallpaper group  $G_s$ , because a lot of cohomology relations of  $G_s$  will be absent when projected to a finite group by imposing  $T_1^n = T_2^n = 1$  for some integer  $n$ . More precisely, write  $G_s = (\mathbb{Z} \times \mathbb{Z}) \rtimes O_s$ , if we can find an integer  $n$  such that  $\varphi : G_s \rightarrow G_{\text{IR}}$  factorizes as the composition of projection and another embedding

$$\varphi = \tilde{\varphi} \circ p : \quad G_s = (\mathbb{Z} \times \mathbb{Z}) \rtimes O_s \xrightarrow{p} \tilde{G}_s \equiv (\mathbb{Z}_n \times \mathbb{Z}_n) \rtimes O_s \xrightarrow{\tilde{\varphi}} G_{\text{IR}}, \quad (5.40)$$

then  $\tilde{\varphi}^*(\Omega_{\text{IR}}) \in H^4(\tilde{G}_s \times G_{\text{int}}, U(1)_\rho)$  will generically not be in the form of  $\exp(i\pi\lambda\eta)$  with  $\lambda \in H^2(\tilde{G}_s, \mathbb{Z}_2)$  and  $\eta \in H^2(G_{\text{int}}, \mathbb{Z}_2)$ , but contains a nonzero piece that nevertheless vanishes when pulled back to  $G_s$ , using certain cohomology relations of  $G_s$  that is not present in  $\tilde{G}_s$ . Specifically, when  $n = 2$ , of the 3 important relations displayed in Appendix 2.D, the first two relations, i.e.,  $x^2 = 0$  in  $p1$  and  $x^2 = xm$  in  $p1m$ , will be absent when

projected to  $\tilde{G}_s$ , while the third relation, i.e.,  $A_{x+y}A_m = 0$  in  $cm$ , will still be present when projected to  $\tilde{G}_s$ .

For example, when the IR effective theory is the DQCP emergent from a square lattice spin-1/2 system with wallpaper group  $p4m$ , we can choose  $n = 2$  and  $\tilde{G}_s = (\mathbb{Z}_2 \times \mathbb{Z}_2) \rtimes D_4$ . The  $\mathbb{Z}_2$  cohomology ring of  $\tilde{G}_s$  is

$$\mathbb{Z}_2[A_{x+y}, A_m, A_c, B_{xy}, B_{c^2}, B_{c(x+y)}] / (A_{x+y}A_c = 0, (A_m + A_c)A_c = 0, B_{c(x+y)}A_c = 0, B_{c(x+y)}(B_{c(x+y)} + A_{x+y}(A_m + A_c)) = (A_m^2 + A_c^2)B_{xy} + A_{x+y}^2B_{c^2}), \quad (5.41)$$

with the pullback of  $B_{c(x+y)}$  equal to  $A_{x+y}(A_{x+y} + A_m)$  in  $H^*(p4m, \mathbb{Z}_2)$ , and the pullback of  $A_{x+y}, A_m, A_c, B_{xy}, B_{c^2}$  their namesake. Then from the fact that the IR anomaly of DQCP corresponds to  $w_5^{O(5)} \in H^5(O(5), \mathbb{Z}_2)$ , we have

$$\begin{aligned} \tilde{\varphi}^* \left( w_5^{O(5)} \right) &= (B_{xy} + B_{c(x+y)} + B_{c^2}) \left( w_3^{SO(3)} + (t + A_{x+y})w_2^{SO(3)} + (t + A_{x+y})^3 \right) \\ &= \mathcal{S}\mathcal{Q}^1 \left( (B_{xy} + B_{c(x+y)} + B_{c^2}) w_2^{O(3)T} + (B_{xy} + B_{c(x+y)} + B_{c^2}) A_{x+y}^2 \right). \end{aligned} \quad (5.42)$$

The first term  $(B_{xy} + B_{c(x+y)} + B_{c^2}) w_2^{O(3)T}$  is again the intrinsic anomaly, while the second term  $(B_{xy} + B_{c(x+y)} + B_{c^2}) A_{x+y}^2$  is the emergent anomaly that vanishes when pulled back to  $G_s = p4m$ . This is a slight generalization of the result in Ref. [38] to the whole group  $p4m$ .

## 5.A.2 DSL

Next consider DSL [15, 81, 171], whose IR symmetry  $G_{\text{IR}}$  is  $\frac{O(6) \times O(2)}{\mathbb{Z}_2}$ , where an improper rotation of either  $O(6)$  or  $O(2)$  complex conjugates the  $U(1)$  coefficient of  $H^4(G_{\text{IR}}, U(1)_\rho)$ . The precise form of the anomaly term for  $G_{\text{IR}}$  is unknown, yet it is possible to write down its pullback to  $O(6) \times O(2)$  under the projection  $p : O(6) \times O(2) \rightarrow \frac{O(6) \times O(2)}{\mathbb{Z}_2}$  [15]

$$\begin{aligned} \tilde{\Omega}_{\text{IR}} &\equiv \exp(i\pi \tilde{L}_{\text{IR}}) \\ &= \exp \left[ i\pi \left( w_4^{O(6)} + w_2^{O(6)} \left( w_2^{O(2)} + (w_1^{O(2)})^2 \right) + \left( (w_2^{O(2)})^2 + w_2^{O(2)}(w_1^{O(2)})^2 + (w_1^{O(2)})^4 \right) \right) \right] \end{aligned} \quad (5.43)$$

where  $\tilde{L}_{\text{IR}} \in H^4(O(6) \times O(2), \mathbb{Z}_2)$ . On a triangular lattice, we consider the following example embedding  $\varphi$  of  $G_{\text{UV}} = p6m \times O(3)^T$  into  $G_{\text{IR}}$ ,

$$\begin{aligned}
T_1 : n &\rightarrow \begin{pmatrix} I_3 & & & \\ & 1 & & \\ & & -1 & \\ & & & -1 \end{pmatrix} n \begin{pmatrix} -\frac{1}{2} & -\frac{\sqrt{3}}{2} \\ \frac{\sqrt{3}}{2} & -\frac{1}{2} \end{pmatrix} \\
T_2 : n &\rightarrow \begin{pmatrix} I_3 & & & \\ & -1 & & \\ & & -1 & \\ & & & -1 \end{pmatrix} n \begin{pmatrix} -\frac{1}{2} & -\frac{\sqrt{3}}{2} \\ \frac{\sqrt{3}}{2} & -\frac{1}{2} \end{pmatrix} \\
C_6 : n &\rightarrow \begin{pmatrix} I_3 & & & \\ & 1 & & \\ & & 1 & \\ & -1 & & \end{pmatrix} n \begin{pmatrix} 1 & \\ & -1 \end{pmatrix} \\
M : n &\rightarrow \begin{pmatrix} I_3 & & & \\ & & -1 & \\ & -1 & & \\ & & & 1 \end{pmatrix} n \\
O(3)^T : n &\rightarrow \begin{pmatrix} O(3)^T & & & \\ & I_3 & & \end{pmatrix} n
\end{aligned} \tag{5.44}$$

Note that  $\varphi$  factorizes into an embedding  $\tilde{\varphi}$  into  $O(6) \times O(2)$  composed with the projection  $p$ , i.e.,  $\varphi = p \circ \tilde{\varphi}$ . In fact, for  $G_{\text{UV}} = G_s \times O(3)^T$  with any  $G_s$ , if  $\varphi$  satisfies the condition that some but not all entries of  $n$  are left invariant under  $SO(3)$ , then  $\varphi$  can always factorize into  $p \circ \tilde{\varphi}$ , where  $\tilde{\varphi}$  is a homomorphism from  $G_{\text{UV}}$  to  $O(6) \times O(2)$ . Therefore, we can think of the IR symmetry as  $O(6) \times O(2)$  for simplicity in the calculation of pullback. Moreover, we can always choose  $\tilde{\varphi}$  such that  $G_s$  acts as identity and  $\mathbb{Z}_2^T$  acts as minus identity in the block where  $SO(3)$  acts.

The LSM anomaly of a triangular lattice spin-1/2 system has been obtained in Appendix 2.D, and we repeat it here

$$\Omega_{\text{UV}} \equiv \exp(i\pi L_{\text{UV}}) = \exp\left(i\pi (B_{xy} + A_c(A_c + A_m)) w_2^{O(3)^T}\right), \tag{5.45}$$

where  $L_{\text{UV}} \in H^4(G_{\text{UV}}, \mathbb{Z}_2)$ . We wish to prove that  $\Omega_{\text{UV}} = \varphi^* \Omega_{\text{IR}}$ , which amounts to proving  $\Omega_{\text{UV}} = \tilde{\varphi}^* \tilde{\Omega}_{\text{IR}}$ . Again, from the commuting diagram Eq. (5.5) (with  $G_{\text{IR}}$  changed to  $O(6) \times O(2)$  and  $\varphi$  changed to  $\tilde{\varphi}$ ), we just need to prove that

$$\mathcal{S}\mathcal{Q}^1(L_{\text{UV}}) = \tilde{\varphi}^* \left( \mathcal{S}\mathcal{Q}^1(\tilde{L}_{\text{IR}}) \right). \tag{5.46}$$

According to Lemma A.4.1, we have

$$\begin{aligned} \mathcal{S}\mathcal{Q}^1(\tilde{L}_{\text{IR}}) = & w_5^{O(6)} + w_4^{O(6)} w_1^{O(2)} + w_3^{O(6)} \left( w_2^{O(2)} + (w_1^{O(2)})^2 \right) + w_2^{O(6)} (w_1^{O(2)})^3 \\ & + w_1^{O(6)} \left( (w_2^{O(2)})^2 + w_2^{O(2)} (w_1^{O(2)})^2 + (w_1^{O(2)})^4 \right) + \left( (w_2^{O(2)})^2 w_1^{O(2)} + (w_1^{O(2)})^5 \right). \end{aligned} \quad (5.47)$$

On the other hand,

$$\mathcal{S}\mathcal{Q}^1(L_{\text{UV}}) = ((B_{xy} + A_c(A_c + A_m)) w_3^{O(3)T}, \quad (5.48)$$

where  $w_3^{O(3)T} = w_3^{SO(3)} + t w_2^{SO(3)} + t^3$  and  $t \in H^1(\mathbb{Z}_2^T, \mathbb{Z}_2)$  corresponds to the gauge field of time-reversal symmetry when pulled back to the spacetime manifold  $\mathcal{M}_4$ .

What remains is the calculation of the pullback  $\tilde{\varphi}^* \left( \mathcal{S}\mathcal{Q}^1(\tilde{L}_{\text{IR}}) \right)$ , which is a straightforward application of the Whitney product formula. In particular, considering the  $O(2)$  block, the pullback gives

$$\begin{aligned} \tilde{\varphi}^* \left( w_1^{O(2)} \right) &= A_c \\ \tilde{\varphi}^* \left( w_2^{O(2)} \right) &= 0 \end{aligned} \quad (5.49)$$

On the other hand,  $O(6)$  factorizes into two  $3 \times 3$  blocks, and for the lower  $3 \times 3$  block we have

$$\begin{aligned} \tilde{\varphi}^* \left( w_1^{O(3)} \right) &= A_c + A_m \\ \tilde{\varphi}^* \left( w_2^{O(3)} \right) &= B_{xy} + A_c^2 \\ \tilde{\varphi}^* \left( w_3^{O(3)} \right) &= A_c B_{xy} + A_c^2 (A_c + A_m) \end{aligned} \quad (5.50)$$

Assembling the Stiefel-Whitney class of the lower  $O(3)$  and upper  $O(3)^T$  into the Stiefel-Whitney class of  $O(6)$ , we have

$$\begin{aligned} \tilde{\varphi}^* \left( w_5^{O(6)} \right) &= w_3^{O(3)T} (B_{xy} + A_c^2) + w_2^{O(3)T} (A_c B_{xy} + A_c^2 (A_c + A_m)) \\ \tilde{\varphi}^* \left( w_4^{O(6)} \right) &= w_3^{O(3)T} (A_c + A_m) + w_2^{O(3)T} (B_{xy} + A_c^2) + t (A_c B_{xy} + A_c^2 (A_c + A_m)) \\ \tilde{\varphi}^* \left( w_3^{O(6)} \right) &= w_3^{O(3)T} + w_2^{O(3)T} (A_c + A_m) + t (B_{xy} + A_c^2) + (A_c B_{xy} + A_c^2 (A_c + A_m)) \\ \tilde{\varphi}^* \left( w_2^{O(6)} \right) &= w_2^{O(3)T} + t (A_c + A_m) + (A_c B_{xy} + A_c^2 (A_c + A_m)) \\ \tilde{\varphi}^* \left( w_1^{O(6)} \right) &= t + (A_c + A_m) \end{aligned} \quad (5.51)$$

Combining Eqs. (5.47), (5.48), (5.49) and (5.51), indeed we get Eq. (5.46). Hence we establish that  $\Omega_{\text{UV}} = \varphi^* \Omega_{\text{IR}}$ .

### 5.A.3 $\text{SL}^{(7)}$

The next examples we want to consider are two realizations of  $N = 7$  Stiefel liquid, i.e.  $\text{SL}^{(7)}$ , proposed in Ref. [15] (see Sec. VII D therein). The IR symmetry  $G_{\text{IR}}$  of the theory is  $\frac{O(7) \times O(3)}{\mathbb{Z}_2}$ , and the precise form of the anomaly is given in Eq. (3.18) for  $N = 7$ . However, following the example in Appendix 5.A.2, for the sake of the analysis of anomaly-matching, we can again think of the IR symmetry as  $O(7) \times O(3)$  and consider the pullback of the anomaly under the projection  $p : O(7) \times O(3) \rightarrow \frac{O(7) \times O(3)}{\mathbb{Z}_2}$ ,

$$\begin{aligned} \tilde{\Omega}_{\text{IR}} &\equiv \exp(i\pi \tilde{L}_{\text{IR}}) \\ &= \exp\left(i\pi \left( w_4^{O(7)} + w_2^{O(7)} \left( w_2^{O(3)} + (w_1^{O(3)})^2 \right) + \left( (w_2^{O(3)})^2 + w_2^{O(3)}(w_1^{O(3)})^2 + (w_1^{O(3)})^4 \right) \right)\right) \end{aligned} \quad (5.52)$$

where  $\tilde{L}_{\text{IR}} \in H^4(O(7) \times O(3), \mathbb{Z}_2)$ . We will omit the tilde symbol in the following calculation.

On a triangular lattice, we consider the following embedding  $\varphi$  of  $G_{\text{UV}} = p6m \times O(3)^T$

into  $O(7) \times O(3)$ ,

$$\begin{aligned}
T_1 : n &\rightarrow \begin{pmatrix} I_3 & & & & & & \\ & -\frac{1}{2} & \frac{\sqrt{3}}{2} & & & & \\ & -\frac{\sqrt{3}}{2} & -\frac{1}{2} & & & & \\ & & & -\frac{1}{2} & \frac{\sqrt{3}}{2} & & \\ & & & -\frac{\sqrt{3}}{2} & -\frac{1}{2} & & \\ & & & & & & \\ & & & & & & \end{pmatrix} n \begin{pmatrix} 1 & & \\ & -1 & \\ & & -1 \end{pmatrix} \\
T_2 : n &\rightarrow \begin{pmatrix} I_3 & & & & & & \\ & -\frac{1}{2} & \frac{\sqrt{3}}{2} & & & & \\ & -\frac{\sqrt{3}}{2} & -\frac{1}{2} & & & & \\ & & & -\frac{1}{2} & \frac{\sqrt{3}}{2} & & \\ & & & -\frac{\sqrt{3}}{2} & -\frac{1}{2} & & \\ & & & & & & \\ & & & & & & \end{pmatrix} n \begin{pmatrix} -1 & & \\ & 1 & \\ & & -1 \end{pmatrix} \\
C_6 : n &\rightarrow \begin{pmatrix} I_3 & & & & & & \\ & 1 & & & & & \\ & & -1 & & & & \\ & & & 1 & & & \\ & & & & -1 & & \\ & & & & & & \\ & & & & & & \end{pmatrix} n \begin{pmatrix} & & 1 \\ 1 & & \\ & 1 & \end{pmatrix} \\
M : n &\rightarrow \begin{pmatrix} I_3 & & & & & & \\ & -1 & & & & & \\ & & -1 & & & & \\ & & & 1 & & & \\ & & & & 1 & & \\ & & & & & & \\ & & & & & & \end{pmatrix} n \begin{pmatrix} & & 1 \\ 1 & & \\ & & 1 \end{pmatrix} \\
O(3)^T : n &\rightarrow \begin{pmatrix} O(3)^T & & \\ & I_4 & \end{pmatrix} n
\end{aligned} \tag{5.53}$$

Again, the LSM anomaly of a triangular lattice spin-1/2 system is

$$\Omega_{UV} \equiv \exp(i\pi L_{UV}) = \exp\left(i\pi (B_{xy} + A_c(A_c + A_m)) w_2^{O(3)^T}\right), \tag{5.54}$$

where  $L_{UV} \in H^4(G_{UV}, \mathbb{Z}_2)$ . We wish to prove that  $\Omega_{UV} = \varphi^* \Omega_{IR}$ . From the commuting diagram Eq. (5.5), we just need to prove that

$$\mathcal{S}\mathcal{Q}^1(L_{UV}) = \varphi^* (\mathcal{S}\mathcal{Q}^1(L_{IR})). \tag{5.55}$$

According to Lemma A.4.1, we have

$$\begin{aligned}
\mathcal{S}\mathcal{Q}^1(L_{IR}) = & w_5^{O(7)} + w_4^{O(7)} w_1^{O(3)} + w_3^{O(7)} \left( w_2^{O(3)} + (w_1^{O(3)})^2 \right) + w_2^{O(7)} \left( w_3^{O(3)} + (w_1^{O(3)})^3 \right) \\
& + w_1^{O(7)} \left( (w_2^{O(3)})^2 + w_2^{O(3)} (w_1^{O(3)})^2 + (w_1^{O(3)})^4 \right) + \left( w_3^{O(3)} (w_1^{O(3)})^2 + (w_2^{O(3)})^2 w_1^{O(3)} + (w_1^{O(3)})^5 \right).
\end{aligned} \tag{5.56}$$

Also,

$$\mathcal{SQ}^1(L_{UV}) = ((B_{xy} + A_c(A_c + A_m)) w_3^{O(3)T}), \quad (5.57)$$

where  $w_3^{O(3)T} = w_3^{SO(3)} + t w_2^{SO(3)} + t^3$  and  $t \in H^1(\mathbb{Z}_2^T, \mathbb{Z}_2)$  corresponds to the gauge field of time-reversal symmetry when pulled back to the spacetime manifold  $\mathcal{M}_4$ .

What remains is the calculation of the pullback  $\varphi^*(\mathcal{SQ}^1(L_{IR}))$ , which is a straightforward application of the Whitney product formula. In particular,  $O(7)$  factorizes into one  $3 \times 3$  block and two  $2 \times 2$  block, and for the  $O(3)$  part and the  $O(7)$  part separately, the pullback gives

$$\begin{aligned} \varphi^*(w_1^{O(3)}) &= A_m, \\ \varphi^*(w_2^{O(3)}) &= B_{xy}, \\ \varphi^*(w_3^{O(3)}) &= 0, \\ \varphi^*(w_1^{O(7)}) &= t, \\ \varphi^*(w_2^{O(7)}) &= w_2^{SO(3)} + t^2 + A_c^2 + A_m^2 + A_m A_c, \\ \varphi^*(w_3^{O(7)}) &= (w_3^{SO(3)} + t w_2^{SO(3)} + t^3) + t(A_c^2 + A_m^2 + A_m A_c) + A_c A_m (A_c + A_m), \\ \varphi^*(w_4^{O(7)}) &= (w_2^{SO(3)} + t^2)(A_c^2 + A_m^2 + A_m A_c) + t A_c A_m (A_c + A_m), \\ \varphi^*(w_5^{O(7)}) &= (w_3^{SO(3)} + t w_2^{SO(3)} + t^3)(A_c^2 + A_m^2 + A_m A_c) + (w_2^{SO(3)} + t^2) A_c A_m (A_c + A_m), \end{aligned} \quad (5.58)$$

Substituting them back into Eq. (5.56), and using the cohomology relation  $B_{xy}^2 = B_{c^2} B_{xy}$ , indeed we get Eq. (5.57) as promised. Hence we establish that  $\Omega_{UV} = \varphi^* \Omega_{IR}$ .

On a Kagome lattice spin-1/2 system, we consider the following embedding  $\varphi$  of  $G_{UV} =$



$p6m \times O(3)^T$  into  $O(7) \times O(3)$ ,

$$\begin{aligned}
T_1 : n &\rightarrow n \begin{pmatrix} 1 & & \\ & -1 & \\ & & -1 \end{pmatrix} \\
T_2 : n &\rightarrow n \begin{pmatrix} -1 & & \\ & 1 & \\ & & -1 \end{pmatrix} \\
C_6 : n &\rightarrow \begin{pmatrix} I_3 & & & \\ & -1 & & \\ & & 1 & \\ & & & -1 & \\ & & & & -1 \end{pmatrix} n \begin{pmatrix} & & -1 \\ 1 & & \\ & 1 & \end{pmatrix} \\
M : n &\rightarrow \begin{pmatrix} I_3 & & & \\ & -1 & & \\ & & -1 & \\ & & & 1 \\ & & & & 1 \end{pmatrix} n \begin{pmatrix} & -1 & \\ -1 & & \\ & & 1 \end{pmatrix} \\
O(3)^T : n &\rightarrow \begin{pmatrix} O(3)^T & \\ & I_4 \end{pmatrix} n
\end{aligned} \tag{5.59}$$

The LSM anomaly of a Kagome lattice spin-1/2 system is

$$\Omega_{UV} \equiv \exp(i\pi L_{UV}) = \exp\left(i\pi B_{xy} w_2^{O(3)^T}\right). \tag{5.60}$$

Again, we wish to prove that  $\Omega_{UV} = \varphi^* \Omega_{IR}$  by proving  $\mathcal{S}Q^1(L_{UV}) = \varphi^*(\mathcal{S}Q^1(L_{IR}))$ .  $\mathcal{S}Q^1(L_{IR})$  is given in Eq. (5.56), while for  $\mathcal{S}Q^1(L_{UV})$  we have

$$\mathcal{S}Q^1(L_{UV}) = B_{xy} w_3^{O(3)^T}. \tag{5.61}$$

It is now straightforward to calculate the pullback of various Stiefel-Whitney classes in Eq.

(5.56),

$$\begin{aligned}
\varphi^* \left( w_1^{O(3)} \right) &= A_m + A_c \\
\varphi^* \left( w_2^{O(3)} \right) &= B_{xy} + A_c^2 \\
\varphi^* \left( w_3^{O(3)} \right) &= A_c^3 + A_c^2 A_m + A_c B_{xy} \\
\varphi^* \left( w_1^{O(7)} \right) &= t + A_c, \\
\varphi^* \left( w_2^{O(7)} \right) &= w_2^{SO(3)} + t^2 + t A_c + A_c^2 + A_c A_m + A_m^2, \\
\varphi^* \left( w_3^{O(7)} \right) &= \left( w_3^{SO(3)} + t w_2^{SO(3)} + t^3 \right) A_c + \left( w_2^{SO(3)} + t^2 \right) A_c + t \left( A_c^2 + A_c A_m + A_m^2 \right) + A_c^3, \\
\varphi^* \left( w_4^{O(7)} \right) &= \left( w_3^{SO(3)} + t w_2^{SO(3)} + t^3 \right) A_c + \left( w_2^{SO(3)} + t^2 \right) \left( A_c^2 + A_c A_m + A_m^2 \right) + t A_c^3 + A_c^2 A_m \left( A_c + A_m \right), \\
\varphi^* \left( w_5^{O(7)} \right) &= \left( w_3^{SO(3)} + t w_2^{SO(3)} + t^3 \right) \left( A_c^2 + A_c A_m + A_m^2 \right) + \left( w_2^{SO(3)} + t^2 \right) A_c^3 + t A_c^2 A_m \left( A_c + A_m \right).
\end{aligned} \tag{5.62}$$

Substituting them into (5.56) and using the cohomology relation  $B_{xy}^2 = B_c^2 B_{xy}$ , indeed we get Eq. (5.61), and thus establish that  $\mathcal{SQ}^1(L_{UV}) = \varphi^* (\mathcal{SQ}^1(L_{IR}))$ .

#### 5.A.4 Five dimensional representation of $SO(3)$

In all previous examples presented in this appendix, the  $SO(3)$  spin rotation symmetry is embedded into the IR symmetry  $G_{IR}$  as a 3 dimensional representation. It is natural to consider embedding involving other representations of  $SO(3)$ , whose physical relevance is illustrated in Section 5.3. In this sub-appendix, we present formula relevant to mapping  $SO(3)$  into  $G_{IR}$  as a 5 dimensional representation of  $SO(3)$ .

First consider the 5 dimensional representation  $\varphi_5 : SO(3) \rightarrow O(5)$  of  $SO(3)$  alone, which can be thought of as a symmetric traceless tensor  $V_5$ , whose 5 basis are

$$\begin{aligned}
&\frac{1}{\sqrt{2}} (n_1 \otimes n_2 + n_2 \otimes n_1), \quad \frac{1}{\sqrt{2}} (n_2 \otimes n_3 + n_3 \otimes n_2), \quad \frac{1}{\sqrt{2}} (n_3 \otimes n_1 + n_1 \otimes n_3), \\
&\frac{1}{\sqrt{2}} (n_2 \otimes n_2 - n_3 \otimes n_3), \quad \frac{1}{\sqrt{6}} (2n_1 \otimes n_1 - n_2 \otimes n_2 - n_3 \otimes n_3),
\end{aligned} \tag{5.63}$$

where  $n_{1,2,3}$  form an  $SO(3)$  vector. Consider the  $\mathbb{Z}_2^2$  subgroup of  $SO(3)$ , generated by  $\pi$ -rotations around the  $x$ - and  $y$ -axes, respectively. Using the above 5 basis, these two  $\pi$ -rotations are mapped into  $\text{diag}(-1, 1, -1, 1, 1)$  and  $\text{diag}(-1, -1, 1, 1, 1)$ , respectively, from which (or from the splitting principle [172]) we see that

$$\begin{aligned}
\varphi_5^* \left( w_2^{O(5)} \right) &= w_2^{SO(3)}, \quad \varphi_5^* \left( w_3^{O(5)} \right) = w_3^{SO(3)}, \\
\varphi_5^* \left( w_1^{O(5)} \right) &= 0, \quad \varphi_5^* \left( w_4^{O(5)} \right) = 0, \quad \varphi_5^* \left( w_5^{O(5)} \right) = 0
\end{aligned} \tag{5.64}$$

Now go back to  $G_{UV} = SO(3) \times \tilde{G}$  and consider a 5 dimensional representation  $\varphi_5 : G_{UV} \rightarrow O(5)$  that can be written as  $V_5 \otimes V_1$ , where  $V_5$  denotes the 5 dimensional representation of  $SO(3)$  while  $V_1$  denotes a 1 dimensional real representation of  $\tilde{G}$  corresponding to  $x \in H^1(\tilde{G}, \mathbb{Z}_2)$ . Again from inspecting the action of the diagonal  $\mathbb{Z}_2^2$  subgroup, we have

$$\begin{aligned}
\varphi_5^* \left( w_1^{O(5)} \right) &= x, \\
\varphi_5^* \left( w_2^{O(5)} \right) &= w_2^{SO(3)}, \\
\varphi_5^* \left( w_3^{O(5)} \right) &= w_3^{SO(3)} + x w_2^{SO(3)}, \\
\varphi_5^* \left( w_4^{O(5)} \right) &= x^2 w_2^{SO(3)} + x^4, \\
\varphi_5^* \left( w_5^{O(5)} \right) &= x^2 w_3^{SO(3)} + x^3 w_2^{SO(3)} + x^5.
\end{aligned} \tag{5.65}$$

## 5.B Strategy of exhaustive search of SEP and results

In this appendix, we briefly review our strategy of the exhaustive search of SEP. We also illustrate how to check all the SEPs from the *csv* data files we provide in the *Data\_and\_Codes* folder and the mathematica file *embedding.m*, which transforms the data in *csv* files into matrices representing generators  $C_6/C_4$ ,  $M$ ,  $T_1$ ,  $T_2$  and  $\mathcal{T}$ . Some interesting realizations have been shown in Sections 5.2 and 5.3.

In order to enumerate all SEPs that match LSM constraints with IR anomaly, we just need to enumerate all embeddings from  $G_{UV}$  to  $G_{IR}$  and, following Section 5.1 and Appendix 5.A, calculate the pullback  $\varphi^*(\Omega_{IR})$  to see if it is identical to  $\Omega_{UV}$  corresponding to a particular LSM constraint. Motivated by quantum magnetism, we assume that the IR theory will emerge as a consequence of the competition between a magnetic state and a non-magnetic state. Therefore, we only consider embeddings such that, in terms of the  $N \times (N - 4)$  matrix  $n$  for  $SL^{(N)}$ , some but not all entries of  $n$  transform under the  $SO(3)$  symmetry.

For DQCP, since the IR symmetry is  $O(5)$ , all embeddings are just composed of representations of  $G_{UV}$ . For DSL and  $SL^{(7)}$ , even though the IR symmetry is  $\frac{O(6) \times O(2)}{\mathbb{Z}_2}$  and  $\frac{O(7) \times O(3)}{\mathbb{Z}_2}$ , respectively, because of the constraints on the embeddings, it suffices to only consider embeddings into  $\frac{O(6) \times O(2)}{\mathbb{Z}_2}$  and  $\frac{O(7) \times O(3)}{\mathbb{Z}_2}$  which can be respectively lifted to an embedding into  $O(6) \times O(2)$  or  $O(7) \times O(3)$ , as discussed below Eq. (5.44). Therefore, all

embeddings we consider are just composed of real representations of  $G_{UV}$ . In other words, our task to specify an embedding becomes finding appropriate irreducible representations of  $G_{UV}$ , and fill them into the  $O(N)$  and  $O(N - 4)$  matrices in a block diagonal form.

Hence let us make a detour and discuss representations of  $G_{UV} = G_s \times SO(3) \times \mathbb{Z}_2^T$ . For any two groups  $G_{1,2}$ , an irreducible representation  $V$  of  $G_1 \times G_2$  is  $V_1 \otimes V_2$ , where  $V_{1,2}$  is an irreducible representation of  $G_{1,2}$ , respectively. So any irreducible representation  $V$  of  $G_{UV}$  takes the form of  $V = V_{SO(3)}^{2n+1} \otimes V_s \otimes V_T$ , where  $V_{SO(3)}^{2n+1}$  is a  $(2n + 1)$ -dimensional irreducible representation of  $SO(3)$  with  $n \in \mathbb{N}$ ,  $V_s$  is an irreducible representation of  $G_s$ , and  $V_T = \pm 1$  is an irreducible representation of  $\mathbb{Z}_2^T$ . The complete list of irreducible representations  $V_s$  of  $G_s$  can be found using the method of induced representations [173–175], and we provide complete lists of irreducible representations of  $p4m$  and  $p6m$  in the Mathematica file *Representation.nb*.

To figure out which representations of  $G_{UV}$  are relevant to our discussions, it is useful to analyze in which blocks the  $SO(3)$  can act nontrivially, with the assumption that some but not all entries of  $n$  transform under the  $SO(3)$  symmetry. For DQCP,  $SO(3)$  must act nontrivially in a 3-d block, while the rest 2-d block should be a reducible or irreducible representation of  $G_s \times \mathbb{Z}_2^T$ . That is, the relevant representation  $V$  of  $G_{UV}$  schematically takes the form

$$V_{\text{DQCP}} = \begin{pmatrix} \left( V_{SO(3)}^3 \otimes V_s^1 \otimes V_T^1 \right)^{3 \times 3} & \\ & \left( V_{SO(3)}^1 \otimes V_{G_s \times \mathbb{Z}_2^T}^2 \right)^{2 \times 2} \end{pmatrix}, \quad (5.66)$$

where  $V_s^1$  and  $V_T^1$  are 1-d representations of  $G_s$  and  $\mathbb{Z}_2^T$  respectively, and  $V_{G_s \times \mathbb{Z}_2^T}^2$  is a 2-d (reducible or irreducible) representation of  $G_s \times \mathbb{Z}_2^T$ .

For DSL, the block involving nontrivial  $SO(3)$  actions can be 3-d or 5-d, and it has to lie in  $O(6)$ . For  $SL^{(7)}$ , the block involving  $SO(3)$  should embed into  $O(7)$  and can be 3-d, 5-d or 6-d. The 6-d representation takes the form of  $V_{SO(3)} \otimes V_{G_s \times \mathbb{Z}_2^T}^2$ , where  $V_{SO(3)}$  is the 3-d representation of  $SO(3)$ , and  $V_{G_s \times \mathbb{Z}_2^T}^2$  involves either two 1-d representations of  $G_s \times \mathbb{Z}_2^T$  or one irreducible 2-d representation of  $G_s \times \mathbb{Z}_2^T$ . However, it turns out that it is impossible to match the anomaly with any LSM constraint in the presence of some 6-d block involving  $SO(3)$ . Therefore, for DSL and  $SL^{(7)}$ , we consider two cases, i.e., either  $SO(3)$  embeds as a 3-d representation, corresponding to deconfined quantum critical points or quantum critical spin liquids in Section 5.2, or as a 5-d representation, corresponding to quantum critical spin-quadrupolar liquids in Section 5.3.

For DSL and  $SL^{(7)}$ , we still have freedom to choose the lifting to  $O(6) \times O(2)$  or  $O(7) \times O(3)$ , and different embeddings into  $O(6) \times O(2)$  or  $O(7) \times O(3)$  may correspond to the

same embedding into  $\frac{O(6) \times O(2)}{\mathbb{Z}_2}$  or  $\frac{O(7) \times O(3)}{\mathbb{Z}_2}$ . For embeddings involving 3-d representation of  $SO(3)$ , we choose such that only  $\mathcal{T}$  acts in the  $3 \times 3$  block as  $-I_3$ , while  $G_s$  acts trivially in that block. That is, for DSL and  $SL^{(7)}$ , the relevant representations  $V$  of  $G_{UV}$  schematically take the form as follows

$$V_{\text{DSL}} = \left( \begin{array}{c} \left( V_{SO(3)}^3 \otimes 1_s \otimes (-1_T) \right)^{3 \times 3} \\ \left( V_{SO(3)}^1 \otimes V_{G_s \times \mathbb{Z}_2^T}^3 \right)^{3 \times 3} \end{array} \right) \times \left( V_{SO(3)}^1 \otimes V_{G_s \times \mathbb{Z}_2^T}^2 \right)^{2 \times 2} \quad (5.67)$$

and

$$V_{\text{SL}^{(7)}} = \left( \begin{array}{c} \left( V_{SO(3)}^3 \otimes 1_s \otimes (-1_T) \right)^{3 \times 3} \\ \left( V_{SO(3)}^1 \otimes V_{G_s \times \mathbb{Z}_2^T}^4 \right)^{4 \times 4} \end{array} \right) \times \left( V_{SO(3)}^1 \otimes V_{G_s \times \mathbb{Z}_2^T}^3 \right)^{3 \times 3} \quad (5.68)$$

where  $1_s$  is the 1-d trivial representation of  $G_s$ , and  $-1_T$  is the 1-d non-trivial representation of  $\mathbb{Z}_2^T$ . For embeddings involving 5-d representation of  $SO(3)$ , we choose such that both  $\mathbb{Z}_2^T$  and  $G_s$  act trivially in the  $5 \times 5$  block. That is, the relevant representations  $V$  of  $G_{UV}$  schematically take the form

$$V_{\text{DSL}} = \left( \begin{array}{c} \left( V_{SO(3)}^5 \otimes 1_s \otimes 1_T \right)^{5 \times 5} \\ \left( V_{SO(3)}^1 \otimes V_{G_s \times \mathbb{Z}_2^T}^1 \right)^{1 \times 1} \end{array} \right) \times \left( V_{SO(3)}^1 \otimes V_{G_s \times \mathbb{Z}_2^T}^2 \right)^{2 \times 2} \quad (5.69)$$

and

$$V_{\text{SL}^{(7)}} = \left( \begin{array}{c} \left( V_{SO(3)}^5 \otimes 1_s \otimes 1_T \right)^{5 \times 5} \\ \left( V_{SO(3)}^1 \otimes V_{G_s \times \mathbb{Z}_2^T}^2 \right)^{2 \times 2} \end{array} \right) \times \left( V_{SO(3)}^1 \otimes V_{G_s \times \mathbb{Z}_2^T}^3 \right)^{3 \times 3} \quad (5.70)$$

where  $1_s$  and  $1_T$  are 1-d trivial representations of  $G_s$  and  $\mathbb{Z}_2^T$ , respectively.

Having identified all possible embeddings, it is a straightforward exercise to calculate the pullback in each case following Section 5.1 and Appendix 5.A. We use *Mathematica* to automate the computation and store results in *csv* files in the ancillary folder [127]. For example, *data.csv* contains data for matching LSM constraints with IR anomaly of  $SL^{(N=5,6,7)}$  when  $SO(3)$  embeds into  $O(6)$  as a 3-d representation, while *dataSL5Rep.csv* contains data for matching LSM constraints of  $p4m$  with IR anomaly of  $SL^{(7)}$  when  $SO(3)$  embeds into  $O(7)$  as a 5-d representation. Moreover, for both  $p4m$  and  $p6m$ , there is a single embedding involving 5-d representation of  $SO(3)$  that can match IR anomaly of DSL, shown in Eq. (5.22), which actually matches IR anomaly with zero LSM constraint.

To read the embeddings, i.e., to read the explicit image of the generators  $C_4/C_6$ ,  $M$ ,  $T_1$ ,  $T_2$  and  $\mathcal{T}$  in  $G_{\text{IR}}$ , we provide a wrapper file *Embedding.m*. When  $SO(3)$  embeds into  $G_{\text{IR}}$  as a 3-d representation, it provides two functions

$$p4mPrintEmbedding[n\_Integer, lsm\_Integer, p\_Integer]$$

$$p6mPrintEmbedding[n\_Integer, lsm\_Integer, p\_Integer]$$

The arguments are  $n = 5, 6, 7$  corresponding to DQCP, DSL and  $SL^{(7)}$  respectively,  $lsm = 1, \dots, 8$  in  $p4m$  or  $lsm = 1, \dots, 4$  corresponding to a particular LSM constraint with the order shown in Table 5.1, and  $p$  corresponding to a position in the array for a particular embedding/realization. When  $SO(3)$  embeds into  $G_{\text{IR}}$  as a 5-d representation and the IR theory is  $SL^{(7)}$ , it also provides two functions

$$p4m5dPrintEmbedding[lsm\_Integer, p\_Integer]$$

$$p6m5dPrintEmbedding[lsm\_Integer, p\_Integer]$$

with similar arguments and output. Note that in this scenario for DQCP there is no realization, and for DSL there is a single realization in  $p4m$  or  $p6m$  shown in Eq. (5.22). For  $p4m$  and  $SL^{(7)}$ , it also provides a function

$$IncommensuratePrintEmbedding[lsm\_Integer, p\_Integer]$$

to check whether some embedding corresponds to an incommensurate order, and if it does, output the corresponding incommensurate embedding. An illustration of how to use these functions is provided in *ReadMe.nb*.

## 5.C Stable realizations on various lattice spin systems

In this appendix, we list all stable realizations of DQCP, DSL and  $SL^{(7)}$  on triangular, kagome, and square lattice half-integer spin systems, as well as those on  $p6m$ -anomaly-free systems (including honeycomb lattice half-integer spin systems and all integer-spin systems with  $p6m$  lattice symmetry) and  $p4m$ -anomaly-free systems (including all integer-spin systems with  $p4m$  lattice symmetry). For square lattice, we only list the realizations in lattice homotopy class with PR at the type-a IWP, from which the ones with PR at the type-b IWP can be obtained by redefining the  $C_4$  center. As in the main text, here a stable DQCP means a realization with only a single relevant perturbation allowed by microscopic symmetries, so that it can be realized as a generic (pseudo-)critical point. A stable DSL

means a realization with no relevant perturbation allowed by microscopic symmetries, so that it can be realized as a stable phase. A stable  $SL^{(7)}$  means a realization with either no relevant perturbation allowed by microscopic symmetries, or a single symmetry-allowed relevant perturbation that does not change the emergent order but only shifts the “zero momenta”, so that this realization can still be viewed as a stable phase. All stable realizations of these states, including those on lattice systems discussed here and also those on other lattice systems, are explicitly documented in *ReadMe.nb*.

### 5.C.1 Stable realizations of DQCP

On all these systems, there is a single new stable realization of DQCP, given by Eq. (5.17), adjacent to ferromagnetic order on triangular lattice, kagome lattice integer spin systems or honeycomb lattice half-integer/integer spin systems. There is a known stable realization of DQCP on the square lattice half-integer spin system, given by Eq. (5.10), adjacent to anti-ferromagnetic (Neel) order. There is another known stable realization of DQCP on  $p6m$ -anomaly-free system [19], adjacent to anti-ferromagnetic order on honeycomb lattice half-integer/integer spin systems, given by

$$\begin{aligned}
 T_{1,2} : n &\rightarrow \begin{pmatrix} I_3 & & \\ & -\frac{1}{2} & \frac{\sqrt{3}}{2} \\ & -\frac{\sqrt{3}}{2} & -\frac{1}{2} \end{pmatrix} n, & C_6 : n &\rightarrow \begin{pmatrix} -I_3 & & \\ & 1 & \\ & & -1 \end{pmatrix} n, \\
 M : n &\rightarrow \begin{pmatrix} -I_3 & & \\ & 1 & \\ & & 1 \end{pmatrix} n, & O(3)^T : n &\rightarrow \begin{pmatrix} O(3)^T & & \\ & & \\ & & I_2 \end{pmatrix} n
 \end{aligned} \tag{5.71}$$

These three are all stable realizations of DQCP.

### 5.C.2 Stable realizations of DSL

On  $p6m$ -anomaly-free systems, there is a single stable realization of DSL where the most relevant spin fluctuations carry spin-1, given by Eq. (5.18). On both  $p6m$ -anomaly-free systems and  $p4m$ -anomaly-free systems, there is also a single stable realization of DSL where the most relevant spinful fluctuations carry spin-2, given by Eq. (5.22). Below we discuss the other systems.

### Triangular lattice half-integer spin systems

On triangular lattice half-integer spin systems, there are 3 stable realizations of DSL. One of them is known [15, 81, 83, 136–140], given by Eq. (5.24), adjacent to  $120^\circ$  order. The other two have identical actions of  $T_{1,2}$ ,  $C_6$  and  $O(3)^T$ :

$$\begin{aligned}
 T_1 : n &\rightarrow \begin{pmatrix} I_3 & & & \\ & 1 & & \\ & & -1 & \\ & & & -1 \end{pmatrix} n, & T_2 : n &\rightarrow \begin{pmatrix} I_3 & & & \\ & -1 & & \\ & & 1 & \\ & & & -1 \end{pmatrix} n \\
 C_6 : n &\rightarrow \begin{pmatrix} I_3 & & & \\ & 1 & & \\ & & 1 & \\ & -1 & & \end{pmatrix} n \begin{pmatrix} -1 & \\ & 1 \end{pmatrix}, & O(3)^T : n &\rightarrow \begin{pmatrix} O(3)^T & \\ & I_3 \end{pmatrix} n
 \end{aligned} \tag{5.72}$$

The action of the mirror symmetry  $M$  in these two realizations are respectively

$$M : n \rightarrow \begin{pmatrix} I_3 & & & \\ & -1 & & \\ & & -1 & \\ & & & 1 \end{pmatrix} n \tag{5.73}$$

and

$$M : n \rightarrow \begin{pmatrix} I_3 & & & \\ & 1 & & \\ & & 1 & \\ & & & -1 \end{pmatrix} n \begin{pmatrix} -1 & \\ & 1 \end{pmatrix} \tag{5.74}$$



## Kagome lattice half-integer spin systems

On kagome lattice half-integer spin systems, there are 3 stable realizations of DSL. One of them is known [15, 24, 81, 83, 132–135], adjacent to  $q = 0$  order, given by

$$\begin{aligned}
 T_1 : n &\rightarrow \begin{pmatrix} I_3 & & & \\ & 1 & & \\ & & -1 & \\ & & & -1 \end{pmatrix} n, & T_2 : n &\rightarrow \begin{pmatrix} I_3 & & & \\ & -1 & & \\ & & 1 & \\ & & & -1 \end{pmatrix} n, \\
 C_6 : n &\rightarrow \begin{pmatrix} I_3 & & & \\ & 1 & & \\ & & 1 & \\ & & & 1 \end{pmatrix} n \begin{pmatrix} -\frac{1}{2} & -\frac{\sqrt{3}}{2} \\ \frac{\sqrt{3}}{2} & -\frac{1}{2} \end{pmatrix}, \\
 M : n &\rightarrow \begin{pmatrix} I_3 & & & \\ & -1 & & \\ & & -1 & \\ & & & -1 \end{pmatrix} n \begin{pmatrix} -1 & \\ & 1 \end{pmatrix}, \\
 O(3)^T : n &\rightarrow \begin{pmatrix} O(3)^T & & & \\ & I_3 & & \\ & & I_3 & \\ & & & I_3 \end{pmatrix} n
 \end{aligned} \tag{5.75}$$

The other two have the same actions of  $T_{1,2}$ ,  $C_6$  and  $O(3)^T$ :

$$\begin{aligned}
 T_1 : n &\rightarrow \begin{pmatrix} I_3 & & & \\ & 1 & & \\ & & -1 & \\ & & & -1 \end{pmatrix} n, & T_2 : n &\rightarrow \begin{pmatrix} I_3 & & & \\ & -1 & & \\ & & 1 & \\ & & & -1 \end{pmatrix} n, \\
 C_6 : n &\rightarrow \begin{pmatrix} I_3 & & & \\ & 1 & & \\ & & 1 & \\ & & & 1 \end{pmatrix} n, & O(3)^T : n &\rightarrow \begin{pmatrix} O(3)^T & & & \\ & I_3 & & \\ & & I_3 & \\ & & & I_3 \end{pmatrix} n
 \end{aligned} \tag{5.76}$$

And the action of  $M$  in the two realizations are respectively

$$M : n \rightarrow \begin{pmatrix} I_3 & & & \\ & 1 & & \\ & & 1 & \\ & & & 1 \end{pmatrix} n \tag{5.77}$$

and

$$M : n \rightarrow \begin{pmatrix} I_3 & & & \\ & -1 & & \\ & & -1 & \\ & & & -1 \end{pmatrix} n \begin{pmatrix} -1 & \\ & 1 \end{pmatrix} \quad (5.78)$$

### Square lattice half-integer spin systems

On square lattice half-integer spin systems, there are 3 stable realizations of DSLs. One of them is given by Eq. (5.19). The other two have the same actions of  $T_{1,2}$ ,  $C_4$  and  $O(3)^T$ :

$$\begin{aligned} T_1 : n \rightarrow \begin{pmatrix} I_3 & & & \\ & -1 & & \\ & & 1 & \\ & & & 1 \end{pmatrix} n \begin{pmatrix} -1 & \\ & 1 \end{pmatrix}, T_2 : n \rightarrow \begin{pmatrix} I_3 & & & \\ & 1 & & \\ & & -1 & \\ & & & 1 \end{pmatrix} n \begin{pmatrix} -1 & \\ & 1 \end{pmatrix} \\ C_4 : n \rightarrow \begin{pmatrix} I_3 & & & \\ & -1 & & \\ & & 1 & \\ & & & -1 \end{pmatrix} n \begin{pmatrix} -1 & \\ & 1 \end{pmatrix}, O(3)^T : n \rightarrow \begin{pmatrix} O(3)^T & \\ & I_3 \end{pmatrix} n \end{aligned} \quad (5.79)$$

The action of  $M$  on these two realizations are respectively

$$M : n \rightarrow \begin{pmatrix} I_3 & & & \\ & 1 & & \\ & & -1 & \\ & & & 1 \end{pmatrix} n \quad (5.80)$$

and

$$M : n \rightarrow \begin{pmatrix} I_3 & & & \\ & -1 & & \\ & & 1 & \\ & & & -1 \end{pmatrix} n \begin{pmatrix} -1 & \\ & 1 \end{pmatrix} \quad (5.81)$$

### 5.C.3 Stable realizations of $SL^{(7)}$

Below we list the stable realizations of  $SL^{(7)}$  on various systems.

### $p6m$ -anomaly-free systems

On  $p6m$ -anomaly-free systems, there are two stable realizations of  $SL^{(7)}$ , both of which have the most relevant spinful fluctuations carrying spin-2. The symmetry actions of one of them is given by Eq. (5.23). The other one has symmetry actions:

$$\begin{aligned}
 SO(3) : n &\rightarrow \begin{pmatrix} \varphi_5(SO(3)) & & \\ & I_2 & \end{pmatrix} n, & \mathcal{T} : n &\rightarrow \begin{pmatrix} I_5 & & \\ & -1 & \\ & & -1 \end{pmatrix} n \begin{pmatrix} -1 & & \\ & 1 & \\ & & 1 \end{pmatrix}, \\
 T_{1,2} : n &\rightarrow \begin{pmatrix} I_5 & & \\ & -\frac{1}{2} & \frac{\sqrt{3}}{2} \\ & -\frac{\sqrt{3}}{2} & -\frac{1}{2} \end{pmatrix} n, \\
 C_6 : n &\rightarrow \begin{pmatrix} I_5 & & \\ & 1 & \\ & & -1 \end{pmatrix} n \begin{pmatrix} -1 & & \\ & 1 & \\ & & 1 \end{pmatrix}, \\
 M : n &\rightarrow \begin{pmatrix} I_5 & & \\ & -1 & \\ & & -1 \end{pmatrix} n \begin{pmatrix} -1 & & \\ & 1 & \\ & & 1 \end{pmatrix},
 \end{aligned} \tag{5.82}$$

### Triangular lattice half-integer spin systems

On triangular lattice half-integer spin systems, there are 8 stable realizations of  $SL^{(7)}$ . The first has appeared in Ref. [15], given by Eq. (5.53).

The second has symmetry actions:

$$\begin{aligned}
 T_1 : n &\rightarrow n \begin{pmatrix} 1 & & \\ & -1 & \\ & & -1 \end{pmatrix}, & T_2 : n &\rightarrow n \begin{pmatrix} -1 & & \\ & 1 & \\ & & -1 \end{pmatrix}, \\
 C_6 : n &\rightarrow \begin{pmatrix} I_3 & & & \\ & -1 & & \\ & & 1 & \\ & & & -1 \\ & & & & 1 \end{pmatrix} n \begin{pmatrix} & & 1 \\ & 1 & \\ & & 1 \end{pmatrix}, \\
 M : n &\rightarrow \begin{pmatrix} I_3 & & & \\ & -1 & & \\ & & -1 & \\ & & & 1 \\ & & & & 1 \end{pmatrix} n \begin{pmatrix} & & 1 \\ & 1 & \\ & & 1 \end{pmatrix}, \\
 O(3)^T : n &\rightarrow \begin{pmatrix} O(3)^T & \\ & I_4 \end{pmatrix} n
 \end{aligned} \tag{5.83}$$

The third has symmetry actions:

$$\begin{aligned}
T_1 : n &\rightarrow \begin{pmatrix} I_3 & & & \\ & -\frac{1}{2} & \frac{\sqrt{3}}{2} & \\ & -\frac{\sqrt{3}}{2} & -\frac{1}{2} & \\ & & & 1 \\ & & & & 1 \end{pmatrix} n \begin{pmatrix} 1 & & \\ & -1 & \\ & & -1 \end{pmatrix}, \\
T_2 : n &\rightarrow \begin{pmatrix} I_3 & & & \\ & -\frac{1}{2} & \frac{\sqrt{3}}{2} & \\ & -\frac{\sqrt{3}}{2} & -\frac{1}{2} & \\ & & & 1 \\ & & & & 1 \end{pmatrix} n \begin{pmatrix} -1 & & \\ & 1 & \\ & & -1 \end{pmatrix}, \\
C_6 : n &\rightarrow \begin{pmatrix} I_3 & & & \\ & 1 & & \\ & & -1 & \\ & & & -1 \\ & & & & 1 \end{pmatrix} n \begin{pmatrix} & & 1 \\ 1 & & \\ & 1 & \end{pmatrix}, \\
M : n &\rightarrow \begin{pmatrix} I_3 & & & \\ & -1 & & \\ & & -1 & \\ & & & 1 \\ & & & & 1 \end{pmatrix} n \begin{pmatrix} & & 1 \\ 1 & & \\ & & 1 \end{pmatrix}, \\
O(3)^T : n &\rightarrow \begin{pmatrix} O(3)^T & \\ & I_4 \end{pmatrix} n
\end{aligned} \tag{5.84}$$

The fourth has symmetry actions:

$$\begin{aligned}
T_1 : n &\rightarrow \begin{pmatrix} I_3 & & & \\ & -\frac{1}{2} & \frac{\sqrt{3}}{2} & \\ & -\frac{\sqrt{3}}{2} & -\frac{1}{2} & \\ & & & 1 \\ & & & & 1 \end{pmatrix} n \begin{pmatrix} 1 & & \\ & -1 & \\ & & -1 \end{pmatrix}, \\
T_2 : n &\rightarrow \begin{pmatrix} I_3 & & & \\ & -\frac{1}{2} & \frac{\sqrt{3}}{2} & \\ & -\frac{\sqrt{3}}{2} & -\frac{1}{2} & \\ & & & 1 \\ & & & & 1 \end{pmatrix} n \begin{pmatrix} -1 & & \\ & 1 & \\ & & -1 \end{pmatrix}, \\
C_6 : n &\rightarrow \begin{pmatrix} I_3 & & & \\ & 1 & & \\ & & -1 & \\ & & & -1 \\ & & & & 1 \end{pmatrix} n \begin{pmatrix} & & 1 \\ 1 & & \\ & 1 & \end{pmatrix}, \\
M : n &\rightarrow \begin{pmatrix} I_3 & & & \\ & 1 & & \\ & & 1 & \\ & & & -1 \\ & & & & -1 \end{pmatrix} n \begin{pmatrix} & & 1 \\ 1 & & \\ & & 1 \end{pmatrix}, \\
O(3)^T : n &\rightarrow \begin{pmatrix} O(3)^T & & \\ & I_4 & \end{pmatrix} n
\end{aligned} \tag{5.85}$$

The first to the fourth realization are all adjacent to tetrahedral order.

The fifth has symmetry actions:

$$\begin{aligned}
T_1 : n &\rightarrow n \begin{pmatrix} 1 & & \\ & -1 & \\ & & -1 \end{pmatrix}, & T_2 : n &\rightarrow n \begin{pmatrix} -1 & & \\ & 1 & \\ & & -1 \end{pmatrix}, \\
C_6 : n &\rightarrow \begin{pmatrix} I_3 & & \\ & -1 & \\ & & 1 & \\ & & & 1 & \\ & & & & -1 \end{pmatrix} n \begin{pmatrix} & & 1 \\ & 1 & \\ & & 1 \end{pmatrix}, \\
M : n &\rightarrow \begin{pmatrix} I_3 & & \\ & -1 & \\ & & -1 & \\ & & & -1 & \\ & & & & 1 \end{pmatrix} n \begin{pmatrix} & & -1 \\ -1 & & \\ & & -1 \end{pmatrix}, \\
O(3)^T : n &\rightarrow \begin{pmatrix} O(3)^T & \\ & I_4 \end{pmatrix} n
\end{aligned} \tag{5.86}$$

The sixth has symmetry actions:

$$\begin{aligned}
T_1 : n &\rightarrow \begin{pmatrix} I_3 & & & \\ & -\frac{1}{2} & \frac{\sqrt{3}}{2} & \\ & -\frac{\sqrt{3}}{2} & -\frac{1}{2} & \\ & & & 1 \\ & & & & 1 \end{pmatrix} n \begin{pmatrix} 1 & & \\ & -1 & \\ & & -1 \end{pmatrix}, \\
T_2 : n &\rightarrow \begin{pmatrix} I_3 & & & \\ & -\frac{1}{2} & \frac{\sqrt{3}}{2} & \\ & -\frac{\sqrt{3}}{2} & -\frac{1}{2} & \\ & & & 1 \\ & & & & 1 \end{pmatrix} n \begin{pmatrix} -1 & & \\ & 1 & \\ & & -1 \end{pmatrix}, \\
C_6 : n &\rightarrow \begin{pmatrix} I_3 & & & \\ & 1 & & \\ & & -1 & \\ & & & 1 \\ & & & & -1 \end{pmatrix} n \begin{pmatrix} & & 1 \\ 1 & & \\ & 1 & \end{pmatrix}, \\
M : n &\rightarrow \begin{pmatrix} I_3 & & & \\ & -1 & & \\ & & -1 & \\ & & & -1 \\ & & & & 1 \end{pmatrix} n \begin{pmatrix} & & -1 \\ -1 & & \\ & -1 & \\ & & -1 \end{pmatrix}, \\
O(3)^T : n &\rightarrow \begin{pmatrix} O(3)^T & \\ & I_4 \end{pmatrix} n
\end{aligned} \tag{5.87}$$



The seventh has symmetry actions:

$$\begin{aligned}
T_1 : n &\rightarrow \begin{pmatrix} I_3 & & & \\ & 1 & & \\ & & 1 & \\ & & & -1 \\ & & & & -1 \end{pmatrix} n \begin{pmatrix} -\frac{1}{2} & -\frac{\sqrt{3}}{2} & \\ \frac{\sqrt{3}}{2} & -\frac{1}{2} & \\ & & 1 \end{pmatrix}, \\
T_2 : n &\rightarrow \begin{pmatrix} I_3 & & & \\ & 1 & & \\ & & -1 & \\ & & & 1 \\ & & & & -1 \end{pmatrix} n \begin{pmatrix} -\frac{1}{2} & -\frac{\sqrt{3}}{2} & \\ \frac{\sqrt{3}}{2} & -\frac{1}{2} & \\ & & 1 \end{pmatrix}, \\
C_6 : n &\rightarrow \begin{pmatrix} I_3 & & & \\ & -1 & & \\ & & 1 & \\ & & & 1 \\ & & & & -1 \end{pmatrix} n \begin{pmatrix} 1 & & \\ & -1 & \\ & & -1 \end{pmatrix}, \\
M : n &\rightarrow \begin{pmatrix} I_3 & & & \\ & 1 & & \\ & & 1 & \\ & & & 1 \\ & & & & -1 \end{pmatrix} n \begin{pmatrix} 1 & & \\ & 1 & \\ & & -1 \end{pmatrix}, \\
O(3)^T : n &\rightarrow \begin{pmatrix} O(3)^T & \\ & I_4 \end{pmatrix} n
\end{aligned} \tag{5.88}$$

The eighth has symmetry actions:

$$\begin{aligned}
T_1 : n &\rightarrow \begin{pmatrix} I_3 & & & \\ & 1 & & \\ & & 1 & \\ & & & -1 & \\ & & & & -1 \end{pmatrix} n \begin{pmatrix} -\frac{1}{2} & -\frac{\sqrt{3}}{2} & \\ \frac{\sqrt{3}}{2} & -\frac{1}{2} & \\ & & 1 \end{pmatrix}, \\
T_2 : n &\rightarrow \begin{pmatrix} I_3 & & & \\ & 1 & & \\ & & -1 & \\ & & & 1 & \\ & & & & -1 \end{pmatrix} n \begin{pmatrix} -\frac{1}{2} & -\frac{\sqrt{3}}{2} & \\ \frac{\sqrt{3}}{2} & -\frac{1}{2} & \\ & & 1 \end{pmatrix}, \\
C_6 : n &\rightarrow \begin{pmatrix} I_3 & & & \\ & 1 & & \\ & & 1 & \\ & & & 1 & \\ & & & & -1 \end{pmatrix} n \begin{pmatrix} 1 & & \\ & -1 & \\ & & 1 \end{pmatrix}, \\
M : n &\rightarrow \begin{pmatrix} I_3 & & & \\ & -1 & & \\ & & 1 & \\ & & & 1 & \\ & & & & -1 \end{pmatrix} n \begin{pmatrix} -1 & & \\ & -1 & \\ & & 1 \end{pmatrix}, \\
O(3)^T : n &\rightarrow \begin{pmatrix} O(3)^T & & \\ & I_4 & \end{pmatrix} n
\end{aligned} \tag{5.89}$$

### Kagome lattice half-integer spin systems

On kagome lattice half-integer spin systems, there are 9 stable realizations of  $SL^{(7)}$ . The first has appeared in Ref. [15] and is given by Eq. (5.59). The second is given by Eq. (5.20). Both realizations are adjacent to cuboc1 order.

The third has symmetry actions

$$\begin{aligned}
T_1 : n &\rightarrow n \begin{pmatrix} 1 & & \\ & -1 & \\ & & -1 \end{pmatrix}, & T_2 : n &\rightarrow n \begin{pmatrix} -1 & & \\ & 1 & \\ & & -1 \end{pmatrix}, \\
C_6 : n &\rightarrow \begin{pmatrix} I_3 & & \\ & -1 & \\ & & -1 \\ & & & 1 \\ & & & & -1 \end{pmatrix} n \begin{pmatrix} & & -1 \\ & 1 & \\ & & 1 \end{pmatrix}, \\
M : n &\rightarrow \begin{pmatrix} I_3 & & \\ & -1 & \\ & & -1 \\ & & & -1 \\ & & & & 1 \end{pmatrix} n \begin{pmatrix} & & 1 \\ & 1 & \\ & & -1 \end{pmatrix}, \\
O(3)^T : n &\rightarrow \begin{pmatrix} O(3)^T & \\ & I_4 \end{pmatrix}
\end{aligned} \tag{5.90}$$

The fourth has symmetry actions

$$\begin{aligned}
T_1 : n &\rightarrow \begin{pmatrix} I_3 & & & \\ & -\frac{1}{2} & \frac{\sqrt{3}}{2} & \\ & -\frac{\sqrt{3}}{2} & -\frac{1}{2} & \\ & & & 1 \\ & & & & 1 \end{pmatrix} n \begin{pmatrix} 1 & & \\ & -1 & \\ & & -1 \end{pmatrix}, \\
T_2 : n &\rightarrow \begin{pmatrix} I_3 & & & \\ & -\frac{1}{2} & \frac{\sqrt{3}}{2} & \\ & -\frac{\sqrt{3}}{2} & -\frac{1}{2} & \\ & & & 1 \\ & & & & 1 \end{pmatrix} n \begin{pmatrix} -1 & & \\ & 1 & \\ & & -1 \end{pmatrix}, \\
C_6 : n &\rightarrow \begin{pmatrix} I_3 & & & \\ & 1 & & \\ & & -1 & \\ & & & -1 \\ & & & & -1 \end{pmatrix} n \begin{pmatrix} & & -1 \\ 1 & & \\ & 1 & \end{pmatrix}, \\
M : n &\rightarrow \begin{pmatrix} I_3 & & & \\ & -1 & & \\ & & -1 & \\ & & & -1 \\ & & & & 1 \end{pmatrix} n \begin{pmatrix} & & 1 \\ 1 & & \\ & & -1 \end{pmatrix}, \\
O(3)^T : n &\rightarrow \begin{pmatrix} O(3)^T & \\ & I_4 \end{pmatrix} n,
\end{aligned} \tag{5.91}$$

The fifth has symmetry actions

$$\begin{aligned}
T_1 : n &\rightarrow \begin{pmatrix} I_3 & & & \\ & 1 & & \\ & & 1 & \\ & & & -\frac{1}{2} & \frac{\sqrt{3}}{2} \\ & & & -\frac{\sqrt{3}}{2} & -\frac{1}{2} \end{pmatrix} n \begin{pmatrix} 1 & & \\ & -1 & \\ & & -1 \end{pmatrix}, \\
T_2 : n &\rightarrow \begin{pmatrix} I_3 & & & \\ & 1 & & \\ & & 1 & \\ & & & -\frac{1}{2} & \frac{\sqrt{3}}{2} \\ & & & -\frac{\sqrt{3}}{2} & -\frac{1}{2} \end{pmatrix} n \begin{pmatrix} -1 & & \\ & 1 & \\ & & -1 \end{pmatrix}, \\
C_6 : n &\rightarrow \begin{pmatrix} I_3 & & & \\ & \frac{1}{2} & \frac{\sqrt{3}}{2} & \\ & -\frac{\sqrt{3}}{2} & \frac{1}{2} & \\ & & & 1 & \\ & & & & -1 \end{pmatrix} n \begin{pmatrix} & & -1 \\ 1 & & \\ & 1 & \end{pmatrix}, \\
M : n &\rightarrow \begin{pmatrix} I_3 & & & \\ & -1 & & \\ & & 1 & \\ & & & -1 & \\ & & & & -1 \end{pmatrix} n \begin{pmatrix} & & 1 \\ 1 & & \\ & & -1 \end{pmatrix}, \\
O(3)^T : n &\rightarrow \begin{pmatrix} O(3)^T & \\ & I_4 \end{pmatrix} n
\end{aligned} \tag{5.92}$$

The third to the fifth realization are all adjacent to cuboc2 order.

The sixth has symmetry actions:

$$\begin{aligned}
T_1 : n &\rightarrow \begin{pmatrix} I_3 & & & \\ & 1 & & \\ & & 1 & \\ & & & -1 & \\ & & & & -1 \end{pmatrix} n, \\
T_2 : n &\rightarrow \begin{pmatrix} I_3 & & & \\ & 1 & & \\ & & -1 & \\ & & & 1 & \\ & & & & -1 \end{pmatrix} n, \\
C_6 : n &\rightarrow \begin{pmatrix} I_3 & & & \\ & 1 & & \\ & & 1 & \\ & & & 1 \end{pmatrix} n \begin{pmatrix} -\frac{1}{2} & -\frac{\sqrt{3}}{2} & \\ \frac{\sqrt{3}}{2} & -\frac{1}{2} & \\ & & 1 \end{pmatrix}, \\
M : n &\rightarrow \begin{pmatrix} I_3 & & & \\ & -1 & & \\ & & 1 & \\ & & & 1 & \\ & & & & 1 \end{pmatrix} n \begin{pmatrix} -1 & & \\ & 1 & \\ & & 1 \end{pmatrix}, \\
O(3)^T : n &\rightarrow \begin{pmatrix} O(3)^T & \\ & I_4 \end{pmatrix} n
\end{aligned} \tag{5.93}$$

The sixth realization is adjacent to  $q = 0$  umbrella order.

The seventh has symmetry actions:

$$\begin{aligned}
T_1 : n &\rightarrow \begin{pmatrix} I_3 & & & \\ & 1 & & \\ & & 1 & \\ & & & -1 \\ & & & & -1 \end{pmatrix} n \begin{pmatrix} -\frac{1}{2} & -\frac{\sqrt{3}}{2} & \\ \frac{\sqrt{3}}{2} & -\frac{1}{2} & \\ & & 1 \end{pmatrix}, \\
T_2 : n &\rightarrow \begin{pmatrix} I_3 & & & \\ & 1 & & \\ & & -1 & \\ & & & 1 \\ & & & & -1 \end{pmatrix} n \begin{pmatrix} -\frac{1}{2} & -\frac{\sqrt{3}}{2} & \\ \frac{\sqrt{3}}{2} & -\frac{1}{2} & \\ & & 1 \end{pmatrix}, \\
C_6 : n &\rightarrow \begin{pmatrix} I_3 & & & \\ & -1 & & \\ & & 1 & \\ & & & 1 \\ & & & & 1 \end{pmatrix} n \begin{pmatrix} 1 & & \\ & -1 & \\ & & 1 \end{pmatrix}, \\
M : n &\rightarrow \begin{pmatrix} I_3 & & & \\ & 1 & & \\ & & 1 & \\ & & & 1 \\ & & & & 1 \end{pmatrix} n, \\
O(3)^T : n &\rightarrow \begin{pmatrix} O(3)^T & \\ & I_4 \end{pmatrix} n
\end{aligned} \tag{5.94}$$

The seventh realization is adjacent to  $q = \sqrt{3} \times \sqrt{3}$  umbrella order.

The eighth has symmetry actions:

$$\begin{aligned}
T_1 : n &\rightarrow \begin{pmatrix} I_3 & & & \\ & 1 & & \\ & & 1 & \\ & & & -1 \\ & & & & -1 \end{pmatrix} n \begin{pmatrix} -\frac{1}{2} & -\frac{\sqrt{3}}{2} & \\ \frac{\sqrt{3}}{2} & -\frac{1}{2} & \\ & & 1 \end{pmatrix}, \\
T_2 : n &\rightarrow \begin{pmatrix} I_3 & & & \\ & 1 & & \\ & & -1 & \\ & & & 1 \\ & & & & -1 \end{pmatrix} n \begin{pmatrix} -\frac{1}{2} & -\frac{\sqrt{3}}{2} & \\ \frac{\sqrt{3}}{2} & -\frac{1}{2} & \\ & & 1 \end{pmatrix}, \\
C_6 : n &\rightarrow \begin{pmatrix} I_3 & & & \\ & -1 & & \\ & & 1 & \\ & & & 1 \\ & & & & 1 \end{pmatrix} n \begin{pmatrix} 1 & & \\ & -1 & \\ & & 1 \end{pmatrix}, \\
M : n &\rightarrow \begin{pmatrix} I_3 & & & \\ & 1 & & \\ & & -1 & \\ & & & -1 \\ & & & & -1 \end{pmatrix} n \begin{pmatrix} 1 & & \\ & 1 & \\ & & -1 \end{pmatrix}, \\
O(3)^T : n &\rightarrow \begin{pmatrix} O(3)^T & \\ & I_4 \end{pmatrix} n
\end{aligned} \tag{5.95}$$



The ninth has symmetry actions:

$$\begin{aligned}
T_1 : n &\rightarrow \begin{pmatrix} I_3 & & & & \\ & 1 & & & \\ & & 1 & & \\ & & & -1 & \\ & & & & -1 \end{pmatrix} n \begin{pmatrix} -\frac{1}{2} & -\frac{\sqrt{3}}{2} & \\ \frac{\sqrt{3}}{2} & -\frac{1}{2} & \\ & & 1 \end{pmatrix}, \\
T_2 : n &\rightarrow \begin{pmatrix} I_3 & & & & \\ & 1 & & & \\ & & -1 & & \\ & & & 1 & \\ & & & & -1 \end{pmatrix} n \begin{pmatrix} -\frac{1}{2} & -\frac{\sqrt{3}}{2} & \\ \frac{\sqrt{3}}{2} & -\frac{1}{2} & \\ & & 1 \end{pmatrix}, \\
C_6 : n &\rightarrow \begin{pmatrix} I_3 & & & & \\ & -1 & & & \\ & & 1 & & \\ & & & 1 & \\ & & & & 1 \end{pmatrix} n \begin{pmatrix} 1 & & \\ & -1 & \\ & & 1 \end{pmatrix}, \\
M : n &\rightarrow \begin{pmatrix} I_3 & & & & \\ & -1 & & & \\ & & & -1 & \\ & & & & -1 \\ & & -1 & & \\ & & & & -1 \end{pmatrix} n \begin{pmatrix} -1 & & \\ & -1 & \\ & & 1 \end{pmatrix}, \\
O(3)^T : n &\rightarrow \begin{pmatrix} O(3)^T & & \\ & I_4 & \end{pmatrix} n
\end{aligned} \tag{5.96}$$

### ***p4m*-anomaly-free systems**

On *p4m*-anomaly-free systems, there are 4 stable realizations of  $SL^{(\tau)}$ , all of which has the most relevant spinful fluctuations carrying spin-2.

The first has symmetry actions:

$$\begin{aligned}
SO(3) : n &\rightarrow \begin{pmatrix} \varphi_5(SO(3)) & & \\ & I_2 & \\ & & \end{pmatrix} n, & \mathcal{T} : n &\rightarrow \begin{pmatrix} I_5 & & \\ & -1 & \\ & & 1 \end{pmatrix} n, \\
T_{1,2} : n &\rightarrow \begin{pmatrix} I_5 & & \\ & 1 & \\ & & -1 \end{pmatrix} n \begin{pmatrix} -1 & & \\ & 1 & \\ & & 1 \end{pmatrix}, & & (5.97) \\
C_4 : n &\rightarrow \begin{pmatrix} I_5 & & \\ & 1 & \\ & & -1 \end{pmatrix} n \begin{pmatrix} 1 & & \\ & -1 & \\ & & 1 \end{pmatrix}, & M : n &\rightarrow \begin{pmatrix} I_5 & & \\ & -1 & \\ & & 1 \end{pmatrix} n
\end{aligned}$$

The second has symmetry actions:

$$\begin{aligned}
SO(3) : n &\rightarrow \begin{pmatrix} \varphi_5(SO(3)) & & \\ & I_2 & \\ & & \end{pmatrix} n, & \mathcal{T} : n &\rightarrow \begin{pmatrix} I_5 & & \\ & -1 & \\ & & 1 \end{pmatrix} n, \\
T_{1,2} : n &\rightarrow \begin{pmatrix} I_5 & & \\ & 1 & \\ & & -1 \end{pmatrix} n \begin{pmatrix} -1 & & \\ & 1 & \\ & & 1 \end{pmatrix}, & & (5.98) \\
C_4 : n &\rightarrow n \begin{pmatrix} -1 & & \\ & -1 & \\ & & 1 \end{pmatrix}, & M : n &\rightarrow \begin{pmatrix} I_5 & & \\ & -1 & \\ & & -1 \end{pmatrix} n \begin{pmatrix} -1 & & \\ & 1 & \\ & & 1 \end{pmatrix}
\end{aligned}$$

The third has symmetry actions:

$$\begin{aligned}
SO(3) : n &\rightarrow \begin{pmatrix} \varphi_5(SO(3)) & & \\ & I_2 & \\ & & \end{pmatrix} n, & \mathcal{T} : n &\rightarrow \begin{pmatrix} I_5 & & \\ & -1 & \\ & & -1 \end{pmatrix} n \begin{pmatrix} -1 & & \\ & 1 & \\ & & 1 \end{pmatrix}, \\
T_{1,2} : n &\rightarrow \begin{pmatrix} I_5 & & \\ & -1 & \\ & & 1 \end{pmatrix} n \begin{pmatrix} -1 & & \\ & 1 & \\ & & 1 \end{pmatrix}, & & (5.99) \\
C_4 : n &\rightarrow \begin{pmatrix} I_5 & & \\ & -1 & \\ & & -1 \end{pmatrix} n, & M : n &\rightarrow \begin{pmatrix} I_5 & & \\ & 1 & \\ & & -1 \end{pmatrix} n
\end{aligned}$$

The fourth has symmetry actions:

$$\begin{aligned}
SO(3) : n &\rightarrow \begin{pmatrix} \varphi_5(SO(3)) & & \\ & I_2 & \\ & & \end{pmatrix} n, & \mathcal{T} : n &\rightarrow \begin{pmatrix} I_5 & & \\ & -1 & \\ & & -1 \end{pmatrix} n \begin{pmatrix} -1 & & \\ & 1 & \\ & & 1 \end{pmatrix}, \\
T_{1,2} : n &\rightarrow \begin{pmatrix} I_5 & & \\ & -1 & \\ & & 1 \end{pmatrix} n \begin{pmatrix} -1 & & \\ & 1 & \\ & & 1 \end{pmatrix}, \\
C_4 : n &\rightarrow \begin{pmatrix} I_5 & & \\ & 1 & \\ & & -1 \end{pmatrix} n \begin{pmatrix} -1 & & \\ & 1 & \\ & & 1 \end{pmatrix}, \\
M : n &\rightarrow \begin{pmatrix} I_5 & & \\ & -1 & \\ & & -1 \end{pmatrix} n \begin{pmatrix} -1 & & \\ & 1 & \\ & & 1 \end{pmatrix}
\end{aligned} \tag{5.100}$$

### Square lattice half-integer spin systems

On square lattice half-integer spin systems, there are 2 stable realizations of  $SL^{(7)}$  where the most relevant spinful fluctuations have spin-1 and all  $n$  modes are at high-symmetry momenta in the Brillouin zone. There are also three realizations where some  $n$  modes can have continuously changing momenta, among which two of them have only a single symmetric relevant perturbation that shifts the momenta of the  $n$  modes, as long as these momenta are not tuned to high-symmetry point. This is the case for the third family of realizations for most non-high-symmetry momenta, except at two special momentum points (see below). Furthermore, there is also one stable realization where the most relevant spinful fluctuations have spin-2 and all  $n$  modes are at high-symmetry momenta.

We start with the 2 realizations with the most relevant spinful fluctuations carrying spin-1 and all  $n$  modes locating at high-symmetry momenta. The first has symmetry

actions:

$$\begin{aligned}
 T_1 : n &\rightarrow \begin{pmatrix} I_3 & & & \\ & -1 & & \\ & & 1 & \\ & & & 1 \end{pmatrix} n \begin{pmatrix} -1 & & \\ & 1 & \\ & & 1 \end{pmatrix}, \\
 T_2 : n &\rightarrow \begin{pmatrix} I_3 & & & \\ & 1 & & \\ & & -1 & \\ & & & 1 \end{pmatrix} n \begin{pmatrix} -1 & & \\ & 1 & \\ & & 1 \end{pmatrix}, \\
 C_4 : n &\rightarrow \begin{pmatrix} I_3 & & & \\ & -1 & & \\ & & 1 & \\ & & & 1 \end{pmatrix} n \begin{pmatrix} 1 & & \\ & -1 & \\ & & -1 \end{pmatrix}, \\
 M : n &\rightarrow \begin{pmatrix} I_3 & & & \\ & -1 & & \\ & & 1 & \\ & & & -1 \\ & & & & -1 \end{pmatrix} n \begin{pmatrix} -1 & & \\ & -1 & \\ & & 1 \end{pmatrix}, \\
 O(3)^T : n &\rightarrow \begin{pmatrix} O(3)^T & \\ & I_4 \end{pmatrix} n
 \end{aligned} \tag{5.101}$$

The second has symmetry actions:

$$\begin{aligned}
T_1 : n &\rightarrow \begin{pmatrix} I_3 & & & \\ & -1 & & \\ & & 1 & \\ & & & -1 & \\ & & & & 1 \end{pmatrix} n \begin{pmatrix} -1 & & \\ & -1 & \\ & & 1 \end{pmatrix}, \\
T_2 : n &\rightarrow \begin{pmatrix} I_3 & & & \\ & 1 & & \\ & & -1 & \\ & & & -1 & \\ & & & & 1 \end{pmatrix} n \begin{pmatrix} -1 & & \\ & -1 & \\ & & 1 \end{pmatrix}, \\
C_4 : n &\rightarrow \begin{pmatrix} I_3 & & & \\ & -1 & & \\ & & 1 & \\ & & & 1 & \\ & & & & 1 \end{pmatrix} n \begin{pmatrix} -1 & & \\ & -1 & \\ & & 1 \end{pmatrix}, \\
M : n &\rightarrow \begin{pmatrix} I_3 & & & \\ & -1 & & \\ & & 1 & \\ & & & 1 & \\ & & & & -1 \end{pmatrix} n \begin{pmatrix} -1 & & \\ & 1 & \\ & & 1 \end{pmatrix}, \\
O(3)^T : n &\rightarrow \begin{pmatrix} O(3)^T & \\ & I_4 \end{pmatrix} n
\end{aligned} \tag{5.102}$$

Next, we turn to the three realizations with some  $n$  modes at continuously changing momenta. The first has symmetry actions given by Eq. (5.21), adjacent to tetrahedral

umbrella order, and the second has symmetry actions

$$\begin{aligned}
C_4 : n &\rightarrow \begin{pmatrix} I_3 & & & \\ & 1 & & \\ & & 1 & \\ & & & 1 \end{pmatrix} n \begin{pmatrix} & 1 & \\ & & 1 \\ 1 & & \\ & & 1 \end{pmatrix}, \\
M : n &\rightarrow \begin{pmatrix} I_3 & & & \\ & -1 & & \\ & & -1 & \\ & & & -1 \end{pmatrix} n \begin{pmatrix} -1 & & \\ & -1 & \\ & & 1 \end{pmatrix}, \\
T_1 : n &\rightarrow \begin{pmatrix} I_3 & & & \\ & \cos k & \sin k & \\ & -\sin k & \cos k & \\ & & & I_2 \end{pmatrix} n \begin{pmatrix} -1 & & \\ & 1 & \\ & & -1 \end{pmatrix}, \\
T_2 : n &\rightarrow \begin{pmatrix} I_3 & & & \\ & I_2 & & \\ & & \cos k & -\sin k \\ & & \sin k & \cos k \end{pmatrix} n \begin{pmatrix} 1 & & \\ & -1 & \\ & & -1 \end{pmatrix}, \\
O(3)^T : n &\rightarrow \begin{pmatrix} O(3)^T & & \\ & & I_4 \end{pmatrix} n
\end{aligned} \tag{5.103}$$

where  $k \in (-\pi, \pi)$  is a generic momentum. In both of these two realizations, the only relevant perturbation that is allowed by microscopic symmetries is the one that shifts the momenta of the  $n$  modes.

The third has symmetry actions:

$$\begin{aligned}
C_4 : n &\rightarrow \begin{pmatrix} I_3 & & & \\ & & 1 & \\ & & & 1 \\ & 1 & & \\ & & & & 1 \end{pmatrix} n \begin{pmatrix} & & 1 & \\ & & & \\ 1 & & & \\ & & & 1 \end{pmatrix}, \\
M : n &\rightarrow \begin{pmatrix} I_3 & & & & \\ & & & & -1 \\ & & & -1 & \\ & & -1 & & \\ & -1 & & & \end{pmatrix} n \begin{pmatrix} & & 1 & \\ & & & \\ 1 & & & \\ & & & -1 \end{pmatrix}, \\
T_1 : n &\rightarrow \begin{pmatrix} I_3 & & & & \\ & \cos k & \sin k & & \\ & -\sin k & \cos k & & \\ & & & \cos k & \sin k \\ & & & -\sin k & \cos k \end{pmatrix} n \begin{pmatrix} -1 & & \\ & 1 & \\ & & -1 \end{pmatrix}, \\
T_2 : n &\rightarrow \begin{pmatrix} I_3 & & & & \\ & \cos k & \sin k & & \\ & -\sin k & \cos k & & \\ & & & \cos k & -\sin k \\ & & & \sin k & \cos k \end{pmatrix} n \begin{pmatrix} & & 1 & \\ & & & -1 \\ 1 & & & \\ & & & -1 \end{pmatrix}, \\
O(3)^T : n &\rightarrow \begin{pmatrix} O(3)^T & \\ & I_4 \end{pmatrix} n
\end{aligned} \tag{5.104}$$

where  $k \in (-\pi, \pi)$  is a generic momentum. For this family of realizations, as long as  $k \neq \pm\pi/2$ , the only symmetric relevant perturbation is the one that shifts the momenta of the  $n$  modes. When  $k = \pm\pi/2$ , besides this symmetric relevant perturbation, there is an additional one that can change the emergent order of  $SL^{(7)}$  and make it unstable.

Finally, there is one realization where all  $n$  modes are at high-symmetry momentum,

and the most spinful fluctuations have spin-2. It has symmetry actions:

$$\begin{aligned}
SO(3) : n &\rightarrow \begin{pmatrix} \varphi_5(SO(3)) & & \\ & I_2 & \\ & & \end{pmatrix} n, & \mathcal{T} : n &\rightarrow \begin{pmatrix} I_5 & & \\ & -1 & \\ & & -1 \end{pmatrix} n \begin{pmatrix} -1 & & \\ & 1 & \\ & & 1 \end{pmatrix} \\
T_1 : n &\rightarrow \begin{pmatrix} I_5 & & \\ & -1 & \\ & & 1 \end{pmatrix} n \begin{pmatrix} -1 & & \\ & 1 & \\ & & 1 \end{pmatrix}, \\
T_2 : n &\rightarrow \begin{pmatrix} I_5 & & \\ & 1 & \\ & & -1 \end{pmatrix} n \begin{pmatrix} -1 & & \\ & 1 & \\ & & 1 \end{pmatrix}, \\
C_4 : n &\rightarrow \begin{pmatrix} I_5 & & \\ & & 1 \\ & & -1 \end{pmatrix} n, & M : n &\rightarrow \begin{pmatrix} I_5 & & \\ & 1 & \\ & & -1 \end{pmatrix} n
\end{aligned} \tag{5.105}$$

## 5.D Classical regular magnetic orders

Ref. [128] studied regular magnetic orders, i.e., magnetic orders that respect all the lattice symmetries modulo global  $O(3)^T$  spin transformations (rotations and/or spin flips). In particular, on triangular, kagome, honeycomb and square lattices, all *classical* regular magnetic orders are classified. These classical orders can all be realized by a product state, where each spin moment on the lattice can be assigned a definite orientation. In this appendix, we explicitly write down the spin configurations of these classical regular magnetic orders, and the lattice symmetry actions on the order parameters.

In terms of the symmetry breaking pattern of the spin  $O(3)^T$  symmetry, there are three types of magnetic orders: collinear, coplanar and non-coplanar. The order parameter of a collinear magnetic order is a three-component vector,  $\mathbf{n}$ , which transforms in the spin-1 representation of the  $O(3)^T$  spin symmetry. The order parameters of a coplanar magnetic order consists of two orthonormal three-component vectors,  $\mathbf{n}_{1,2}$ , both transforming in the spin-1 representation of the  $O(3)^T$  spin symmetry. The order parameters of a non-coplanar magnetic order consists of three orthonormal three-component vectors,  $\mathbf{n}_{1,2,3}$ , all transforming in the spin-1 representation of the  $O(3)^T$  spin symmetry.

We start from the triangular lattice. We will denote the position  $\mathbf{r}$  of a site on a triangular lattice by its coordinates in the basis of translation vectors of  $T_{1,2}$  (see Fig. 2.1), such that  $\mathbf{r} = x\mathbf{T}_1 + y\mathbf{T}_2$ , where  $\mathbf{T}_{1,2}$  is the translation vector of  $T_{1,2}$ . Under the  $p6m$



symmetry,

$$\begin{aligned}
T_1 &: (x, y) \rightarrow (x + 1, y) \\
T_2 &: (x, y) \rightarrow (x, y + 1) \\
C_6 &: (x, y) \rightarrow (x - y, x) \\
M &: (x, y) \rightarrow (y, x)
\end{aligned} \tag{5.106}$$

1. There is a single collinear classical regular magnetic order, the ferromagnetic order, where  $\mathbf{S}(x, y) = \mathbf{n}$ . Under the  $p6m$  symmetry,  $\mathbf{n}$  is invariant.
2. There is a single coplanar classical regular magnetic order, the  $120^\circ$  order, where  $\mathbf{S}(x, y) = (-1)^{x+y} \cos \frac{\pi(x+y)}{3} \mathbf{n}_1 + (-1)^{x+y} \sin \frac{\pi(x+y)}{3} \mathbf{n}_2$ . Under the  $p6m$  symmetry,

$$\begin{aligned}
T_{1,2} &: \mathbf{n}_1 \rightarrow -\frac{1}{2} \mathbf{n}_1 - \frac{\sqrt{3}}{2} \mathbf{n}_2, \quad \mathbf{n}_2 \rightarrow \frac{\sqrt{3}}{2} \mathbf{n}_1 - \frac{1}{2} \mathbf{n}_2 \\
C_6 &: \mathbf{n}_1 \rightarrow \mathbf{n}_1, \quad \mathbf{n}_2 \rightarrow -\mathbf{n}_2 \\
M &: \mathbf{n}_{1,2} \rightarrow \mathbf{n}_{1,2}
\end{aligned} \tag{5.107}$$

3. There are two non-coplanar classical regular magnetic order. The first is the tetrahedral order, where  $\mathbf{S}(x, y) = (-1)^x \mathbf{n}_1 + (-1)^y \mathbf{n}_2 + (-1)^{x+y} \mathbf{n}_3$ . Under the  $p6m$  symmetry,

$$\begin{aligned}
T_1 &: \mathbf{n}_1 \rightarrow -\mathbf{n}_1, \quad \mathbf{n}_2 \rightarrow \mathbf{n}_2, \quad \mathbf{n}_3 \rightarrow -\mathbf{n}_3 \\
T_2 &: \mathbf{n}_1 \rightarrow \mathbf{n}_1, \quad \mathbf{n}_2 \rightarrow -\mathbf{n}_2, \quad \mathbf{n}_3 \rightarrow -\mathbf{n}_3 \\
C_6 &: \mathbf{n}_1 \rightarrow \mathbf{n}_2, \quad \mathbf{n}_2 \rightarrow \mathbf{n}_3, \quad \mathbf{n}_3 \rightarrow \mathbf{n}_1 \\
M &: \mathbf{n}_1 \rightarrow \mathbf{n}_2, \quad \mathbf{n}_2 \rightarrow \mathbf{n}_1, \quad \mathbf{n}_3 \rightarrow \mathbf{n}_3
\end{aligned} \tag{5.108}$$

4. The second non-coplanar classical regular magnetic order is the F-umbrella order, where  $\mathbf{S}(x, y) = (-1)^{x+y} \cos \frac{\pi(x+y)}{3} \sin \theta \mathbf{n}_1 + (-1)^{x+y} \sin \frac{\pi(x+y)}{3} \sin \theta \mathbf{n}_2 + \cos \theta \mathbf{n}_3$ , with  $\theta$  a free parameter. Under the  $p6m$  symmetry,

$$\begin{aligned}
T_{1,2} &: \mathbf{n}_1 \rightarrow -\frac{1}{2} \mathbf{n}_1 + \frac{\sqrt{3}}{2} \mathbf{n}_2, \quad \mathbf{n}_2 \rightarrow -\frac{\sqrt{3}}{2} \mathbf{n}_1 - \frac{1}{2} \mathbf{n}_2, \quad \mathbf{n}_3 \rightarrow \mathbf{n}_3 \\
C_6 &: \mathbf{n}_1 \rightarrow \mathbf{n}_1, \quad \mathbf{n}_2 \rightarrow -\mathbf{n}_2, \quad \mathbf{n}_3 \rightarrow \mathbf{n}_3 \\
M &: \mathbf{n}_{1,2,3} \rightarrow \mathbf{n}_{1,2,3}
\end{aligned} \tag{5.109}$$

Next we turn to the kagome lattice. Each unit cell in a kagome lattice includes three sites, so the spin configuration will be written as  $\mathbf{S}_i(x, y)$ , where  $(x, y)$  labels the position of the unit cell in the same way as the triangular lattice, and  $i = 1, 2, 3$  represents the site obtained by applying a half translation  $\mathbf{T}_1/2$ ,  $\mathbf{T}_2/2$  and  $(\mathbf{T}_1 + \mathbf{T}_2)/2$  to the  $C_6$  center of the unit cell, respectively.

1. There is a single collinear classical regular magnetic order, the ferromagnetic order, where  $\mathbf{S}_i(x, y) = \mathbf{n}$  for  $i = 1, 2, 3$ . Under the  $p6m$  symmetry,  $\mathbf{n}$  is invariant.
2. There are two coplanar classical regular magnetic orders. The first is the  $\mathbf{q} = 0$  order, where  $\mathbf{S}_1(x, y) = \mathbf{n}_1$ ,  $\mathbf{S}_2(x, y) = -\frac{1}{2}\mathbf{n}_1 + \frac{\sqrt{3}}{2}\mathbf{n}_2$ , and  $\mathbf{S}_3(x, y) = -\frac{1}{2}\mathbf{n}_1 - \frac{\sqrt{3}}{2}\mathbf{n}_2$ . Under the  $p6m$  symmetry,

$$\begin{aligned}
T_{1,2} : \mathbf{n}_{1,2} &\rightarrow \mathbf{n}_{1,2} \\
C_6 : \mathbf{n}_1 &\rightarrow -\frac{1}{2}\mathbf{n}_1 - \frac{\sqrt{3}}{2}\mathbf{n}_2, \quad \mathbf{n}_2 \rightarrow \frac{\sqrt{3}}{2}\mathbf{n}_1 - \frac{1}{2}\mathbf{n}_2 \\
M : \mathbf{n}_1 &\rightarrow -\frac{1}{2}\mathbf{n}_1 + \frac{\sqrt{3}}{2}\mathbf{n}_2, \quad \mathbf{n}_2 \rightarrow \frac{\sqrt{3}}{2}\mathbf{n}_1 + \frac{1}{2}\mathbf{n}_2
\end{aligned} \tag{5.110}$$

3. The second coplanar classical regular magnetic order is the  $\mathbf{q} = \sqrt{3} \times \sqrt{3}$  order, where  $\mathbf{S}_1(x, y) = (-1)^{x+y} \cos \frac{\pi(x+y)}{3} \mathbf{n}_1 + (-1)^{x+y} \sin \frac{\pi(x+y)}{3} \mathbf{n}_2$ ,  $\mathbf{S}_2(x, y) = \mathbf{S}_1(x, y)$ , and  $\mathbf{S}_3(x, y) = (-1)^{x+y} \cos \frac{\pi(x+y+2)}{3} \mathbf{n}_1 + (-1)^{x+y} \sin \frac{\pi(x+y+2)}{3} \mathbf{n}_2$ . Under the  $p6m$  symmetry,

$$\begin{aligned}
T_{1,2} : \mathbf{n}_1 &\rightarrow -\frac{1}{2}\mathbf{n}_1 - \frac{\sqrt{3}}{2}\mathbf{n}_2, \quad \mathbf{n}_2 \rightarrow \frac{\sqrt{3}}{2}\mathbf{n}_1 - \frac{1}{2}\mathbf{n}_2 \\
C_6 : \mathbf{n}_1 &\rightarrow -\frac{1}{2}\mathbf{n}_1 + \frac{\sqrt{3}}{2}\mathbf{n}_2, \quad \mathbf{n}_2 \rightarrow \frac{\sqrt{3}}{2}\mathbf{n}_1 + \frac{1}{2}\mathbf{n}_2 \\
M : \mathbf{n}_{1,2} &\rightarrow \mathbf{n}_{1,2}
\end{aligned} \tag{5.111}$$

4. There are five non-coplanar classical regular magnetic orders. The first is the octahedral order, where  $\mathbf{S}_1(x, y) = (-1)^y \mathbf{n}_1$ ,  $\mathbf{S}_2(x, y) = (-1)^x \mathbf{n}_2$  and  $\mathbf{S}_3(x, y) = (-1)^{x+y} \mathbf{n}_3$ . Under the  $p6m$  symmetry,

$$\begin{aligned}
T_1 : \mathbf{n}_1 &\rightarrow \mathbf{n}_1, \quad \mathbf{n}_2 \rightarrow -\mathbf{n}_2, \quad \mathbf{n}_3 \rightarrow (-1)^{x+y} \mathbf{n}_3 \\
T_2 : \mathbf{n}_1 &\rightarrow -\mathbf{n}_1, \quad \mathbf{n}_2 \rightarrow \mathbf{n}_2, \quad \mathbf{n}_3 \rightarrow -\mathbf{n}_3 \\
C_6 : \mathbf{n}_1 &\rightarrow \mathbf{n}_3, \quad \mathbf{n}_2 \rightarrow \mathbf{n}_1, \quad \mathbf{n}_3 \rightarrow \mathbf{n}_2 \\
M : \mathbf{n}_1 &\rightarrow \mathbf{n}_2, \quad \mathbf{n}_2 \rightarrow \mathbf{n}_1, \quad \mathbf{n}_3 \rightarrow \mathbf{n}_3
\end{aligned} \tag{5.112}$$

5. The second non-coplanar classical regular magnetic order is the cuboc1 order, where  $\mathbf{S}_1(x, y) = (-1)^x \mathbf{n}_2 + (-1)^{x+y} \mathbf{n}_3$ ,  $\mathbf{S}_2(x, y) = (-1)^y \mathbf{n}_1 + (-1)^{x+y} \mathbf{n}_3$  and  $\mathbf{S}_3(x, y) = -(-1)^x \mathbf{n}_2 - (-1)^y \mathbf{n}_1$ . Under the  $p6m$  symmetry,

$$\begin{aligned}
T_1 : \mathbf{n}_1 &\rightarrow \mathbf{n}_1, & \mathbf{n}_2 &\rightarrow -\mathbf{n}_2, & \mathbf{n}_3 &\rightarrow -\mathbf{n}_3 \\
T_2 : \mathbf{n}_1 &\rightarrow -\mathbf{n}_1, & \mathbf{n}_2 &\rightarrow \mathbf{n}_2, & \mathbf{n}_3 &\rightarrow -\mathbf{n}_3 \\
C_6 : \mathbf{n}_1 &\rightarrow -\mathbf{n}_3, & \mathbf{n}_2 &\rightarrow -\mathbf{n}_1, & \mathbf{n}_3 &\rightarrow -\mathbf{n}_2 \\
M : \mathbf{n}_1 &\rightarrow \mathbf{n}_2, & \mathbf{n}_2 &\rightarrow \mathbf{n}_1, & \mathbf{n}_3 &\rightarrow \mathbf{n}_3
\end{aligned} \tag{5.113}$$

6. The third non-coplanar classical regular magnetic order is the cuboc2 order, where  $\mathbf{S}_1(x, y) = (-1)^x \mathbf{n}_2 - (-1)^{x+y} \mathbf{n}_3$ ,  $\mathbf{S}_2(x, y) = (-1)^y \mathbf{n}_1 + (-1)^{x+y} \mathbf{n}_3$  and  $\mathbf{S}_3(x, y) = (-1)^x \mathbf{n}_2 + (-1)^y \mathbf{n}_1$ . Under the  $p6m$  symmetry,

$$\begin{aligned}
T_1 : \mathbf{n}_1 &\rightarrow \mathbf{n}_1, & \mathbf{n}_2 &\rightarrow -\mathbf{n}_2, & \mathbf{n}_3 &\rightarrow -\mathbf{n}_3 \\
T_2 : \mathbf{n}_1 &\rightarrow -\mathbf{n}_1, & \mathbf{n}_2 &\rightarrow \mathbf{n}_2, & \mathbf{n}_3 &\rightarrow -\mathbf{n}_3 \\
C_6 : \mathbf{n}_1 &\rightarrow \mathbf{n}_3, & \mathbf{n}_2 &\rightarrow \mathbf{n}_1, & \mathbf{n}_3 &\rightarrow -\mathbf{n}_2 \\
M : \mathbf{n}_1 &\rightarrow \mathbf{n}_2, & \mathbf{n}_2 &\rightarrow \mathbf{n}_1, & \mathbf{n}_3 &\rightarrow -\mathbf{n}_3
\end{aligned} \tag{5.114}$$

7. The fourth non-coplanar is the  $\mathbf{q} = 0$  umbrella order, where  $\mathbf{S}_1(x, y) = \sin \theta \mathbf{n}_1 + \cos \theta \mathbf{n}_3$ ,  $\mathbf{S}_2(x, y) = -\frac{1}{2} \sin \theta \mathbf{n}_1 + \frac{\sqrt{3}}{2} \sin \theta \mathbf{n}_2 + \cos \theta \mathbf{n}_3$ , and  $\mathbf{S}_3(x, y) = -\frac{1}{2} \sin \theta \mathbf{n}_1 - \frac{\sqrt{3}}{2} \sin \theta \mathbf{n}_2 + \cos \theta \mathbf{n}_3$ , with  $\theta$  a free parameter. Under the  $p6m$  symmetry,

$$\begin{aligned}
T_{1,2} : \mathbf{n}_{1,2,3} &\rightarrow \mathbf{n}_{1,2,3} \\
C_6 : \mathbf{n}_1 &\rightarrow -\frac{1}{2} \mathbf{n}_1 - \frac{\sqrt{3}}{2} \mathbf{n}_2, & \mathbf{n}_2 &\rightarrow \frac{\sqrt{3}}{2} \mathbf{n}_1 - \frac{1}{2} \mathbf{n}_2, & \mathbf{n}_3 &\rightarrow \mathbf{n}_3 \\
M : \mathbf{n}_1 &\rightarrow -\frac{1}{2} \mathbf{n}_1 + \frac{\sqrt{3}}{2} \mathbf{n}_2, & \mathbf{n}_2 &\rightarrow \frac{\sqrt{3}}{2} \mathbf{n}_1 + \frac{1}{2} \mathbf{n}_2, & \mathbf{n}_3 &\rightarrow \mathbf{n}_3
\end{aligned} \tag{5.115}$$

8. The last non-coplanar classical regular magnetic order is the  $\mathbf{q} = \sqrt{3} \times \sqrt{3}$  umbrella order, where  $\mathbf{S}_1(x, y) = (-1)^{x+y} \cos \frac{\pi(x+y)}{3} \sin \theta \mathbf{n}_1 + (-1)^{x+y} \sin \frac{\pi(x+y)}{3} \sin \theta \mathbf{n}_2 + \cos \theta \mathbf{n}_3$ ,  $\mathbf{S}_2(x, y) = \mathbf{S}_1(x, y)$ , and  $\mathbf{S}_3(x, y) = -(-1)^{x+y} \cos \frac{\pi(x+y-1)}{3} \sin \theta \mathbf{n}_1 - (-1)^{x+y} \sin \frac{\pi(x+y-1)}{3} \sin \theta \mathbf{n}_2 + \cos \theta \mathbf{n}_3$ . Under the  $p6m$  symmetry,

$$\begin{aligned}
T_{1,2} : \mathbf{n}_1 &\rightarrow -\frac{1}{2} \mathbf{n}_1 - \frac{\sqrt{3}}{2} \mathbf{n}_2, & \mathbf{n}_2 &\rightarrow \frac{\sqrt{3}}{2} \mathbf{n}_1 - \frac{1}{2} \mathbf{n}_2, & \mathbf{n}_3 &\rightarrow \mathbf{n}_3 \\
C_6 : \mathbf{n}_1 &\rightarrow -\frac{1}{2} \mathbf{n}_1 + \frac{\sqrt{3}}{2} \mathbf{n}_2, & \mathbf{n}_2 &\rightarrow \frac{\sqrt{3}}{2} \mathbf{n}_1 + \frac{1}{2} \mathbf{n}_2, & \mathbf{n}_3 &\rightarrow \mathbf{n}_3 \\
M : \mathbf{n}_{1,2,3} &\rightarrow \mathbf{n}_{1,2,3}
\end{aligned} \tag{5.116}$$

Now we turn to the honeycomb lattice. Each unit cell of a honeycomb lattice includes two sites, so the spin configuration will be written in terms of  $\mathbf{S}_A(x, y)$  and  $\mathbf{S}_B(x, y)$ , where the  $A$  and  $B$  sublattice can be obtained by translating by  $\frac{2\mathbf{T}_1+\mathbf{T}_2}{3}$  and  $\frac{\mathbf{T}_1-\mathbf{T}_2}{3}$  from the  $C_6$  center, respectively.

1. There are two collinear classical regular magnetic orders. The first is the ferromagnetic order, where  $\mathbf{S}_A(x, y) = \mathbf{S}_B(x, y) = \mathbf{n}$ . Under the  $p6m$  symmetry,  $\mathbf{n}$  is invariant.
2. The second collinear classical regular magnetic order is the anti-ferromagnetic order, where  $\mathbf{S}_A(x, y) = -\mathbf{S}_B(x, y) = \mathbf{n}$ . Under the  $p6m$  symmetry,

$$\begin{aligned} T_{1,2} : \mathbf{n} &\rightarrow \mathbf{n} \\ C_6 : \mathbf{n} &\rightarrow -\mathbf{n} \\ M : \mathbf{n} &\rightarrow -\mathbf{n} \end{aligned} \tag{5.117}$$

3. There is a single coplanar classical regular magnetic order, the  $V$  order, where  $\mathbf{S}_A(x, y) = \cos\theta\mathbf{n}_1 - \sin\theta\mathbf{n}_2$  and  $\mathbf{S}_B(x, y) = \cos\theta\mathbf{n}_1 + \sin\theta\mathbf{n}_2$ , with  $\theta$  a free parameter. Under the  $p6m$  symmetry,

$$\begin{aligned} T_{1,2} : \mathbf{n}_{1,2} &\rightarrow \mathbf{n}_{1,2} \\ C_6 : \mathbf{n}_1 &\rightarrow \mathbf{n}_1, \quad \mathbf{n}_2 \rightarrow -\mathbf{n}_2 \\ M : \mathbf{n}_1 &\rightarrow \mathbf{n}_1, \quad \mathbf{n}_2 \rightarrow -\mathbf{n}_2 \end{aligned} \tag{5.118}$$

4. There are two non-coplanar classical regular magnetic orders. The first is the cubic order, where  $\mathbf{S}_A(x, y) = (-1)^x\mathbf{n}_1 + (-1)^y\mathbf{n}_2 + (-1)^{x+y}\mathbf{n}_3$  and  $\mathbf{S}_B(x, y) = (-1)^x\mathbf{n}_1 - (-1)^y\mathbf{n}_2 + (-1)^{x+y}\mathbf{n}_3$ . Under the  $p6m$  symmetry,

$$\begin{aligned} T_1 : \mathbf{n}_1 &\rightarrow -\mathbf{n}_1, \quad \mathbf{n}_2 \rightarrow \mathbf{n}_2, \quad \mathbf{n}_3 \rightarrow -\mathbf{n}_3 \\ T_2 : \mathbf{n}_1 &\rightarrow \mathbf{n}_1, \quad \mathbf{n}_2 \rightarrow -\mathbf{n}_2, \quad \mathbf{n}_3 \rightarrow -\mathbf{n}_3 \\ C_6 : \mathbf{n}_1 &\rightarrow \mathbf{n}_2, \quad \mathbf{n}_2 \rightarrow -\mathbf{n}_3, \quad \mathbf{n}_3 \rightarrow \mathbf{n}_1 \\ M : \mathbf{n}_1 &\rightarrow \mathbf{n}_2, \quad \mathbf{n}_2 \rightarrow \mathbf{n}_1, \quad \mathbf{n}_3 \rightarrow -\mathbf{n}_3 \end{aligned} \tag{5.119}$$

5. The second non-coplanar classical regular magnetic order is the tetrahedral order, where  $\mathbf{S}_A(x, y) = (-1)^x\mathbf{n}_1 + (-1)^y\mathbf{n}_2 + (-1)^{x+y}\mathbf{n}_3$  and  $\mathbf{S}_B(x, y) = -(-1)^x\mathbf{n}_1 +$

$(-1)^y \mathbf{n}_2 - (-1)^{x+y} \mathbf{n}_3$ . Under the  $p6m$  symmetry,

$$\begin{aligned}
T_1 : \mathbf{n}_1 &\rightarrow -\mathbf{n}_1, & \mathbf{n}_2 &\rightarrow \mathbf{n}_2, & \mathbf{n}_3 &\rightarrow -\mathbf{n}_3 \\
T_2 : \mathbf{n}_1 &\rightarrow \mathbf{n}_1, & \mathbf{n}_2 &\rightarrow -\mathbf{n}_2, & \mathbf{n}_3 &\rightarrow -\mathbf{n}_3 \\
C_6 : \mathbf{n}_1 &\rightarrow -\mathbf{n}_2, & \mathbf{n}_2 &\rightarrow \mathbf{n}_3, & \mathbf{n}_3 &\rightarrow -\mathbf{n}_1 \\
M : \mathbf{n}_1 &\rightarrow -\mathbf{n}_2, & \mathbf{n}_2 &\rightarrow -\mathbf{n}_1, & \mathbf{n}_3 &\rightarrow \mathbf{n}_3
\end{aligned} \tag{5.120}$$

Finally, we discuss the square lattice. We will denote the position of a site by its coordinates in the basis of translation vectors of  $T_{1,2}$  (see Fig. 2.2). such that  $\mathbf{r} = x\mathbf{T}_1 + y\mathbf{T}_2$ , where  $\mathbf{T}_{1,2}$  is the translation vector of  $T_{1,2}$ . Under the  $p4m$  symmetry,

$$\begin{aligned}
T_1 : (x, y) &\rightarrow (x + 1, y) \\
T_2 : (x, y) &\rightarrow (x, y + 1) \\
C_4 : (x, y) &\rightarrow (-y, x) \\
M : (x, y) &\rightarrow (-x, y)
\end{aligned} \tag{5.121}$$

1. There are two collinear classical regular magnetic orders. The first is the ferromagnetic order, where  $\mathbf{S}(x, y) = \mathbf{n}$ . Under the  $p4m$  symmetry,  $\mathbf{n}$  is invariant.
2. The second collinear classical regular magnetic order is the anti-ferromagnetic order, where  $\mathbf{S}(x, y) = (-1)^{x+y} \mathbf{n}$ . Under the  $p4m$  symmetry,

$$\begin{aligned}
T_{1,2} : \mathbf{n} &\rightarrow -\mathbf{n} \\
C_4 : \mathbf{n} &\rightarrow -\mathbf{n} \\
M : \mathbf{n} &\rightarrow \mathbf{n}
\end{aligned} \tag{5.122}$$

3. There are two coplanar classical regular magnetic orders. The first is the orthogonal order, where  $\mathbf{S}(x, y) = \frac{(-1)^x + (-1)^y}{2} \mathbf{n}_1 + \frac{-(-1)^x + (-1)^y}{2} \mathbf{n}_2$ . Under the  $p4m$  symmetry,

$$\begin{aligned}
T_1 : \mathbf{n}_1 &\rightarrow \mathbf{n}_2, & \mathbf{n}_2 &\rightarrow \mathbf{n}_1 \\
T_2 : \mathbf{n}_1 &\rightarrow -\mathbf{n}_2, & \mathbf{n}_2 &\rightarrow -\mathbf{n}_1 \\
C_4 : \mathbf{n}_1 &\rightarrow \mathbf{n}_1, & \mathbf{n}_2 &\rightarrow -\mathbf{n}_2 \\
M : \mathbf{n}_{1,2} &\rightarrow \mathbf{n}_{1,2}
\end{aligned} \tag{5.123}$$

4. The second coplanar classical regular magnetic order is the  $V$  order, where  $\mathbf{S}(x, y) = \cos \theta \mathbf{n}_1 - (-1)^{x+y} \sin \theta \mathbf{n}_2$ , where  $\theta$  a free parameter. Under the  $p4m$  symmetry,

$$\begin{aligned}
T_{1,2} : \mathbf{n}_1 &\rightarrow \mathbf{n}_1, & \mathbf{n}_2 &\rightarrow -\mathbf{n}_2 \\
C_4 : \mathbf{n}_{1,2} &\rightarrow \mathbf{n}_{1,2} \\
M : \mathbf{n}_{1,2} &\rightarrow \mathbf{n}_{1,2}
\end{aligned} \tag{5.124}$$

5. There are two non-coplanar classical regular magnetic orders. The first is the tetrahedral umbrella order (also known as the AF umbrella order), where  $\mathbf{S}(x, y) = \frac{(-1)^x \sin \theta}{\sqrt{2}} \mathbf{n}_1 - \frac{(-1)^y \sin \theta}{\sqrt{2}} \mathbf{n}_2 - (-1)^{x+y} \cos \theta \mathbf{n}_3$ , with  $\theta$  a free parameter. Under the  $p4m$  symmetry,

$$\begin{aligned}
T_1 : \mathbf{n}_1 &\rightarrow -\mathbf{n}_1, & \mathbf{n}_2 &\rightarrow \mathbf{n}_2, & \mathbf{n}_3 &\rightarrow -\mathbf{n}_3 \\
T_2 : \mathbf{n}_1 &\rightarrow \mathbf{n}_1, & \mathbf{n}_2 &\rightarrow -\mathbf{n}_2, & \mathbf{n}_3 &\rightarrow -\mathbf{n}_3 \\
C_4 : \mathbf{n}_1 &\rightarrow -\mathbf{n}_2, & \mathbf{n}_2 &\rightarrow -\mathbf{n}_1, & \mathbf{n}_3 &\rightarrow \mathbf{n}_3 \\
M : \mathbf{n}_{1,2,3} &\rightarrow \mathbf{n}_{1,2,3}
\end{aligned} \tag{5.125}$$

6. The second non-coplanar classical regular magnetic order is the umbrella order (also known as the F umbrella order), where  $\mathbf{S}(x, y) = \cos \theta \mathbf{n}_1 + \frac{(-1)^x \sin \theta}{\sqrt{2}} \mathbf{n}_2 + \frac{(-1)^y \sin \theta}{\sqrt{2}} \mathbf{n}_3$ . Under the  $p4m$  symmetry,

$$\begin{aligned}
T_1 : \mathbf{n}_1 &\rightarrow \mathbf{n}_1, & \mathbf{n}_2 &\rightarrow -\mathbf{n}_2, & \mathbf{n}_3 &\rightarrow \mathbf{n}_3 \\
T_2 : \mathbf{n}_1 &\rightarrow \mathbf{n}_1, & \mathbf{n}_2 &\rightarrow \mathbf{n}_2, & \mathbf{n}_3 &\rightarrow -\mathbf{n}_3 \\
C_4 : \mathbf{n}_1 &\rightarrow \mathbf{n}_1, & \mathbf{n}_2 &\rightarrow \mathbf{n}_3, & \mathbf{n}_3 &\rightarrow \mathbf{n}_2 \\
M : \mathbf{n}_{1,2,3} &\rightarrow \mathbf{n}_{1,2,3}
\end{aligned} \tag{5.126}$$

## 5.E Stability of DSL realizations on NaYbO<sub>2</sub> and twisted bilayer WSe<sub>2</sub>

In this appendix, we discuss the stability of a few more examples of DSL realizations on systems with spin-orbit coupling (SOC). The specific systems we have in mind are NaYbO<sub>2</sub> and twisted bilayer WSe<sub>2</sub> (tWSe<sub>2</sub>). Recently, it was pointed out that tWSe<sub>2</sub> is a good quantum simulator of triangular lattice Hubbard model, which can be effectively described by a triangular lattice spin-1/2 system in the strong coupling regime [153–155].

The symmetries of NaYbO<sub>2</sub> are given in Eq. (5.25). The symmetries of tWSe<sub>2</sub> are

$$T_{1,2}, C_3 \equiv C_6^2, SO(2), \mathcal{T} \tag{5.127}$$

where  $SO(2)$  is a reduced spin rotational symmetry<sup>11</sup>.

---

<sup>11</sup>These are the symmetries of tWSe<sub>2</sub> in the presence of a displacement field, which is satisfied in the generic experimental setting. If there is no displacement field, there is an extra mirror symmetry.

On triangular lattice spin-1/2 systems with the full  $p6m \times O(3)^T$  symmetry, our exhaustive search finds 3 realizations of DSL, given by Eqs. (5.24), (5.72) and (5.73). Using these symmetry actions, it is straightforward to see that for all three realizations, the remaining symmetries of NaYbO<sub>2</sub> are sufficient to forbid all relevant operators of DSL listed in Sec. 3.4.2. However, for the symmetry setting of tWSe<sub>2</sub> and for all three realizations, the  $(A_L, A_R)$  operator (the fermion mass that transforms in the adjoint representation of the flavor symmetry) is always symmetry-allowed and will destabilize the DSL. This means if a DSL is stably realized in tWSe<sub>2</sub>, that realization cannot be compatible with a full  $p6m \times O(3)^T$  symmetry.

# Chapter 6

## Summary and Discussion

In summary, we have developed systematic methods to calculate the anomaly of various systems relevant to condensed matter physics, primarily in  $(2 + 1)$ -d, including i) deriving the topological partition functions corresponding to the LSM constraints in a large class of systems relevant to the study of quantum magnetism, ii) anomaly of recently-proposed Stiefel Liquid, and iii) systematic methods to calculate the anomaly of bosonic topological orders. We then apply these results, and, motivated by the hypothesis of emergibility, use the method of anomaly matching to study the emergibility of various Stiefel liquids in lattice spin systems, and discuss many interesting realizations.

Being able to calculate the anomaly is extremely useful, because the anomaly is powerful in constraining the possible low-energy dynamics of a strongly interacting field theory, which is often challenging to understand by other means. For example, if a strongly interacting field theory with some symmetry has an anomaly different from the ones we calculate for some IR phase, this field theory cannot flow to this IR phase at low energies under renormalization group. Moreover, according to the hypothesis of emergibility, the ability to calculate the anomaly of a quantum phase or phase transition is crucial to understand whether this phase or transition can emerge in a given quantum many-body system, whose robust microscopic properties are compactly encoded in their Lieb-Schultz-Mattis-type anomalies. Going one step further, this hypothesis provides a possible route to solve the open problem of classifying possible phase diagrams with given lattice symmetries, in a way similar to the classification of various symmetry-enriched quantum criticality. We believe that this work is an important step towards these goals.

We remark that our philosophy to study the emergibility of a quantum phase or phase transition is different from the conventional one. Our strategy is based on anomaly-



matching, while the conventional one is based on explicit constructions of this phase or phase transition, often in terms of a mean field (including parton gauge mean field) or a wave function. We believe that the anomaly-based strategy captures the intrinsic essence of emergibility. After all, any mean-field construction is also a way of doing anomaly-matching in disguise, and such a construction by itself cannot rigorously prove the emergibility. On the other hand, although a microscopic wave function can guarantee the emergibility, it is generically difficult to read off the universal physics encoded in a wave function, and there is no guarantee that a proposed wave function indeed describes the quantum phase or phase transition of interest - in fact, in general there is no guarantee that such a wave function could be realized as the ground state of any local Hamiltonian. So the significance of this work is not only reflected by the specific results, but also by the fact that it demonstrates the feasibility of the anomaly-based framework of emergibility, and the fact that this framework can yield interesting results not envisioned before. This anomaly-based framework of emergibility is established for lattice spin systems in this paper. An interesting and important open problem is to generalize the topological characterizations of LSM constraints to other systems, and apply the results to study the emergibility of other quantum phases and phase transitions. Systems of particular relevance are those in  $(3+1)$ -d, those with spin-orbit coupling, those with a filling constraint due to a  $U(1)$  symmetry, those with long-range interactions, those with a constrained Hilbert space, fermionic systems, etc. We leave these for future work.

We have assumed that the hypothesis of emergibility is a necessary and sufficient condition of emergibility. As mentioned before, its necessity has been established, while the sufficiency is a reasonable conjecture. It is important to further justify or disprove (the sufficiency of) this hypothesis. If it is disproved, it will be extremely interesting and valuable to identify a correct necessary and sufficient condition of emergibility.

# References

- [1] W. Ye, M. Guo, Y.-C. He, C. Wang, and L. Zou, Topological characterization of Lieb-Schultz-Mattis constraints and applications to symmetry-enriched quantum criticality, *SciPost Physics* **13**, 066 (2022), [arXiv:2111.12097 \[cond-mat.str-el\]](#) .
- [2] W. Ye and L. Zou, Anomaly of  $(2 + 1)$ -Dimensional Symmetry-Enriched Topological Order from  $(3 + 1)$ -Dimensional Topological Quantum Field Theory, [arXiv e-prints](#) , [arXiv:2210.02444 \(2022\)](#), [arXiv:2210.02444 \[cond-mat.str-el\]](#) .
- [3] W. Ye, S.-S. Lee, and L. Zou, Ultraviolet-Infrared Mixing in Marginal Fermi Liquids, *Phys. Rev. Lett.* **128**, 106402 (2022), [arXiv:2109.00004 \[cond-mat.str-el\]](#) .
- [4] C.-J. Lin, W. Ye, Y. Zou, S. Sang, and T. H. Hsieh, Probing sign structure using measurement-induced entanglement, *Quantum* **7**, 910 (2023), [arXiv:2205.05692 \[quant-ph\]](#) .
- [5] L. Landau, E. Lifshits, L. Pitaevskiĭ, J. Sykes, and M. Kearsley, *Statistical Physics*, Course of theoretical physics No. Vol 1 (Pergamon Press, 1980).
- [6] S. Sachdev, *Quantum Phase Transitions* (Cambridge University Press, 2001).
- [7] X. Wen, *Quantum Field Theory of Many-Body Systems: From the Origin of Sound to an Origin of Light and Electrons*, Oxford Graduate Texts (OUP Oxford, 2004).
- [8] L. Savary and L. Balents, Quantum spin liquids: a review, *Reports on Progress in Physics* **80**, 016502 (2017).
- [9] Y. Zhou, K. Kanoda, and T.-K. Ng, Quantum spin liquid states, *Reviews of Modern Physics* **89**, 025003 (2017), [arXiv:1607.03228 \[cond-mat.str-el\]](#) .
- [10] C. Broholm, R. J. Cava, S. A. Kivelson, D. G. Nocera, M. R. Norman, and T. Senthil, Quantum Spin Liquids, *Science* **367**, eaay0668 (2020), [arXiv:1905.07040 \[cond-mat.str-el\]](#) .

- [11] B. Bakalov and A. Kirillov, *Lectures on Tensor Categories and Modular Functors*, Translations of Mathematical Monographs (American Mathematical Society, 2001).
- [12] V. Turaev, *Quantum Invariants of Knots and 3-manifolds*, De Gruyter studies in mathematics (W. de Gruyter, 1994).
- [13] T. Lan and X.-G. Wen, Classification of 3 +1 D Bosonic Topological Orders (II): The Case When Some Pointlike Excitations Are Fermions, *Physical Review X* **9**, 021005 (2019), [arXiv:1801.08530 \[cond-mat.str-el\]](#) .
- [14] T. Johnson-Freyd and M. Yu, Topological Orders in (4+1)-Dimensions, *SciPost Phys.* **13**, 068 (2022), [arXiv:2104.04534 \[hep-th\]](#) .
- [15] L. Zou, Y.-C. He, and C. Wang, Stiefel Liquids: Possible Non-Lagrangian Quantum Criticality from Intertwined Orders, *Physical Review X* **11**, 031043 (2021), [arXiv:2101.07805 \[cond-mat.str-el\]](#) .
- [16] J. Wess and B. Zumino, Consequences of anomalous ward identities, *Physics Letters B* **37**, 95 – 97 (1971).
- [17] E. Witten, Global Aspects of Current Algebra, *Nucl. Phys. B* **223**, 422–432 (1983).
- [18] T. Senthil, A. Vishwanath, L. Balents, S. Sachdev, and M. P. A. Fisher, Deconfined Quantum Critical Points, *Science* **303**, 1490–1494 (2004), [arXiv:cond-mat/0311326 \[cond-mat.str-el\]](#) .
- [19] T. Senthil, L. Balents, S. Sachdev, A. Vishwanath, and M. P. A. Fisher, Quantum criticality beyond the Landau-Ginzburg-Wilson paradigm, *Phys. Rev. B* **70**, 144407 (2004), [arXiv:cond-mat/0312617 \[cond-mat.str-el\]](#) .
- [20] T. Senthil and M. P. A. Fisher, Competing orders, nonlinear sigma models, and topological terms in quantum magnets, *Phys. Rev. B* **74**, 064405 (2006), [arXiv:cond-mat/0510459 \[cond-mat.str-el\]](#) .
- [21] C. Wang, A. Nahum, M. A. Metlitski, C. Xu, and T. Senthil, Deconfined Quantum Critical Points: Symmetries and Dualities, *Physical Review X* **7**, 031051 (2017), [arXiv:1703.02426 \[cond-mat.str-el\]](#) .
- [22] I. Affleck and J. B. Marston, Large-n limit of the heisenberg-hubbard model: Implications for high- $T_c$  superconductors, *Phys. Rev. B* **37**, 3774–3777 (1988).

- [23] X.-G. Wen and P. A. Lee, Theory of Underdoped Cuprates, *Phys. Rev. Lett.* **76**, 503–506 (1996), [arXiv:cond-mat/9506065 \[cond-mat\]](#) .
- [24] M. B. Hastings, Dirac structure, rvb, and goldstone modes in the kagomé antiferromagnet, *Phys. Rev. B* **63**, 014413 (2000).
- [25] G. Hooft, Naturalness, chiral symmetry, and spontaneous chiral symmetry breaking, in *Recent Developments in Gauge Theories*, edited by G. Hooft, C. Itzykson, A. Jaffe, H. Lehmann, P. K. Mitter, I. M. Singer, and R. Stora (Springer US, Boston, MA, 1980) pp. 135–157.
- [26] X. Chen, Z.-C. Gu, Z.-X. Liu, and X.-G. Wen, Symmetry protected topological orders and the group cohomology of their symmetry group, *Phys. Rev. B* **87**, 155114 (2013), [arXiv:1106.4772 \[cond-mat.str-el\]](#) .
- [27] A. Kapustin, Symmetry Protected Topological Phases, Anomalies, and Cobordisms: Beyond Group Cohomology, arXiv e-prints, [arXiv:1403.1467 \(2014\)](#), [arXiv:1403.1467 \[cond-mat.str-el\]](#) .
- [28] X.-G. Wen, Classifying gauge anomalies through symmetry-protected trivial orders and classifying gravitational anomalies through topological orders, *Phys. Rev. D* **88**, 045013 (2013), [arXiv:1303.1803 \[hep-th\]](#) .
- [29] D. Gaiotto, A. Kapustin, Z. Komargodski, and N. Seiberg, Theta, time reversal and temperature, *Journal of High Energy Physics* **2017**, 91 (2017), [arXiv:1703.00501 \[hep-th\]](#) .
- [30] Z. Komargodski and N. Seiberg, A symmetry breaking scenario for QCD<sub>3</sub>, *Journal of High Energy Physics* **2018**, 109 (2018), [arXiv:1706.08755 \[hep-th\]](#) .
- [31] E. Lieb, T. Schultz, and D. Mattis, Two soluble models of an antiferromagnetic chain, *Annals of Physics* **16**, 407 – 466 (1961).
- [32] M. Oshikawa, Commensurability, Excitation Gap, and Topology in Quantum Many-Particle Systems on a Periodic Lattice, *Phys. Rev. Lett.* **84**, 1535–1538 (2000), [arXiv:cond-mat/9911137 \[cond-mat.str-el\]](#) .
- [33] M. B. Hastings, Lieb-Schultz-Mattis in higher dimensions, *Phys. Rev. B* **69**, 104431 (2004), [arXiv:cond-mat/0305505 \[cond-mat.str-el\]](#) .

- [34] M. Cheng, M. Zaletel, M. Barkeshli, A. Vishwanath, and P. Bonderson, Translational Symmetry and Microscopic Constraints on Symmetry-Enriched Topological Phases: A View from the Surface, *Physical Review X* **6**, 041068 (2016), [arXiv:1511.02263 \[cond-mat.str-el\]](#) .
- [35] H. C. Po, H. Watanabe, C.-M. Jian, and M. P. Zaletel, Lattice Homotopy Constraints on Phases of Quantum Magnets, *Phys. Rev. Lett.* **119**, 127202 (2017), [arXiv:1703.06882 \[cond-mat.str-el\]](#) .
- [36] C.-M. Jian, Z. Bi, and C. Xu, Lieb-Schultz-Mattis theorem and its generalizations from the perspective of the symmetry-protected topological phase, *Phys. Rev. B* **97**, 054412 (2018), [arXiv:1705.00012 \[cond-mat.str-el\]](#) .
- [37] G. Y. Cho, C.-T. Hsieh, and S. Ryu, Anomaly manifestation of Lieb-Schultz-Mattis theorem and topological phases, *Phys. Rev. B* **96**, 195105 (2017), [arXiv:1705.03892 \[cond-mat.str-el\]](#) .
- [38] M. A. Metlitski and R. Thorngren, Intrinsic and emergent anomalies at deconfined critical points, *Phys. Rev. B* **98**, 085140 (2018), [arXiv:1707.07686 \[cond-mat.str-el\]](#) .
- [39] S.-J. Huang, H. Song, Y.-P. Huang, and M. Hermele, Building crystalline topological phases from lower-dimensional states, *Phys. Rev. B* **96**, 205106 (2017), [arXiv:1705.09243 \[cond-mat.str-el\]](#) .
- [40] D. V. Else and R. Thorngren, Topological theory of Lieb-Schultz-Mattis theorems in quantum spin systems, *Phys. Rev. B* **101**, 224437 (2020), [arXiv:1907.08204 \[cond-mat.str-el\]](#) .
- [41] M. P. Zaletel and A. Vishwanath, Constraints on Topological Order in Mott Insulators, *Phys. Rev. Lett.* **114**, 077201 (2015), [arXiv:1410.2894 \[cond-mat.str-el\]](#) .
- [42] Y. Qi, M. Cheng, and C. Fang, Symmetry fractionalization of visons in  $\mathbb{Z}_2$  spin liquids, arXiv e-prints , [arXiv:1509.02927 \(2015\)](#), [arXiv:1509.02927 \[cond-mat.str-el\]](#) .
- [43] Y. Qi and M. Cheng, Classification of symmetry fractionalization in gapped  $\mathbb{Z}_2$  spin liquids, *Phys. Rev. B* **97**, 115138 (2018), [arXiv:1606.04544 \[cond-mat.str-el\]](#) .
- [44] S.-Q. Ning, L. Zou, and M. Cheng, Fractionalization and anomalies in symmetry-enriched U(1) gauge theories, *Physical Review Research* **2**, 043043 (2020), [arXiv:1905.03276 \[cond-mat.str-el\]](#) .

- [45] C. Wang and T. Senthil, Interacting fermionic topological insulators/superconductors in three dimensions, *Phys. Rev. B* **89**, 195124 (2014), [arXiv:1401.1142 \[cond-mat.str-el\]](#) .
- [46] H. Watanabe, H. C. Po, A. Vishwanath, and M. Zaletel, Filling constraints for spin-orbit coupled insulators in symmorphic and nonsymmorphic crystals, *Proceedings of the National Academy of Science* **112**, 14551–14556 (2015), [arXiv:1505.04193 \[cond-mat.str-el\]](#) .
- [47] I. Kimchi, S. A. Parameswaran, A. M. Turner, F. Wang, and A. Vishwanath, Featureless and nonfractionalized Mott insulators on the honeycomb lattice at 1/2 site filling, *Proceedings of the National Academy of Science* **110**, 16378–16383 (2013), [arXiv:1207.0498 \[cond-mat.str-el\]](#) .
- [48] C.-M. Jian and M. Zaletel, Existence of featureless paramagnets on the square and the honeycomb lattices in 2+1 dimensions, *Phys. Rev. B* **93**, 035114 (2016), [arXiv:1507.00361 \[cond-mat.str-el\]](#) .
- [49] P. Kim, H. Lee, S. Jiang, B. Ware, C.-M. Jian, M. Zaletel, J. H. Han, and Y. Ran, Featureless quantum insulator on the honeycomb lattice, *Phys. Rev. B* **94**, 064432 (2016), [arXiv:1509.04358 \[cond-mat.str-el\]](#) .
- [50] K. Latimer and C. Wang, Correlated fragile topology: A parton approach, *Phys. Rev. B* **103**, 045128 (2021), [arXiv:2007.15605 \[cond-mat.str-el\]](#) .
- [51] R. Dijkgraaf and E. Witten, Topological gauge theories and group cohomology, *Communications in Mathematical Physics* **129**, 393 – 429 (1990).
- [52] C. Wang and M. Levin, Braiding Statistics of Loop Excitations in Three Dimensions, *Phys. Rev. Lett.* **113**, 080403 (2014), [arXiv:1403.7437 \[cond-mat.str-el\]](#) .
- [53] R. Thorngren and D. V. Else, Gauging spatial symmetries and the classification of topological crystalline phases, *Phys. Rev. X* **8**, 011040 (2018), [arXiv:1612.00846 \[cond-mat.str-el\]](#) .
- [54] C. Wang and T. Senthil, Boson topological insulators: A window into highly entangled quantum phases, *Phys. Rev. B* **87**, 235122 (2013), [arXiv:1302.6234 \[cond-mat.str-el\]](#) .
- [55] C. Wang and T. Senthil, Time-Reversal Symmetric U(1) Quantum Spin Liquids, *Physical Review X* **6**, 011034 (2016), [arXiv:1505.03520 \[cond-mat.str-el\]](#) .

- [56] L. Zou, C. Wang, and T. Senthil, Symmetry enriched U(1) quantum spin liquids, [Phys. Rev. B \*\*97\*\*, 195126 \(2018\)](#), [arXiv:1710.00743 \[cond-mat.str-el\]](#) .
- [57] L. Zou, Bulk characterization of topological crystalline insulators: Stability under interactions and relations to symmetry enriched U (1) quantum spin liquids, [Phys. Rev. B \*\*97\*\*, 045130 \(2018\)](#), [arXiv:1711.03090 \[cond-mat.str-el\]](#) .
- [58] P.-S. Hsin and A. Turzillo, Symmetry-enriched quantum spin liquids in (3 + 1)d, [Journal of High Energy Physics \*\*2020\*\*, 22 \(2020\)](#), [arXiv:1904.11550 \[cond-mat.str-el\]](#) .
- [59] T. T. Wu and C. N. Yang, Concept of nonintegrable phase factors and global formulation of gauge fields, [Phys. Rev. D \*\*12\*\*, 3845–3857 \(1975\)](#).
- [60] M. Barkeshli, P. Bonderson, M. Cheng, and Z. Wang, Symmetry Fractionalization, Defects, and Gauging of Topological Phases, [Phys. Rev. B \*\*100\*\*, 115147 \(2019\)](#), [arXiv:1410.4540 \[cond-mat.str-el\]](#) .
- [61] N. Tarantino, N. H. Lindner, and L. Fidkowski, Symmetry fractionalization and twist defects, [New Journal of Physics \*\*18\*\*, 035006 \(2016\)](#), [arXiv:1506.06754 \[cond-mat.str-el\]](#) .
- [62] Z. Song, C. Fang, and Y. Qi, Real-space recipes for general topological crystalline states, [Nature Communications \*\*11\*\*, 4197 \(2020\)](#), [arXiv:1810.11013 \[cond-mat.str-el\]](#) .
- [63] J.-H. Zhang, S. Yang, Y. Qi, and Z.-C. Gu, Real-space construction of crystalline topological superconductors and insulators in 2D interacting fermionic systems, [Physical Review Research \*\*4\*\*, 033081 \(2022\)](#), [arXiv:2012.15657 \[cond-mat.str-el\]](#) .
- [64] H. Song, S.-J. Huang, L. Fu, and M. Hermele, Topological Phases Protected by Point Group Symmetry, [Physical Review X \*\*7\*\*, 011020 \(2017\)](#), [arXiv:1604.08151 \[cond-mat.str-el\]](#) .
- [65] T. Senthil, J. B. Marston, and M. P. A. Fisher, Spin quantum Hall effect in unconventional superconductors, [Phys. Rev. B \*\*60\*\*, 4245–4254 \(1999\)](#), [arXiv:cond-mat/9902062 \[cond-mat.supr-con\]](#) .
- [66] X. Chen, Y.-M. Lu, and A. Vishwanath, Symmetry-protected topological phases from decorated domain walls, [Nature Communications \*\*5\*\*, 3507 \(2014\)](#), [arXiv:1303.4301 \[cond-mat.str-el\]](#) .

- [67] K. Brown, *Cohomology of Groups*, Graduate Texts in Mathematics (Springer New York, 2012).
- [68] C. Weibel, *An Introduction to Homological Algebra*, Cambridge Studies in Advanced Mathematics (Cambridge University Press, 1995).
- [69] J. Kirk, J. Davis, P. Kirk, and A. M. Society, *Lecture Notes in Algebraic Topology*, Crm Proceedings & Lecture Notes (American Mathematical Society, 2001).
- [70] M. Nakahara, *Geometry, Topology and Physics, Second Edition*, Graduate student series in physics (Taylor & Francis, 2003).
- [71] Y. Lee, K. Ohmori, and Y. Tachikawa, Revisiting Wess-Zumino-Witten terms, *SciPost Physics* **10**, 061 (2021), [arXiv:2009.00033 \[hep-th\]](#) .
- [72] E. Witten, On Holomorphic factorization of WZW and coset models, *Commun. Math. Phys.* **144**, 189–212 (1992).
- [73] D. S. Freed, Pions and Generalized Cohomology, *J. Diff. Geom.* **80**, 45–77 (2008), [arXiv:hep-th/0607134](#) .
- [74] V. Gorbenko, S. Rychkov, and B. Zan, Walking, weak first-order transitions, and complex CFTs, *Journal of High Energy Physics* **2018**, 108 (2018), [arXiv:1807.11512 \[hep-th\]](#) .
- [75] R. Ma and C. Wang, Theory of deconfined pseudocriticality, *Phys. Rev. B* **102**, 020407 (2020), [arXiv:1912.12315 \[cond-mat.str-el\]](#) .
- [76] A. Nahum, Note on Wess-Zumino-Witten models and quasiuniversality in 2 +1 dimensions, *Phys. Rev. B* **102**, 201116 (2020), [arXiv:1912.13468 \[cond-mat.str-el\]](#) .
- [77] Y.-C. He, J. Rong, and N. Su, Non-Wilson-Fisher kinks of  $O(N)$  numerical bootstrap: from the deconfined phase transition to a putative new family of CFTs, *SciPost Physics* **10**, 115 (2021), [arXiv:2005.04250 \[hep-th\]](#) .
- [78] D. B. Kaplan, J.-W. Lee, D. T. Son, and M. A. Stephanov, Conformality lost, *Phys. Rev. D* **80**, 125005 (2009).
- [79] V. Borokhov, A. Kapustin, and X. Wu, Topological Disorder Operators in Three-Dimensional Conformal Field Theory, *Journal of High Energy Physics* **11**, 049 (2002), [hep-th/0206054](#) .



- [80] E. Dyer, M. Mezei, and S. S. Pufu, Monopole Taxonomy in Three-Dimensional Conformal Field Theories, arXiv e-prints (2013), [arXiv:1309.1160 \[hep-th\]](#) .
- [81] X.-Y. Song, Y.-C. He, A. Vishwanath, and C. Wang, From spinon band topology to the symmetry quantum numbers of monopoles in dirac spin liquids, [Phys. Rev. X](#) **10**, 011033 (2020), [arXiv:1811.11182 \[cond-mat.str-el\]](#) .
- [82] Y.-C. He, J. Rong, and N. Su, Conformal bootstrap bounds for the U(1) Dirac spin liquid and N=7 Stiefel liquid, [SciPost Physics](#) **13**, 014 (2022), [arXiv:2107.14637 \[cond-mat.str-el\]](#) .
- [83] X.-Y. Song, C. Wang, A. Vishwanath, and Y.-C. He, Unifying description of competing orders in two-dimensional quantum magnets, [Nature Communications](#) **10**, 4254 (2019), [arXiv:1811.11186 \[cond-mat.str-el\]](#) .
- [84] A. Kitaev, Anyons in an exactly solved model and beyond, [Annals of Physics](#) **321**, 2–111 (2006), [arXiv:cond-mat/0506438 \[cond-mat.mes-hall\]](#) .
- [85] L. Kong and Z.-H. Zhang, An invitation to topological orders and category theory, arXiv e-prints , [arXiv:2205.05565 \(2022\)](#), [arXiv:2205.05565 \[cond-mat.str-el\]](#) .
- [86] P. Etingof, S. Gelaki, D. Nikshych, and V. Ostrik, *Tensor Categories*, Mathematical Surveys and Monographs (American Mathematical Society, 2016).
- [87] P. Selinger, A survey of graphical languages for monoidal categories, in *New Structures for Physics*, edited by B. Coecke (Springer Berlin Heidelberg, Berlin, Heidelberg, 2011) pp. 289–355.
- [88] P. Etingof, D. Nikshych, V. Ostrik, and w. a. a. b. Ehud Meir, Fusion categories and homotopy theory, [Quantum topology](#) **1**, 209–273 (2010), [arXiv:0909.3140 \[math.QA\]](#) .
- [89] F. Benini, C. Córdova, and P.-S. Hsin, On 2-group global symmetries and their anomalies, [Journal of High Energy Physics](#) **2019**, 118 (2019), [arXiv:1803.09336 \[hep-th\]](#) .
- [90] P. Bonderson, K. Shtengel, and J. K. Slingerland, Interferometry of non-Abelian anyons, [Annals of Physics](#) **323**, 2709–2755 (2008), [arXiv:0707.4206 \[quant-ph\]](#) .
- [91] L. Crane and D. N. Yetter, A categorical construction of 4D TQFTs, arXiv e-prints , [hep-th/9301062 \(1993\)](#), [arXiv:hep-th/9301062 \[hep-th\]](#) .

- [92] D. Bulmash and M. Barkeshli, Absolute anomalies in (2+1)D symmetry-enriched topological states and exact (3+1)D constructions, [Physical Review Research](#) **2**, 043033 (2020), [arXiv:2003.11553 \[cond-mat.str-el\]](#) .
- [93] K. Walker, TQFTs <https://canyon23.net/math/tc.pdf>.
- [94] M. Barkeshli, P. Bonderson, M. Cheng, C.-M. Jian, and K. Walker, Reflection and Time Reversal Symmetry Enriched Topological Phases of Matter: Path Integrals, Non-orientable Manifolds, and Anomalies, [Communications in Mathematical Physics](#) **374**, 1021–1124 (2019), [arXiv:1612.07792 \[cond-mat.str-el\]](#) .
- [95] K. Walker, A universal state sum, arXiv e-prints , [arXiv:2104.02101 \(2021\)](#), [arXiv:2104.02101 \[math.QA\]](#) .
- [96] M. Atiyah, Topological quantum field theories, [Inst. Hautes Etudes Sci. Publ. Math.](#) **68**, 175–186 (1989).
- [97] J. Lurie, On the Classification of Topological Field Theories, arXiv e-prints , [arXiv:0905.0465 \(2009\)](#), [arXiv:0905.0465 \[math.CT\]](#) .
- [98] S. Kochman, *Bordism, Stable Homotopy, and Adams Spectral Sequences*, Fields Institute for Research in Mathematical Sciences Toronto: Fields Institute monographs (American Mathematical Soc.).
- [99] D. S. Freed and M. J. Hopkins, Reflection positivity and invertible topological phases, [Geometry & Topology](#) **25**, 1165–1330 (2021), [arXiv:1604.06527 \[hep-th\]](#) .
- [100] D. Freed, *Lectures on Field Theory and Topology*, CBMS Regional Conference Series in Mathematics (Conference Board of the Mathematical Sciences, 2019).
- [101] J. Roberts, Skein theory and turaev-viro invariants, [Topology](#) **34**, 771–787 (1995).
- [102] L. Crane, L. H. Kauffman, and D. N. Yetter, State-Sum Invariants of 4-Manifolds I, arXiv e-prints , [hep-th/9409167 \(1994\)](#), [arXiv:hep-th/9409167 \[hep-th\]](#) .
- [103] T. Lan and X.-G. Wen, Classification of 3 +1 D Bosonic Topological Orders (II): The Case When Some Pointlike Excitations Are Fermions, [Physical Review X](#) **9**, 021005 (2019), [arXiv:1801.08530 \[cond-mat.str-el\]](#) .
- [104] K. Walker and Z. Wang, (3+1)-TQFTs and topological insulators, [Frontiers of Physics](#) **7**, 150–159 (2012), [arXiv:1104.2632 \[cond-mat.str-el\]](#) .

- [105] E. Witten, Quantum Field Theory and the Jones Polynomial, [Commun. Math. Phys.](#) **121**, 351–399 (1989).
- [106] J. Wang, X.-G. Wen, and E. Witten, Symmetric Gapped Interfaces of SPT and SET States: Systematic Constructions, [Physical Review X](#) **8**, 031048 (2018), [arXiv:1705.06728 \[cond-mat.str-el\]](#) .
- [107] Y. Tachikawa, On gauging finite subgroups, [SciPost Phys.](#) **8**, 015 (2020), [arXiv:1712.09542 \[hep-th\]](#) .
- [108] D. S. Freed, The cobordism hypothesis, arXiv e-prints , [arXiv:1210.5100](#) (2012), [arXiv:1210.5100 \[math.AT\]](#) .
- [109] A. Brochier, D. Jordan, and N. Snyder, On dualizability of braided tensor categories, [Compositio Mathematica](#) **157**, 435–483 (2021), [arXiv:1804.07538 \[math.QA\]](#) .
- [110] Y. H. Tham, On the Category of Boundary Values in the Extended Crane-Yetter TQFT, arXiv e-prints , [arXiv:2108.13467](#) (2021), [arXiv:2108.13467 \[math.QA\]](#) .
- [111] R. Gompf and A. Stipsicz, *4-Manifolds and Kirby Calculus*, Graduate studies in mathematics (American Mathematical Society, 1999).
- [112] S. Akbulut, *4-manifolds*, Oxford graduate texts in mathematics (Oxford University Press, 2016).
- [113] A. Scorpan, *The Wild World of 4-Manifolds* (American Mathematical Society, 2005).
- [114] C. L. Kane and M. P. A. Fisher, Quantized thermal transport in the fractional quantum Hall effect, [Phys. Rev. B](#) **55**, 15832–15837 (1997), [arXiv:cond-mat/9603118 \[cond-mat\]](#) .
- [115] L. Crane, L. H. Kauffman, and D. N. Yetter, Evaluating the Crane-Yetter Invariant, arXiv e-prints , [hep-th/9309063](#) (1993), [arXiv:hep-th/9309063 \[hep-th\]](#) .
- [116] C. Wang and M. Levin, Anomaly Indicators for Time-Reversal Symmetric Topological Orders, [Phys. Rev. Lett.](#) **119**, 136801 (2017), [arXiv:1610.04624 \[cond-mat.str-el\]](#) .
- [117] A. Vishwanath and T. Senthil, Physics of Three-Dimensional Bosonic Topological Insulators: Surface-Deconfined Criticality and Quantized Magnetoelectric Effect, [Physical Review X](#) **3**, 011016 (2013), [arXiv:1209.3058 \[cond-mat.str-el\]](#) .

- [118] F. J. Burnell, X. Chen, L. Fidkowski, and A. Vishwanath, Exactly soluble model of a three-dimensional symmetry-protected topological phase of bosons with surface topological order, *Phys. Rev. B* **90**, 245122 (2014), [arXiv:1302.7072 \[cond-mat.str-el\]](https://arxiv.org/abs/1302.7072) .
- [119] M. Barkeshli and M. Cheng, Relative anomalies in (2+1)D symmetry enriched topological states, *SciPost Physics* **8**, 028 (2020), [arXiv:1906.10691 \[cond-mat.str-el\]](https://arxiv.org/abs/1906.10691) .
- [120] E. H. Brown, The cohomology of  $bso_n$  and  $bo_n$  with integer coefficients, *Proceedings of the American Mathematical Society* **85**, 283–288 (1982).
- [121] C. Córdova and K. Ohmori, Anomaly constraints on gapped phases with discrete chiral symmetry, *Phys. Rev. D* **102**, 025011 (2020), [arXiv:1912.13069 \[hep-th\]](https://arxiv.org/abs/1912.13069) .
- [122] C. Cordova and K. Ohmori, Anomaly Obstructions to Symmetry Preserving Gapped Phases, arXiv e-prints , [arXiv:1910.04962 \(2019\)](https://arxiv.org/abs/1910.04962), [arXiv:1910.04962 \[hep-th\]](https://arxiv.org/abs/1910.04962) .
- [123] S.-Q. Ning, B.-B. Mao, Z. Li, and C. Wang, Anomaly indicators and bulk-boundary correspondences for three-dimensional interacting topological crystalline phases with mirror and continuous symmetries, *Phys. Rev. B* **104**, 075111 (2021), [arXiv:2105.02682 \[cond-mat.str-el\]](https://arxiv.org/abs/2105.02682) .
- [124] M. F. Lapa and M. Levin, Anomaly indicators for topological orders with U(1) and time-reversal symmetry, *Phys. Rev. B* **100**, 165129 (2019), [arXiv:1905.00435 \[cond-mat.str-el\]](https://arxiv.org/abs/1905.00435) .
- [125] M. Bärenz and J. Barrett, Dichromatic State Sum Models for Four-Manifolds from Pivotal Functors, *Communications in Mathematical Physics* **360**, 663–714 (2018), [arXiv:1601.03580 \[math-ph\]](https://arxiv.org/abs/1601.03580) .
- [126] D. S. Freed, Short-range entanglement and invertible field theories, arXiv e-prints , [arXiv:1406.7278 \(2014\)](https://arxiv.org/abs/1406.7278), [arXiv:1406.7278 \[cond-mat.str-el\]](https://arxiv.org/abs/1406.7278) .
- [127] Codes and data available at <https://arxiv.org/src/2111.12097v2/anc>.
- [128] L. Messio, C. Lhuillier, and G. Misguich, Lattice symmetries and regular magnetic orders in classical frustrated antiferromagnets, *Phys. Rev. B* **83**, 184401 (2011), [arXiv:1101.1212 \[cond-mat.str-el\]](https://arxiv.org/abs/1101.1212) .
- [129] A. W. Sandvik, Evidence for Deconfined Quantum Criticality in a Two-Dimensional Heisenberg Model with Four-Spin Interactions, *Phys. Rev. Lett.* **98**, 227202 (2007), [arXiv:cond-mat/0611343 \[cond-mat.str-el\]](https://arxiv.org/abs/cond-mat/0611343) .

- [130] A. W. Sandvik, Continuous Quantum Phase Transition between an Antiferromagnet and a Valence-Bond Solid in Two Dimensions: Evidence for Logarithmic Corrections to Scaling, *Phys. Rev. Lett.* **104**, 177201 (2010), [arXiv:1001.4296 \[cond-mat.str-el\]](#) .
- [131] S. Pujari, K. Damle, and F. Alet, Néel-State to Valence-Bond-Solid Transition on the Honeycomb Lattice: Evidence for Deconfined Criticality, *Phys. Rev. Lett.* **111**, 087203 (2013), [arXiv:1302.1408 \[cond-mat.str-el\]](#) .
- [132] Y. Ran, M. Hermele, P. A. Lee, and X.-G. Wen, Projected-Wave-Function Study of the Spin-1/2 Heisenberg Model on the Kagomé Lattice, *Phys. Rev. Lett.* **98**, 117205 (2007), [arXiv:cond-mat/0611414 \[cond-mat.str-el\]](#) .
- [133] M. Hermele, Y. Ran, P. A. Lee, and X.-G. Wen, Properties of an algebraic spin liquid on the kagome lattice, *Phys. Rev. B* **77**, 224413 (2008), [arXiv:0803.1150 \[cond-mat.str-el\]](#) .
- [134] Y. Iqbal, F. Becca, S. Sorella, and D. Poilblanc, Gapless spin-liquid phase in the kagome spin-(1)/(2) Heisenberg antiferromagnet, *Phys. Rev. B* **87**, 060405 (2013), [arXiv:1209.1858 \[cond-mat.str-el\]](#) .
- [135] Y.-C. He, M. P. Zaletel, M. Oshikawa, and F. Pollmann, Signatures of Dirac Cones in a DMRG Study of the Kagome Heisenberg Model, *Physical Review X* **7**, 031020 (2017), [arXiv:1611.06238 \[cond-mat.str-el\]](#) .
- [136] Y. Zhou and X.-G. Wen, Quantum Orders and Spin Liquids in  $\text{Cs}_2\text{CuCl}_4$ , *arXiv e-prints* , cond-mat/0210662 (2002), [arXiv:cond-mat/0210662 \[cond-mat.str-el\]](#) .
- [137] Y.-M. Lu, Symmetric  $Z_2$  spin liquids and their neighboring phases on triangular lattice, *Phys. Rev. B* **93**, 165113 (2016), [arXiv:1505.06495 \[cond-mat.str-el\]](#) .
- [138] Y. Iqbal, W.-J. Hu, R. Thomale, D. Poilblanc, and F. Becca, Spin liquid nature in the Heisenberg  $J_1$ - $J_2$  triangular antiferromagnet, *Phys. Rev. B* **93**, 144411 (2016), [arXiv:1601.06018 \[cond-mat.str-el\]](#) .
- [139] S. Hu, W. Zhu, S. Eggert, and Y.-C. He, Dirac Spin Liquid on the Spin-1/2 Triangular Heisenberg Antiferromagnet, *Phys. Rev. Lett.* **123**, 207203 (2019), [arXiv:1905.09837 \[cond-mat.str-el\]](#) .
- [140] C.-M. Jian, A. Thomson, A. Rasmussen, Z. Bi, and C. Xu, Deconfined quantum critical point on the triangular lattice, *Phys. Rev. B* **97**, 195115 (2018), [arXiv:1710.04668 \[cond-mat.str-el\]](#) .

- [141] J. Alicea, Monopole quantum numbers in the staggered flux spin liquid, *Phys. Rev. B* **78**, 035126 (2008), [arXiv:0804.0786 \[cond-mat.str-el\]](#) .
- [142] Y. Ran, A. Vishwanath, and D.-H. Lee, A direct transition between a Neel ordered Mott insulator and a  $d_{x^2-y^2}$  superconductor on the square lattice, arXiv e-prints (2008), [arXiv:0806.2321 \[cond-mat.str-el\]](#) .
- [143] C.-J. Lin and L. Zou, Entanglement-enabled symmetry-breaking orders, arXiv e-prints , [arXiv:2207.08828 \(2022\)](#), [arXiv:2207.08828 \[cond-mat.str-el\]](#) .
- [144] S.-S. Gong, W. Zhu, L. Balents, and D. N. Sheng, Global phase diagram of competing ordered and quantum spin-liquid phases on the kagome lattice, *Phys. Rev. B* **91**, 075112 (2015), [arXiv:1412.1571 \[cond-mat.str-el\]](#) .
- [145] E. Eichten and J. Preskill, Chiral gauge theories on the lattice, *Nuclear Physics B* **268**, 179–208 (1986).
- [146] R. Narayanan and H. Neuberger, Chiral fermions on the lattice, *Phys. Rev. Lett.* **71**, 3251–3254 (1993).
- [147] S. Randjbar-Daemi and J. Strathdee, Chiral fermions on the lattice, *Nuclear Physics B* **443**, 386–416 (1995).
- [148] H. Neuberger, Chiral fermions on the lattice, *Nuclear Physics B Proceedings Supplements* **83**, 67–76 (2000), [arXiv:hep-lat/9909042 \[hep-lat\]](#) .
- [149] X.-G. Wen, A Lattice Non-Perturbative Definition of an SO(10) Chiral Gauge Theory and Its Induced Standard Model, *Chinese Physics Letters* **30**, 111101 (2013), [arXiv:1305.1045 \[hep-lat\]](#) .
- [150] Y. Kikukawa, On the gauge-invariant path-integral measure for the overlap Weyl fermions in 16 of SO(10), *Progress of Theoretical and Experimental Physics* **2019**, 10.1093/ptep/ptz115 (2019), 113B03, [arXiv:1710.11618 \[hep-lat\]](#) .
- [151] J. Wang and X.-G. Wen, A Non-Perturbative Definition of the Standard Models, *Phys. Rev. Research* **2**, 023356 (2020), [arXiv:1809.11171 \[hep-th\]](#) .
- [152] S. S. Razamat and D. Tong, Gapped Chiral Fermions, *Physical Review X* **11**, 011063 (2021), [arXiv:2009.05037 \[hep-th\]](#) .

- [153] L. Wang, E.-M. Shih, A. Ghiotto, L. Xian, D. A. Rhodes, C. Tan, M. Claassen, D. M. Kennes, Y. Bai, B. Kim, K. Watanabe, T. Taniguchi, X. Zhu, J. Hone, A. Rubio, A. N. Pasupathy, and C. R. Dean, Correlated electronic phases in twisted bilayer transition metal dichalcogenides, *Nature Materials* **19**, 861–866 (2020).
- [154] H. Pan, F. Wu, and S. Das Sarma, Band topology, Hubbard model, Heisenberg model, and Dzyaloshinskii-Moriya interaction in twisted bilayer WSe<sub>2</sub>, *Physical Review Research* **2**, 033087 (2020), [arXiv:2004.04168 \[cond-mat.str-el\]](#) .
- [155] Z. Zhang, Y. Wang, K. Watanabe, T. Taniguchi, K. Ueno, E. Tutuc, and B. J. LeRoy, Flat bands in twisted bilayer transition metal dichalcogenides, *Nature Physics* **16**, 1093–1096 (2020), [arXiv:1910.13068 \[cond-mat.str-el\]](#) .
- [156] W. Liu, Z. Zhang, J. Ji, Y. Liu, J. Li, X. Wang, H. Lei, G. Chen, and Q. Zhang, Rare-Earth Chalcogenides: A Large Family of Triangular Lattice Spin Liquid Candidates, *Chinese Physics Letters* **35**, 117501 (2018), [arXiv:1809.03025 \[cond-mat.str-el\]](#) .
- [157] K. M. Ranjith, D. Dmytriieva, S. Khim, J. Sichelschmidt, S. Luther, D. Ehlers, H. Yasuoka, J. Wosnitza, A. A. Tsirlin, H. Kühne, and M. Baenitz, Field-induced instability of the quantum spin liquid ground state in the  $J_{eff}=1/2$  triangular-lattice compound NaYbO<sub>2</sub>, *Phys. Rev. B* **99**, 180401 (2019), [arXiv:1901.07760 \[cond-mat.str-el\]](#) .
- [158] L. Ding, P. Manuel, S. Bachus, F. Grubler, P. Gegenwart, J. Singleton, R. D. Johnson, H. C. Walker, D. T. Adroja, A. D. Hillier, and A. A. Tsirlin, Gapless spin-liquid state in the structurally disorder-free triangular antiferromagnet NaYbO<sub>2</sub>, *Phys. Rev. B* **100**, 144432 (2019), [arXiv:1901.07810 \[cond-mat.str-el\]](#) .
- [159] M. M. Bordelon, E. Kenney, C. Liu, T. Hogan, L. Posthuma, M. Kavand, Y. Lyu, M. Sherwin, N. P. Butch, C. Brown, M. J. Graf, L. Balents, and S. D. Wilson, Field-tunable quantum disordered ground state in the triangular-lattice antiferromagnet NaYbO<sub>2</sub>, *Nature Physics* **15**, 1058–1064 (2019), [arXiv:1901.09408 \[cond-mat.str-el\]](#) .
- [160] M. M. Bordelon, C. Liu, L. Posthuma, P. M. Sarte, N. P. Butch, D. M. Pajerowski, A. Banerjee, L. Balents, and S. D. Wilson, Spin excitations in the frustrated triangular lattice antiferromagnet NaYbO<sub>2</sub>, *Phys. Rev. B* **101**, 224427 (2020), [arXiv:2005.10375 \[cond-mat.str-el\]](#) .
- [161] M. Baenitz, P. Schlender, J. Sichelschmidt, Y. A. Onykiienko, Z. Zangeneh, K. M. Ranjith, R. Sarkar, L. Hozoi, H. C. Walker, J. C. Orain, H. Yasuoka, J. van den Brink, H. H. Klauss, D. S. Inosov, and T. Doert, NaYbS<sub>2</sub>: A planar spin-1/2

- triangular-lattice magnet and putative spin liquid, *Phys. Rev. B* **98**, 220409 (2018), [arXiv:1809.01947 \[cond-mat.str-el\]](#) .
- [162] J. Sichelschmidt, P. Schlender, B. Schmidt, M. Baenitz, and T. Doert, Electron spin resonance on the spin-1/2 triangular magnet NaYbS<sub>2</sub>, *Journal of Physics Condensed Matter* **31**, 205601 (2019), [arXiv:1812.07871 \[cond-mat.str-el\]](#) .
- [163] K. M. Ranjith, S. Luther, T. Reimann, B. Schmidt, P. Schlender, J. Sichelschmidt, H. Yasuoka, A. M. Strydom, Y. Skourski, J. Wosnitza, H. Kühne, T. Doert, and M. Baenitz, Anisotropic field-induced ordering in the triangular-lattice quantum spin liquid NaYbSe<sub>2</sub>, *Phys. Rev. B* **100**, 224417 (2019), [arXiv:1911.12712 \[cond-mat.str-el\]](#) .
- [164] J. Ma, J. Li, Y. Hao Gao, C. Liu, y. Qingyong Ren, Z. Zhang, Z. Wang, R. Chen, J. Embs, E. Feng, F. Zhu, Q. Huang, Z. Xiang, L. Chen, E. S. Choi, Z. Qu, L. Li, J. Wang, H. Zhou, Y. Su, X. Wang, Q. Zhang, and G. Chen, Spin-orbit-coupled triangular-lattice spin liquid in rare-earth chalcogenides, arXiv e-prints , [arXiv:2002.09224 \(2020\)](#), [arXiv:2002.09224 \[cond-mat.str-el\]](#) .
- [165] P.-L. Dai, G. Zhang, Y. Xie, C. Duan, Y. Gao, Z. Zhu, E. Feng, Z. Tao, C.-L. Huang, H. Cao, A. Podlesnyak, G. E. Granroth, M. S. Everett, J. C. Neufeind, D. Voneshen, S. Wang, G. Tan, E. Morosan, X. Wang, H.-Q. Lin, L. Shu, G. Chen, Y. Guo, X. Lu, and P. Dai, Spinon Fermi Surface Spin Liquid in a Triangular Lattice Antiferromagnet NaYbSe<sub>2</sub>, *Physical Review X* **11**, 021044 (2021), [arXiv:2004.06867 \[cond-mat.str-el\]](#) .
- [166] J. Iaconis, C. Liu, G. Halász, and L. Balents, Spin Liquid versus Spin Orbit Coupling on the Triangular Lattice, *SciPost Physics* **4**, 003 (2018), [arXiv:1708.07856 \[cond-mat.str-el\]](#) .
- [167] D. Sénéchal, An introduction to bosonization, arXiv e-prints , [cond-mat/9908262 \(1999\)](#), [arXiv:cond-mat/9908262 \[cond-mat.str-el\]](#) .
- [168] E. Witten, Nonabelian Bosonization in Two-Dimensions, *Commun. Math. Phys.* **92**, 455–472 (1984).
- [169] M. Lajkó, K. Wamer, F. Mila, and I. Affleck, Generalization of the Haldane conjecture to SU(3) chains, *Nuclear Physics B* **924**, 508–577 (2017), [arXiv:1706.06598 \[cond-mat.str-el\]](#) .



- [170] I. Hason, Z. Komargodski, and R. Thorngren, Anomaly matching in the symmetry broken phase: Domain walls, CPT, and the Smith isomorphism, [SciPost Physics](#) **8**, 062 (2020), [arXiv:1910.14039 \[hep-th\]](#) .
- [171] V. Calvera and C. Wang, Theory of Dirac Spin-Orbital Liquids: monopoles, anomalies, and applications to  $SU(4)$  honeycomb models, arXiv e-prints , [arXiv:2103.13405](#) (2021), [arXiv:2103.13405 \[cond-mat.str-el\]](#) .
- [172] R. Bott and L. Tu, *Differential Forms in Algebraic Topology*, Graduate Texts in Mathematics (Springer New York, 2013).
- [173] C. Bradley and A. Cracknell, *The Mathematical Theory of Symmetry in Solids: Representation Theory for Point Groups and Space Groups*, EBSCO ebook academic collection (OUP Oxford, 2010).
- [174] S. Weinberg, *The Quantum Theory of Fields: Volume 1, Foundations* (Cambridge University Press, 2005).
- [175] P. Etingof, O. Golberg, S. Hensel, T. Liu, A. Schwendner, D. , and E. Yudovina, *Introduction to Representation Theory*, Student mathematical library (American Mathematical Society, 2011).
- [176] A. Hatcher, C. U. Press, and C. U. D. of Mathematics, *Algebraic Topology*, Algebraic Topology (Cambridge University Press, 2002).

# APPENDIX

# Appendix A

## Review of Mathematical Background

In this appendix, we briefly review various mathematical concepts used in this paper. We also define some new concepts that will be useful in the paper.

### A.1 Group cohomology

In this sub-appendix, we provide a brief review of the fundamentals of group cohomology. See Refs. [26, 67, 68] for more details.

Given a (discrete) group  $G$ , let  $X$  be an Abelian group equipped with a  $G$  action  $\rho : G \times X \rightarrow X$ , which is compatible with group multiplication, i.e., for any  $g, h \in G$ ,  $e$  the identity element in  $G$  and  $a, b \in X$ , we have

$$\begin{aligned} \text{Identity of Group Action} &: \rho_e(a) = a, \\ \text{Compatibility of Group Action} &: \rho_g(\rho_h(a)) = \rho_{gh}(a), \\ \text{Compatibility of Module} &: \rho_g(ab) = \rho_g(a)\rho_g(b). \end{aligned} \tag{A.1}$$

We leave the group multiplication symbols implicit in the above. Such an Abelian group  $X$  with  $G$  action  $\rho$  is called a  $G$ -module, denoted by  $X_\rho$ . In this paper, we will mainly consider three different cases of  $X$ , i.e.,  $\mathbb{Z}_2$ ,  $U(1)$  and  $\mathbb{Z}$ . In particular, when  $X = \mathbb{Z}_2$ , the action  $\rho_g$  is always trivial for any  $g \in G$ . When  $X = U(1)$  ( $X = \mathbb{Z}$ ), the action  $\rho_g$  is either trivial or complex conjugation (multiplication by  $-1$ ), i.e., a  $\mathbb{Z}_2$  action. Therefore,  $\rho$  can be defined by a homomorphism  $\tilde{\rho} : G \rightarrow \mathbb{Z}_2$ , and whether  $\tilde{\rho}(g)$  equals  $+1$  or  $-1$  determines whether the action of  $\rho_g$  on  $U(1)$  and  $\mathbb{Z}$  is trivial or non-trivial.

Let  $\omega(g_1, \dots, g_n) \in X$  be a function of  $n$  group elements with  $g_i \in G$  for  $i = 1, \dots, n$ . Such a function is called an  $n$ -cochain, and the set of all  $n$ -cochains is denoted by  $C^n(G, X_\rho)$ . They naturally form an Abelian group under multiplication,

$$(\omega \cdot \omega')(g_1, \dots, g_n) = \omega(g_1, \dots, g_n)\omega'(g_1, \dots, g_n), \quad (\text{A.2})$$

and the identity element is the trivial cochain  $\omega(g_1, \dots, g_n) = 1$  for every  $(g_1, \dots, g_n)$ , where 1 is the identity element in  $X$ .

We now define the coboundary map  $d : C^n(G, X_\rho) \rightarrow C^{n+1}(G, X_\rho)$  acting on cochains to be

$$(d\omega)(g_1, \dots, g_{n+1}) = \rho_{g_1}(\omega(g_2, \dots, g_{n+1})) \prod_{j=1}^n (\omega(g_1, \dots, g_{j-1}, g_j g_{j+1}, g_{j+2}, \dots, g_{n+1}))^{(-1)^j} (\omega(g_1, \dots, g_n))^{(-1)^{n+1}}. \quad (\text{A.3})$$

One can directly verify that  $d(d\omega) = 1$  for any  $\omega \in C^n(G, X_\rho)$ , where 1 denotes the trivial cochain in  $C^{n+2}(G, X_\rho)$ . With the coboundary map, we next define  $\omega \in C^n(G, X_\rho)$  to be an  $n$ -cocycle if it satisfies the condition  $d\omega = 1$ , and all  $n$ -cocycles naturally form an Abelian group

$$Z^n(G, X_\rho) = \ker[d : C^n(G, X_\rho) \rightarrow C^{n+1}(G, X_\rho)] = \{ \omega \in C^n(G, X_\rho) \mid d\omega = 1 \}. \quad (\text{A.4})$$

We also define  $\omega \in C^n(G, X_\rho)$  to be an  $n$ -coboundary if it satisfies the condition  $\omega = d\mu$  for some  $(n-1)$ -cochain  $\mu \in C^{n-1}(G, X_\rho)$ , and all  $n$ -coboundaries naturally form an Abelian group

$$\begin{aligned} B^n(G, X_\rho) &= \text{im}[d : C^{n-1}(G, X_\rho) \rightarrow C^n(G, X_\rho)] \\ &= \{ \omega \in C^n(G, X_\rho) \mid \exists \mu \in C^{n-1}(G, X_\rho) : \omega = d\mu \}. \end{aligned} \quad (\text{A.5})$$

Clearly,  $B^n(G, X_\rho) \subseteq Z^n(G, X_\rho) \subseteq C^n(G, X_\rho)$ , and we define the  $n$ -th group cohomology of  $G$  to be the quotient group

$$H^n(G, X_\rho) = \frac{Z^n(G, X_\rho)}{B^n(G, X_\rho)}. \quad (\text{A.6})$$

In other words,  $H^n(G, X_\rho)$  collects the equivalence classes of  $n$ -cocycles, where two  $n$ -cocycles are considered equivalent if they differ by an  $n$ -coboundary.

It is instructive to look at the lowest cohomology groups. Let us first consider  $H^1(G, X_\rho)$ :

$$\begin{aligned} Z^1(G, X_\rho) &= \{ \omega \mid \omega(g_1)\rho_{g_1}(\omega(g_2)) = \omega(g_1 g_2) \} \\ B^1(G, X_\rho) &= \{ \omega \mid \omega(g) = \rho_g(\mu)\mu^{-1} \}. \end{aligned} \quad (\text{A.7})$$

If the  $G$ -action on  $X$  is trivial, then  $B^1(G, X_\rho) = \{1\}$  and  $Z^1(G, X_\rho)$  consists of group homomorphisms from  $G$  to  $X$ , which, in particular, map elements in the same conjugacy class to the same image, i.e.,

$$\omega(g_2^{-1}g_1g_2) = \omega(g_1). \quad (\text{A.8})$$

for any  $g_{1,2} \in G$ .

For the second cohomology, we have

$$\begin{aligned} Z^2(G, X_\rho) &= \{ \omega \mid \rho_{g_1}(\omega(g_2, g_3))\omega(g_1, g_2g_3) = \omega(g_1, g_2)\omega(g_1g_2, g_3) \} \\ B^2(G, X_\rho) &= \{ \omega \mid \omega(g_1, g_2) = \rho_{g_1}(\mu(g_2))(\mu(g_1g_2))^{-1}\mu(g_1) \}. \end{aligned} \quad (\text{A.9})$$

In particular,  $H^2(G, \text{U}(1)_\rho)$  classifies all inequivalent complex projective representations of  $G$ , while  $H^2(G, \mathbb{Z}_2)$  classifies all inequivalent real orthogonal projective representations of  $G$ , which will be most useful throughout the paper.

## A.2 Maps of group Cohomology

In this sub-appendix, we review various maps of group cohomology, which will be used throughout the paper.

The first map we consider is the pullback of group cohomology. Consider a map between two groups  $\varphi : G \rightarrow H$  compatible with their respective group action  $\rho_G$  and  $\rho_H$  on  $X$ , in the sense that  $\rho_{\varphi(g)}(a) = \rho_g(a)$  for any  $a \in X$  and any  $g \in G$  or, in the case of  $X = \text{U}(1), \mathbb{Z}$ ,  $\tilde{\rho}_H \circ \varphi = \tilde{\rho}_G$ . Given such a map, we can define the pullback from  $H^n(H, X_\rho)$  to  $H^n(G, X_\rho)$ , which can be defined on the representative cochain  $\omega \in C^n(H, X_\rho)$  as follows

$$(\varphi^*(\omega))(g_1, \dots, g_n) \equiv \omega(\varphi(g_1), \dots, \varphi(g_n)). \quad (\text{A.10})$$

It is straightforward to check that it maps cocycles to cocycles, and coboundaries to coboundaries, so it gives a well-defined map from  $H^n(H, X_\rho)$  to  $H^n(G, X_\rho)$ ,

$$\varphi^* : H^n(H, X_\rho) \rightarrow H^n(G, X_\rho). \quad (\text{A.11})$$

The second map we consider is the map of group cohomology induced by a map of  $G$ -modules  $i : X \rightarrow Y$ . Here  $i$  is any map from  $G$ -module  $X$  to  $G$ -module  $Y$  that preserves

the action of  $G$ , i.e., for any  $a \in X$  and  $g \in G$  we have  $\rho_g(i(a)) = i(\rho_g(a))$ . Then for any  $n$ -cochain  $\omega(g_1, \dots, g_n) \in C^n(G, X_\rho)$ , we can map it to another  $n$ -cochain  $\tilde{i}(\omega)$  such that

$$(\tilde{i}(\omega))(g_1, \dots, g_n) \equiv i(\omega(g_1, \dots, g_n)). \quad (\text{A.12})$$

It is straightforward to check that it maps cocycles to cocycles, and coboundaries to coboundaries, so it gives a well-defined map from  $H^n(G, X_\rho)$  to  $H^n(G, Y_\rho)$ ,

$$\tilde{i} : H^n(G, X_\rho) \rightarrow H^n(G, Y_\rho). \quad (\text{A.13})$$

We will frequently use this map to convert cohomology elements in  $H^n(G, \mathbb{Z}_2)$  to elements in  $H^n(G, U(1)_\rho)$ , induced by the inclusion  $i$  of  $\mathbb{Z}_2 = \{\pm 1\}$  into  $U(1)$ . Note that the representative cochains  $\omega$  and  $\tilde{i}(\omega)$  as a function from  $G^n$  to  $\mathbb{Z}_2$  and  $U(1)$  are manifestly the same, but a function representing a nontrivial element in  $H^n(G, \mathbb{Z}_2)$  can represent a trivial element in  $H^n(G, U(1)_\rho)$ , because the module  $U(1)_\rho$  in general yields more coboundaries compared to the module  $\mathbb{Z}_2$ . We also consider the map of group cohomology  $\tilde{p}$  induced by the projection  $p$  of  $\mathbb{Z}$  onto  $\mathbb{Z}_2 = \{0, 1\}$

The third map which will be useful in the analysis of anomaly/anomaly-matching is the Bockstein homomorphism [69, 176]. Consider a short exact sequence of  $G$ -modules,

$$1 \longrightarrow X \xrightarrow{i} Z \xrightarrow{p} Y \longrightarrow 1 \quad (\text{A.14})$$

with the map  $i : X \rightarrow Z$  injective, the map  $p : Z \rightarrow Y$  surjective and  $\ker[p] = \text{im}[i]$ . There is a long exact sequence of the cohomology of  $G$  associated to this short exact sequence, such that  $\ker = \text{im}$  at any place of the following chain of maps,

$$\longrightarrow H^n(G, X_\rho) \xrightarrow{\tilde{i}} H^n(G, Z_\rho) \xrightarrow{\tilde{p}} H^n(G, Y_\rho) \xrightarrow{\beta} H^{n+1}(G, X_\rho) \xrightarrow{\tilde{i}} \dots \quad (\text{A.15})$$

The map  $\beta$ , called the Bockstein homomorphism, is defined as follows. For  $[\omega] \in H^n(G, Y_\rho)$  and a representative cochain  $\omega$ , choose a function  $\tilde{\omega}$  from  $G^n$  to  $Z_\rho$  such that

$$p((\tilde{\omega})(g_1, \dots, g_n)) = \omega(g_1, \dots, g_n). \quad (\text{A.16})$$

Because  $p$  is surjective,  $\tilde{\omega}$  always exists. For any choice of  $\tilde{\omega}$ , it is straightforward to see that  $p((d\tilde{\omega})(g_1, \dots, g_n)) = 0$  and as a result  $(d\tilde{\omega})(g_1, \dots, g_n)$  is in the image of  $i$ . Then we define this (unique) preimage to be the image of  $\omega$  under the Bockstein homomorphism, i.e., we have

$$\beta(\omega) \equiv \tilde{i}^{-1}(d\tilde{\omega}). \quad (\text{A.17})$$

There are several short exact sequences that we should pay special attention to. The first one is

$$1 \longrightarrow \mathbb{Z} \xrightarrow{\times 2\pi} \mathbb{R} \xrightarrow{\text{mod } 2\pi} \text{U}(1) \longrightarrow 1. \quad (\text{A.18})$$

When  $H^n(G, \mathbb{Z}_\rho)$  and  $H^{n+1}(G, \mathbb{Z}_\rho)$  contain torsion elements only,  $H^n(G, \mathbb{R}_\rho) = H^{n+1}(G, \mathbb{R}_\rho) = 0$ , and from Eq. (A.15) we see that the associated Bockstein homomorphism  $\beta : H^n(G, \text{U}(1)_\rho) \rightarrow H^{n+1}(G, \mathbb{Z}_\rho)$  is an isomorphism. For most discussions in this paper, especially when  $G$  is a finite group (and  $n > 0$ ), this Bockstein homomorphism is indeed an isomorphism, and only in the example in Appendix 5.A.1 it is not, on which we will comment explicitly.

The second short exact sequence that is important to us is

$$1 \longrightarrow \mathbb{Z} \xrightarrow{\times 2} \mathbb{Z} \xrightarrow{\text{mod } 2} \mathbb{Z}_2 \longrightarrow 1 \quad (\text{A.19})$$

For  $x \in H^n(G, \mathbb{Z}_2)$ , the Bockstein homomorphism  $\beta_2$  is sometimes written as

$$\beta_2(x) = \frac{1}{2}dx. \quad (\text{A.20})$$

When  $H^n(G, \mathbb{Z}_\rho) = (\mathbb{Z}_2)^k$  with some non-negative integer  $k$ ,  $\tilde{i}$  maps  $H^n(G, \mathbb{Z}_\rho)$  to 0 in  $H^n(G, \mathbb{Z}_\rho)$ . Therefore, from Eq. (A.15), we see that  $\tilde{p}$  is injective while  $\beta_2$  is surjective.

We can also consider the natural map from Eq. (A.19) to Eq. (A.18), which is inclusion for every factor as follows,

$$\begin{array}{ccccccc} 1 & \longrightarrow & \mathbb{Z} & \xrightarrow{\times 2\pi} & \mathbb{R} & \xrightarrow{\text{mod } 2\pi} & \text{U}(1) \longrightarrow 1 \\ & & \cong \uparrow & & \times \pi \uparrow & & i \uparrow \\ 1 & \longrightarrow & \mathbb{Z} & \xrightarrow{\times 2} & \mathbb{Z} & \xrightarrow{\text{mod } 2} & \mathbb{Z}_2 \longrightarrow 1 \end{array} \quad (\text{A.21})$$

where  $i$  is again the inclusion of  $\mathbb{Z}_2 = \{\pm 1\}$  into  $\text{U}(1)$ . As a result, we have a map of long exact sequences,

$$\begin{array}{ccccccc} \dots & \longrightarrow & H^n(G, \mathbb{Z}_2) & \xrightarrow{\beta_2} & H^{n+1}(G, \mathbb{Z}_\rho) & \longrightarrow & H^{n+1}(G, \mathbb{Z}_\rho) \longrightarrow \dots \\ & & \downarrow \tilde{i} & & \downarrow \cong & & \downarrow \\ \dots & \longrightarrow & H^n(G, \text{U}(1)_\rho) & \xrightarrow{\beta} & H^{n+1}(G, \mathbb{Z}_\rho) & \longrightarrow & H^{n+1}(G, \mathbb{R}_\rho) \longrightarrow \dots \end{array} \quad (\text{A.22})$$

Here we distinguish the first Bockstein homomorphism by denoting it by  $\beta_2$ , and  $\tilde{i}$  denotes the map induced by  $i : \mathbb{Z}_2 \rightarrow \text{U}(1)$  specifically. Hence, we have  $\beta_2 = \beta \circ \tilde{i}$ . When

$H^n(G, \mathbb{Z}_\rho) = (\mathbb{Z}_2)^k$ , since  $\beta$  is an isomorphism while  $\beta_2$  is surjective,  $\tilde{i}$  is surjective as well. It suggests that in this case every element  $\Omega \in H^n(G, U(1)_\rho)$  can be written as  $\tilde{i}(L)$  or  $e^{i\pi L}$  for some  $L \in H^n(G, \mathbb{Z}_2)$ . In fact, every element  $\Omega \in H^n(G, U(1)_\rho)$  whose inverse is itself can be written as  $e^{i\pi L}$  for some  $L \in H^n(G, \mathbb{Z}_2)$ . We use this fact throughout the paper.

### A.3 Cup product and $\mathbb{Z}_2$ cohomology ring

In this sub-appendix, we review cup product and  $\mathbb{Z}_2$  cohomology ring in group cohomology that we will use [67, 68, 176]. We will specialize to the case where the module is  $\mathbb{Z}_2 = \{0, 1\}$  and the group action  $\rho$  is trivial. The special feature of  $\mathbb{Z}_2$ , contrary to e.g.  $U(1)$ , is the fact that  $\mathbb{Z}_2$  is a ring. Note that here addition in  $\mathbb{Z}_2$  is regarded as the group multiplication used in Eq. (A.2), and we will use  $+$  to denote this addition in this sub-appendix. There is another ring multiplication that will be important later, which should be distinguished with the group multiplication used in Appendix A.1.

The cross product is defined as the following operation on group cohomology,

$$\times : H^m(G, \mathbb{Z}_2) \otimes H^n(H, \mathbb{Z}_2) \rightarrow H^{m+n}(G \times H, \mathbb{Z}_2), \quad (\text{A.23})$$

such that for  $x \in H^m(G, \mathbb{Z}_2)$  and  $y \in H^n(H, \mathbb{Z}_2)$ , after choosing cochain representatives  $\tilde{x}$  and  $\tilde{y}$ , we have the cochain representative of  $x \times y$  as follows,

$$\widetilde{x \times y}((g_1, h_1), \dots, (g_{m+n}, h_{m+n})) \equiv \tilde{x}(g_1, \dots, g_m) \cdot \tilde{y}(h_{m+1}, \dots, h_{m+n}), \quad (\text{A.24})$$

where  $g_i \in G, h_i \in H, i = 1, \dots, m+n$ .

The cup product is defined as the following operation on group cohomology,

$$\cup : H^m(G, \mathbb{Z}_2) \otimes H^n(G, \mathbb{Z}_2) \xrightarrow{\times} H^{m+n}(G \times G, \mathbb{Z}_2) \xrightarrow{\Delta^*} H^{m+n}(G, \mathbb{Z}_2), \quad (\text{A.25})$$

where  $\Delta : G \rightarrow G \times G$  is the diagonal embedding  $g \rightarrow (g, g)$ . We can also define it at the cochain level, i.e., for  $x \in H^m(G, \mathbb{Z}_2)$  and  $y \in H^n(G, \mathbb{Z}_2)$ , after choosing cochain representatives  $\tilde{x}$  and  $\tilde{y}$ , we have the cochain representative of  $x \cup y$  as follows,

$$\widetilde{x \cup y}(g_1, \dots, g_{m+n}) \equiv \tilde{x}(g_1, \dots, g_m) \cdot \tilde{y}(g_{m+1}, \dots, g_{m+n}). \quad (\text{A.26})$$

We can prove that cup product is commutative, i.e.,  $x \cup y = y \cup x$ .

The cup product  $\cup$  gives a multiplication on the direct sum of cohomology groups

$$H^*(G, \mathbb{Z}_2) = \bigoplus_{k \in \mathbb{N}} H^k(G, \mathbb{Z}_2), \quad (\text{A.27})$$



Together with the fact that  $1 \cup x = x$  where  $x$  is any element in  $H^*(G, \mathbb{Z}_2)$  and 1 here denotes the nontrivial element in  $H^0(G, \mathbb{Z}_2) = \mathbb{Z}_2$ , the cup product  $\cup$  turns  $H^*(G, \mathbb{Z}_2)$  into a ring that is naturally  $\mathbb{N}$  graded and commutative. We call this ring *the  $\mathbb{Z}_2$  cohomology ring* of  $G$ .

Moreover,  $H^*(G, \mathbb{Z}_2)$  is also a  $\mathbb{Z}_2$  algebra, and therefore can be presented by generators and relations, i.e., all elements in  $H^n(G, \mathbb{Z}_2)$  for any  $n > 0$  are either generators or can be expressed as sum of (cup) products of generators, and generators satisfy some relations which dictate that certain sums of (cup) products actually yield a trivial cohomology element. We will call a generator in  $H^n(G, \mathbb{Z}_2)$  a degree  $n$  generator. Hence, the  $\mathbb{Z}_2$  cohomology ring of  $G$ , i.e.,  $H^*(G, \mathbb{Z}_2)$ , can be written as follows,

$$H^*(G, \mathbb{Z}_2) = \mathbb{Z}_2[A_\bullet, \dots, B_\bullet, \dots] / \text{relations} \quad (\text{A.28})$$

with  $A_\bullet(B_\bullet)$  generators in degree 1(2) belonging to  $H^1(G, \mathbb{Z}_2)(H^2(G, \mathbb{Z}_2))$ , and  $\bullet$  the name of the generator. Together with potential higher order generators, e.g.,  $C_\bullet$  in degree 3, they are supposed to form a complete list of generators of the entire cohomology ring.

For example, the  $\mathbb{Z}_2$  cohomology ring of the group  $\mathbb{Z}_2$  is

$$\mathbb{Z}_2[A_c], \quad (\text{A.29})$$

where  $A_c$  is the nontrivial element in  $H^1(\mathbb{Z}_2, \mathbb{Z}_2)$  and can be thought of as nothing but the gauge field of e.g.,  $C_2$  rotation when pulled back to the spacetime manifold. In other words, for the  $\mathbb{Z}_2$  cohomology ring of  $\mathbb{Z}_2$ , there is a single generator  $A_c$  in degree 1 and no relation. Accordingly, we can see that  $H^n(G, \mathbb{Z}_2) = \mathbb{Z}_2$  for  $n \in \mathbb{N}$ , with the nontrivial element given by  $A_c^n \equiv A_c \cup A_c \cup \dots \cup A_c$ , the cup product of  $n$   $A_c$ 's.

As another example, the  $\mathbb{Z}_2$  cohomology ring of  $\mathbb{Z}_4$  is

$$\mathbb{Z}_2[A_c, B_{c^2}] / (A_c^2 = 0), \quad (\text{A.30})$$

where here  $A_c$  is the nontrivial element in  $H^1(\mathbb{Z}_4, \mathbb{Z}_2)$  and can be thought of as (the  $\mathbb{Z}_2$  reduction of) the gauge field of  $C_4$  rotation when pulled back to the spacetime manifold, while  $B_{c^2}$  is the nontrivial element in  $H^2(\mathbb{Z}_4, \mathbb{Z}_2)$ , which corresponds to the fractionalization pattern of the  $\mathbb{Z}_4$  symmetry on an  $SO(3)$  monopole, with  $C_4^4 = C_2^2 = -1$ . That is to say, for the  $\mathbb{Z}_2$  cohomology ring of  $\mathbb{Z}_4$ , there are two generators at degree 1 and 2 respectively, with the square of degree 1 generator  $A_c$  equal to 0. Then we see that  $H^n(\mathbb{Z}_4, \mathbb{Z}_2) = \mathbb{Z}_2$  for  $n \in \mathbb{N}$  as well, and the nontrivial element is given by  $B_{c^2}^k$  when  $n = 2k$  and  $A_c B_{c^2}^k$  when  $n = 2k + 1$  ( $k \in \mathbb{N}$ ). Note that for both  $G = \mathbb{Z}_2$  and  $G = \mathbb{Z}_4$ ,  $H^n(G, \mathbb{Z}_2) = \mathbb{Z}_2$  for any  $n \in \mathbb{N}$ , but the  $\mathbb{Z}_2$  cohomology rings give more information that differentiates the two groups.

For any two groups  $G_1$  and  $G_2$ , we have  $H^*(G_1 \times G_2, \mathbb{Z}_2) = H^*(G_1, \mathbb{Z}_2) \otimes H^*(G_2, \mathbb{Z}_2)$ . Moreover, if  $G$  can be written as  $G_1 \rtimes G_2$ , where  $G_1$  is a normal subgroup of  $G$  and  $G_2$  acts on  $G_1$  by conjugation, the calculation of the  $\mathbb{Z}_2$  cohomology ring of  $G$  can be achieved with the help of Lyndon–Hochschild–Serre spectral sequence [67, 68] that also connects  $H^*(G, \mathbb{Z}_2)$  with  $H^*(G_1, \mathbb{Z}_2)$  and  $H^*(G_2, \mathbb{Z}_2)$  which we possibly already know. The general strategy for calculating the  $\mathbb{Z}_2$  cohomology ring of wallpaper groups  $G$  is as follows:

1. Identify all generators and elements in the  $\mathbb{Z}_2$  cohomology ring of  $G$  through Lyndon–Hochschild–Serre spectral sequence.
2. If there is no relation, given generators  $A_1, A_2, B_1, C_1 \dots$ , all elements of the form  $A_1^m A_2^n B_1^p C_1^q \dots, m, n, p, q \dots \in \mathbb{N}$  will appear explicitly as different elements in the  $\mathbb{Z}_2$  cohomology ring. Therefore, when e.g., some  $A_1^2$  is missing, we should identify some relation that relates  $A_1^2$  to elements that appear explicitly, which can be achieved through pulling back to (enough) subgroups of  $G$ .

To illustrate the strategy, in the following we calculate the  $\mathbb{Z}_2$  cohomology ring of three space groups in one or two spatial dimensions, including the generators and relations.

- $p1$ :  $\mathbb{Z}_2[x]/(x^2 = 0)$ .

Consider the line group  $p1$ , generated by a single translation  $T$ . The cohomology of  $p1$  is  $H^1(p1, \mathbb{Z}_2) \cong \mathbb{Z}_2$  while  $H^n(p1, \mathbb{Z}_2) \cong 0, n > 1$ . Denote the nontrivial element in  $H^1(p1, \mathbb{Z}_2)$  as  $x$ , which corresponds to (the  $\mathbb{Z}_2$  reduction of) the gauge field of translation, the  $\mathbb{Z}_2$  cohomology ring of  $p1$  is given by  $\mathbb{Z}_2[x]/(x^2 = 0)$ .

- $p1m$ :  $\mathbb{Z}_2[x, m]/(x^2 = xm)$ .

Consider the line group  $p1m$ , generated by translation  $T$  and mirror symmetry  $M$  with relation  $MTM = T^{-1}$ . The cohomology of  $p1m$  is  $H^n(p1m, \mathbb{Z}_2) \cong \mathbb{Z}_2^2, n \geq 1$ . Since  $p1m \cong \mathbb{Z} \rtimes \mathbb{Z}_2$ , with the help of the corresponding Serre spectral sequence, we know that  $H^n(p1m, \mathbb{Z}_2), n \geq 1$  is spanned by 2 elements, i.e.,  $m^n$  and  $m^{n-1}x$ . where  $m, x \in H^1(p1m, \mathbb{Z}_2)$  are two generators that correspond to the gauge field of mirror symmetry and (the  $\mathbb{Z}_2$  reduction of) the gauge field of translation, respectively.

The next thing to do is to identify  $x^2$ , which does not explicitly appear as elements of the  $\mathbb{Z}_2$  cohomology ring. Write  $x^2$  as  $a_1xm + a_2m^2, a_{1,2} \in \{0, 1\}$ . By restricting to  $\mathbb{Z}_2$  subgroup generated by  $M$ , whose  $\mathbb{Z}_2$  cohomology ring can be denoted by  $\mathbb{Z}_2[m']$ , we see that  $x$  becomes 0 while  $m$  becomes  $m'$ , and thus  $a_2 = 0$ . By restricting to the  $\mathbb{Z}_2$  subgroup generated by  $TM$ , whose  $\mathbb{Z}_2$  cohomology ring can be denoted by

$\mathbb{Z}_2[m'']$ , we see that both  $x$  and  $m$  become  $m''$ , and thus  $a_1 = 1$ . Therefore, we have  $x^2 = xm$ .

Therefore, the  $\mathbb{Z}_2$  cohomology ring of  $p1m$  is  $\mathbb{Z}_2[x, m]/(x^2 = xm)$ .

- $cm$ :  $\mathbb{Z}_2[A_{x+y}, A_m, B_{xy}]/(A_{x+y}A_m = 0, A_{x+y}^2 = 0, B_{xy}A_{x+y} = 0, B_{xy}^2 = 0)$ .

Consider  $2d$  wallpaper group  $cm$ , generated by two translation symmetries  $T_1, T_2$  as well as mirror symmetry  $M$  that interchanges the two translations, i.e.,  $MT_1M = T_2$  and  $MT_2M = T_1$ . The cohomology of  $cm$  is  $H^n(cm, \mathbb{Z}_2) \cong (\mathbb{Z}_2)^2$ ,  $n \geq 1$ . Since  $cm \cong (\mathbb{Z} \times \mathbb{Z}) \rtimes \mathbb{Z}_2$ , with the help of the corresponding Serre spectral sequence, we know that  $H^1(cm, \mathbb{Z}_2)$  is spanned by  $A_{x+y}$  and  $A_m$ , while  $H^n(cm, \mathbb{Z}_2), n \geq 2$  is spanned by  $B_{xy}A_m^{n-2}$  and  $A_m^n$ . Here  $A_m, A_{x+y} \in H^1(cm, \mathbb{Z}_2)$  correspond to the gauge field of mirror symmetry and (the  $\mathbb{Z}_2$  reduction of) the sum of gauge fields of  $T_1$  and  $T_2$ , respectively. Note that since  $T_1$  and  $T_2$  map to each other under conjugation by  $M$ , the gauge field of the two translations  $x$  and  $y$  individually is not invariant under conjugation by  $M$ , yet their sum that we denote by  $A_{x+y}$  is invariant under conjugation by  $M$ , which is a necessary condition for it to be a cohomology element, as required by Eq. (A.8). To conform to the notation, we also denote the gauge field of mirror symmetry by  $A_m$  when considering wallpaper groups. Moreover, there is an extra degree-2 generator  $B_{xy}$ , i.e., an element belonging to  $H^2(cm, \mathbb{Z}_2)$  that cannot be written as sum of cup product of elements in  $H^1(cm, \mathbb{Z}_2)$ . The name  $xy$  comes from the fact that its restriction to subgroup  $p1$  generated by  $T_1, T_2$  is  $A_xA_y$  (see Appendix 2.D).

To identify the relations, we note that there are now 4 missing elements:  $A_{x+y}A_m, A_{x+y}^2, B_{xy}A_{x+y}, B_{xy}^2$ . By restricting to the subgroup  $p1$  generated by  $T_1, T_2$  as well as the subgroup  $\mathbb{Z}_2$  generated by  $M$ , we see that  $A_{x+y}A_m = A_{x+y}^2 = 0$ . By restricting to the subgroup  $pm$  generated by  $T_1T_2^{-1}, T_1T_2, M$ , we see that  $B_{xy}A_{x+y} = 0$  as well as  $B_{xy}^2 = 0$ . Note that the pullback of  $A_{x+y}, A_m$  and  $B_{xy}$  to the subgroup  $pm$  is 0,  $A_m$  and  $A_yA_m$ , respectively.

Therefore, the  $\mathbb{Z}_2$  cohomology ring of  $cm$  is

$$\mathbb{Z}_2[A_{x+y}, A_m, B_{xy}]/(A_{x+y}A_m = 0, A_{x+y}^2 = 0, B_{xy}A_{x+y} = 0, B_{xy}^2 = 0)$$

## A.4 $\mathcal{S}Q^1$

In this sub-appendix, we define a new map we call  $\mathcal{S}Q^1$ , reminiscent of  $Sq^1$  in regular Steenrod algebra, as follows

$$\mathcal{S}Q^1 : H^n(G, \mathbb{Z}_2) \xrightarrow{\tilde{i}} H^n(G, U(1)_\rho) \xrightarrow{\beta} H^{n+1}(G, \mathbb{Z}_\rho) \xrightarrow{\tilde{p}} H^{n+1}(G, \mathbb{Z}_2), \quad (\text{A.31})$$

i.e.  $\mathcal{S}Q^1 \equiv \tilde{p} \circ \beta \circ \tilde{i}$ , where  $\tilde{i}$  and  $\tilde{p}$  are the map of group cohomology induced by the homomorphism of modules  $i : \mathbb{Z}_2 \rightarrow U(1)$  and  $p : \mathbb{Z} \rightarrow \mathbb{Z}_2$ , and  $\beta$  is the Bockstein homomorphism associated with the short exact sequence  $1 \rightarrow \mathbb{Z} \rightarrow \mathbb{R} \rightarrow U(1) \rightarrow 1$ . Note that  $\beta \circ \tilde{i}$  is the Bockstein homomorphism  $\beta_2$  associated with the short exact sequence  $1 \rightarrow \mathbb{Z} \rightarrow \mathbb{Z} \rightarrow \mathbb{Z}_2 \rightarrow 1$ , and therefore when the action  $\rho$  is trivial,  $\mathcal{S}Q^1$  is exactly  $Sq^1$  in regular Steenrod algebra.

Moreover,  $\mathcal{S}Q^1$  is related to  $Sq^1$  via the following simple fact

**Lemma A.4.1.** *For  $x \in H^n(G, \mathbb{Z}_2)$ , we have*

$$\mathcal{S}Q^1(x) = \mathcal{S}Q^1(1) \cup x + Sq^1(x). \quad (\text{A.32})$$

*Proof.* According to Eq. (A.17), choosing a cochain  $\tilde{x} \in C^n(G, \mathbb{Z})$  such that the  $\mathbb{Z}_2$  reduction of  $\tilde{x}$  is  $x$ , we have

$$\begin{aligned} \mathcal{S}Q^1(x) &= \frac{1}{2} \left( (-1)^{\tilde{\rho}(g_1)} \tilde{x}(g_2, \dots, g_{n+1}) + \sum_{j=1}^n (-1)^j \tilde{x}(g_1, \dots, g_j g_{j+1}, \dots, g_{n+1}) \right. \\ &\quad \left. + (-1)^{n+1} \tilde{x}(g_1, \dots, g_n) \right) \\ &= \frac{1}{2} \left( (-1)^{\tilde{\rho}(g_1)} - 1 \right) \tilde{x}(g_2, \dots, g_{n+1}) + Sq^1(x) \\ &= \mathcal{S}Q^1(1) \cup x + Sq^1(x) \pmod{2}. \end{aligned} \quad (\text{A.33})$$

■

For example, for  $\mathbb{Z}_2^T$  with nontrivial action on  $U(1)$  or  $\mathbb{Z}$ , we have,

$$\mathcal{S}Q^1(t^{2n+1}) = 0, \quad \mathcal{S}Q^1(t^{2n}) = t^{2n+1}, \quad (\text{A.34})$$

where  $t \in H^1(\mathbb{Z}_2^T, \mathbb{Z}_2)$  is the generator of the  $\mathbb{Z}_2$  cohomology ring of  $\mathbb{Z}_2^T$ . We see that in the presence of nontrivial  $\rho$ , the operation  $\mathcal{S}\mathcal{Q}^1$  is not distributive with respect to the cup product. Note that  $\mathcal{S}\mathcal{Q}^1(1)$  is nonzero and equals  $t$ , which when pulled back to the spacetime manifold  $\mathcal{M}$  equals  $w_1$  as well, i.e., the first Stiefel-Whitney class of  $\mathcal{M}$ . In contrast, for  $\mathbb{Z}_2$  with trivial action on  $U(1)$  or  $\mathbb{Z}$ , we have

$$\mathcal{S}\mathcal{Q}^1(A_c^{2n}) = 0, \quad \mathcal{S}\mathcal{Q}^1(A_c^{2n+1}) = A_c^{2n+2}, \quad (\text{A.35})$$

where  $A_c \in H^1(\mathbb{Z}_2, \mathbb{Z}_2)$  is the generator of the  $\mathbb{Z}_2$  cohomology ring of  $\mathbb{Z}_2$  as well.

As another example, consider  $O(5)$  with  $\tilde{\rho} : O(5) \rightarrow \mathbb{Z}_2$  the determinant, i.e., an  $O(5)$  element complex conjugates a  $U(1)$  element or multiplies a  $\mathbb{Z}$  element by  $-1$  if and only if the determinant of the  $O(5)$  element is  $-1$ . From Lemma A.4.1 we immediately have,

$$\mathcal{S}\mathcal{Q}^1(w_4^{O(5)}) = w_5^{O(5)}, \quad (\text{A.36})$$

as suggested by the calculation in the context of DQCP in Refs. [21, 170].

Moreover, even if  $\mathcal{S}\mathcal{Q}^1$  is not distributive with respect to the cup product, from Lemma A.4.1  $\mathcal{S}\mathcal{Q}^1$  is still distributive with respect to the cross product involving two different groups, i.e., we have

**Lemma A.4.2.** *For  $x \in H^m(G, \mathbb{Z}_2)$  and  $y \in H^n(H, \mathbb{Z}_2)$ , we have  $x \times y \in H^{m+n}(G \times H, \mathbb{Z}_2)$  and*

$$\mathcal{S}\mathcal{Q}^1(x \times y) = \mathcal{S}\mathcal{Q}^1(x) \times y + x \times \mathcal{S}\mathcal{Q}^1(y). \quad (\text{A.37})$$

This lemma is also important when calculating  $\mathcal{S}\mathcal{Q}^1$  because it decomposes the calculation into different pieces corresponding to different groups. For example, with the help of Eqs. (A.34) and (A.35), the lemma tells us how to calculate  $\mathcal{S}\mathcal{Q}^1$  for the group  $(\mathbb{Z}_2)^k$  with every  $\mathbb{Z}_2$  piece acting trivially or nontrivially on  $U(1)$  or  $\mathbb{Z}$ .

Finally, from the fact that

$$A_{\text{LH}} \cong \ker [\tilde{i} : H^2(G_s, \mathbb{Z}_2) \rightarrow H^2(G_s, U(1)_\rho)], \quad (\text{A.38})$$

as argued in Section 2.2, for LSM anomaly written as  $\exp(i\pi\lambda\eta)$  where  $\lambda \in H^2(G_s, \mathbb{Z}_2)$  and  $\eta \in H^2(G_{\text{int}}, \mathbb{Z}_2)$ , we have

$$\mathcal{S}\mathcal{Q}^1(\lambda) = 0. \quad (\text{A.39})$$

This can also be mathematically checked by considering different representations  $\rho : G_s \rightarrow O(n)$ . For example, consider  $G_s = p4m$ . Then  $A_{\text{LH}}$  is spanned by  $\lambda_1 = B_{xy} + A_{x+y}(A_{x+y} + A_m) + B_{c^2}$ ,  $\lambda_2 = B_{xy}$ ,  $\lambda_3 = A_{x+y}(A_{x+y} + A_m)$  in  $H^2(p4m, \mathbb{Z}_2)$  (see Appendix 2.D), corresponding to LSM anomaly associated to DOF at the site  $a$ , plaquette center  $b$ , and bond center  $c$  as in Fig. 2.2, respectively. Consider the following three representations of  $p4m$ . The first one is

$$\begin{aligned} T_x &\rightarrow \begin{pmatrix} -1 & 0 & 0 \\ 0 & -1 & 0 \\ 0 & 0 & 1 \end{pmatrix}, & T_y &\rightarrow \begin{pmatrix} -1 & 0 & 0 \\ 0 & 1 & 0 \\ 0 & 0 & -1 \end{pmatrix}, \\ C_4 &\rightarrow \begin{pmatrix} 1 & 0 & 0 \\ 0 & 0 & 1 \\ 0 & -1 & 0 \end{pmatrix}, & M &\rightarrow \begin{pmatrix} 1 & 0 & 0 \\ 0 & 1 & 0 \\ 0 & 0 & -1 \end{pmatrix} \end{aligned} \quad (\text{A.40})$$

The pullback of  $w_2^{O(3)}$  equals  $B_{xy} + B_{c^2}$  while the pullback of  $w_3^{O(3)}$  is zero (see Section 5.1 and especially Eq. (5.16)). From  $\mathcal{S}\mathcal{Q}^1(w_2^{O(3)}) = w_3^{O(3)}$ , we establish that

$$\mathcal{S}\mathcal{Q}^1(B_{xy} + B_{c^2}) = 0. \quad (\text{A.41})$$

The second representation is

$$T_x \rightarrow \begin{pmatrix} 1 & 0 \\ 0 & 1 \end{pmatrix}, \quad T_y \rightarrow \begin{pmatrix} 1 & 0 \\ 0 & 1 \end{pmatrix}, \quad C_4 \rightarrow \begin{pmatrix} 0 & 1 \\ -1 & 0 \end{pmatrix}, \quad M \rightarrow \begin{pmatrix} 1 & 0 \\ 0 & -1 \end{pmatrix} \quad (\text{A.42})$$

The pullback of  $w_2^{O(2)}$  equals  $B_{c^2}$ , and from  $\mathcal{S}\mathcal{Q}^1(w_2^{O(2)}) = 0$ , we establish that

$$\mathcal{S}\mathcal{Q}^1(B_{c^2}) = 0 \quad (\text{A.43})$$

The third representation is

$$T_x \rightarrow \begin{pmatrix} -1 & 0 \\ 0 & -1 \end{pmatrix}, \quad T_y \rightarrow \begin{pmatrix} -1 & 0 \\ 0 & -1 \end{pmatrix}, \quad C_4 \rightarrow \begin{pmatrix} 1 & 0 \\ 0 & 1 \end{pmatrix}, \quad M \rightarrow \begin{pmatrix} 1 & 0 \\ 0 & -1 \end{pmatrix} \quad (\text{A.44})$$

and we have

$$\mathcal{S}\mathcal{Q}^1(A_{x+y}(A_{x+y} + A_m)) = 0. \quad (\text{A.45})$$

Since  $B_{xy} + B_{c^2}, B_{c^2}, A_{x+y}(A_{x+y} + A_m)$  span  $A_{\text{LH}}$  as well, indeed we mathematically show that  $\mathcal{S}\mathcal{Q}^1(\lambda) = 0$  for  $\lambda \in A_{\text{LH}}$  in  $p4m$ . Then according to Lemma A.4.2 we also have

$$\mathcal{S}\mathcal{Q}^1(\lambda\eta) = \mathcal{S}\mathcal{Q}^1(\lambda) \times \eta + \lambda \times \mathcal{S}\mathcal{Q}^1(\eta) = \lambda \times \mathcal{S}\mathcal{Q}^1(\eta) \quad (\text{A.46})$$

This equation will be very useful in the analysis of anomaly-matching. Note that this equation holds for LSM constraints on lattices with any wallpaper group.